frontiers | Research Topics

Updates on radiation-induced lymphopenia

Edited by
Peter Sylvain Nicolas van Rossum, Steven H. Lin and Jian-Yue Jin

Published in
Frontiers in Oncology

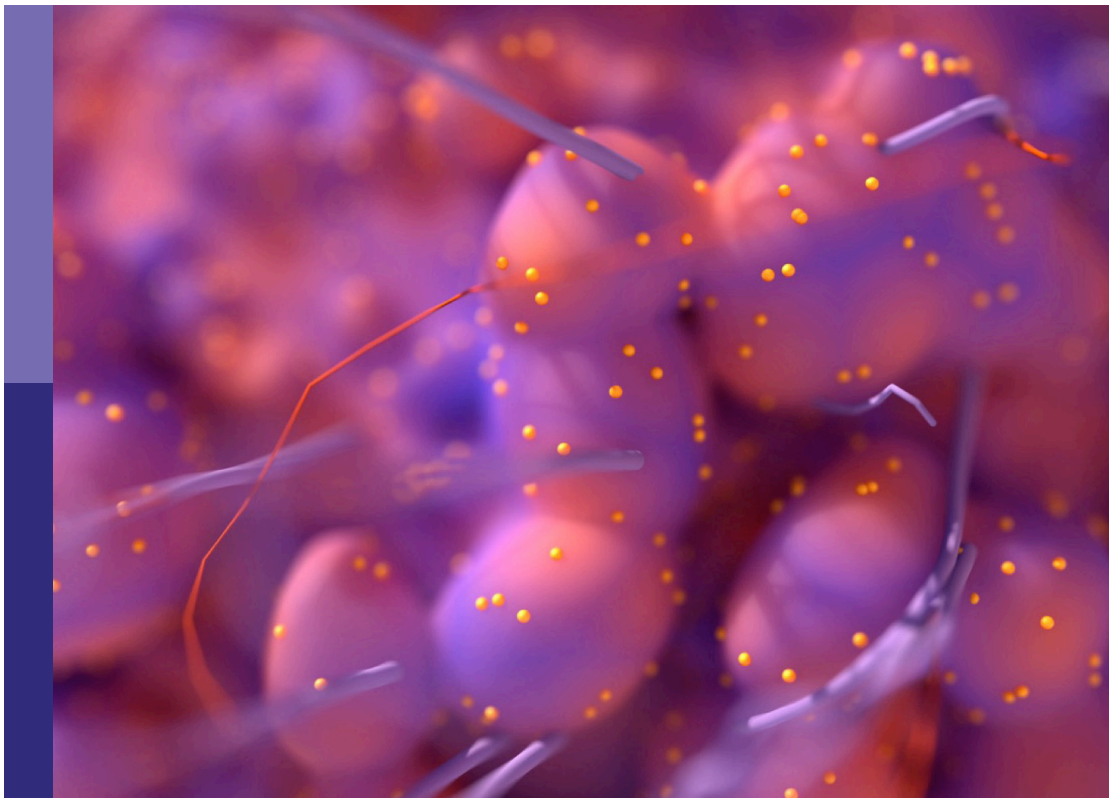

ISSN 1664-8714
ISBN 978-2-8325-5396-1
DOI 10.3389/978-2-8325-5396-1

About Frontiers

Frontiers is more than just an open access publisher of scholarly articles: it is a pioneering approach to the world of academia, radically improving the way scholarly research is managed. The grand vision of Frontiers is a world where all people have an equal opportunity to seek, share and generate knowledge. Frontiers provides immediate and permanent online open access to all its publications, but this alone is not enough to realize our grand goals.

Frontiers journal series

The Frontiers journal series is a multi-tier and interdisciplinary set of open-access, online journals, promising a paradigm shift from the current review, selection and dissemination processes in academic publishing. All Frontiers journals are driven by researchers for researchers; therefore, they constitute a service to the scholarly community. At the same time, the *Frontiers journal series* operates on a revolutionary invention, the tiered publishing system, initially addressing specific communities of scholars, and gradually climbing up to broader public understanding, thus serving the interests of the lay society, too.

Dedication to quality

Each Frontiers article is a landmark of the highest quality, thanks to genuinely collaborative interactions between authors and review editors, who include some of the world's best academicians. Research must be certified by peers before entering a stream of knowledge that may eventually reach the public - and shape society; therefore, Frontiers only applies the most rigorous and unbiased reviews. Frontiers revolutionizes research publishing by freely delivering the most outstanding research, evaluated with no bias from both the academic and social point of view. By applying the most advanced information technologies, Frontiers is catapulting scholarly publishing into a new generation.

What are Frontiers Research Topics?

Frontiers Research Topics are very popular trademarks of the *Frontiers journals series*: they are collections of at least ten articles, all centered on a particular subject. With their unique mix of varied contributions from Original Research to Review Articles, Frontiers Research Topics unify the most influential researchers, the latest key findings and historical advances in a hot research area.

Find out more on how to host your own Frontiers Research Topic or contribute to one as an author by contacting the Frontiers editorial office: frontiersin.org/about/contact

Updates on radiation-induced lymphopenia

Topic editors

Peter Sylvain Nicolas van Rossum — Amsterdam University Medical Center, Netherlands

Steven H. Lin — University of Texas MD Anderson Cancer Center, United States

Jian-Yue Jin — Capital Medical University, China

Citation

van Rossum, P. S. N., Lin, S. H., Jin, J.-Y., eds. (2024). *Updates on radiation-induced lymphopenia*. Lausanne: Frontiers Media SA. doi: 10.3389/978-2-8325-5396-1

Table of contents

frontiers | Frontiers in Oncology

TYPE Editorial
PUBLISHED 02 July 2024
DOI 10.3389/fonc.2024.1448658

OPEN ACCESS

EDITED AND REVIEWED BY
Timothy James Kinsella,
Brown University, United States

*CORRESPONDENCE
Pim J. J. Damen
p.damen@erasmusmc.nl

RECEIVED 13 June 2024
ACCEPTED 14 June 2024
PUBLISHED 02 July 2024

CITATION
Damen PJJ, Lin SH and van Rossum PSN (2024) Editorial: Updates on radiation-induced lymphopenia.
Front. Oncol. 14:1448658.
doi: 10.3389/fonc.2024.1448658

Editorial: Updates on radiation-induced lymphopenia

Pim J. J. Damen[1,2]*, Steven H. Lin[3] and Peter S. N. van Rossum[1]

[1]Department of Radiation Oncology, Amsterdam UMC, Amsterdam, Netherlands, [2]Department of Radiotherapy, Erasmus MC Cancer Institute, University Medical Center Rotterdam, Rotterdam, Netherlands, [3]Department of Radiation Oncology, The University of Texas MD Anderson Cancer Center, Houston, TX, United States

KEYWORDS

lymphopenia, radiotherapy, review, survival, immunotherapy

Editorial on the Research Topic
Updates on radiation-induced lymphopenia

Radiotherapy is a commonly employed and effective treatment for cancer, seeking to achieve an optimal balance between tumor cell death and minimizing damage to healthy tissues. Radiation-induced lymphopenia (RIL) is a common side effect due to the high radiosensitivity of lymphocytes even at low doses (<1Gy), leading to their direct depletion (1). While the detrimental effects of radiotherapy on lymphocytes have been recognized since 1905, its influence on tumor control and survival has remained largely unclear until recently (2). Moreover, awareness and understanding of the prognostic effects of RIL remain limited in daily clinical practice.

Radiotherapy induces a substantial drop in lymphocyte levels during treatment, with the most significant decrease occurring in the first week and continuing in subsequent weeks, which is attributed to lymphocyte cell death and migration toward the tumor (3). The review by Paganetti outlined that differences in radiosensitivity exist among lymphocyte subpopulations (i.e. B cells appear to be more radiosensitive than T cells, whereas natural killer cells appear to be the most radioresistant).The review indicates that not only the absolute lymphocyte counts are affected by radiation, but also lymphocyte diversity and activity. This is supported by the finding that despite the eventual recovery of the lymphocyte counts, the extent of lymphocyte restoration (i.e. lymphocyte quantity) appears unrelated to survival (i.e. lymphocyte quality) (4).

Numerous studies and reviews have addressed the incidence of RIL and its implications for survival (3). Overall, severe RIL appears to occur in 30-50% of patients with solid tumors, and is most severe after radiotherapy of tumors in the brain, thorax and upper abdomen (5). Multiple meta-analyses have shown the detrimental association of RIL with pathologic response, progression-free survival (PFS) and overall survival (OS), both for specific tumor locations (3, 6–8) and for solid tumors in general (e.g. a pooled hazard ratio [HR] of 1.65, and a 95% confidence interval [CI] of 1.43-1.90 were found for the negative impact of RIL on OS in solid tumors) (5).

Multiple factors have been found to contribute to the occurrence and severity of RIL. Clinical characteristics described in the literature associated with RIL (e.g. lower baseline ALC, older age and worse patient performance score) may correspond to a more fragile reserve or compensation system (5). Other factors such as a higher tumor stage, a larger planning target volume (PTV), more radiotherapy fractions and a higher heart, lung or

integral body dose, correspond to a larger proportion of the blood pool (i.e. circulating lymphocytes) being irradiated (4, 7, 9). More recently, the effective dose to immune cells (EDIC) was found to be significantly correlated with severe RIL in esophageal squamous cell carcinoma by Xu et al. and Qiu et al. (10) and in breast cancer by (Chen et al.). The EDIC estimates the dose to immune cells by calculating the radiation dose to circulating blood as a surrogate, with contributions from each blood-containing organ, including the lungs and heart, and large and small blood vessels. Another study confirmed that severe RIL was associated with a higher dose of circulating blood cells. In addition, in a study of hepatocellular carcinoma patients with bone metastases treated with radiotherapy, Chen et al. found that the systemic immune-inflammation index and the neutrophil-to-lymphocyte-ratio were independently correlated with poor prognosis.

A significant finding since the advent of immunotherapy is that a reduction in lymphocyte numbers appears to correlate with decreased effectiveness of lymphocyte-activating immunotherapeutic agents (11, 12). In a meta-analysis by Zhang et al., including 10 cohorts with a total of 1,130 lung cancer patients treated with immunotherapy, RIL was associated with worse PFS (HR 2.05, 95% CI 1.62-2.60) and OS (HR 2.69, 95% CI 2.10-3.43), suggesting the importance of monitoring lymphocyte counts in lung cancer patients undergoing immunotherapy. A study by Pasquier et al. found that the inclusion of at least one tumor-draining lymph node (TDLN) in the clinical target volume was associated with worse PFS in locally advanced non-small cell lung cancer (NSCLC) patients treated with immunotherapy after concurrent chemoradiation therapy. Radiotherapy targeting TDLNs may disrupt the anti-tumor immune response by interfering with the generation of progenitor-exhausted T cells that seed the tumor, resulting in diminished infiltration of CD8+ T cells and decreased expression of T-cell recruiting chemokines.

Identifying patients with an elevated risk of developing RIL is desirable to mitigate this risk and potentially improve oncological outcomes. Such patient selection may help to determine who may benefit most from strategies aimed at avoiding RIL. Multiple prediction models for RIL have been reported in the literature and Van Rossum et al. externally validated two models, developed in lung and esophageal cancer. The PTV-based predictive model yielded better external performance in NSCLC patients when compared to a dosimetry-based model (13). Xu et al. developed and internally validated a machine learning model to predict severe lymphopenia during pelvic radiotherapy in cervical cancer patients. Consequently, these predictive models may assist in identifying patients at increased risk for severe RIL who may benefit from lymphopenia-mitigating strategies, which may ultimately improve survival.

Methods to potentially mitigate lymphopenia are aimed at minimizing unintended radiation exposure to circulating blood and secondary lymphoid organs. This includes avoiding doses to major vessels, the heart, lungs, and lymphocyte-rich organs such as lymph nodes, spleen, and bone marrow. A recent systematic review summarizes the existing literature on dosimetric factors associated with RIL in solid tumors and provides a foundation for potential use in future clinical trials aimed at mitigating RIL risk (14). Since these constraints have not been validated in prospective trials, adhering to the "as low as reasonably achievable" (ALARA) principle for organs at risk remains advisable in current practice. Other methods include reducing the number of radiation fractions (i.e. hypofractionation) or reducing the field size or integral body dose (e.g. with proton-beam therapy or online adaptive [MRI- or CT-based] radiotherapy) (15–17).

In conclusion, RIL is linked to poorer oncologic outcomes in patients with various types of solid tumors. While clinicians may currently have limited awareness of RIL, it is expected to become increasingly important in the coming years with the introduction and advancement of immunotherapy. Future research should determine whether and in which patients' lymphopenia-mitigating strategies could be beneficial in terms of oncological outcomes.

Author contributions

PD: Investigation, Project administration, Writing – original draft. SL: Conceptualization, Investigation, Supervision, Writing – review & editing. Pv: Conceptualization, Investigation, Project administration, Supervision, Writing – review & editing.

Conflict of interest

Author SL discloses grant funding from Beyond Spring Pharmaceuticals, Hitachi Chemical Diagnostics, and IntraOp Corporation, serving on advisory board for Beyond Spring Pharmaceuticals, STCube Pharmaceuticals, and AstraZeneca, being a consultant for XRAD Therapeutics and is cofounder of Scenexo, Inc.

The remaining authors declare that the research was conducted in the absence of any commercial or financial relationships that could be construed as a potential conflict of interest.

The author(s) declared that they were an editorial board member of Frontiers, at the time of submission. This had no impact on the peer review process and the final decision.

Publisher's note

References

1. Sellins KS, Cohen JJ. Gene induction by gamma-irradiation leads to DNA fragmentation in lymphocytes. *J Immunol*. (1987) 139:3199–206. doi: 10.4049/jimmunol.139.10.3199

2. Heineke VH. Experimentelle Untersuchungen über die Einwirkung der Röntgenstrahlen auf das Knochenmark, nebst einigen Bemerkungen über die Röntgentherapie der Leukämie und Pseudoleukämie und des Sarcoms. *Deutsche Z für Chirurgie*. (1905) 78:196–230. doi: 10.1007/BF02798721

3. de Kermenguy F, Meziani L, Mondini M, Clémenson C, Morel D, Deutsch E, et al. Radio-induced lymphopenia in the era of anti-cancer immunotherapy. *Int Rev Cell Mol Biol*. (2023) 378:1–30. doi: 10.1016/bs.ircmb.2023.03.002

4. Deng W, Xu C, Liu A, van Rossum PSN, Deng W, Liao Z, et al. The relationship of lymphocyte recovery and prognosis of esophageal cancer patients with severe radiation-induced lymphopenia after chemoradiation therapy. *Radiother Oncol*. (2019) 133:9–15. doi: 10.1016/j.radonc.2018.12.002

5. Damen PJJ, Kroese TE, van Hillegersberg R, Schuit E, Peters M, Verhoeff JJC, et al. The influence of severe radiation-induced lymphopenia on overall survival in solid tumors: A systematic review and meta-analysis. *Int J Radiat Oncol Biol Phys*. (2021) 111:936–48. doi: 10.1016/j.ijrobp.2021.07.1695

6. Dai D, Tian Q, Shui Y, Li J, Wei Q. The impact of radiation induced lymphopenia in the prognosis of head and neck cancer: A systematic review and meta-analysis. *Radiother Oncol*. (2022) 168:28–36. doi: 10.1016/j.radonc.2022.01.003

7. Dai D, Tian Q, Yu G, Shui Y, Jiang H, Wei Q. Severe radiation-induced lymphopenia affects the outcomes of esophageal cancer: A comprehensive systematic review and meta-analysis. *Cancers (Basel)*. (2022) 14:3024. doi: 10.3390/cancers14123024

8. Upadhyay R, Venkatesulu BP, Giridhar P, Kim BK, Sharma A, Elghazawy H, et al. Risk and impact of radiation related lymphopenia in lung cancer: A systematic review and meta-analysis. *Radiother Oncol*. (2021) 157:225–33. doi: 10.1016/j.radonc.2021.01.034

9. van Rossum PSN, Deng W, Routman DM, Liu AY, Xu C, Shiraishi Y, et al. Prediction of severe lymphopenia during chemoradiation therapy for esophageal cancer: development and validation of a pretreatment nomogram. *Pract Radiat Oncol*. (2020) 10:e16–26. doi: 10.1016/j.prro.2019.07.010

10. Xu C, Jin JY, Zhang M, Liu A, Wang J, Mohan R, et al. The impact of the effective dose to immune cells on lymphopenia and survival of esophageal cancer after chemoradiotherapy. *Radiother Oncol*. (2020) 146:180–6. doi: 10.1016/j.radonc.2020.02.015

11. Pike LRG, Bang A, Mahal BA, Taylor A, Krishnan M, Spektor A, et al. The impact of radiation therapy on lymphocyte count and survival in metastatic cancer patients receiving PD-1 immune checkpoint inhibitors. *Int J Radiat Oncol Biol Phys*. (2019) 103:142–51. doi: 10.1016/j.ijrobp.2018.09.010

12. Friedes C, Chakrabarti T, Olson S, Prichett L, Brahmer JR, Forde PJ, et al. Association of severe lymphopenia and disease progression in unresectable locally advanced non-small cell lung cancer treated with definitive chemoradiation and immunotherapy. *Lung Cancer*. (2021) 154:36–43. doi: 10.1016/j.lungcan.2021.01.022

13. Abravan A, Faivre-Finn C, Kennedy J, McWilliam A, van Herk M. Radiotherapy-related lymphopenia affects overall survival in patients with lung cancer. *J Thorac Oncol*. (2020) 15(10):P1624. doi: 10.1016/j.jtho.2020.06.008

14. Venkatesulu BP, Giridhar P, Pujari L, Chou B, Lee JH, Block AM, et al. Lymphocyte sparing normal tissue effects in the clinic (LymphoTEC): A systematic review of dose constraint considerations to mitigate radiation-related lymphopenia in the era of immunotherapy. *Radiother Oncol*. (2022) 177:81–94. doi: 10.1016/j.radonc.2022.10.019

15. Wang X, Van Rossum PSN, Chu Y, Hobbs BP, Grassberger C, Hong TS, et al. Severe lymphopenia during chemoradiation therapy for esophageal cancer: comprehensive analysis of randomized phase 2B trial of proton beam therapy versus intensity modulated radiation therapy. *Int J Radiat Oncol Biol Phys*. (2024) 118:368–77. doi: 10.1016/j.ijrobp.2023.08.058

16. Raaymakers BW, Lagendijk JJW, Overweg J, Kok JGM, Raaijmakers AJE, Kerkhof EM, et al. Integrating a 1.5 T MRI scanner with a 6 MV accelerator: proof of concept. *Med Biol Phys Med Biol*. (2009) 54:229–37. doi: 10.1088/0031-9155/54/12/N01

17. Morgan HE, Wang K, Yan Y, Desai N, Hannan R, Chambers E, et al. Preliminary evaluation of PTV margins for online adaptive radiation therapy of the prostatic fossa. *Pract Radiat Oncol*. (2023) 13:e345–53. doi: 10.1016/j.prro.2022.11.003

frontiers | Frontiers in Oncology

ORIGINAL RESEARCH
published: 28 April 2022
doi: 10.3389/fonc.2022.768956

Radiation Induced Lymphopenia Is Associated With the Effective Dose to the Circulating Immune Cells in Breast Cancer

Fang Chen[1,2†], Jian-Yue Jin[3†], Timothy S.K. Hui[1], Haiman Jing[1], Hong Zhang[4], Yaqing Nong[1], Ying Han[1], Weili Wang[3], Lingyu Ma[1], Fan Yi[1], Qingqing Chen[1], Yongsheng Zhang[1], Pingfu Fu[5], Li Yang[1], Zhiyuan Xu[1] and Feng-Ming Spring Kong[1,2]*

[1] Department of Clinical Oncology, The University of Hong Kong-Shenzhen Hospital, Shenzhen, China, [2] Department of Clinical Oncology, Hong Kong University Li Ka Shing Medical School, Hong Kong, Hong Kong SAR, China, [3] Department of Radiation Oncology, Case Western Reserve University, Cleveland, OH, United States, [4] Department of Radiation Oncology, University of Maryland School of Medicine, Baltimore, MD, United States, [5] Department of Population and Quantitative Health Sciences, Case Western Reserve University, Cleveland, OH, United States

OPEN ACCESS

Edited by:
Francesca Ballarini,
University of Pavia, Italy

Reviewed by:
Francesco Tommasino,
University of Trento, Italy
Ting Xu,
University of Texas MD Anderson Cancer Center, United States

***Correspondence:**
Feng-Ming Spring Kong
kong0001@hku.hk

†These authors have contributed equally to this work and share first authorship

Specialty section:
This article was submitted to Radiation Oncology, a section of the journal Frontiers in Oncology

Received: 05 September 2021
Accepted: 28 March 2022
Published: 28 April 2022

Citation:
Chen F, Jin J-Y, Hui TSK, Jing H, Zhang H, Nong Y, Han Y, Wang W, Ma L, Yi F, Chen Q, Zhang Y, Fu P, Yang L, Xu Z and Kong F-MS (2022) Radiation Induced Lymphopenia Is Associated With the Effective Dose to the Circulating Immune Cells in Breast Cancer. Front. Oncol. 12:768956. doi: 10.3389/fonc.2022.768956

Background: Lymphopenia is a known significant factor for treatment outcome in cancer patients, with underlying risk factor poorly understood in breast cancer. We hypothesize that the effective dose to the circulating immune cells (EDIC) which was related with lymphopenia in lung cancer will also have significant effect for radiation induced lymphopenia (RIL) in patients with breast cancer.

Material and Methods: Patients treated with adjuvant radiotherapy (RT) and with complete blood tests within one week from RT end/start (post/preRT) were eligible in this study. Radiation dosimetric factors were collected retrospectively, and EDIC for each patient was calculated based on the doses to lung, heart and total body according to the model description, as previously reported. RIL was defined by the CTCAE5.0 based on postRT peripheral lymphocyte count (PLC). Linear regression was first used to test the correlation between EDIC with post/preRT PLC ratio and postRT PLC, using all these as continuous variables. Normal tissue complication probability (NTCP) was used to develop models that predict the CTCAE graded RIL from EDIC.

Results: A total of 735 patients were eligible. The mean post/preRT PLC ratio was 0.66 (95% CI: 0.64-0.68) and mean EDIC of breast cancer was 1.70Gy (95% CI: 1.64-1.75). Both post/preRT PLC ratio and postRT PLC were significantly correlated with EDIC ($P<0.001$), with R^2 of 0.246. For patients with normal preRT PLC, the post/preRT PLC ratio was better associated with EDIC, and postRT PLC was expressed as $PLC_{preRT} \times (0.89 - 0.16 \times EDIC)$. For patients with preRT lymphopenia, postRT PLC was better associated with EDIC and it was $1.1 - 0.17 \times EDIC$. Using binned EDIC as the dose variable, the bootstrap validated NTCPs fit the data nicely with R^2 of 0.93, 0.96, and 0.94 for grade-1, grade-2, and grade-3 RIL, respectively. The corresponding EDIC to induce 50% of grade-1, grade-2 and grade-3 RIL was 1.2, 2.1 and 3.7 Gy, respectively.

Conclusion: EDIC is a significant factor for RIL in patients with breast cancer, and may be used to compute the risk of lymphopenia in each individual patient with the use of the conventional NTCP modeling. External validation is needed before the EDIC can be used to guide RT plan.

Keywords: lymphopenia, radiation, effective dose to the circulating immune cells (EDIC), prediction model, breast cancer

INTRODUCTION

The immune system is critical for the development and management of malignant tumors. Lymphocyte is a major component of the immune system while lymphopenia was reported to be associated with poor prognosis in patients with breast cancer and other malignant cancers (1–4). However, lymphocytes are extremely radiosensitive (5, 6) and exposure to as low as 1 Gy of radiation can destroy mature circulating lymphocytes (7). Therefore, radiotherapy (RT) can damage the immune system and cause potential immunosuppression while it is applied for its role on killing malignant tumor cells.

Radiation induced lymphopenia (RIL) is common and known as a negative prognostic factor in many types of malignant solid tumors (8–15). In breast cancer, we have demonstrated that 60.5% patients had lymphopenia and 92.7% patients had some degree of reduction in peripheral lymphocyte count (PLC) after adjuvant RT (16). RIL or the ratio of nadir PLC and pretreatment PLC were also found to be a potential predictor for ipsilateral breast tumor recurrence or 5-year disease-free survival in breast cancer (17, 18). Meanwhile, several phase III clinical trials involving immunotherapy showed positive results which have significantly changed the treatment strategy for triple negative breast cancer (19, 20). The keynote 522 study (20) had enrolled previously untreated stage II or stage III triple-negative breast cancer and most of them would receive adjuvant RT concurrent with pembrolizumab after surgery. The effect of immunotherapy might be weakened by RIL since patients with low PLC had lower immune response rate while receiving checkpoint inhibitors (21). Therefore, it is important to establish a prediction model of RIL to improve RT plan of a better lymphocyte-sparing technique to reduce treatment-related lymphopenia.

Studies had revealed that radiation dose to the lymphatic system played an important role on RIL (6, 12). Our prior study also found that several radiation dosimetric factors (such as mean lung dose) were significant risk factors for lymphopenia after RT in patients with breast cancer (16). A simple RIL model based on radiation dose to the lymphatic system will be helpful clinically to improve RT plan and minimize lymphopenia. The lymphatic system is a complicated system composed of lymphoid organs such as lymph nodes/ducts, bone marrow and thymus, non-lymphoid organs such as lung and liver where lymphocytes reside, and circulation blood which transport lymphocytes to different parts of the body (22). Here we hypothesized that radiation dose to the lymphocytes in circulation blood to be critical for RIL because it was observed in breast and brain radiation patients while there is little lymphoid tissue in radiation of these regions (13, 23, 24). In addition, RIL is directly measured according to the number of lymphocytes in a unit volume of blood, and the active lymphocytes in circulation blood may be more radiosensitive than non-active lymphocytes in other parts of the lymphatic system (5, 6).

However, it is difficult to determine the radiation dose to the lymphocytes in circulation blood because they are moving targets. We have previously developed a model for the effective dose to the circulating immune cells (EDIC) for thoracic radiation based on planning dosimetric data, and demonstrated that EDIC was associated with both overall survival (OS) and local progression free survival (LPFS) after thoracic radiotherapy in non-small cell lung cancer (NSCLC) patients (25). This EDIC model has been validated externally in NSCLC (26) and esophageal cancer (15, 27), and further extended to abdominal radiation with consideration of other immune organs beyond circulating blood, including spleen, lymphatic ducts and bone marrows (22). Because the main irradiated blood-containing structures of breast cancer are similar to that of other thoracic malignancies, we hypothesized that this modeled EDIC may also be applicable to breast cancer. The purpose of this study is two folds: 1) to investigate whether EDIC is associated with RIL in patients with breast cancer; 2) to develop a normal tissue complication probability (NTCP) model for RIL by considering the EDIC as the dose to the circulating lymphocytes, similar as the conventional NTCP model for other normal structures (such as NTCP of radiation induced pneumonitis versus lung dose).

Abbreviations: EDIC, effective dose to the circulating immune cells; RIL, radiation induced lymphopenia; RT, radiotherapy; PLC, peripheral lymphocyte counts; NSCLC, non-small cell lung cancer; LYM, lymphocytes; Nadir-PLC, the lowest peripheral lymphocyte counts during radiation; PreRT PLC, peripheral lymphocyte counts before radiation; OAR, organ at risk; CTCAE, Common Terminology Criteria for Adverse Events; EUD, equivalent uniform dose; MLD, mean lung doses; MHD, mean heart dose; ITDV, integral dose or integral total dose volume; NTCP, Normal Tissue Complication Probability; OS, overall survival; LPFS, local progression-free survival; CRT, chemoradiotherapy; PFS, progression free survival; DMFS, distant metastasis free survival; ESCC, esophageal squamous cell cancer; SBRT, stereotactic body radiation therapy; MOD, Mean Organ Dose; V5 (20), relative volume receiving more than 5Gy (20Gy).

MATERIALS AND METHODS

Study Population

Patients with breast cancer who had received adjuvant radiation between March 2015 to February 2020 in the

University of Hong Kong-Shenzhen Hospital were enrolled in this study. Inclusion criteria: pathology confirmed invasive breast cancer, aged 18-year-old and above, underwent adjuvant radiation therapy. Exclusion criteria: non-invasive breast cancer, recurrent or stage IV breast cancer, breast lymphoma, immune related diseases, without PLC within 7 days before and after radiation in the University of Hong Kong-Shenzhen Hospital.

Data Collection

Following information of patients were collected: 1) radiation dosimetric factors including RT technique, RT fields, RT fractionations, mean heart dose (MHD), mean lung dose (MLD), and integral dose, which has a unit of dose*volume (to avoid confusion, here we referred it as integral total dose volume [ITDV]); 2) Other clinical factors including age, tumor laterality, ER/PR/HER-2 subtype, stage, surgical approaches, chemotherapy, endocrine therapy, target therapy; 3) PLC within 7 days at the beginning and end of radiation. Lymphopenia was graded by Common Terminology Criteria for Adverse Events (CTCAE) version 5.0. Lymphopenia was defined as PLC cut-off of 1.06×10^9 in our institution. Grade 1, 2, 3 and 4 lymphopenia were defined as PLC cut-off of 1.06-0.8×10^9, 0.8-0.5×10^9, 0.5-0.2×10^9 and 0.2×10^9/L, respectively. The study endpoints were numerical value of post/preRT PLC ratio, and postRT lymphopenia graded by CTCAE5.0 based on postRT PLC.

EDIC Calculation

A recently reported EDIC model was used for this study (25). The details of the EDIC model derivation have been described previously and validated externally (22, 25). Basically, the model derivation includes 4 steps: 1) convert the mean dose of each single blood containing organ (such as lung and heart) in one fraction into blood dose and volume by considering continuous blood flow through the organ during the time of radiation delivery (22, 25); 2) estimate the fractionation effect by considering that the irradiated blood uniformly mixed with un-irradiated blood after each fraction (13); 3) convert the blood dose volume data modified by the fractionation effect into a blood equivalent uniform dose; and 4) finally EDIC is the sum of the blood equivalent uniform doses (EUDs) contributed by each blood-containing organs, including lung, heart, large and small blood vessels with an assumption that large and small vessels are uniformly distributed in the body. The model is finally expressed as $EDIC = 12\% \times MLD + 8\% \times MHD + [45\% + 35\% \times 0.85 \times (\frac{n}{45})^{\frac{1}{2}}] \times ITDV/(61.8 \times 10^3)$, where MLD, MHD, and ITDV are the mean total lung dose, mean heart dose and integral dose (or integral total dose volume), respectively, and n is the number of radiation fractions (25). The ITDV was calculated as the mean external contour dose multiplying with the volume of the external contour. The CT scan region was from the lower jaw to L1 vertebra in this study.

Statistical Method

The effects of potential risk factors of RIL (post/preRT PLC ratio) were estimated using univariate analysis initially and further estimated using multivariable model. To avoid the unstable and inaccurate estimates of the coefficients, the stepwise linear regression based on the Akaike information criterion minimum was used to select variables for inclusion in the multivariate analysis. Meanwhile, the collinearity testing was performed using the variance inflation factor (VIF), and VIF > 10.0 was interpreted as indicating multicollinearity. Variables with VIF > 10.0 were not included in the final model. Coefficients and corresponding 95% confidence interval were calculated for the linear regression model. Another linear regression was used to investigate the numerical correlation between the post/preRT PLC ratio (or postRT PLC) with EDIC. Statistical analysis was performed using R software (version 3.6.2; https://www.R-project.org).

To develop the NTCP model for RIL, the Solver program in Excel was used to fit the clinical data into the NTCP model. The patients were binned into the following 8 groups according to their EDIC values: 1) EDIC <1.0; 2) 1≤ EDIC<1.5; 3) 1.5≤ EDIC<2.0; 4) 2.0≤ EDIC<2.5; 5) 2.5≤ EDIC<3.0; 6) 3.0≤ EDIC<3.5; 7) 3.5≤ EDIC<4.0; and 8) EDIC≥4.0. The average EDIC in each bin was calculated. The percentage of patients had Grade 1+, Grade 2+ and Grade 3+ lymphopenia at each bin was also calculated, respectively. The calculated percentage of patients with lymphopenia was considered as clinically observed NTCP for lymphopenia, and NTCP versus average EDIC was then fitted with the NTCP model expressed as

$$NTCP = 1/\left[1 + \left(\frac{D50}{EDIC}\right)^k\right] \quad (1)$$

where D50 and k are fitting parameters. When the value of EDIC that generated NTCP of 50% was considered to be D50. For better comparison, we also used the original binary data for each patient to fit the NTCP model. Bootstrap validations were also performed for both binning and original binary data settings. Internal generalizability was evaluated over 1000 bootstrap samples, which were obtained by selecting patients randomly from the study cohort, with replacement to produce datasets having the same number of patients as the original cohort. Confidence intervals (CIs) for fit parameters were calculated using the bias corrected and accelerated bootstrap (BCa) method.

RESULTS

Characteristics of Patients and Radiation Dosimetric at Baseline

Between March 2015 to February 2020, 1559 patients with breast cancer received adjuvant RT in the University of Hong Kong-Shenzhen Hospital. Among them, 735 patients with invasive breast cancer were eligible for this study (**Supplementary Figure 1 for patient selection**). **Table 1** lists the characteristics of patient, tumor, pre-radiation treatment factors and radiation dosimetric factors at baseline. The median age was 45 years (range 26-86). The mean doses of lung, heart and integral body were 5.5Gy (95% CI: 5.3-5.6), 2.4Gy (95% CI: 2.2-2.5) and 4.4Gy (95% CI: 4.3-4.5), respectively.

Correlation Between EDIC and postRT/preRT PLC (or postRT PLC)

Overall, 92.7% patients had some degree of reduction in PLC postRT, and 60.5% (445/735) patients had lymphopenia postRT (**Supplementary Table 1**). The mean post/preRT PLC ratio was 0.66 (95% CI: 0.64-0.68). The mean EDIC of breast cancer was 1.70Gy (95% CI: 1.64-1.75). Univariate and multivariable regression analyses showed that EDIC was one of the significant risk factors (P<0.001) for lymphopenia (post/preRT PLC ratio) (**Table 1**).

Linear regression showed that the post/preRT PLC ratio decreased with increasing EDIC (R^2 = 0.246, p<0.001) (**Figure 1A**). However, we noted that a significant number of patients were outliers that not fit to the linear regression. Interestingly, most of these outlier patients had baseline (preRT) lymphopenia (or low preRT PLC), which may had confounded the radiation effect. In this study, 14.3% (105/735, 95%CI: 14.2-14.3%) patients had CTCAE5.0 defined lymphopenia before RT (11.4%, 2.5%, 0.4% and 0 for grade 1, 2, 3 and 4, respectively) (**Supplementary Table 1**). As shown in **Figures 1B–D**, the correlation represented by R^2 was improved from 0.246 to 0.283 by excluding 3 patients with grade-3 baseline lymphopenia, improved to 0.309 by excluding additional 18 patients with grade-2 baseline lymphopenia, and further improved to 0.318 by excluding 84 grade-1 baseline lymphopenia patients. The percentage outliers were 2/3 (66.7%), 3/18 (11.1%), 2/84 (2.4%) and 1/640 (0.1%) for patients with baseline (Pre-RT) grade-3, grade-2, grade-1 and grade-0 lymphopenia, respectively. In patients with normal preRT PLC, the postRT PLC (or potential RIL) might be estimated by the linear regression of the post/preRT PLC ratio with EDIC, and specifically be computed as $PLC_{postRT} = PLC_{preRT} \times (0.89 - 0.16 \times EDIC)$ (**Figure 1D**). Meanwhile, these data also indicated that patients with baseline lymphopenia before RT tended to have a different behavior.

The postRT PLC also decreased with increasing EDIC (R^2 = 0.275, p<0.001) (**Figure 2A**), and its correlation was better than that of post/preRT PLC ratio to EDIC. However, the correlation did not improve when patients with preRT lymphopenia were excluded (**Figures 2B, C**). The correlation was better than that of the post/preRT PLC ratio to EDIC if all patients were considered, but it was not as good as that of the post/preRT PLC ratio to EDIC if patients with preRT lymphopenia were excluded.

We also compared the correlation of post/preRT PLC ratio to EDIC and postRT PLC to EDIC for patients with grade 1+ and grade 2+ pre-RT lymphopenia. As shown in **Figures 3A–D**, the correlation of postRT PLC to EDIC for patients with grade 1+

TABLE 1 | Patient characteristics, dosimetric factors and their predictive values on radiation induced lymphopenia (post/preRT PLC ratio).

	n (%)/Mean (95%CI)	Univariate analysis		Multivariable analysis	
		Coefficient (95%CI)	p value	Coefficient (95%CI)	p value
Age [median (range)]-year	45 (26-86)	-0.001 (-0.003, 0.001)	0.355		
Tumor side (left vs non-left)†	371(50.5%) vs 364 (49.5%)	-0.035 (-0.069, -0.001)	0.046		
Tumor stage*					
IA/IB	193 (26.2%)	0			
IIA/IIB	332 (45.2%)	-0.061 (-0.100, -0.021)	0.003		
IIIA/IIIB/IIIC	210 (28.6%)	-0.224 (-0.268, -0.181)	<0.001		
Node status (N0 vs N+)	290 (39.5%) vs 445 (60.5%)	-0.139 (-0.172, -0.105)	<0.001		
BCT vs Mastectomy	373 (50.7%) vs 362 (49.3%)	0.105 (0.071, 0.138)	<0.001		
SLNB vs ALND	265 (36.1%) vs 470 (63.9%)	0.135 (0.100, 0.170)	<0.001		
Chemotherapy (none vs yes)	69 (9.4%) vs 666 (90.6%)	0.008 (-0.051, 0.067)	0.800		
Target therapy (non vs yes)	556 (75.6%) vs 179 (24.4%)	-0.019 (-0.059, 0.022)	0.364		
Endocrine therapy (none vs yes)	186 (25.3%) vs 549 (74.7%)	-0.004 (-0.044, 0.035)	0.837		
RT technology					
RapidArc	123 (16.7%)	0		0	
2D-fields	277 (37.7%)	0.351 (0.307, 0.395)	<0.001	0.176 (0.078, 0.275)	<0.001
3DCRT	335 (45.6%)	0.268 (0.225, 0.311)	<0.001	0.146 (0.069, 0.223)	<0.001
EDIC (95% CI)—Gy	1.7 (1.6-1.8)	-0.156 (-0.177, -0.136)	<0.001	-0.106 (-0.156, -0.055)	<0.001
RT fields (breast vs breast/chestwall + regional LNs)	277 (37.7%) vs 458 (62.3%)	-0.153 (-0.187, -0.119)	<0.001		
RT Dose (40.5Gy vs 50Gy)	665 (90.5%) vs 70 (9.5%)	-0.109 (-0.167, -0.051)	<0.001	0.056 (-0.009, 0.120)	0.091
Use of breathing control (none vs yes)	721 (98.1%) vs 14 (1.9%)	-0.202 (-0.327, -0.077)	0.002		
RT fractions (15 vs 25)	665 (90.5%) vs 70 (9.5%)	-0.109 (-0.167, -0.051)	<0.001		
Mean heart dose (95% CI)—Gy	2.4 (2.2-2.5)	-0.036 (-0.044, -0.029)	<0.001		
Heart dose_Dmax (95% CI)—Gy	26.5 (25.2-27.9)	-0.001 (-0.002, -0.0001)	0.026	0.001 (0.0002, 0.002)	0.012
Mean dose of the total body (95% CI)—Gy	4.4 (4.3-4.5)	-0.069 (-0.078, -0.060)	<0.001		
V5 of bilateral lungs (95%CI)—Gy	22.3 (21.3-23.2)	-0.009 (-0.010, -0.008)	<0.001		
V20 of bilateral lungs (95%CI)—Gy	10.2 (9.9-10.5)	-0.017 (-0.021, -0.013)	<0.001		
Mean bilateral lung dose (95%CI)—Gy	5.5 (5.3-5.6)	-0.046 (-0.053, -0.040)	<0.001		

RT, radiotherapy; LN, lymph nodes; BCT, Breast conserving therapy; SLNB, Sentinel lymph node biopsy; ALND, Axillary lymph node dissection; EDIC, effective dose to the circulating immune cells); V5 (20), relative volume receiving more than 5Gy (20Gy).

†Non-left included 363 right and 1 bilateral breast cancer.

**Tumor stage was identified as the higher stage between clinical and pathological stage for patients who had received neoadjuvant chemotherapy and was identified as pathological stage for patients who had upfront surgery.*

preRT lymphopenia was the best (R^2 = 0.366, p<0.001). Therefore, for these patients with baseline lymphopenia, the postRT PLC (or potential RIL) might be approximated by linear regression of absolute postRT PLC with EDIC, and specifically be computed as PLC_{postRT} = 1.1 – 0.17 × *EDIC* (**Figure 3D**). Again, all these data (**Figures 1–3**) indicate that overall, the post-RT lymphocytes decreased with increasing EDIC. However, the decreasing models may be different for patients with different pre-RT PLC status.

RIL Normal Tissue Complication Probability (NTCP) Modelling

The NTCP versus mean EDIC based on the binned data was plotted in **Figures 4A–C** for Grade-1 and above, Grade-2 and above, and Grade-3 and above RIL respectively. The data were fitted with the NTCP model in Eq.1, with R^2 = 0.96, 0.98 and 0.98, for Grade-1, Grade-2 and Grade-3 RIL, respectively. The D50 (dose of EDIC at 50% probability of having RIL) for EDIC was 1.2 (95%CI: 1.0-1.4), 2.1 (95%CI: 2.0-2.3) and 3.7 Gy (95% CI: 3.5-3.9), and the k value was 2.4 (95%CI: 1.8-3.2), 4.0 (95%CI: 3.1-5.3), and 4.9 (95%CI: 3.8-6.5), correspondingly. **Table 2** showed the results of model fitting of using binary data of each patient without binning, and Bootstrap validation for both binned data and binary data without binning. The binary data appeared to have quite consistent mean D50 and k values as the binned data, while its 95% CIs were narrower than that of the binned data. On the other hand, the binned data showed much better fittings (R^2 Values) than that of the binary data of individual patient. The Bootstrap validation appeared to show very consistent data as the original data for both the binned data and binary data without binning.

The NTCP models for different grades of RIL could thus be expressed as:

$$NTCP = 1/\left[1+\left(\frac{1.2}{EDIC}\right)^{2.4}\right] \quad \text{for Grade} - 1 \text{ and above RIL (4a)}$$

$$NTCP = 1/\left[1+\left(\frac{2.1}{EDIC}\right)^{4.0}\right] \quad \text{for Grade} - 2 \text{ and above RIL (4b)}$$

$$NTCP = 1/\left[1+\left(\frac{3.7}{EDIC}\right)^{4.9}\right] \quad \text{for Grade} - 3 \text{ and above RIL (4c)}$$

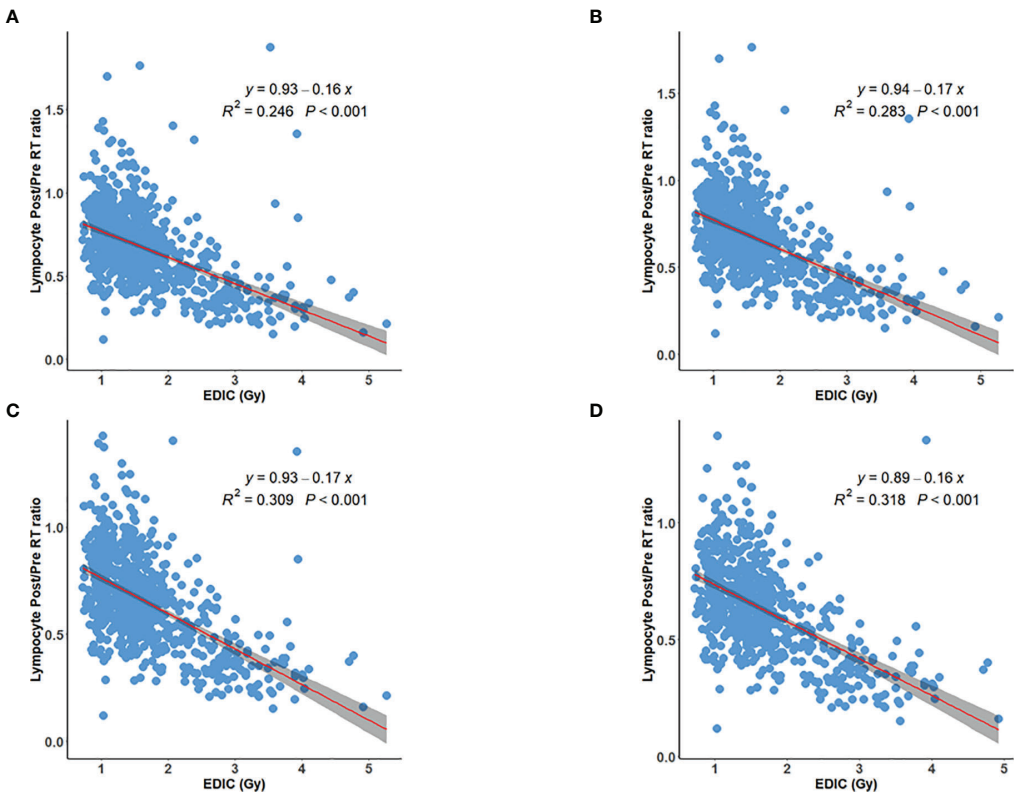

FIGURE 1 | Inverse linear relation between post/preRT PLC Ratio and EDIC for **(A)** all 735 patients; **(B)** 732 patients excluding 3 patients with grade 3 preRT lymphopenia; **(C)** 714 patients excluding additional 18 patients with grade 2 preRT lymphopenia; **(D)** 630 patients excluding additional 84 patients with grade 1 preRT lymphopenia.

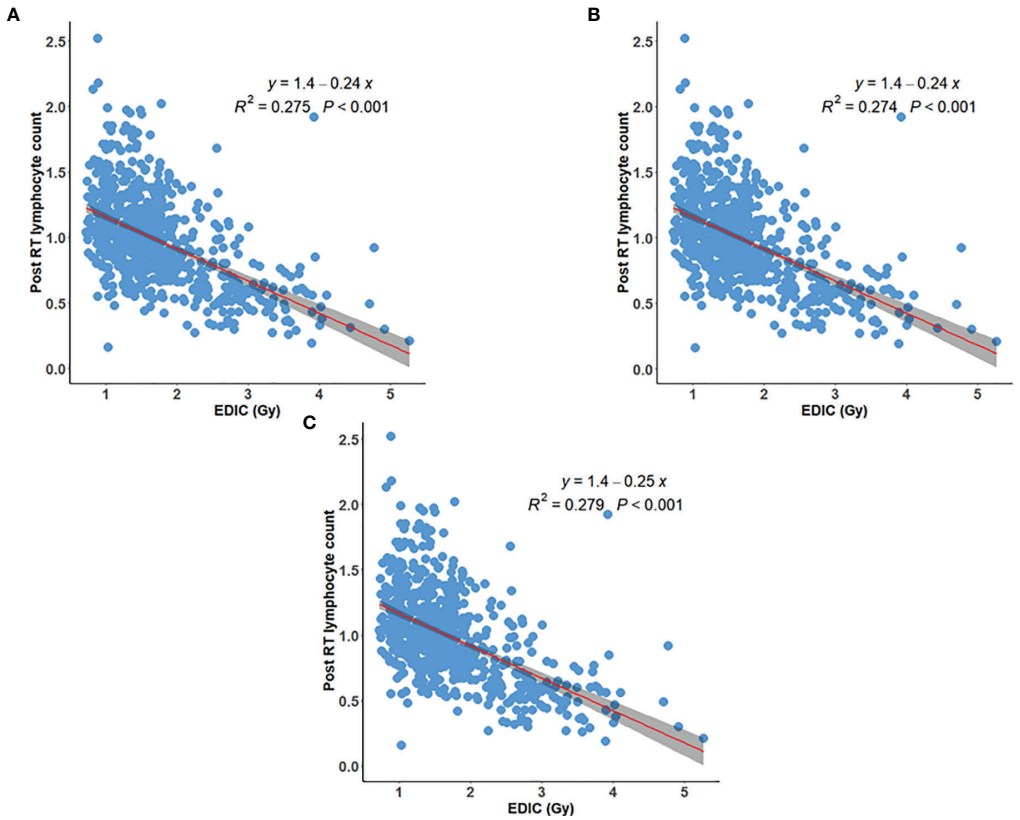

FIGURE 2 | Inverse linear relationship between EDIC and postRT peripheral lymphocyte counts (PLC) for **(A)** all 735 patients; **(B)** 732 patients excluding 3 patients with grade 3 preRT lymphopenia; **(C)** 714 patients excluding additional 18 patients with grade-2 preRT lymphopenia.

DISCUSSION

This study of 735 patients at the first time in breast cancer demonstrated a significant correlation between EDIC and RIL, and that both post/preRT PLC ratio and postRT PLC decreased linearly (R^2<0.4) with increasing EDIC. The post/preRT PLC ratio had a better correlation with EDIC in patients with normal preRT PLC, and the postRT PLC appeared to have a better correlation with EDIC in patients with preRT lymphopenia. Comparing to the numerical correlation by the linear regression, EDIC fitted better into the sigmoid-shaped NTCP model for RIL (R^2>0.96). The EDIC value of 50% incidence of grade-1 RIL was 1.2 Gy, the corresponding EDIC to reach 50% of grade-2 and grade-3 RIL was 2.1 and 3.7 Gy, respectively.

The significance of EDIC for RIL in breast radiation makes biological sense and is supported by radiation physics rationales. Lymphocytes are produced in bone marrow and thymus, and then travel through blood circulation into various functional sites. Radiation can directly kill circulating immune cells as they pass through the irradiated field. EDIC is the estimation of equivalent dose to the circulating immune cells in blood contributed by the irradiation of the blood-containing organs in thoracic radiation according to the mean dose to these organs (such as MLD, MHD and ITDV). In addition, the radiation dose fractionation effect is also considered in the EDIC model (25). EDIC has been reported to be associated with RIL in other thoracic malignancies such as lung and esophageal cancers (15, 25–27). As a type of thoracic cancers, breast cancer is similar to the NSCLC and esophageal cancer in terms of that its main irradiated blood-containing organs are lung and heart. Therefore, the EDIC model may be also applicable in breast cancer. However, the irradiation pattern or dose distribution in these organs may be quite different for breast cancer in comparison to that of the NSCLC and esophageal cancer. The irradiated lung and heart volumes in breast cancer are usually much smaller. According to the EDIC model derivation (25), the contribution of a blood-containing organ (such as lung) to EDIC is approximately expressed as B%*Mean Organ Dose (MOD) when A% is larger than 20% and fraction number is larger than 20, where MOD is the mean organ dose, A% is the percentage blood-current that flow into the organ, B% is the percentage blood-volume that present within the organ. This expression was derived based on the assumption that the blood flow through the organs in a serial pattern, and should be applicable for any blood-containing organs with any non-uniform dose distributions. The lung is composed of 5 lobes and each lobe may be approximately considered as having a serial blood-flow pattern with A%=20%. From the physics model perspective, the EDIC model can be

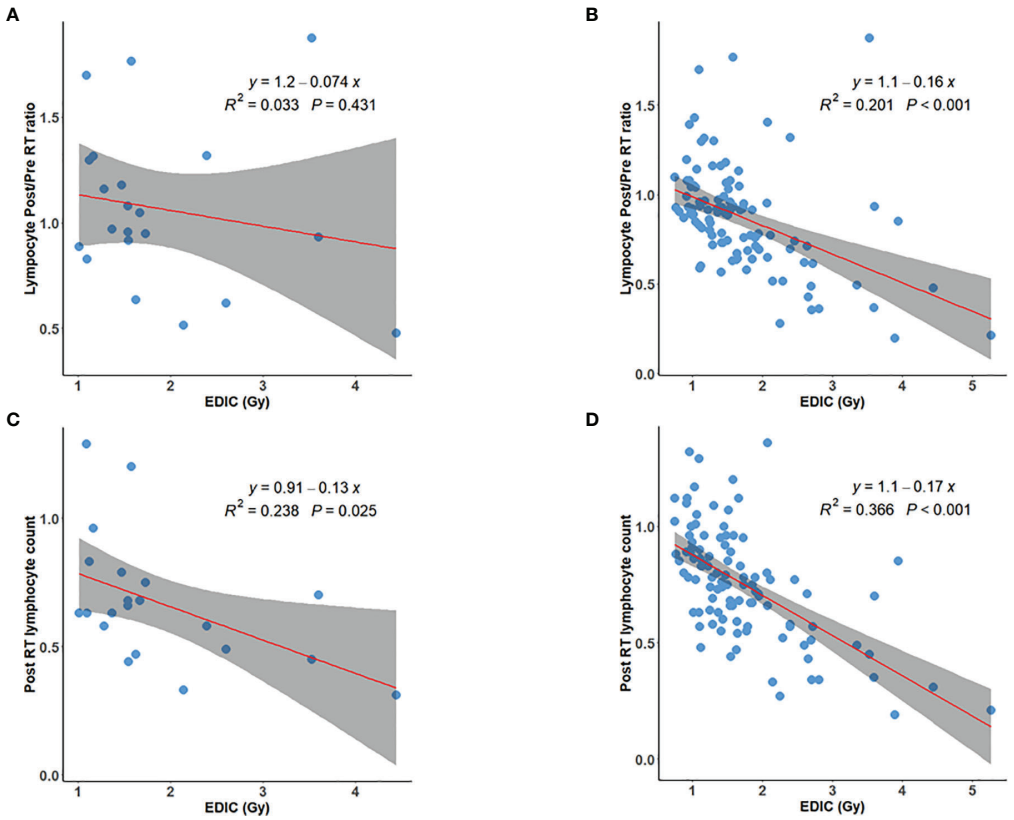

FIGURE 3 | Post/preRT PLC ratio versus EDIC for **(A)** 21 patients with grade-2+ preRT lymphopenia; **(B)** 105 patients with grade-1+ preRT lymphopenia; PostRT PLC versus EDIC for **(C)** 21 patients with grade-2+ preRT lymphopenia; and **(D)** 105 patients with grade-1+ preRT lymphopenia.

applied in breast cancer radiation. Indeed, significance of EDIC on both postRT PLC and RIL of this study support the validity of this model in breast cancer.

It is interesting to note that when a patient had a normal preRT PLC, the post/preRT PLC ratio had better correlation with EDIC. This is consistent with the theory that when the preRT PLC is normal, the killing of circulation lymphocytes in blood by radiation plays the most important role in the reduction of PLC. However, 14.3% patients had preRT lymphopenia in this study, which was reported to be related with prior chemotherapy in our

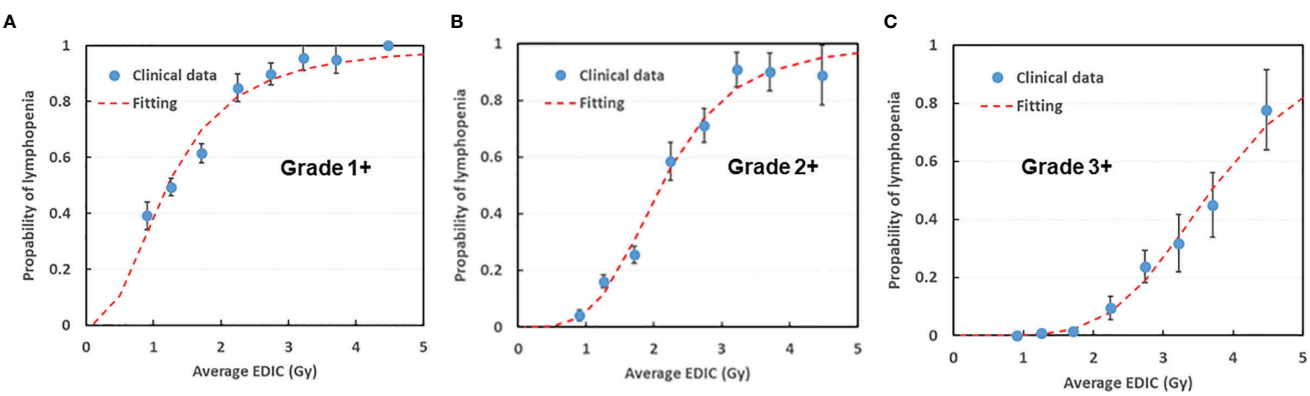

FIGURE 4 | EDIC NTCP model for **(A)** Grade 1+, **(B)** Grade 2+ and **(C)** Grade 3+ postRT lymphopenia. Patients were divided into 8 groups with a 0.5 Gy increment in each group (<1, 1-1.5, 1.5-2, 2-2.5, 2.5-3, 3-3.5, 3.5-4, >4.5). NTCP, Normal Tissue Complication Probability. EDIC, Effective Dose to the circulating Immune Cells.

TABLE 2 | Parameters in NTCP modeling.

			Grade 1+	Grade 2+	Grade 3+
Binned data	Crude	D50 (Gy)	1.2 (95%CI: 1.0-1.4)	2.1 (95%CI: 2.0-2.3)	3.7 (95%CI: 3.5-3.9)
		k	2.4 (95%CI: 1.8-3.2)	4.0 (95%CI: 3.1-5.3)	4.9 (95%CI: 3.8-6.5)
		R^2	0.96	0.98	0.98
	Bootstrap validation	D50 (Gy)	1.2 (95%CI: 1.1-1.3)	2.1 (95%CI: 2.0-2.2)	3.7 (95%CI: 3.3-4.4)
		k	2.4 (95%CI: 2.0-2.9)	4.0 (95%CI: 2.6-4.9)	5.5 (95%CI: 2.6-9.0)
		R^2	0.93	0.96	0.94
Binary data without binning	Crude	D50 (Gy)	1.2 (95%CI: 1.1-1.3)	2.2 (95%CI: 2.1-2.3)	3.7 (95%CI: 3.6-4.0)
		k	2.1 (95%CI: 1.6-2.6)	3.9 (95%CI: 3.2-4.7)	4.4 (95%CI: 3.7-5.3)
		R^2	0.13	0.3	0.27
	Bootstrap validation	D50 (Gy)	1.2 (95%CI: 1.1-1.4)	2.2 (95%CI: 2.0-2.3)	3.7 (95%CI: 3.4-4.4)
		k	2.1 (95%CI: 1.7-2.5)	3.9 (95%CI: 3.2-4.8)	4.4 (95%CI: 3.4-5.9)
		R^2	0.12	0.3	0.27

another study of 1012 patients with early or locally advanced breast cancer (28). Therefore, we also explored the relationship of EDIC and lymphopenia in this population. When a patient had preRT lymphopenia, the absolute postRT PLC was better associated with EDIC. This is consistent with previous report that when the preRT PLC is low, the regeneration of new lymphocytes from other parts of lymphatic system begins to play a role (12). This regeneration of new lymphocytes weakens the association between EDIC and post/preRT PLC ratio. The lower the preRT PLC, the larger the deviation from the correlation of EDIC and post/preRT PLC ratio. For 3 patients with grade-3 preRT lymphopenia, 2 of them were outliers, while 3 over 18 patients were outliers for grade-2 preRT lymphopenia, and 2 over 84 patients were outliers for grade-1 preRT lymphopenia in this study.

It is important to note that this study also provided a NTCP model of RIL based solely on EDIC. The NTCP model of each grade of lymphopenia fits well with the sigmoid-curved dose toxicity relationship, using EDIC for both binned data or binary data for each patient without binning. These two approaches achieved quite consistent results, and bootstrap validation also confirmed the similar results. These data suggest that EDIC is likely a true key dosimetric parameter, or at least a good surrogate of the true dosimetric parameter that directly impacts the RIL. EDIC might be used as a reference for clinician in dose prescription and treatment planning. With the guide of this EDIC model in lymphopenia, we may improve our treatment to limit RIL. For example, adjustment of beam energies, directions and number of beams may be able to reduce EDIC and hence limit RIL. In addition, according to the EDIC derivation (25), reducing the radiation fraction number n may also reduce EDIC through the term of $(n/45)^{1/2}$, which is contributed by blood-containing organs with a relatively small A% (such as A% <25%). Thus, hypofractionated treatments such as stereotactic body radiation therapy (SBRT) may reduce EDIC. Indeed, SBRT was reported to be associated with significantly less RIL than conventionally fractionated RT in locally advanced pancreatic cancer and breast cancer (18, 29, 30). Hypofractionated radiation in this study was also found to have less risk of RIL (**Table 1**).

This is the first study to validate the association of EDIC and RIL in patients with breast cancer. However, it should be noted that several other dosimetric factors were also reported to be significantly associated with RIL. These factors include lung V5 and heart V50 in lung cancer, brain V25 in glioma, and mean whole body dose in esophageal cancer (9, 12, 13, 31–33). In our prior study, lung V5 and volume modulated arc therapy rather than three-dimensional conformal technique were also risk factors for severe RIL (16). Although EDIC is a combination of several dosimetric parameters, it may not be the best model. A more comprehensive model with an optimal combination of other dosimetric parameters (such as lung V5) and likely including immune organs like bone marrow and thymus may turn out to be a better predictor than the EDIC. Adding other clinical factors may further improve the prediction of RIL in breast cancer. Further study is needed to determine these parameters and the best combination of them for better prediction. From a theoretic view point, EDIC is just an approximation of the dose to the immune cells in the circulating blood. The dose to the lymphatic stations, bone marrow and other lymphatic structures may also affect RIL. The regeneration of new lymphocytes may complicate the prediction. It should also be noted that the survival of this study is not mature yet. Future studies will be performed to explore the association of EDIC and other dosimetric parameters with the long-term treatment outcomes of patients.

CONCLUSIONS

This study demonstrated that EDIC was significantly associated with radiation induced lymphopenia (RIL) in breast cancer. Using EDIC as the dose variable, the risk of RIL can be predicted nicely by a conventional NTCP model. The corresponding EDIC to induce 50% of grade-1, grade-2 and grade-3 RIL was 1.2, 2.1 and 3.7 Gy, respectively. Should it be validated by external datasets, these number may be used as reference to guide radiation plan optimization and improve survivals for patients.

DATA AVAILABILITY STATEMENT

The raw data supporting the conclusions of this article will be made available by the authors, without undue reservation.

ETHICS STATEMENT

The studies involving human participants were reviewed and approved by the University of Hong Kong-Shenzhen Hospital (# 2019 098). Written informed consent for participation was not required for this study in accordance with the national legislation and the institutional requirements.

AUTHOR CONTRIBUTIONS

FC: primary investigator: overall study hypothesis, study design, data collection, data analysis, result interpretation, manuscript writing and final manuscript approval; J-YJ and TH: study design, physics modeling, data analysis, manuscript writing and final manuscript approval; HZ, LM, and PF: various parts of statistical analysis, results interpretation and final manuscript approval; YH, FY, QC, YZ: clinic data collection and final manuscript approval; YN: radiation dosimetric factors collection and final manuscript approval; HJ, WW, LY, and ZX: results interpretation and final manuscript approval; F-MK: study idea, study hypothesis/design, data quality control, data analysis, result interpretation, detailed manuscript preparation and final manuscript approval. All authors contributed to the article and approved the submitted version.

FUNDING

This project was partially supported by Shenzhen Key Medical Discipline Construction Fund (No. SZXK014), Shenzhen Science and Technology program (Grant No: KQTD20180411185028798), Health Commission of Guangdong Province, China (A2021114) and a Varian Medical System research grant.

SUPPLEMENTARY MATERIAL

The Supplementary Material for this article can be found online at: https://www.frontiersin.org/articles/10.3389/fonc.2022.768956/full#supplementary-material

Supplementary Figure 1 | Study population profile. As shown, a total of 735 patients with breast cancer were enrolled in this study.

REFERENCES

1. Afghahi A, Purington N, Han SS, Desai M, Pierson E, Mathur MB, et al. Higher Absolute Lymphocyte Counts Predict Lower Mortality From Early-Stage Triple-Negative Breast Cancer. *Clin Cancer Res* (2018) 24(12):2851–8. doi: 10.1158/1078-0432.CCR-17-1323
2. De Giorgi U, Mego M, Scarpi E, Giuliano M, Giordano A, Reuben JM, et al. Relationship Between Lymphocytopenia and Circulating Tumor Cells as Prognostic Factors for Overall Survival in Metastatic Breast Cancer. *Clin Breast Cancer* (2012) 12(4):264–9. doi: 10.1016/j.clbc.2012.04.004
3. Saroha S, Uzzo RG, Plimack ER, Ruth K, Al-Saleem T. Lymphopenia Is an Independent Predictor of Inferior Outcome in Clear Cell Renal Carcinoma. *J Urol* (2013) 189(2):454–61. doi: 10.1016/j.juro.2012.09.166
4. Ceze N, Thibault G, Goujon G, Viguier J, Watier H, Dorval E, et al. Pre-Treatment Lymphopenia as a Prognostic Biomarker in Colorectal Cancer Patients Receiving Chemotherapy. *Cancer Chemother Pharmacol* (2011) 68(5):1305–13. doi: 10.1007/s00280-011-1610-3
5. Nakamura N, Kusunoki Y, Akiyama M. Radiosensitivity of CD4 or CD8 Positive Human T-Lymphocytes by an *In Vitro* Colony Formation Assay. *Radiat Res* (1990) 123(2):224–7. doi: 10.2307/3577549
6. Hall EJ, Giaccia AJ. *Radiobiology for the Radiologist* Vol. 6. Lippincott Williams & Wilkins (2006).
7. Sellins KS, Cohen JJ. Gene Induction by Gamma-Irradiation Leads to DNA Fragmentation in Lymphocytes. *J Immunol* (1987) 139(10):3199–206.
8. Mehrazin R, Uzzo RG, Kutikov A, Ruth K, Tomaszewski JJ, Dulaimi E, et al. Lymphopenia Is an Independent Predictor of Inferior Outcome in Papillary Renal Cell Carcinoma. *Urol Oncol* (2015) 33(9):388.e19–25. doi: 10.1016/j.urolonc.2014.06.004
9. Davuluri R, Jiang W, Fang P, Xu C, Komaki R, Gomez DR, et al. Lymphocyte Nadir and Esophageal Cancer Survival Outcomes After Chemoradiation Therapy. *Int J Radiat Oncol Biol Phys* (2017) 99(1):128–35. doi: 10.1016/j.ijrobp.2017.05.037
10. Liu L-T, Chen Q-Y, Tang L-Q, Guo S-S, Guo L, Mo H-Y, et al. The Prognostic Value of Treatment-Related Lymphopenia in Nasopharyngeal Carcinoma Patients. *Cancer Res Treat* (2018) 50(1):19. doi: 10.4143/crt.2016.595
11. Wild AT, Ye X, Ellsworth SG, Smith JA, Narang AK, Garg T, et al. The Association Between Chemoradiation-Related Lymphopenia and Clinical Outcomes in Patients With Locally Advanced Pancreatic Adenocarcinoma. *Am J Clin Oncol* (2015) 38(3):259. doi: 10.1097/COC.0b013e3182940ff9
12. Tang C, Liao Z, Gomez D, Levy L, Zhuang Y, Gebremichael RA, et al. Lymphopenia Association With Gross Tumor Volume and Lung V5 and Its Effects on Non-Small Cell Lung Cancer Patient Outcomes. *Int J Radiat Oncol Biol Phys* (2014) 89(5):1084–91. doi: 10.1016/j.ijrobp.2014.04.025
13. Yovino S, Kleinberg L, Grossman SA, Narayanan M, Ford E. The Etiology of Treatment-Related Lymphopenia in Patients With Malignant Gliomas: Modeling Radiation Dose to Circulating Lymphocytes Explains Clinical Observations and Suggests Methods of Modifying the Impact of Radiation on Immune Cells. *Cancer Invest* (2013) 31(2):140–4. doi: 10.3109/07357907.2012.762780
14. Lissoni P, Meregalli S, Bonetto E, Mancuso M, Brivio F, Colciago M, et al. Radiotherapy-Induced Lymphocytopenia: Changes in Total Lymphocyte Count and in Lymphocyte Subpopulations Under Pelvic Irradiation in Gynecologic Neoplasms. *J Biol Regulators Homeostatic Agents* (2005) 19(3-4):153–8.
15. So TH, Chan SK, Chan WL, Choi H, Chiang CL, Lee V, et al. Lymphopenia and Radiation Dose to Circulating Lymphocyte With Neoadjuvant Chemoradiation in Esophageal Squamous Cell Carcinoma. *Adv Radiat Oncol* (2020) 5(5):880–8. doi: 10.1016/j.adro.2020.03.021
16. Chen F, Yu H, Zhang H, Nong Y, Wang Q, Jing H, et al. Risk Factors for Radiation Induced Lymphopenia in Patients With Breast Cancer Receiving Adjuvant Radiotherapy. *Ann Trans Med* (2021) 9(16):1288. doi: 10.21037/atm-21-2150
17. Cho O, Chun M, Kim SW, Jung YS, Yim H. Lymphopenia as a Potential Predictor of Ipsilateral Breast Tumor Recurrence in Early Breast Cancer. *Anticancer Res* (2019) 39(8):4467–74. doi: 10.21873/anticanres.13620
18. Sun G-Y, Wang S-L, Song Y-W, Jin J, Wang W-H, Liu Y-P, et al. Radiation-Induced Lymphopenia Predicts Poorer Prognosis in Patients With Breast Cancer: A *Post-Hoc* Analysis of a Randomized Controlled Trial of Postmastectomy Hypofractionated Radiotherapy. *Int J Radiat Oncol Biol Phys* (2020) 108(1):277–85. doi: 10.1016/j.ijrobp.2020.02.633
19. Schmid P, Adams S, Rugo HS, Schneeweiss A, Barrios CH, Iwata H, et al. Atezolizumab and Nab-Paclitaxel in Advanced Triple-Negative Breast Cancer. *N Engl J Med* (2018) 379(22):2108–21. doi: 10.1056/NEJMoa1809615
20. Schmid P, Cortes J, Pusztai L, McArthur H, Kümmel S, Bergh J, et al. Pembrolizumab for Early Triple-Negative Breast Cancer. *N Engl J Med* (2020) 382(9):810–21. doi: 10.1056/NEJMoa1910549

21. Diehl A, Yarchoan M, Hopkins A, Jaffee E, Grossman SA. Relationships Between Lymphocyte Counts and Treatment-Related Toxicities and Clinical Responses in Patients With Solid Tumors Treated With PD-1 Checkpoint Inhibitors. *Oncotarget* (2017) 8(69):114268. doi: 10.18632/oncotarget.23217
22. Jin J-Y, Mereniuk T, Yalamanchali A, Wang W, Machtay M, Ellsworth S. A Framework for Modeling Radiation Induced Lymphopenia in Radiotherapy. *Radiother Oncol* (2020) 144:105–13. doi: 10.1016/j.radonc.2019.11.014
23. Meyer KK. Radiation-Induced Lymphocyte-Immune Deficiency: A Factor in the Increased Visceral Metastases and Decreased Hormonal Responsiveness of Breast Cancer. *Arch Surg* (1970) 101(2):114–21. doi: 10.1001/archsurg.1970.01340260018003
24. Maclennan I, Kay H. Analysis of Treatment in Childhood Leukemia. IV. The Critical Association Between Dose Fractionation and Immunosuppression Induced by Cranial Irradiation. *Cancer* (1978) 41(1):108–11. doi: 10.1002/1097-0142(197801)41:1<108::AID-CNCR2820410116>3.0.CO;2-Z
25. Jin J-Y, Hu C, Xiao Y, Zhang H, Paulus R, Ellsworth SG, et al. Higher Radiation Dose to the Immune Cells Correlates With Worse Tumor Control and Overall Survival in Patients With Stage III NSCLC: A Secondary Analysis of RTOG0617. *Cancers* (2021) 13(24):6193. doi: 10.3390/cancers13246193
26. Ladbury CJ, Rusthoven CG, Camidge DR, Kavanagh BD, Nath SK. Impact of Radiation Dose to the Host Immune System on Tumor Control and Survival for Stage III Non-Small Cell Lung Cancer Treated With Definitive Radiation Therapy. *Int J Radiat Oncol Biol Phys* (2019) 105(2):346–55. doi: 10.1016/j.ijrobp.2019.05.064
27. Xu C, Jin J-Y, Zhang M, Liu A, Wang J, Mohan R, et al. The Impact of the Effective Dose to Immune Cells on Lymphopenia and Survival of Esophageal Cancer After Chemoradiotherapy. *Radiother Oncol* (2020) 146:180–6. doi: 10.1016/j.radonc.2020.02.015
28. Chen F, Ma L, Wang Q, Zhou M, Nong Y, Jing H, et al. Chemotherapy Is a Risk Factor of Lymphopenia Before Adjuvant Radiotherapy in Breast Cancer. *Cancer Rep (Hoboken)* (2021), e1525. doi: 10.1002/cnr2.1525
29. Crocenzi T, Cottam B, Newell P, Wolf RF, Hansen PD, Hammill C, et al. A Hypofractionated Radiation Regimen Avoids the Lymphopenia Associated With Neoadjuvant Chemoradiation Therapy of Borderline Resectable and Locally Advanced Pancreatic Adenocarcinoma. *J Immunother Cancer* (2016) 4(1):1–13. doi: 10.1186/s40425-016-0149-6
30. Yuan C, Wang Q. Comparative Analysis of the Effect of Different Radiotherapy Regimes on Lymphocyte and Its Subpopulations in Breast Cancer Patients. *Clin Trans Oncol* (2018) 20(9):1219–25. doi: 10.1007/s12094-018-1851-2
31. Contreras JA, Lin AJ, Weiner A, Speirs C, Samson P, Mullen D, et al. Cardiac Dose Is Associated With Immunosuppression and Poor Survival in Locally Advanced Non-Small Cell Lung Cancer. *Radiother Oncol* (2018) 128(3):498–504. doi: 10.1016/j.radonc.2018.05.017
32. Huang J, DeWees TA, Badiyan SN, Speirs CK, Mullen DF, Fergus S, et al. Clinical and Dosimetric Predictors of Acute Severe Lymphopenia During Radiation Therapy and Concurrent Temozolomide for High-Grade Glioma. *Int J Radiat Oncol Biol Phys* (2015) 92(5):1000–7. doi: 10.1016/j.ijrobp.2015.04.005
33. Saito T, Toya R, Matsuyama T, Semba A, Oya N. Dosimetric Predictors of Treatment-Related Lymphopenia Induced by Palliative Radiotherapy: Predictive Ability of Dose-Volume Parameters Based on Body Surface Contour. *Radiol Oncol* (2017) 51(2):228–34. doi: 10.1515/raon-2016-0050

Conflict of Interest: The authors declare that the research was conducted in the absence of any commercial or financial relationships that could be construed as a potential conflict of interest.

Publisher's Note: All claims expressed in this article are solely those of the authors and do not necessarily represent those of their affiliated organizations, or those of the publisher, the editors and the reviewers. Any product that may be evaluated in this article, or claim that may be made by its manufacturer, is not guaranteed or endorsed by the publisher.

frontiers | Frontiers in Oncology

TYPE Original Research
PUBLISHED 15 September 2022
DOI 10.3389/fonc.2022.905222

OPEN ACCESS

EDITED BY
Kathy Han,
University Health Network, Canada

REVIEWED BY
Hong Qi Tan,
National Cancer Centre Singapore, Singapore
Anthony Magliocco,
Protean BioDiagnostics Inc., United States

*CORRESPONDENCE
Linlang Guo
linlangg@yahoo.com
Hao Yu
yuhao_zju@163.com

†These authors have contributed equally to this work and share first authorship

SPECIALTY SECTION
This article was submitted to Radiation Oncology, a section of the journal Frontiers in Oncology

RECEIVED 26 March 2022
ACCEPTED 22 August 2022
PUBLISHED 15 September 2022

CITATION
Xu Z, Yang L, Yu H and Guo L (2022) A machine learning model for grade 4 lymphopenia prediction during pelvic radiotherapy in patients with cervical cancer.
Front. Oncol. 12:905222.
doi: 10.3389/fonc.2022.905222

A machine learning model for grade 4 lymphopenia prediction during pelvic radiotherapy in patients with cervical cancer

Zhiyuan Xu[1,2†], Li Yang[1,2†], Hao Yu[3*] and Linlang Guo[4*]

[1]Clinical Oncology Center, The University of Hong Kong - Shenzhen Hospital, Shenzhen, China, [2]Shenzhen Key Laboratory of Translational Research on Recurrent/Metastatic Cancer, The University of Hong Kong - Shenzhen Hospital, Shenzhen, China, [3]Shenzhen Institute of Advanced Technology, Chinese Academy of Sciences, Shenzhen, China, [4]Department of Pathology, Zhujiang Hospital, Southern Medical University, Guangzhou, China

Background/purpose: Severe lymphopenia during pelvic radiotherapy (RT) predicts poor survival in patients with cervical cancer. However, the risk of severe lymphopenia has not been well predicted. We developed a machine learning model using clinical and dosimetric information to predict grade 4 (G4) lymphopenia during pelvic RT in patients with cervical cancer.

Methods: This retrospective study included cervical cancer patients treated with definitive pelvic RT ± induction/concurrent chemotherapy. Clinical information and a set of dosimetric parameters of external beam radiotherapy plan were collected. G4 lymphopenia during RT, which was also referred to as G4 absolute lymphocyte count (ALC) nadir, was defined as ALC nadir $<0.2 \times 10^9$ cells/L during RT according to Common Terminology Criteria for Adverse Events (CTCAE) v4.03. Elastic-net logistic regression models were constructed for the prediction of G4 lymphopenia during pelvic RT using a repeated cross-validation methodology.

Results: A total of 130 patients were eligible, and 43 (33.1%) patients had G4 lymphopenia during RT. On multivariable analysis, G4 ALC nadir was associated with poor overall survival (OS) [hazard ratio (HR), 3.91; 95% confidence interval (CI), 1.34–11.38, p = 0.01]. Seven significant factors [Eastern Cooperative Oncology Group (ECOG) performance score, pre-RT hemoglobin, pre-RT lymphocytes, concurrent chemotherapy, gross tumor volume of regional lymphadenopathy (GTV_N volume), body volume, and maximum dose of planning target volume receiving at least 55 Gy (PTV_5500 Dmax)] were obtained by elastic-net logistic regression models and were included in the final prediction model for G4 ALC nadir. The model's predicting ability in test set was area under the curve (AUC) = 0.77 and accuracy = 0.76. A nomogram of the final predicting model was constructed.

Conclusions: This study developed and validated a comprehensive model integrating clinical and dosimetric parameters by machine learning method, which performed well in predicting G4 lymphopenia during pelvic RT for

cervical cancer and will facilitate physicians to identify patients at high risk of G4 lymphopenia who might benefit from modified treatment approaches.

KEYWORDS

cervical cancer, machine learning model, lymphopenia, prediction, pelvic radiotherapy

1. Introduction

Cervical cancer is the fourth most frequently diagnosed cancer and the fourth leading cause of cancer death in women (1). Pelvic radiotherapy (RT) plays an integral part in the treatment of locally advanced cervical cancer (2), but it can also result in toxicities, including effects on host immunity. A higher radiation dose to immune cells was reported to be associated with poor treatment outcomes in patients with non-small cell lung cancer (NSCLC) (3). Lymphocytes, one of the most important components of the immune system, are especially critical in mediating cellular immunity against malignant tumor cells. In cervical cancer patients treated with concurrent chemoradiotherapy (CCRT), the incidence of grade 3 (G3) and grade 4 (G4) lymphopenia during CCRT, graded by Common Terminology Criteria for Adverse Events (CTCAE), reached as high as 73% and 16%, respectively, and G4 lymphopenia was associated with poor survival (4). Although it has clinical significance, the risk of G4 lymphopenia has not been well predicted in cervical cancer patients.

Many factors were reported to be associated with lymphopenia during RT. Radiation *per se* is among the most important risk factors for lymphopenia because lymphocytes continuously traverse the irradiated field and are extremely sensitive to radiation (5). The modeled RT dose to peripheral lymphocytes were associated with lymphopenia in patients treated with RT (6). Radiation field size, dose per fraction, and fraction number are all correlated with risk of lymphopenia (7). Dose–volume parameter (volume receiving at least 40 Gy) of the pelvic bone marrow was associated with a higher risk of acute G3 [odds ratio (OR)=1.018] or late grade 2 (G2) lymphopenia (OR=1.005) in prostate cancer patients treated with RT (8). The RT dose to the large blood vessels, bone, and whole body were also correlated with lymphopenia (6). Besides these dose–volume parameters, our previous study demonstrated that the International Federation of Gynecology and Obstetrics (FIGO) stage, pre-treatment lymphocyte, and pre-treatment hemoglobin were significantly associated with lymphopenia during CCRT in cervical cancer patients. Other studies showed that baseline lymphocyte had an important role in predicting lymphopenia during RT (8, 9). Integrating both dosimetric and clinical information might improve the prediction performance for lymphopenia.

Machine learning (ML), one of the most relevant subsets of artificial intelligence (AI) in medicine, mainly focuses on making as accurate predictions as possible. Compared with traditional statistical methods, ML could be more suited in highly innovative fields with a huge bulk of data (10). By using deep ML method to integrate dosimetric and clinical information, Cong Zhu et al. (9) developed a model to predict G4 RT-induced lymphopenia in patients with esophageal carcinoma with area under the curve (AUC) at 0.831, accuracy at 0.769, and precision at 0.670.

At present, ML method has not been widely applied in the prediction of G4 lymphopenia during pelvic RT for cervical cancer. By integrating both clinical factors and a set of dosimetric parameters, this study aimed to build an ML model to predict G4 lymphopenia during pelvic RT in patients with cervical cancer, with the hope to aid the physician's decision-making process in clinical practice.

2. Materials and methods

2.1 Patients

This study was approved by the institutional ethics committee of the University of Hong Kong-Shenzhen Hospital [No (2022).020], and informed consent form from each patient for this study was waived. A cohort of patients diagnosed with cervical carcinoma from January 2015 to February 2021 in the University of Hong Kong-Shenzhen Hospital was selected for this study. Patients were included if they met the following criteria: 1) ≥18 years old; 2) newly diagnosed, pathology-confirmed cervical carcinoma; 3) FIGO stage (2018) IB-IVB (only stage IVB with oligo-metastases scheduled for radical pelvic RT were included); 4) major treatment was external beam radiotherapy (EBRT) followed by brachytherapy (BT) or stereotactic body radiotherapy (SBRT, if BT was contraindicated or declined) with or without induction or concurrent chemotherapy; and (5) complete blood counts (CBCs) were tested before and weekly during RT. Patients were excluded if

they had the following: 1) cervical small cell carcinoma; 2) concomitant secondary primary malignant tumor; 3) acquired immune deficiency syndrome (AIDS); 4) pelvic RT in recurrent or adjuvant settings; and 5) did not complete planned EBRT.

2.2 Radiation therapy

All patients received pelvic EBRT followed by BT or SBRT. The simulation computed tomography (CT) scans for EBRT were taken with 3-mm slices from the interspace between thoracic vertebra 9 and 10 to the upper one-third of the femur. EBRT techniques were RapidArc or three-dimensional conformal radiotherapy (3D-CRT). For RapidArc, gross tumor volume (GTV) of the primary tumor (P) and regional pathological lymph nodes (N) detected by physical examination, simulation CT, pelvis magnetic resonance imaging (MRI), or positron emission tomography (PET)/CT were denoted as GTV_P and GTV_N, respectively. CTV_4500 [clinical target volume (CTV) receiving prescribed dose of ≥45Gy], including cervix, bilateral parametrium, uterus, part of vagina, and pelvic lymphatics; CTV_5500 (CTV receiving prescribed dose of ≥55 Gy), pelvic GTV_N + 3 mm margin; CTV_5750 (CTV receiving prescribed dose of ≥57.5 Gy), retroperitoneal GTV_N + 3 mm margin; PTV_4500, PTV_5500, and PTV_5750 [planning target volume (PTV) receiving prescribed doses of ≥45, ≥55, and ≥57.5 Gy], CTV_4500, CTV_5500, and CTV_5750 + 5 mm margin, respectively. Prescription dose was delivered as 45 Gy in 25 fractions (45 Gy/25 Fr) to PTV_4500 with a simultaneous integrated boost (SIB) of 55 Gy to PTV_5500 or 57.5 Gy to PTV_5750. For 3D-CRT, two sequential phases were adopted: 45 Gy/25 Fr to whole pelvis as phase I; boosting to pelvic wall with 16 Gy/8 Fr for FIGO IIIB or 10 Gy/5 Fr for other stages as phase II. All EBRT was delivered daily, five fractions per week. CT- or MRI-guided BT was started 3–4 weeks after the initiation of EBRT with ^{192}Ir (iridium) high-dose rate, once a week for a total of 4 weeks. Cumulative equivalent doses in 2 Gy/Fr (EQD2) of > 84 Gy for stage IB–IIIA and >90 Gy for ≥ stage IIIB were set to cervical primary tumor.

2.3 Chemotherapy

Concurrent cisplatin (40 mg/m^2) was given weekly during EBRT for up to 5–6 weeks. If creatinine clearance ≤50 ml/min, carboplatin at the dose of AUC = 2 mg/ml/min was given weekly as an alternative. Induction chemotherapy (IC) with paclitaxel and carboplatin was given if anticipated RT waiting time exceeded about 3 weeks. For patients aged over 70 or with FIGO stage IB1, no chemotherapy was recommended.

2.4 End points and dose–volume histogram metrics

Absolute lymphocyte count (ALC) was measured as $\times 10^9$ cells/L and graded by CTCAE v4.03. G4 lymphopenia during RT, which was also referred to as G4 ALC nadir, was defined as ALC nadir < 0.2×10^9 cells/L during RT. Progression-free survival (PFS) was the time between the initiation of RT and the date of disease progression or death from any cause. Overall survival (OS) was the time between the initiation of RT and the date of death from any cause. Dose–volume histogram (DVH) metrics of both tumor targets and organs at risk (OARs) during EBRT were extracted directly from the Varian eclipse treatment planning system (version15.0, External Beam Planning, Varian) with anisotropic analytical algorithm. The tumor targets of interest included GTV_P, GTV_N, CTV_4500, PTV_4500, and PTV_5500. The OARs of interest included body (defined as the part of body within the range of simulation CT scan for EBRT) and bones (defined as bones within 2 cm beyond PTV). For each structure, the whole volume [in cubic centimeter (cc)], maximum dose (Dmax, in Gy), mean dose (Dmean, in Gy), and the percentage of the whole volume receiving ≥5, ≥10, ≥20, ≥30, ≥40, and ≥45 Gy (denoted as V5, V10, V20, V30, V40, and V45, respectively) were extracted.

2.5 Univariate and multivariable analysis

For the outcomes of OS and PFS, G4 ALC nadir and all clinical characteristics were analyzed by the univariate and multivariable Cox proportional hazards regression (cox-PH) models. Kaplan–Meier product-limit estimates with time-to-event curves were generated. To classify factors associated with G4 ALC nadir, all clinical characteristics and DVH metrics from tumor targets and OARs were analyzed between patient groups with or without G4 ALC nadir by the univariate logistic regression method.

2.6 Elastic-net logistic regression modeling

Elastic-net logistic regression is a type of penalized logistic regression (11, 12). Elastic-net uses both L1 and L2 norm penalty on the regression covariates and uses a mixing parameter that defines the proportion (alpha parameter) of penalty applied to the covariates between both L1 and L2 norms. Taken together, the elastic-net regression method allows retention of correlated covariates and also regularizes model predictors in a manner that allows for improved prediction performance. The risk factors selected from clinical characteristics and DVH metrics

by elastic-net logistic regression models were applied to construct the multivariable logistic regression model.

Elastic-net logistic regression models were constructed for G4 ALC nadir prediction using a repeated cross-validation (CV) methodology to approximate the models' generalization abilities when lacking an external validation dataset (13, 14). To determine the important features for G4 ALC nadir by elastic-net logistic regression models, we selected the best alpha parameter in one randomly separated train set as the first step; then, one elastic-net model was established in the train set and validated in the rest of the test set in 10-fold CV; finally, the 10-fold CV process was repeated 100 times in different held-out sets to estimate model mean efficacy [95% confidence interval (CI)], which is called repeated CV, considering to reduce overfitting in the small sample size. The statistically significant features were selected as the important features for G4 ALC nadir.

2.7 Statistical considerations

The Wilcoxon paired rank test was applied to compare the performances between two models. A p-value <0.05 was considered statistically significant in all statistical analysis. The Bonferroni correction was applied in multiple statistical testing. R software (version 4.0.2, R Development Core Team, Vienna, Austria) was used to conduct all statistical analyses. Elastic-net logistic regression modeling was implemented by the R package glmnet.

3. Results

3.1 Patient characteristics and clinical outcomes

Both pre-RT characteristics and clinical outcomes of the patients are listed in Table 1. A total of 130 patients formed the study cohort. The median age at diagnosis was 53 [interquartile range (IQR), 46–63] years. RapidArc was used in 79.2% of the patients. Twenty percent of patients had IC, and 83.8% received concurrent chemotherapy. The median (IQR) follow-up was 26.4 (14.2–41.6) months. The incidence of death, disease progression, local failure, regional lymph node metastasis, and distant metastasis during follow-up was 19.2%, 24.6%,11.5%, 3.8%, and 15.4%, respectively.

ALC of all patients declined during RT and generally recovered to some extent at the completion of RT, as shown in Figure 1A. The median pre-RT ALC was 1.74×10^9 cells/L. The counts declined during RT to the median ALC nadir as 0.24×10^9 cells/L, and the median onset time of ALC nadir was 33 days from the initiation of RT. Finally, ALC partially recovered to the median counts of 0.57×10^9 cells/L at the end of RT. The incidence of pre-, during-, and post-RT G4 lymphopenia were 0%, 33.1%, and 4.6%, respectively (Figure 1B).

TABLE 1 Baseline characteristics and clinical outcomes of the patients.

Features	Categories	Median (IQR)or num (%)
Death	No	105 (80.8%)
	Yes	25 (19.2%)
Disease progression	No	98 (75.4%)
	Yes	32 (24.6%)
Post-RT local failure	No	115 (88.5%)
	Yes	15 (11.5%)
Post-RT regional LN metastasis	No	125 (96.2%)
	Yes	5 (3.8%)
Post-RT distant metastasis	No	110 (84.6%)
	Yes	20 (15.4%)
Age (years)		53 (46-63)
ECOG	0-1	114 (87.7%)
	2	16 (12.3%)
FIGO stage (2018)	I–II	36 (27.7%)
	III	84 (64.6%)
	IV	10 (7.7%)
Body mass index		23.1 (20.1-25.1)
RT technique	3D-CRT	27 (20.8%)
	RapidArc	103 (79.2%)
Induction chemotherapy	No	104 (80%)
	Yes	26 (20%)
Concurrent chemotherapy	No	21 (16.2%)
	Yes	109 (83.8%)
Pre-RT regional LN metastasis	No	45 (34.6%)
	Yes	85 (65.4%)
Pre-RT CBCs ($\times10^9$ cells/L)	Leukocytes	6.6 (5.1-8.1)
	Hemoglobin (g/L)	118 (103-130)
	Platelets	260 (216.5-316.8)
	Neutrophils	4.3 (3.1-5.6)
	Lymphocytes	1.7 (1.3-2.1)
	Monocytes	0.3 (0.2-0.4)

CBCs, complete blood counts; ECOG, Eastern Cooperative Oncology Group; FIGO, International Federation of Gynecology and Obstetrics; IQR, interquartile range; LN, lymph node; OS, overall survival; PFS, progression-free survival; RT, radiotherapy; 3D-CRT, three-dimensional conformal radiotherapy.

3.2 G4 ALC nadir during RT was associated with poor clinical outcomes

During follow-up, there were a total of 25 deaths. G4 ALC nadir was seen in 33.1% of patients. Patients with G4 ALC nadir had worse OS (p = 0.023) and PFS (p = 0.054) than those without G4 ALC nadir as shown in Figures 2A, B. On univariate analysis, OS was significantly worse in patients with G4 ALC

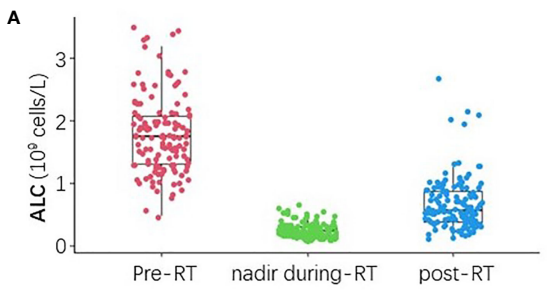

B

Total 130 Patients		RT		
		Pre	During	Post
ALC (10^9 cells/L)		1.74	0.24	0.57
G4 lymphopenia	without (%)	130 (100)	87 (66.9)	124 (95.4)
	with (%)	0 (0)	43 (33.1)	6 (4.6)

FIGURE 1
The change of absolute lymphocyte count (ALC) from baseline to post-RT. **(A)** ALC declined during RT and generally recovered to some extent at the completion of RT. **(B)** The median ALC and incidence of G4 lymphopenia at different time points (pre-, nadir during-, and post-RT).

nadir than those without G4 ALC nadir [hazard ratio (HR), 2.44; 95% CI, 1.1–5.39; p = 0.03], and PFS was also worse in patients with G4 ALC nadir (HR, 1.96; 95% CI, 0.98–3.94; p = 0.05), as shown in Table 2. On multivariable analysis, patients with G4 ALC nadir still had significantly poor OS and a trend of poor PFS than those without G4 ALC nadir (HR, 3.91; 95% CI, 1.34–11.38; p = 0.01, and HR, 1.82; 95% CI, 0.75–4.42; p = 0.19, respectively). Although without statistical significance (p > 0.05), G4 ALC nadir showed a trend of promotion effects in the occurrence of local failure, regional lymph node metastasis, and distant metastasis after RT (OR, 1.41, 1.37, and 1.83, respectively) (Figure 2C).

3.3 Clinical and DVH characteristics and their correlations with G4 ALC nadir

The clinical characteristics were compared between the patient groups with or without G4 ALC nadir, and the univariate analysis results (ORs and p-values) are listed in Supplementary Table S1. Age, Eastern Cooperative Oncology

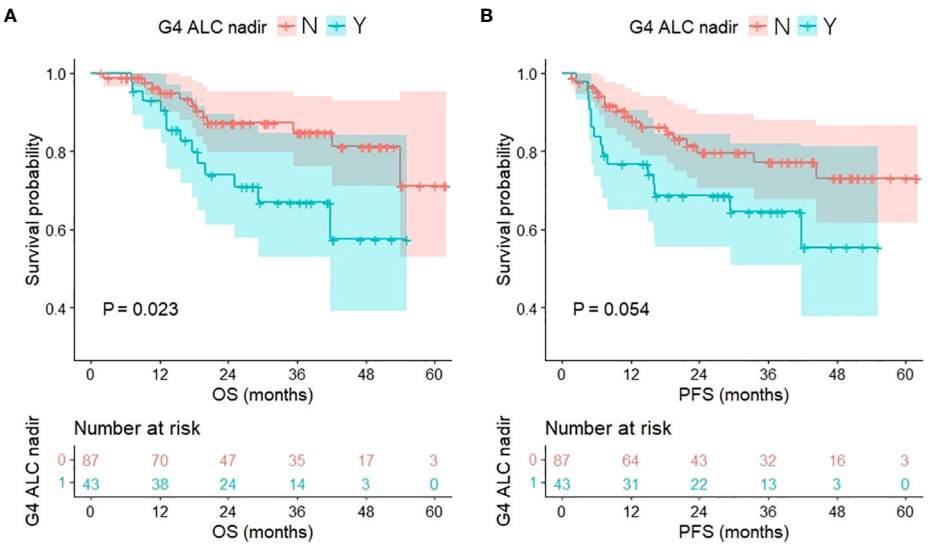

C

Patients Number		Local failure		Regional lymph node metastasis		Distant metastasis	
		without	with	without	with	without	with
G4 ALC nadir	without (%)	78 (89.7)	9 (10.3)	84 (96.6)	3 (3.4)	76 (87.4)	11 (12.6)
	with (%)	37 (86)	6 (14)	41 (95.3)	2 (4.7)	34 (79.1)	9 (20.9)
	OR (95%CI)	1.41 (0.68-2.88)		1.37 (0.67-2.8)		1.83 (0.89-2.75)	
	P-value	0.35		0.39		0.1	

FIGURE 2
G4 ALC nadir and different treatment outcomes. **(A)** Patients with G4 ALC nadir had worse overall survival (OS) (p = 0.023). **(B)** Patients with G4 ALC nadir had worse progression-free survival (PFS) (p = 0.054). **(C)** The incidence and risk of local failure, regional lymph node metastasis, and distant metastasis after RT in patients with G4 ALC nadir.

10.3389/fonc.2022.905222

TABLE 2 Univariate and multivariable analysis of potential factors associated with survivals.

Features	OS			PFS		
	HR	95% CI	p-value	HR	95% CI	p-value
Univariate analysis						
G4 ALC nadir: yes vs. no	2.44	1.1–5.39	0.03	1.96	0.98–3.94	0.05
Multivariable analysis						
G4 ALC nadir: yes vs. no	3.91	1.34–11.38	0.01	1.82	0.75–4.42	0.19
Age	0.01	2.09e−05–5.67	0.16	0.13	8.39e−04–18.91	0.42
ECOG: 2 vs. 0 and 1	1.81	0.46–7.17	0.4	1.75	0.49–6.25	0.39
FIGO stage III vs. I–II	0.8	0.22–2.91	0.74	1.26	0.43–3.67	0.68
FIGO stage IV vs. I–II	5.83	1.01–33.71	0.05	5.45	1.39–21.45	0.02
Body mass index	3.28e−03	4.37e−07–24.6	0.21	0.55	6.34e−04–478.03	0.86
RT technique: RapidArc vs. 3D-CRT	0.28	0.07–1.08	0.06	0.92	0.32–2.65	0.88
Induction chemotherapy: yes vs. no	1.4	0.35–5.67	0.64	0.77	0.24–2.45	0.65
Concurrent chemotherapy: yes vs. no	0.11	0.02–0.56	8.43e−03	0.79	0.21–2.98	0.73
Pre-RT regional LN metastasis: yes vs. no	3.78	0.88–16.3	0.07	1.11	0.38–3.3	0.85
Pre-RT leukocytes	6.92e−10	1.01e−27–4.72e+08	0.31	0.06	1.55e−14–2.27e+11	0.85
Pre-RT hemoglobin	9.30e−04	2.23e−07–3.87	0.1	0.04	7.04e−05–28.45	0.35
Pre-RT platelets	16.28	0.52–514.45	0.11	1.27	0.07–23.36	0.87
Pre-RT neutrophils	1.60e+09	1.5e−05–1.71e+23	0.2	60.81	1.41e−08–2.62e+11	0.72
Pre-RT lymphocytes	7.17e+04	0.04–1.33e+11	0.13	4.89	1.15e−04–2.08e+05	0.77
Pre-RT monocytes	1.18e−09	4.64e−18–0.3	0.04	1.13e−04	3.92e−10–32.55	0.16

ALC, absolute lymphocyte count; CI, confidence interval; ECOG, Eastern Cooperative Oncology Group; FIGO, International Federation of Gynecology and Obstetrics; G4, grade 4; HR, hazard ratio; LN, lymph node; OS, overall survival; PFS, progression-free survival; RT, radiotherapy; 3D-CRT, three-dimensional conformal radiotherapy.

Group (ECOG) performance status score, pre-RT hemoglobin, and pre-RT lymphocytes had protective effects from the occurrence of G4 ALC nadir (OR, 0.97, p = 0.03; OR, 0.11, p =0.04; OR, 0.97, p = 5.6e−3; OR, 0.22, p = 2.0e−4, respectively), while the usage of concurrent chemotherapy promoted the occurrence of G4 ALC nadir (OR, 5.73; p = 0.02). Body mass index (BMI) had protective (OR, 0.9; p = 0.06) and pre-RT regional lymph node metastasis had promotive (OR, 2.22; p = 0.06) effects from the occurrence of G4 ALC nadir with borderline significance.

All DVH metrics of interest were summarized in the format of median (IQR) in Supplementary Table S2. The radiation dosimetrics of different structures had high correlations (Pearson's correlations > 0.5). There were little correlations among clinical characteristics and DVH dosimetrics, also among radiation dosimetrics and volumes, as shown in Supplementary Figure S1.

The DVH dosimetrics of each structure were compared between the patient groups with or without G4 ALC nadir as shown in Figure 3, and univariate logistic regression analysis results of each DVH dosimetrics in each structure for G4 ALC nadir are listed in Supplementary Table S3. The volume of GTV_N was correlated with the occurrence of G4 ALC nadir (OR, 1.07; p = 0.01). The volume of GTV_P, all dosimetrics of PTV_5500, and the volume, V5, and V10 of the body showed a tendency to correlate with the occurrence of G4 ALC nadir (all p-values <0.1).

3.4 Elastic-net regression modeling for selecting risk factors affecting G4 ALC nadir

In searching grids from 0 to 1 step 0.05, the best alpha in the elastic-net logistic regression model with best performances was selected as 0.6 in one randomly separated train set. Then, elastic-net models were established in differently separated train sets and validated in the rest of the test sets in 10-fold CV for 100 iterations to summarize the prediction performances. As summarized in all models, mean AUC value in train sets was 0.84 (IQR, 0.82–0.86) and that in test sets was 0.76 (IQR, 0.69–0.83). The selected frequencies of all the 14 clinical characteristics and 63 DVH parameters in elastic-net regression models in 100 iterations bootstrapping are shown in Supplementary Figure S2.

The most moderate elastic-net model was selected as the final model. In building the model, the correlations between regression coefficients and lambda are shown in Figures 4A, B. The final model is shown in Figure 4C. Considering both the significance and selected frequency in bootstrapping, seven

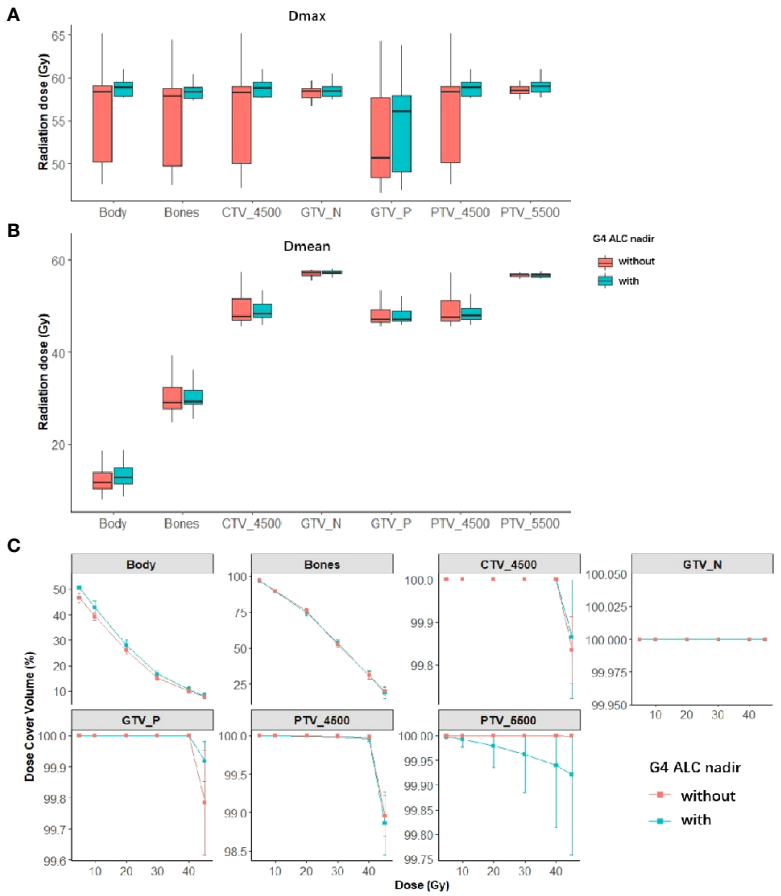

FIGURE 3
Summary of dose–volume histogram (DVH) metrics of both tumor targets and organs at risk (OARs) in patients with or without G4 ALC nadir (red is the summary of DVH metrics in patients without G4 ALC nadir; green is the summary of DVH metrics in patients with G4 ALC nadir). Panels **(A, B)** show the median (95%CI) of Dmax and Dmean of both tumor targets and OARs in patients with or without G4 ALC nadir. Panel **(C)** shows the relative volume (in percentage) covered by different dose levels of both tumor targets and OARs in patients with or without G4 ALC nadir.

important risk factors were included in the final model (Figure 4C), including four clinical characteristics (ECOG, pre-RT hemoglobin, pre-RT lymphocytes, and concurrent chemotherapy) and three DVH parameters (GTV_N volume, PTV_5500 Dmax, and body volume).

3.5 Development and validation of the prediction model for G4 ALC nadir

The final multivariable logistic regression model was further constructed with these seven factors selected by elastic-net model in one seldomly separated train set, as shown in Figure 4C. Among clinical characteristics, ECOG (OR, 0.16; 95% CI, 0.02–1.15; p = 0.07), pre-RT lymphocytes (OR, 3.01e−04;95% CI,0–0.13; p < 0.01), and pre-RT hemoglobin (OR, 6.16e−05; 95% CI, 0–0.08; p < 0.01) were protective factors for occurrence of G4 ALC nadir, while concurrent chemotherapy was a promoting factor for G4 ALC nadir (OR, 10.12; 95% CI, 1.76–58.18; p < 0.01). Among DVH parameters, body volume played as a protective factor (OR, 0.56; 95% CI, 0.35–0.89, p = 0.01), while the GTV_N volume and PTV_5500 Dmax promoted the incidence of G4 ALC nadir (OR, 1.16; 95% CI, 0.7–1.93; p = 0.56; OR, 1.58; 95% CI, 1–2.51; p = 0.05, respectively). It was consistent with the coefficient in the final LASSO-net regression model.

The final multivariable logistic regression model with seven important factors was compared with the multivariable logistic regression model with four clinical characteristics selected by elastic-net model. Their prediction abilities were testified in both train and test sets, as summarized in Figure 5B, and one example of AUC in the train and test sets was shown in Figure 5A. Four evaluation criteria, including sensitivity, specificity, accuracy, and AUC were all summarized and compared in Figure 5B.

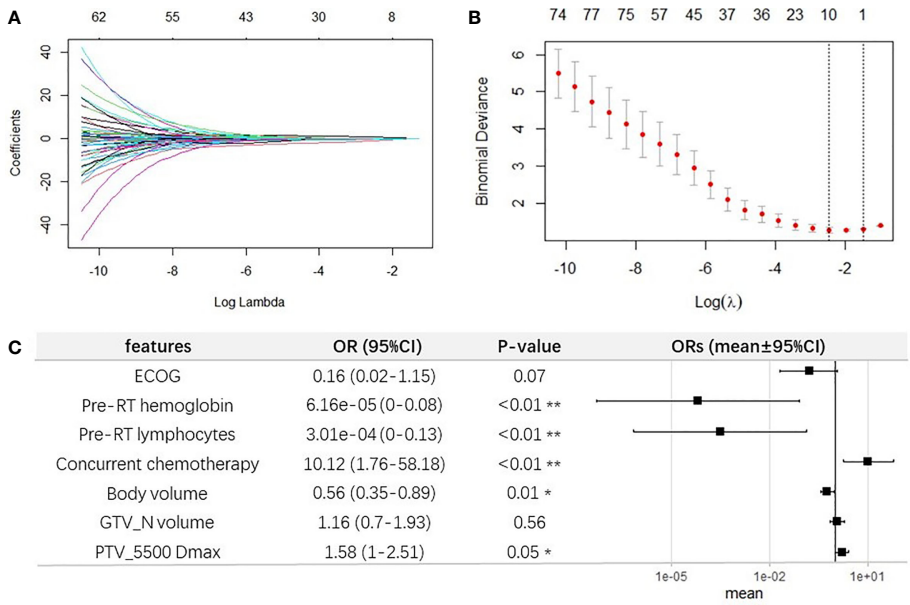

FIGURE 4
Elastic-net regression modeling for selecting important features for G4 ALC nadir. **(A)** Elastic-net coefficient profiles of all factors. **(B)** The selected optimal parameter (lambda) in the most moderate elastic-net model. **(C)** Forest plot of the seven selected important features for G4 ALC nadir.

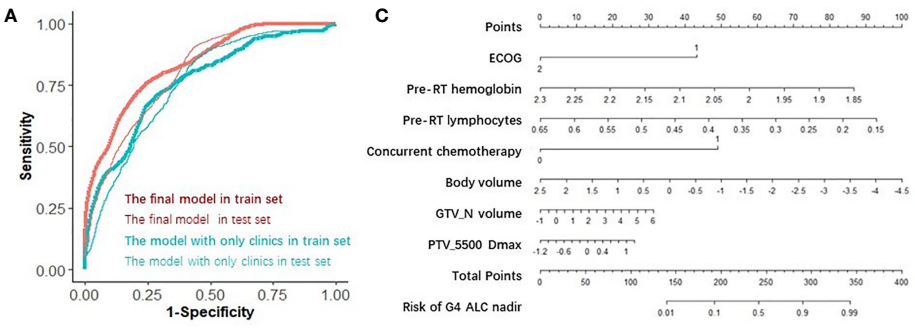

B

Criteria mean (95%CI)	The final model		The model with only clinical features	
	Train Set	Test set	Train Set	Test set
Sensitivity	0.77 (0.76 - 0.78)	0.76 (0.74 - 0.79)	0.78 (0.76 - 0.8)	0.8 (0.78 - 0.82)
Specificity	0.78 (0.77 - 0.79)	0.76 (0.74 - 0.79)	0.69 (0.68 - 0.71)	0.7 (0.67 - 0.72)
Accuracy	0.78 (0.77 - 0.79)	0.76 (0.75 - 0.78)	0.72 (0.72 - 0.73)	0.73 (0.72 - 0.75)
AUC	0.84 (0.83 - 0.84)	0.77 (0.76 - 0.79)	0.8 (0.8 - 0.81)	0.76 (0.75 - 0.78)

FIGURE 5
Evaluations of the models and nomogram for G4 ALC nadir prediction. **(A)** One example of receiver operating characteristic (ROC) curve of the prediction models in train and test sets. **(B)** Comparison of four evaluation criteria of different prediction models in train and test sets. **(C)** Nomogram of the final prediction model with seven parameters.

The final model with seven important factors had significantly higher AUC (mean, 0.84; 95% CI, 0.83–0.84) than the model with four clinical features (AUC mean, 0.8; 95% CI, 0.8–0.81) in train sets (a Wilcoxon paired rank test, $p < 0.01$), and the final model also had significantly higher AUC (mean, 0.77; 95% CI, 0.76–0.79) than the model with only four clinical features (mean, 0.76; 95% CI, 0.75–0.78) in test sets (a Wilcoxon paired rank test, $p < 0.01$). These results indicated that the DVH parameters improved the prediction performance for G4 ALC nadir. Finally, for the purpose of clinical usage in the future, the corresponding nomogram of the final multivariable logistic regression model with seven important factors for predicting G4 ALC nadir was plotted, as shown in Figure 5C.

4. Discussion

Lymphocytes are the most radiosensitive cells among the erythroid, myeloid, and lymphoid lineage with LD50 (lethal dose required to reduce the surviving fraction of lymphocytes by 50%) of only 2 Gy (5). RT-induced lymphopenia was common and correlated with poor survival in patients with different types of solid tumors, such as thoracic malignancies, brain tumors, head and neck cancers, and cervical cancer (15). In cervical cancer, the reported incidence of G4 lymphopenia during CCRT was 16%, and G4 lymphopenia could predict poor survival (4). The current study confirmed the results of previous studies. In our study, the incidence of G4 ALC nadir during pelvic (chemo)RT was as high as 33.1%, and G4 ALC nadir was associated with poor survival outcomes. Therefore, studies that focused on the prediction model for G4 lymphopenia are justified.

In this study, using the important risk factors selected from elastic-net models in machine learning framework, we developed and validated a multivariable logistic regression model for predicting G4 lymphopenia during pelvic (chemo)RT in cervical cancer patients with mean AUC = 0.84 (95% CI, 0.83–0.84), mean accuracy = 0.78 (95% CI, 0.77–0.79) in train sets and mean AUC = 0.77 (95% CI, 0.76–0.79), mean accuracy = 0.76 (95% CI, 0.75–0.78) in test sets. The final multivariable logistic regression model included four clinical characteristics (ECOG, pre-RT hemoglobin, pre-RT lymphocytes, and concurrent chemotherapy) and three DVH parameters (GTV_N volume, PTV_5500 Dmax, and body volume). Until now, we are not aware of any similar prediction models in cervical cancer. There are some other studies using machine learning algorithms to predict RT-induced lymphopenia in esophageal cancer (9, 16). Zhu and colleagues (9) constructed a novel deep learning model using dosimetric and clinical information to predict G4 lymphopenia during CCRT for esophageal cancer. Compared with their novel hybrid deep learning model in the train set, the AUC (0.84 vs. 0.831) and accuracy (0.78 vs. 0.769) of our final model were numerically similar (9). The performance of the final proposed model with both clinical and dosimetric factors was evaluated based on four prediction metrics and compared to the multivariable model with only clinical factors selected by elastic-net model. As expected, the model including both clinical and dosimetric factors outperformed the model including only clinical factors [mean AUC, 0.84 (95% CI, 0.83–0.84) vs. 0.8 (95% CI, 0.8–0.81), $p < 0.01$ in train sets, and mean AUC of 0.77 (95% CI, 0.76–0.79) vs. 0.76 (95% CI, 0.75–0.78), $p < 0.01$ in test sets]. With regard to potential clinical applications, we speculated that our model might play a role in the following clinical scenarios. First, as our model was totally based on pre-RT clinical and dosimetric parameters, it will enable physicians to assess EBRT plans for G4 lymphopenia risk and to identify patients at high risk who might benefit from modified treatment approaches and to guide modification of treatment approaches. Second, with the success of immunotherapy in solid tumors, the immunomodulatory effects of RT in conjunction with immune checkpoint blockade are currently under active investigation in cervical cancer (17). Lymphocytes are key effectors of immunotherapy, and lymphopenia was predictive for compromised efficacy of immunotherapy (18). It was reported that treatment-related severe lymphopenia was correlated with disease progression in NSCLC patients receiving consolidative immunotherapy after definitively chemoradiation (19). Applying lymphocyte-sparing RT has been recommended when combining RT with immunotherapy (20). RT-induced lymphopenia, which can be predicted using our model, should be one of the issues to take into consideration in designing clinical trials of RT combined with immunotherapy in cervical cancer (21).

In our proposed model, concurrent chemotherapy was a significant promote clinical factor for G4 ALC nadir (OR, 10.12; 95% CI, 1.76–58.18, $p < 0.01$), which was consistent with some previous studies (22, 23). In a study with large cohort of patients (N = 3,920) with different cancer types, the use of concurrent chemotherapy, particularly platinum compounds versus none, was associated with a lower ALC at end of RT (612 vs. 937 cells/ml, $p < 0.001$) (22). Another study with 711 patients who received definitive RT for NSCLC revealed that receipt of concurrent chemotherapy was associated with lower lymphocyte nadirs in multivariable analysis ($p < 0.0001$) (23). However, the contribution of concurrent chemotherapy to lymphocyte depletion is difficult to conclusively establish in studies demonstrating decreased ALC after CCRT. There were studies that showed that lymphopenia during CCRT was not significantly different among patients receiving different chemotherapy regimens, suggesting that no chemotherapy regimen *per se* was more likely to be cytotoxic to lymphocyte (24). In a study comparing effects of concurrent cisplatin administration during RT to RT alone on the immune function of patients with cervical cancer, administration of concurrent cisplatin might synergistically increase cytotoxic effects of radiation on tumor cells but did not alter the magnitude and the characteristics of radiation-induced

immunosuppression (25). When patients received induction chemotherapy followed by consolidation chemoradiation, the drop in ALC occurred after consolidation therapy but not induction therapy, suggesting that induction chemotherapy did not play a major immediate role in causing lymphopenia (24, 26). Our study also showed that induction chemotherapy did not correlate with G4 ALC nadir during RT (OR, 1.09; p = 0.85). In esophageal cancer, neither induction chemotherapy nor the type of concurrent chemotherapy [e.g., taxane and 5-fluorouracil (5-FU) versus platinum and 5-FU or taxane and platinum or other] was associated with G4 lymphopenia (27). All these results suggest that the effect of concurrent chemotherapy on lymphopenia during RT is complex. More studies on the synergistic mechanism of chemotherapy and RT on the immune system are needed. Our study showed that ECOG was a protective factor from developing G4 ALC nadir. Patients with ECOG of 2 were less likely to develop G4 ALC nadir than those with ECOG of 0–1 (OR, 0.16; 95% CI, 0.02–1.15; p = 0.07). The possible reason for this result might be that patients with ECOG of 2 received less concurrent chemotherapy (p = 0.002).

Other two factors that promoted the incidence of G4 ALC nadir in our final model were GTV_N volume and PTV_5500 Dmax. In clinical practice, the dose level of 55 Gy was prescribed for metastatic locoregional lymph nodes. Both the two parameters indicated that the irradiation dose of the lymphatic system was positively correlated with G4 ALC nadir. Studies about the role of nodal irradiation for solid tumors on the reduction in circulating lymphocytes are scarce. Haas et al. studied the immunological effects of nodal irradiation for Hodgkin's disease and showed that lymphoid irradiation (LI) was cytotoxic to peripheral blood T cells (28). They also postulated that the bone marrow outside the irradiation fields was a major source of T cells repopulating the peripheral blood after LI (28).

Among the clinical factors, pre-RT hemoglobin and lymphocytes were protective from developing G4 ALC nadir, which were consistent with results from previous studies (8, 9, 27, 29). Zhu et al. reported that patients with G4 lymphopenia during CCRT for esophageal cancer had lower level of baseline hemoglobin (12.94 vs. 13.28 g/dl, p = 0.008) and baseline ALC (1.42 vs. 1.78 x 10^9/L, p <0.001) (9). Sini et al. also suggested that baseline ALC played an extremely important role in the development of lymphopenia in patients treated with pelvis RT for prostate cancer (8). Baseline ALCs below 1.83 x 10^9/L were predictive of an enhanced probability of acute G3 lymphopenia (8). Recent studies found that erythroid cells can regulate immune responses (30). CD71+erythroid cells (CECs), which are immature red blood cells, including erythroblasts and reticulocytes, exert immunosuppressive functions by producing reactive oxygen species to decrease T-cell proliferation or secreting cytokines, including transforming growth factor β (TGF-β), which promotes T-cell differentiation into regulatory T cells (30, 31). In patients with cancer, anemia leads to increased frequency of CECs in the peripheral blood contributing to diminished immunity (30), and late-stage tumors can induce anemia and immunosuppressive extramedullary erythroid progenitor cells (32). In addition to affecting erythroid cells, as a systemic disease, cancer induces many functional and compositional changes to the immune system as a whole (33). Reduced abundance and decreased function of T cells in the blood was observed in cancer (33). All these studies can partly explain our results that pre-RT hemoglobin and lymphocytes were protective factors for G4 lymphopenia occurrence.

We observed that body volume was included in our final model as a protective factor for the occurrence of lymphopenia (OR, 0.56; 95% CI, 0.35–0.89, p = 0.01). In our study, body volume was defined as the part of body within the range of simulation CT scan for EBRT. On the condition of same irradiation dose, patients with larger body volume would receive lower dose per unit of body volume. We further did linear regression analysis and demonstrated that body volume was moderately correlated with BMI (R^2 = 0.602, p <0.01). Univariate analysis of this study also showed that BMI had a propensity to protect patients from developing G4 ALC nadir (OR = 0.9, p = 0.06), which was consistent with previous studies (9, 27). Due to the significant correlation, BMI was not included in the final prediction model by the machine learning framework, while it might improve the model's generalizability in external dataset.

Bone marrow displays structural and functional features resembling a secondary lymphoid organ and contains follicle-like structures similar to lymph nodes or spleen. Approximately 8%–20% of bone marrow mononuclear cells are lymphocytes (34). The correlation of bone marrow irradiation with lymphopenia is controversial. Some studies showed that the doses to the pelvic bone marrow was correlated with RT-induced lymphopenia (8, 35). However, a study on dosimetric predictors of lymphopenia induced by palliative RT showed that bone marrow dose–volume parameters did not predict lymphopenia. Our study did not find any relationship between DVH parameters of bones and occurrence of G4 ALC nadir. We postulate two possible reasons for the negative results of this study. First, lymphocytes are extremely radiosensitive to radiation (5), the doses to the pelvic bone exceeded the lethal dose of the lymphocyte (mean dose of bone was as high as 29.2 Gy). Second, the whole irradiated bones were treated as a whole organ during the process of our analysis. However, radiation to different parts of the pelvic bones may contribute differently to hematological toxicities. A study in patients treated with whole-pelvis RT for prostate cancer showed that the model for acute G3 lymphopenia included V40 of the whole pelvis, and the 1-year G2 lymphopenia model included V40 of the ilium (8).

It is also meaningful to explore the relationship between tumor biology and the risk of developing G4 ALC nadir. Squamous cell carcinoma accounted for approximately 80% of all cervical cancers, and adenocarcinoma accounted for approximately 20% (36). In our study, the majority of patients

(95.4%) had squamous cell carcinoma, and histology types were not associated with the incidence of G4 ALC nadir (squamous vs. non-squamous: 33.1% vs. 33.3%, $p > 0.999$). Cho et al. also reported that histology types did not correlate with chemoradiation-induced lymphopenia in cervical cancer ($p = 0.713$) (4). Most cervical cancers are positive for human papillomavirus (HPV) (37). In our study, it was not possible to analyze the relationship between HPV and occurrence of G4 ALC nadir because there were a lot of missing data on HPV and we are not aware of any such analysis by others as well. With regard to FIGO stage, it had no significant impact on the occurrence of G4 ALC nadir in univariate analysis in our study, which was consistent with the results from Cho et al. (4). In FIGO (2018), locoregional lymph nodes (pelvic and paraaortic) are indicators for staging, and patients with locoregional lymph nodes metastases only are staged as IIIC. In clinical practice, radiation dose boosts mainly to locoregional metastatic lymph nodes, which was included in the final model.

With regard to ways of reducing the risk of lymphopenia or restoration of the number of lymphocytes in the peripheral blood, several measures can be attempted. First, according to our proposed model, if patients are at high risk of G4 lymphopenia, measures can be taken before treatment, such as correcting anemia, modifying EBRT plan to reduce PTV_5500 Dmax, or restoring a physiological number of lymphocytes in the peripheral blood by use of cytokines IL-2, IL-7, and IL-15, which play a role in the development, proliferation, and survival of T cells (18).

This study had some limitations. First, there were some discordances on the time points of blood tests due to the retrospective nature of the study. Second, lymphocyte subtypes changed differently after pelvic RT (38, 39) and had different impacts on treatment outcomes (40, 41). However, lymphocyte subtypes were unavailable for the patients included in the study, as lymphocyte subtypes were not routinely tested in our clinical practice, and no blood was collected for further tests. Third, body volume in the final model is determined by the extent of the simulation CT scans, which might be hard to synchronize across different centers. However, body volume was selected as a protective factor for the occurrence of G4 ALC nadir through elastic-net regression modeling; we think it is still meaningful to keep it in the final model to remind readers of its potential role in the occurrence of G4 ALC nadir during CCRT in cervical cancer, and we also recommend external validation of the role of body volume. Fourth, although the data were split into a training and a testing set, it would be better to use external data from different institutions to validate our results.

In conclusion, the present study developed and validated a comprehensive model integrating clinical and dosimetric parameters by machine learning method, which performed well in predicting G4 lymphopenia during pelvic RT for cervical cancer and may facilitate physicians to identify patients at high risk of G4 lymphopenia who might benefit from modified treatment approaches.

Data availability statement

The raw data supporting the conclusions of this article will be made available by the authors, without undue reservation.

Ethics statement

This study was reviewed and approved by Ethics committee of the University of Hong Kong-Shenzhen Hospital. The ethics committee waived the requirement of written informed consent for participation.

Author contributions

LY: Primary data collection, data analysis, manuscript writing, and manuscript approval. ZX: Primary data collection, data analysis, manuscript editing, and manuscript approval. HY: Corresponding author, data double check, data analysis, result interpretation, study design, and manuscript approval. LG: Corresponding author, study design oversight, data quality control, results check and manuscript approval. All authors contributed to the article and approved the submitted version.

Funding

This project is supported in part by Health Commission of Guangdong Province, China (NO. B2020100); Shenzhen Science and Technology Program (NO. KQTD20180411185028798 and JCYJ20210324114600002); High Level-Hospital Program, Health Commission of Guangdong Province, China (NO. HKUSZH201902031 and HKUSZH201901038); Shenzhen Fundamental Research Program (NO. JCYJ2020109150427184) and Shenzhen Key Medical Discipline Construction Fund (NO. SZXK014).

Conflict of interest

The authors declare that the research was conducted in the absence of any commercial or financial relationships that could be construed as a potential conflict of interest.

Publisher's note

Supplementary material

The Supplementary Material for this article can be found online at: https://www.frontiersin.org/articles/10.3389/fonc.2022.905222/full#supplementary-material

SUPPLEMENTARY FIGURE 1
The Pearson's correlations among clinical characteristics and dose-volume histogram (DVH) metrics.

SUPPLEMENTARY FIGURE 2
The selected frequencies of 14 clinical characteristics and 63 dose-volume histogram (DVH) parameters in Elastic-net regression models in 100 iterations bootstrapping.

References

1. Sung H, Ferlay J, Siegel RL, Laversanne M, Soerjomataram I, Jemal A, et al. Global cancer statistics 2020: GLOBOCAN estimates of incidence and mortality worldwide for 36 cancers in 185 countries. *CA: Cancer J Clin* (2021) 71(3):209–49. doi: 10.3322/caac.21660

2. Koh WJ, Abu-Rustum NR, Bean S, Bradley K, Campos SM, Cho KR, et al. Cervical cancer, version 3.2019, NCCN clinical practice guidelines in oncology. *J Natl Compr Cancer Network JNCCN* (2019) 17(1):64–84. doi: 10.6004/jnccn.2019.0001

3. Jin JY, Hu C, Xiao Y, Zhang H, Paulus R, Ellsworth SG, et al. Higher radiation dose to the immune cells correlates with worse tumor control and overall survival in patients with stage III NSCLC: A secondary analysis of RTOG0617. *Cancers* (2021) 13(24):6193. doi: 10.3390/cancers13246193

4. Cho O, Chun M, Chang SJ, Oh YT, Noh OK. Prognostic value of severe lymphopenia during pelvic concurrent chemoradiotherapy in cervical cancer. *Anticancer Res* (2016) 36(7):3541–7.

5. Nakamura N, Kusunoki Y, Akiyama M. Radiosensitivity of CD4 or CD8 positive human T-lymphocytes by an *in vitro* colony formation assay. *Radiat Res* (1990) 123(2):224–7. doi: 10.2307/3577549

6. Qian JM, Akama-Garren E, Shin J, Gunasti L, Bang A, Pike LRG, et al. Dosimetric modeling of lymphopenia in patients with metastatic cancer receiving palliative radiation and PD-1 immune checkpoint inhibitors. *Adv Radiat Oncol* (2022) 7(2):100880. doi: 10.1016/j.adro.2021.100880

7. Ellsworth SG. Field size effects on the risk and severity of treatment-induced lymphopenia in patients undergoing radiation therapy for solid tumors. *Adv Radiat Oncol* (2018) 3(4):512–9. doi: 10.1016/j.adro.2018.08.014

8. Sini C, Fiorino C, Perna L, Noris Chiorda B, Deantoni CL, Bianchi M, et al. Dose-volume effects for pelvic bone marrow in predicting hematological toxicity in prostate cancer radiotherapy with pelvic node irradiation. *Radiother Oncol J Eur Soc Ther Radiol Oncol* (2016) 118(1):79–84. doi: 10.1016/j.radonc.2015.11.020

9. Zhu C, Lin SH, Jiang X, Xiang Y, Belal Z, Jun G, et al. A novel deep learning model using dosimetric and clinical information for grade 4 radiotherapy-induced lymphopenia prediction. *Phys Med Biol* (2020) 65(3):035014. doi: 10.1088/1361-6560/ab63b6

10. Rajula HSR, Verlato G, Manchia M, Antonucci N, Fanos V. Comparison of conventional statistical methods with machine learning in medicine: Diagnosis, drug development, and treatment. *Medicina (Kaunas Lithuania)* (2020) 56(9):455. doi: 10.3390/medicina56090455

11. Zou H, Hastie T. Regularization and variable selection *via* the elastic net. *J R Stat Society: Ser B (Statistical Methodol* (2005) 67(2):301–20. doi: 10.1111/j.1467-9868.2005.00503.x

12. Hastie T TR, Friedman J. *The elements of statistical learning: data mining, inference, and prediction. 2nd ed.* New York, NY: Springer (2009).

13. Deist TM, Dankers F, Valdes G, Wijsman R, Hsu IC, Oberije C, et al. Machine learning algorithms for outcome prediction in (chemo)radiotherapy: An empirical comparison of classifiers. *Med Phys* (2018) 45(7):3449–59. doi: 10.1002/mp.12967

14. Xu CJ, van der Schaaf A, Schilstra C, Langendijk JA, van't Veld AA. Impact of statistical learning methods on the predictive power of multivariate normal tissue complication probability models. *Int J Radiat oncol biology Phys* (2012) 82 (4):e677–84. doi: 10.1016/j.ijrobp.2011.09.036

15. Venkatesulu BP, Mallick S, Lin SH, Krishnan S. A systematic review of the influence of radiation-induced lymphopenia on survival outcomes in solid tumors. *Crit Rev oncol/hematol* (2018) 123:42–51. doi: 10.1016/j.critrevonc.2018.01.003

16. Ebrahimi S, Lim G, Hobbs BP, Lin SH, Mohan R, Cao W. A hybrid deep learning model for forecasting lymphocyte depletion during radiation therapy. *Med Phys* (2022) 49(5):3507–22. doi: 10.1002/mp.15584

17. Dyer BA, Feng CH, Eskander R, Sharabi AB, Mell LK, McHale M, et al. Current status of clinical trials for cervical and uterine cancer using immunotherapy combined with radiation. *Int J Radiat oncol biology Phys* (2021) 109(2):396–412. doi: 10.1016/j.ijrobp.2020.09.016

18. Ménétrier-Caux C, Ray-Coquard I, Blay JY, Caux C. Lymphopenia in cancer patients and its effects on response to immunotherapy: an opportunity for combination with cytokines? *J immunother Cancer* (2019) 7(1):85. doi: 10.1186/s40425-019-0549-5

19. Friedes C, Chakrabarti T, Olson S, Prichett L, Brahmer JR, Forde PM, et al. Association of severe lymphopenia and disease progression in unresectable locally advanced non-small cell lung cancer treated with definitive chemoradiation and immunotherapy. *Lung Cancer (Amsterdam Netherlands)* (2021) 154:36–43. doi: 10.1016/j.lungcan.2021.01.022

20. Lambin P, Lieverse RIY, Eckert F, Marcus D, Oberije C, van der Wiel AMA, et al. Lymphocyte-sparing radiotherapy: The rationale for protecting lymphocyte-rich organs when combining radiotherapy with immunotherapy. *Semin Radiat Oncol* (2020) 30(2):187–93. doi: 10.1016/j.semradonc.2019.12.003

21. Holub K, Vargas A, Biete A. Radiation-induced lymphopenia: the main aspects to consider in immunotherapy trials for endometrial and cervical cancer patients. *Clin Trans Oncol Off Publ Fed Spanish Oncol Societies Natl Cancer Institute Mexico* (2020) 22(11):2040–8. doi: 10.1007/s12094-020-02345-3

22. Terrones-Campos C, Ledergerber B, Vogelius IR, Specht L, Helleberg M, Lundgren J. Lymphocyte count kinetics, factors associated with the end-of-Radiation-Therapy lymphocyte count, and risk of infection in patients with solid malignant tumors treated with curative-intent radiation therapy. *Int J Radiat oncol biology Phys* (2019) 105(4):812–23. doi: 10.1016/j.ijrobp.2019.07.013

23. Tang C, Liao Z, Gomez D, Levy L, Zhuang Y, Gebremichael RA, et al. Lymphopenia association with gross tumor volume and lung V5 and its effects on non-small cell lung cancer patient outcomes. *Int J Radiat oncol biology Phys* (2014) 89(5):1084–91. doi: 10.1016/j.ijrobp.2014.04.025

24. Campian JL, Ye X, Brock M, Grossman SA. Treatment-related lymphopenia in patients with stage III non-small-cell lung cancer. *Cancer Invest* (2013) 31 (3):183–8. doi: 10.3109/07357907.2013.767342

25. Santin AD, Hermonat PL, Ravaggi A, Bellone S, Roman J, Pecorelli S, et al. Effects of concurrent cisplatinum administration during radiotherapy vs. radiotherapy alone on the immune function of patients with cancer of the uterine cervix. *Int J Radiat oncol biology Phys* (2000) 48(4):997–1006. doi: 10.1016/s0360-3016(00)00769-0

26. Chadha AS, Liu G, Chen HC, Das P, Minsky BD, Mahmood U, et al. Does unintentional splenic radiation predict outcomes after pancreatic cancer radiation therapy? *Int J Radiat oncol biology Phys* (2017) 97(2):323–32. doi: 10.1016/j.ijrobp.2016.10.046

27. van Rossum PSN, Deng W, Routman DM, Liu AY, Xu C, Shiraishi Y, et al. Prediction of severe lymphopenia during chemoradiation therapy for esophageal cancer: Development and validation of a pretreatment nomogram. *Pract Radiat Oncol* (2020) 10(1):e16–26. doi: 10.1016/j.prro.2019.07.010

28. Haas GS, Halperin E, Doseretz D, Linggood R, Russell PS, Colvin R, et al. Differential recovery of circulating T cell subsets after nodal irradiation for hodgkin's disease. *J Immunol (Baltimore Md 1950)* (1984) 132(2):1026–30.

29. Yang L, Xu Z, Ma L, Liu Q, Chang ATY, Wang Q, et al. Early onset of severe lymphopenia during definitive radiotherapy correlates with mean body dose and predicts poor survival in cervical cancer. *Cancer Biomarkers section A Dis Markers* (2022) 34(1):149–59. doi: 10.3233/CBM-210292

30. Grzywa TM, Nowis D, Golab J. The role of CD71(+) erythroid cells in the regulation of the immune response. *Pharmacol Ther* (2021) 228:107927. doi: 10.1016/j.pharmthera.2021.107927

31. Elahi S, Ertelt JM, Kinder JM, Jiang TT, Zhang X, Xin L, et al. Immunosuppressive CD71+ erythroid cells compromise neonatal host defence against infection. *Nature* (2013) 504(7478):158–62. doi: 10.1038/nature12675

32. Zhao L, He R, Long H, Guo B, Jia Q, Qin D, et al. Late-stage tumors induce anemia and immunosuppressive extramedullary erythroid progenitor cells. *Nat Med* (2018) 24(10):1536–44. doi: 10.1038/s41591-018-0205-5

33. Hiam-Galvez KJ, Allen BM, Spitzer MH. Systemic immunity in cancer. *Nat Rev Cancer* (2021) 21(6):345–59. doi: 10.1038/s41568-021-00347-z

34. Zhao E, Xu H, Wang L, Kryczek I, Wu K, Hu Y, et al. Bone marrow and the control of immunity. *Cell Mol Immunol* (2012) 9(1):11–9. doi: 10.1038/cmi.2011.47

35. Albuquerque K, Giangreco D, Morrison C, Siddiqui M, Sinacore J, Potkul R, et al. Radiation-related predictors of hematologic toxicity after concurrent chemoradiation for cervical cancer and implications for bone marrow-sparing pelvic IMRT. *Int J Radiat oncol biology Phys* (2011) 79(4):1043–7. doi: 10.1016/j.ijrobp.2009.12.025

36. National Comprehensive Cancer Network. *Cervical cancer (version 1.2021)* . Available at: http://www.nccn.org/professionals/physician_gls/ pdf/cervical.pdf (Accessed October 2, 2020).

37. Walboomers JM, Jacobs MV, Manos MM, Bosch FX, Kummer JA, Shah KV, et al. Human papillomavirus is a necessary cause of invasive cervical cancer worldwide. *J Pathol* (1999) 189(1):12–9. doi: 10.1002/(SICI)1096-9896(199909)189:1<12::AID-PATH431>3.0.CO;2-F

38. Eric A, Juranic Z, Tisma N, Plesinac V, Borojevic N, Jovanovic D, et al. Radiotherapy-induced changes of peripheral blood lymphocyte subpopulations in cervical cancer patients: relationship to clinical response. *J BUON Off J Balkan Union Oncol* (2009) 14(1):79–83.

39. Swanson GP, Jhavar SG, Hammonds K. The effect of pelvic radiation alone on lymphocyte subgroups. *Clin Transl Radiat Oncol* (2020) 23:100–2. doi: 10.1016/j.ctro.2020.05.010

40. Jordanova ES, Gorter A, Ayachi O, Prins F, Durrant LG, Kenter GG, et al. Human leukocyte antigen class I, MHC class I chain-related molecule a, and CD8+/regulatory T-cell ratio: which variable determines survival of cervical cancer patients? *Clin Cancer Res* (2008) 14(7):2028–35. doi: 10.1158/1078-0432.CCR-07-4554

41. Ozsahin M, Crompton NE, Gourgou S, Kramar A, Li L, Shi Y, et al. CD4 and CD8 T-lymphocyte apoptosis can predict radiation-induced late toxicity: a prospective study in 399 patients. *Clin Cancer Res* (2005) 11(20):7426–33. doi: 10.1158/1078-0432.CCR-04-2634

frontiers | Frontiers in Oncology

TYPE Original Research
PUBLISHED 27 February 2023
DOI 10.3389/fonc.2023.1119173

OPEN ACCESS

EDITED BY
Kevin Ni,
St George Hospital Cancer Care Centre, Australia

REVIEWED BY
Antonino Romeo,
Scientific Institute of Romagna for the Study and Treatment of Tumors (IRCCS), Italy
Atsuto Katano,
The University of Tokyo Hospital, Japan

*CORRESPONDENCE
Nalee Kim
rodr.naleekim@gmail.com

†These authors have contributed equally to this work

SPECIALTY SECTION
This article was submitted to Radiation Oncology, a section of the journal Frontiers in Oncology

RECEIVED 10 January 2023
ACCEPTED 14 February 2023
PUBLISHED 27 February 2023

CITATION
Kim N, Shin J, Ahn SH, Pyo H, Noh JM, Yang K, Lee W and Park B (2023) Reduced radiation exposure to circulating blood cells in proton therapy compared with X-ray therapy in locally advanced lung cancer: Computational simulation based on circulating blood cells.
Front. Oncol. 13:1119173.
doi: 10.3389/fonc.2023.1119173

Reduced radiation exposure to circulating blood cells in proton therapy compared with X-ray therapy in locally advanced lung cancer: Computational simulation based on circulating blood cells

Nalee Kim[1*†], Jungwook Shin[2†], Sung Hwan Ahn[1†], Hongryull Pyo[1], Jae Myoung Noh[1], Kyungmi Yang[1], Woojin Lee[1] and Byoungsuk Park[1]

[1]Department of Radiation Oncology, Samsung Medical Center, Sungkyunkwan University School of Medicine, Seoul, Republic of Korea, [2]Division of Cancer Epidemiology and Genetics, National Cancer Institute, National Institutes of Health, Rockville, MD, United States

Background: We estimated the dose of circulating blood cells (CBCs) in patients with locally advanced non-small cell lung cancer for predicting severe radiation-induced lymphopenia (SRIL) and compared pencil-beam scanning proton therapy (PBSPT) and intensity-modulated (photon) radiotherapy (IMRT).

Materials and methods: After reviewing 325 patients who received definitive chemoradiotherapy with PBSPT (n = 37) or IMRT (n = 164). SRIL was diagnosed when two or more events of an absolute lymphocyte count < 200 μL occurred during the treatment course. Dose information for the heart and lungs was utilized for the time-dependent computational dose calculation of CBCs.

Results: The dose distribution of CBCs was significantly lesser in the PBSPT group than that in the IMRT group. Overall, 75 (37.3%) patients experienced SRIL during the treatment course; 72 and 3 patients were treated with IMRT and PBSPT, respectively. SRIL was associated with poor progression-free and overall survival outcomes. Upon incorporating the dose information of CBCs for predicting SRIL, CBC D90% > 2.6 GyE was associated with the development of SRIL with the baseline lymphocyte count and target volume. Furthermore, PBSPT significantly reduced the dose of CBC D90% (odds ratio = 0.11; p = 0.004) compared with IMRT.

Conclusion: The results of this study demonstrate the significance of the dose distribution of CBCs in predicting SRIL. Furthermore, reducing the dose of CBCs after PBSPT minimized the risk of SRIL. Lymphocyte-sparing radiotherapy in PBSPT could improve outcomes, particularly in the setting of maintenance immunotherapy.

KEYWORDS

proton beam therapy, lung cancer, lymphopenia, radiation therapy, blood

1 Introduction

Given the physical characteristics of proton and photon (X-ray) beam therapies, proton beam radiation therapy (RT) has intrigued physicians by improving treatment outcomes in patients with non-small cell lung cancer (NSCLC) (1). However, a randomized controlled trial comparing intensity-modulated (photon) RT (IMRT) and proton beam therapy failed to demonstrate clinical benefit in terms of oncologic outcomes and normal tissue toxicities (2). Furthermore, previous retrospective studies showed a trend but no significant benefit in preventing radiation pneumonitis following proton beam therapy (3–5).

Severe radiation-induced lymphopenia (SRIL), which is significant depletion of lymphocytes due to radiation exposure, has been investigated with the emerging interest in immune responses against tumors (6–8). Its clinical significance has been evaluated in various solid tumors (6, 9–12). In this context, we previously showed that pencil-beam scanning proton therapy (PBSPT), an advanced beam delivery technique in proton beam therapy, decreased the occurrence of SRIL (12). Although the etiology of SRIL is multifaceted, the consensus is lacking for dose constraints, which could lead to SRIL because of the lack of tools to compute the dose to circulating lymphocytes.

We previously developed a time-dependent computational framework called the hematological dose (HEDOS), which estimates the dose to circulating blood cells (CBCs) based on a whole-body blood flow simulation and is used to construct the dose–volume histogram of blood cells (bDVH) (13). It has been applied to selective cases. Xing et al. demonstrated the impact of external beam delivery techniques, including IMRT, volumetric-modulated arc therapy, passive proton beam, and PBSPT for the liver treatment plan without clinical data (14). Qian et al. applied HEDOS to correlate the dose to CBCs for patients with metastatic NSCLC, melanoma, or renal cell carcinoma who received immunotherapy and underwent palliative RT (15).

The present study aimed to investigate the clinical effect of the dose information of CBCs on the occurrence of SRIL in patients with NSCLC undergoing concurrent chemoradiotherapy (CCRT) and further determine the association between the occurrence of SRIL and the treatment modality (IMRT or PBPST).

2 Materials and methods

2.1 Patient population

Upon approval from the institutional review board (approval no.: 2020-01-034), we retrospectively reviewed the data obtained from 325 patients treated with CCRT between November 2016 and December 2019. A total of 124 patients were excluded from the analysis for the following reasons (Supplementary Figure 1): lacking information for the dose distribution to the healthy organs (n = 40), missing follow-up data (n = 26), incomplete CCRT course (n = 20), provision of induction chemotherapy before CCRT (n = 18), use of the hybrid IMRT/PBSPT technique (n = 15), and missing weekly blood test reports (n = 5). Finally, the data obtained from 201 patients were analyzed (164 in the IMRT group and 37 in the PBSPT group). The requirement to obtain informed consent was waived because of the retrospective nature of this study.

2.2 Treatment

The detailed institutional policies of planning IMRT and PBSPT have been previously described (3). Briefly, based on four-dimensional computed tomography in ten breathing phases, the planning target volume (PTV) was delineated with a 5-mm margin from the clinical target/gross tumor volume. A total dose of 66 GyE in 30 fractions was prescribed in both IMRT and PBSPT groups. Supplementary Table 1 summarizes the planning criteria for the organs at risk. In the IMRT group, the volumetric-modulated arc therapy was the most frequently used (n = 100, 61.0%), followed by the step-and-shoot method with the 6-MV photon coplanar beam (n = 64, 39.0%). In the PBSPT group, single-field optimization was adopted in 22 (59.5%) patients. The two-field plan was used in 23 (62.2%) patients, and the pencil beam algorithm was applied to all patients. Pinnacle (version 9.2, Royal Phillips Electronics, Miami, FL, USA) and RayStation (RaySearch Laboratories, Stockholm, Sweden) were used for planning IMRT and PBSPT, respectively.

Regarding chemotherapy, 189 (94.0%) patients received six cycles of paclitaxel/cisplatin; six patients received paclitaxel/carboplatin; four patients received gemcitabine/cisplatin; and two patients received combined etoposide and cisplatin. Subsequently, 19 (9.5%) patients received maintenance therapy with durvalumab.

2.3 SRIL

Following weekly peripheral blood count assessments during CCRT, lymphopenia was graded based on the Common Terminology Criteria for Adverse Events version 5.00. Based on the absolute lymphocyte count (ALC), SRIL was diagnosed when two or more events of ALC < 200/μL (grade 4) occurred during the CCRT course.

2.4 bDVH

We used the pre-generated spatiotemporal blood distribution based on International Commission on Radiological Protection 89th publication that has been described before (13). Dose data of the heart and lungs from each patient's treatment plan were utilized for HEDOS calculations. The beam-on-time of IMRT and PBPST were both assumed to be 60 s/beam, and the detailed time structure of beam delivery was not considered. We used the dose after all fractions for the analysis. Also, we used 5.3 L for total CBC volume for all patients to compute dose distribution to CBC and thus the volume of one CBC was 0.053 mL (16).

2.5 Statistical analysis

Overall survival (OS) rates were calculated from the first date of CCRT to the date of death or last follow-up. Progression-free survival (PFS) rates were calculated from the first date of CCRT to the date of progression, death, or the last follow-up. Baseline characteristics were evaluated using the chi-squared test or Fisher's exact and Mann–Whitney U tests to assess categorical and continuous variables, respectively. The Kaplan–Meier method and log-rank test were used for OS and PFS. A Cox regression model was used for the multivariable analysis of factors affecting OS and PFS that had a *p*-value < 0.05 in the univariable analysis. The logistic regression analysis was performed to evaluate the predictive factors of SRIL. The factors were selected in stepwise regression after ten-fold cross-validation and included in the multivariate analysis of SRIL. To identify the optimal cutoffs for dosimetric parameters of CBCs, maximally selected rank statistics were performed. A null multivariate model was built based on patient and tumor characteristics. The Akaike information criterion (AIC) was used to compare multivariate models to select the most discriminative dosimetric predictor of SRIL. Statistical significance was set at a two-tailed *p*-value < 0.05. All statistical analyses were performed using SPSS version 25.0 (IBM Corp., Armonk, NY, USA) and R version 4.0.2 (R Foundation for Statistical Computing, Vienna, Austria).

3 Results

3.1 Patient population

Overall, compared with the patients in the PBSPT group, patients in the IMRT group were younger, more frequently diagnosed with adenocarcinoma, and had a more advanced nodal disease (Supplementary Table 2). Although the target volume or prescription dose did not differ between the two groups (PBSPT and IMRT groups), the dose parameters for V5GyE, V10GyE, and V20GyE of the lungs, mean lung dose, V30GyE of the heart, and mean heart dose were significantly lower in the PBPST group than those in the IMRT group (Table 1). Moreover, bDVH was significantly lower in the PBPST group than that in the IMRT group (Table 1). Figure 1 shows bDVHs for the entire population stratified by RT modality.

TABLE 1 Detailed information on dose parameters according to the radiation therapy modality.

		Total	IMRT	PBSPT	*p*-value
		n = 201	n = 164	n = 37	
GTV, cc		108.9 [67.4–203.4]	109.4 [67.9–205.8]	104.7 [66.0–194.1]	0.966
CTV, cc		314.4 [208.1–495.2]	310.2 [202.0–489.2]	350.2 [232.9–520.4]	0.269
PTV, cc		575.8 [387.4–805.9]	572.6 [385.9–792.5]	592.3 [389.3–890.4]	0.522
CTV V100%, %		96.3 [95.0–97.8]	96.2 [95.0–97.2]	99.0 [96.0–99.1]	<.001
PTV V95%, %		97.1 [94.1–98.8]	97.1 [94.2–99.0]	96.8 [94.1–98.4]	0.174
Radiotherapy	Total dose, GyE	66.0 [66.0–66.0]	66.0 [66.0–66.0]	66.0 [66.0–66.0]	0.769
	BED, Gy	80.5 [80.5–80.5]	80.5 [80.5–80.5]	80.5 [80.5–80.5]	0.997
Lungs	V_{5GyE}, %	51.2 [42.6–61.3]	54.9 [47.2–63.2]	35.2 [27.2–41.5]	<0.001
	V_{10GyE}, %	40.9 [33.8–47.1]	43.4 [36.2–49.7]	30.7 [23.7–36.1]	<0.001
	V_{20GyE}, %	31.3 [24.1–36.5]	32.3 [26.4–37.4]	23.5 [20.1–27.5]	<0.001
	Mean dose, GyE	17.6 [14.3–20.6]	19.0 [15.3–21.3]	13.9 [11.1–16.2]	<0.001
Heart	V_{30GyE}, %	12.6 [5.9–26.3]	14.6 [5.7–28.2]	9.1 [6.0–12.9]	0.013
	V_{45GyE}, %	7.2 [2.9–16.2]	8.0 [2.9–17.4]	5.4 [3.0–8.5]	0.090
	Mean dose, GyE	12.0 [6.0–18.9]	13.3 [7.1–21.5]	7.5 [5.1–10.3]	<0.001
CBC	Mean, GyE	2.93 [2.22–3.93]	3.10 [2.29–4.09]	2.39 [1.76–3.02]	0.002
	D10, GyE	3.49 [2.66–4.64]	3.66 [2.73–4.76]	2.94 [2.12–3.64]	0.003
	D20, GyE	3.30 [2.50–4.36]	3.47 [2.58–4.52]	2.74 [1.99–3.43]	0.003
	D30, GyE	3.16 [2.39–4.19]	3.32 [2.47–4.35]	2.60 [1.90–3.25]	0.002
	D40, GyE	3.03 [2.30–4.05]	3.20 [2.37–4.21]	2.48 [1.82–3.12]	0.002
	D50, GyE	2.92 [2.21–3.92]	3.09 [2.29–4.08]	2.38 [1.76–3.01]	0.002

(Continued)

TABLE 1 Continued

		Total	IMRT	PBSPT	*p*-value
		n = 201	n = 164	n = 37	
	D60, GyE	2.81 [2.12–3.78]	2.98 [2.20–3.95]	2.29 [1.68–2.89]	0.002
	D70, GyE	2.70 [2.04–3.63]	2.83 [2.11–3.80]	2.19 [1.61–2.77]	0.001
	D80, GyE	2.57 [1.93–3.46]	2.70 [2.00–3.61]	2.07 [1.53–2.64]	0.001
	D90, GyE	2.39 [1.79–3.22]	2.52 [1.86–3.33]	1.91 [1.41–2.45]	<0.001
CBC	$V_{0.5GyE}$, %	100.0 [100.0–100.0]	100.0 [100.0–100.0]	100.0 [100.0–100.0]	0.290
	$V_{1.0GyE}$, %	100.0 [100.0–100.0]	100.0 [100.0–100.0]	100.0 [99.9–100.0]	<.001
	$V_{1.5GyE}$, %	100.0 [98.53–100.00]	100.00 [99.22–100.00]	99.2 [82.7–100.0]	<.001
	$V_{2.0GyE}$, %	98.9 [73.7–100.0]	99.5 [80.4–100.0]	85.2 [19.3–99.1]	<.001
	$V_{2.5GyE}$, %	84.4 [20.1–99.7]	91.0 [26.8–99.8]	38.2 [0.6–87.7]	0.001
	$V_{3.0GyE}$, %	42.4 [1.3–95.9]	57.7 [2.2–96.9]	7.8 [0.0–50.5]	0.002
	$V_{3.5GyE}$, %	9.7 [0.0–77.7]	18.3 [0.0–84.6]	0.5 [0.0–16.2]	0.002

Values are expressed as median [interquartile range].
IMRT, intensity-modulated radiation (photon) therapy; PBSPT, pencil-beam scanning proton therapy; GTV, gross tumor volume; CTV, clinical target volume; PTV, planning target volume; GyE, gray equivalent; BED10, biological effective dose with α/β of 10; Vxx%, volume receiving more than proportion to prescribed dose; Dxx, dose to XX% of volume; V_{XXGyE}, volume receiving over XX GyE; CBC, circulating blood cell.

3.2 SRIL

ALC in the entire cohort decreased gradually during the CCRT course and recovered afterward (Supplementary Figure 2). From week 4 to the last week of the CCRT course, ALCs were significantly lower in the IMRT group than in the PBSPT group (Supplementary Figure 2, Supplementary Table 3). Among 107 (53.2%) patients who developed grade 4 lymphopenia during the CCRT course, 75 (37.3% of entire patients) experienced SRIL, including three (8.1% of PBPST group) in the PBPST group and 72 (43.9% of IMRT group) in the IMRT group ($p < 0.001$). In addition, none of the patient or tumor characteristics, except for baseline ALC values, differed between the two groups. Patients with SRIL showed significantly lower baseline ALC than those without SRIL (median, 2,010/μL vs. 2,140/μL, $p = 0.029$, Table 2). Regarding dose-volume parameters, patients with SRIL had a larger target volume and showed a higher dose distribution to the lung and heart than those without SRIL (all $p < 0.001$, Table 2). Moreover, bDVH for patients with SRIL also differed from that for patients without SRIL (Figure 2).

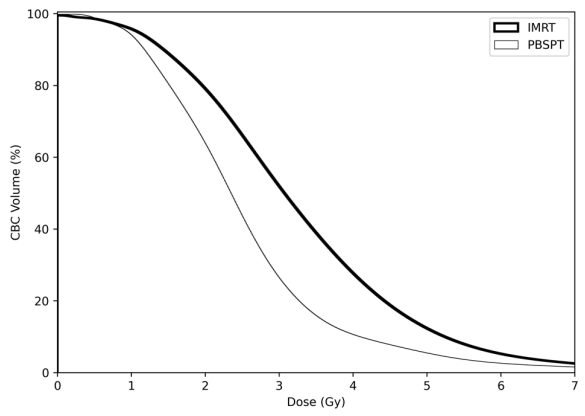

FIGURE 1
Dose-volume parameters of circulating blood cells in both treatment modalities for all patients.

3.3 Prognostic value of SRIL

With a median follow-up of 39.8 (IQR [interquartile range], 21.0–49.4) months, the 3-year OS and PFS rates were 62.4% and 26.2% for the entire cohort, respectively. Patients with SRIL showed poorer OS and PFS outcomes than those without SRIL (3-year OS, 48.3% vs. 70.9%, $p < 0.001$; 3-year PFS, 10.5% vs. 36.1%, $p < 0.001$, Figures 3A, B). The multivariable analysis revealed that SRIL remained a significantly unfavorable factor for both OS and PFS (Table 3).

3.4 Factors predicting SRIL

First, we performed a multivariate analysis to predict the development of SRIL based on clinical and treatment factors other than dose information of CBCs. Both baseline ALC (odds ratio [OR] = 0.60, 95% confidence interval [CI]: 0.37–0.94, $p = 0.026$) and PTV (OR = 1.02, 95% CI: 1.01–1.03, $p = 0.001$) were related to an increased risk of SRIL (Table 4, Supplementary Table 4). AIC in the null model, including baseline ALC and PTV, was 245.52 (Supplementary Table 5). Subsequent analysis showed that bDVH was related to an increased risk of SRIL in the univariate analysis (Supplementary Table 4). In the stepwise regression model, CBC of D90% as the continuous variable (OR = 3.25, 95% CI: 1.98–5.67, $p < 0.001$) was the

TABLE 2 Patient, tumor, and treatment characteristics stratified by severe radiation-induced lymphopenia. .

Patient and tumor characteristics		SRIL	No SRIL	
		n = 75	n = 126	*p*-value
Sex	Female	18 (24.0)	24 (19.0)	0.404
	Male	57 (76.0)	102 (81.0)	
Age		63 [57–68]	64 [58–69]	0.340
ECOG	0	6 (8.0)	22 (17.5)	0.061
	1 or 2	69 (92.0)	104 (82.5)	
Smoking history	Never-smoker	18 (24.0)	21 (16.7)	0.204
	Ex- or current-smoker	57 (76.0)	105 (83.3)	
Tumor laterality	Left	25 (33.3)	53 (42.1)	0.110
	Right	49 (65.3)	66 (52.4)	
	Central	1 (1.3)	7 (5.6)	
Tumor location	Upper lobe	42 (56.0)	69 (54.8)	0.226
	Middle lobe	5 (6.7)	18 (14.3)	
	Lower lobe	28 (37.3)	39 (31.0)	
Pathology	Non-ADC	36 (48.0)	57 (45.2)	0.704
	ADC	39 (52.0)	69 (54.8)	
T-stage	*c*T1 or *c*T2	43 (57.3)	81 (64.3)	0.327
	*c*T3 or *c*T4	32 (42.7)	45 (35.7)	
N-stage	cN2	24 (32.0)	46 (36.5)	0.516
	cN3	51 (68.0)	80 (63.5)	
Clinical stage	IIIA	7 (9.3)	25 (19.8)	0.086
	IIIB	55 (73.3)	75 (59.5)	
	IIIC	13 (17.3)	26 (20.6)	
Baseline ALC,	($\times 10^3$/μL)	2.01 [1.48–2.33]	2.14 [1.68–2.60]	0.029
Baseline ANC	($\times 10^3$/μL)	4.82 [3.74–6.40]	5.01 [3.47–5.99]	0.973
Details of radiation therapy				
Modality	IMRT	72 (96.0)	92 (73.0)	<.001
	PBSPT	3 (4.0)	34 (27.0)	
GTV, cc		171.8 [93.4–275.2]	89.7 [46.8–154.0]	<.001
CTV, cc		441.4 [283.4–613.4]	264.9 [174.6–411.7]	<.001
PTV, cc		739.5 [531.2–938.5]	471.4 [339.1–707.6]	<.001
Total dose, GyE		66.0 [66.0–66.0]	66.0 [66.0–66.0]	0.782
BED10, Gy		80.5 [80.5–80.5]	80.5 [80.5–80.5]	0.960
Lung	V_{5GyE}, %	58.4 [51.2–64.5]	47.0 [36.4–58.4]	<.001
	V_{10GyE}, %	44.7 [40.9–48.8]	37.7 [30.7–45.9]	<.001
	V_{20GyE}, %	33.8 [29.9–38.5]	28.2 [22.3–33.4]	<.001
	Mean dose, GyE	20.1 [17.1–22.3]	16.2 [13.1–19.4]	<.001
Heart	V_{30GyE}, %	21.4 [10.8–35.0]	9.5 [3.5–19.5]	<.001
	V_{45GyE}, %	13.0 [5.6–18.6]	5.3 [1.5–11.2]	<.001

(Continued)

TABLE 2 Continued

Patient and tumor characteristics		SRIL	No SRIL	
		n = 75	n = 126	*p*-value
	Mean dose, GyE	9.4 [3.9–15.6]	4.0 [1.2– 7.7]	<.001
CBC	Mean, GyE	3.81 [2.80–4.81]	2.55 [1.86–3.34]	<.001
	D10, GyE	4.53 [3.34–5.72]	3.05 [2.23–3.92]	<.001
	D20, GyE	4.28 [3.15–5.40]	2.87 [2.10–3.72]	<.001
	D30, GyE	4.11 [3.01–5.17]	2.75 [2.01–3.58]	<.001
	D40, GyE	3.96 [2.90–4.98]	2.64 [1.93–3.45]	<.001
	D50, GyE	3.79 [2.79–4.80]	2.54 [1.85–3.32]	<.001
	D60, GyE	3.66 [2.69–4.62]	2.45 [1.78–3.14]	<.001
	D70, GyE	3.52 [2.59–4.43]	2.35 [1.69–3.02]	<.001
	D80, GyE	3.36 [2.46–4.21]	2.21 [1.60–2.87]	<.001
	D90, GyE	3.14 [2.30–3.89]	2.05 [1.48–2.67]	<.001

Values are expressed as number of patients (%) or median [interquartile range].
ECOG, Eastern Cooperative Oncology Group; ADC, adenocarcinoma; ALC, absolute lymphocyte count; ANC, absolute neutrophil count; IMRT, intensity-modulated radiation (photon) therapy; PBSPT, pencil-beam scanning proton therapy; GTV, gross tumor volume; CTV, clinical target volume; PTV, planning target volume; GyE, gray equivalent; BED10, biological effective dose with α/β of 10; Dxx, dose to XX% of volume; VXXGyE, volume receiving over XX GyE; CBC, circulating blood cell.

only significant factor among bDVH along with baseline ALC (OR = 0.46, 95% CI: 0.27–0.76, $p = 0.004$, Table 4).

Finally, we separately generated models with each significant dosimetric variable of CBCs together with the null model. After comparing AIC, the model including CBC D90% > 2.6 GyE was associated with the lowest AIC at 218.46 (Supplementary Table 5) and remained significant in the multivariate analysis (OR = 6.38, 95% CI: 3.19–13.26, $p < 0.001$), along with baseline ALC and PTV (all $p < 0.05$, Table 4).

A dose-volume relationship between CBC D90% and the probability of SRIL was observed (Figure 4). In addition, the number of grade 4 lymphopenia events and CBC D90% were positively correlated (Supplementary Figure 3). When analyzing factors affecting D90% > 2.6 GyE, PBSPT significantly satisfied the dose criteria for CBC D90% of 2.6 GyE (OR = 0.11, 95% CI: 0.03–0.31, $p = 0.004$, Table 5). Furthermore, CBC D90% > 2.6 GyE was associated with poorer OS and PFS outcomes after excluding SRIL from the multivariable analysis (Supplementary Table 6).

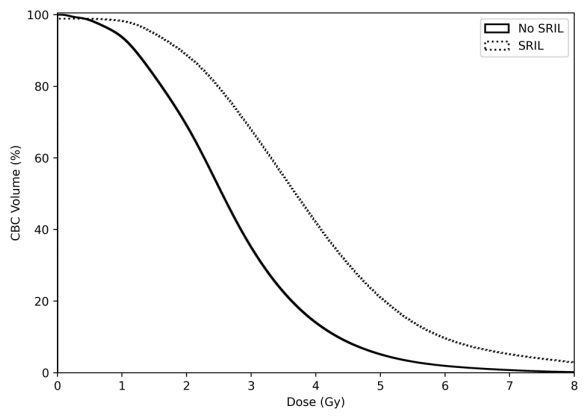

FIGURE 2
Dose-volume parameters for circulating blood cells stratified by severe radiation-induced lymphopenia.

4 Discussion

In this study, we investigated the prognostic value of SRIL and the correlation of bDVH with the development of SRIL in patients with locally advanced NSCLC treated with CCRT. SRIL was associated with poorer OS and PFS outcomes compared with the control. Moreover, at CBC D90% > 2.6 GyE, the risk of SRIL significantly increased together with baseline ALC and PTV. Moreover, PBPST was a significant contributor to minimizing CBC D90%. In addition, CBC D90% had a prognostic value for OS and PFS outcomes. To the best of our knowledge, this was the first study to discover the clinical impact of CBCs in patients with NSCLC and the potential benefit of PBSPT in minimizing radiation exposure to CBCs compared with IMRT (photon).

The negative impact of treatment-related lymphopenia on treatment outcomes in NSCLC has been widely investigated in recent studies (12, 17–23). Upadhyay et al. systematically reviewed 14 studies involving patients with lung cancer and reported that severe lymphopenia increased the risk of death with a pooled hazard ratio of 1.59 ($p < 0.001$) and the risk of death/progression with a pooled hazard ratio of 2.1 ($p < 0.001$) (17). Considering the radiosensitivity of lymphocytes, thoracic RT, which inevitably irradiates highly vascularized lymphocyte-rich organs, such as the lungs and heart, is a major contributor to lymphopenia or SRIL (24). We had previously reported the prognostic value of SRIL in patients with NSCLC (12). Although we could not perform subgroup analyses for patients treated with immunotherapy owing to the small sample size, the clinical significance of SRIL in

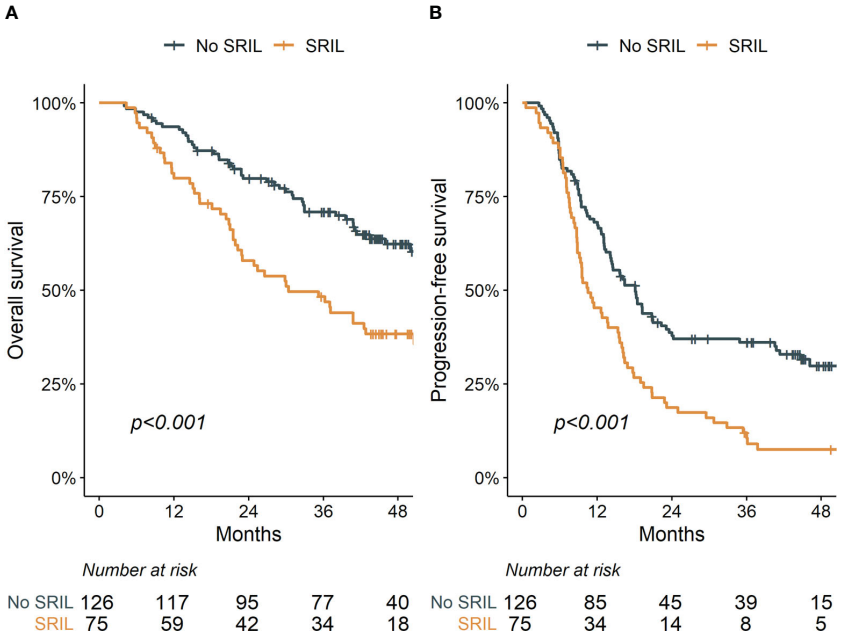

FIGURE 3
Overall **(A)** and progression-free **(B)** survival stratified by severe radiation-induced lymphopenia.

TABLE 3 Prognostic factors for overall and progression-free survival.

Overall survival		Univariable analysis			Multivariable analysis		
Variables		HR	95% CI	*p*-value	HR	95% CI	*p*-value
Treatment modality	(IMRT vs. PBSPT)	0.84	0.46–1.50	0.551			
Sex	(Female vs. male)	1.62	0.94–2.78	0.083			
Age	(<65 vs. ≥ 65 years)	1.18	0.78–1.77	0.442			
Histology	(non-ADC vs. ADC)	0.52	0.35–0.79	0.002	0.61	0.40–0.93	0.021
Clinical T-stage	(T1–2 vs. T3–4)	1.18	0.78–1.79	0.444			
Clinical N-stage	(N2 vs. N3)	0.73	0.48–1.12	0.151			
GTV	Continuous (per 10cc)	1.33	1.12–1.57	0.001	1.01	1.00–1.02	0.142
Total dose	(>66 vs. ≤66 GyE)	1.56	0.72–3.37	0.263			
BED10	(<80 vs. ≥80 GyE)	1.20	0.73–1.95	0.469			
Baseline ALC	(continuous)	0.41	0.20–1.11	0.137			
SRIL	(No vs. yes)	1.54	1.02–2.33	0.040	1.42	1.01–2.25	0.043
Progression-free survival		**Univariable analysis**			**Multivariable analysis**		
Variables		HR	95% CI	*p*-value	HR	95% CI	*p*-value
Treatment modality	(IMRT vs. PBSPT)	0.57	0.36–0.91	0.019	0.75	0.45–1.22	0.244
Sex	(Female vs. male)	0.84	0.57–1.21	0.344			
Age	(<65 vs. ≥ 65 years)	0.63	0.45–0.87	0.005	0.68	0.48–0.94	0.021
Histology	(non-ADC vs. ADC)	1.08	0.78–1.48	0.651			
Clinical T-stage	(T1–2 vs. T3–4)	0.98	0.71–1.35	0.881			
Clinical N-stage	(N2 vs. N3)	1.11	0.79–1.55	0.550			

(Continued)

TABLE 3 Continued

Progression-free survival		Univariable analysis			Multivariable analysis		
Variables		HR	95% CI	*p*-value	HR	95% CI	*p*-value
GTV	Continuous (per 10 cc)	1.01	1.00–1.02	0.142			
Total dose	(>66 vs. ≤66 GyE)	1.09	0.63–1.88	0.768			
BED10	(<80 vs. ≥80 GyE)	1.43	0.98–2.10	0.065			
Baseline ALC	(Continuous)	0.75	0.60–0.93	0.009	1.33	0.91–1.93	0.139
SRIL	(No vs. yes)	1.91	1.39–2.64	<.001	1.65	1.17–2.33	0.004

*The foreparts of parentheses were set as the reference group.
HR, hazard ratio; CI, confidence interval; IMRT, intensity-modulated radiation (photon) therapy; PBSPT, pencil-beam scanning proton therapy; ADC, adenocarcinoma; GTV, gross tumor volume; GyE, gray equivalent; BED10, biological effective dose with α/β of 10; ALC, absolute lymphocyte count; SRIL, severe radiation-induced lymphopenia.

the context of immunotherapy for NSCLC was highlighted (18, 19, 21–23). Jing et al. discovered that SRIL (defined as ALC < 230/μL at the end of CCRT) disrupted survival benefits of maintenance therapy with durvalumab following CCRT (21). In addition to the development of SRIL, Cho et al. reported that recovery from SRIL at 3 months after CCRT was significantly related to PFS and OS outcomes in patients treated with maintenance immunotherapy (18). The dismal effect of SRIL might stem from the reduced systemic anti-tumor immune response by lymphocytes and depletion of tumor-infiltrating lymphocyte (7, 25). The depletion of $CD4^+$ T cells from SRIL, which control cell-mediated immunity against tumors and exert anti-tumor effects on $CD8^+$ T cells, could influence the prognosis (26).

In view of decreasing the incidence of SRIL, several studies suggested various dose-volume criteria for predicting SRIL (12, 17, 20, 23, 27–29). In addition to the baseline ALC and target volume, most studies revealed that the dose to the lung or heart was predictive of SRIL (17). In this context, we had previously reported that lung V5Gy (OR = 1.07) and baseline ALC (OR = 0.73) were independent predictive factors of SRIL in 223 patients with NSCLC treated with CCRT (12). However, a dose–volume correlation in the lung or heart only indirectly provides the potential impact of RT on SRIL. Joseph et al. reported a negative correlation between the integral body dose and post-RT ALC in patients with lung cancer (29). Furthermore, neither dose to the lungs nor heart was significantly related to post-RT ALC. In addition, several reports highlighted that the effective dose to circulating immune cells (EDIC), which incorporates the mean lung dose, mean heart dose, and integral dose, was related to SRIL in lung, breast, and esophageal cancers (29–31). However, the EDIC equation was formulated based on limited patient data, i.e., patients receiving IMRT with over 25 fractions, and built for thoracic radiation fields only. The EDIC equation is yet to be validated with proton patient data. We chose HEDOS over EDIC in this study because using HEDOS, we can calculate the dose to CBCs utilizing the organ DVH from any treatment modality or treatment site. With a patient-specific bDVH from HEDOS results, the various DVH metrics were tested to find the most significant dosimetric factors for SRIL that could be used to guide the treatment plan in a way to reduce the SRIL risk. The last feature we

TABLE 4 Multivariate analysis to predict severe radiation-induced lymphopenia.

Variables		Multivariate analysis		
		OR	95% CI	*p*-value
Model 1 (without CBC data)				
Baseline ALC	(Continuous)	0.60	0.37–0.93	0.026
PTV	(Continuous, per 10 cc)	1.02	1.01–1.03	0.001
Model 2 (Stepwise model)				
Baseline ALC	(Continuous)	0.47	0.27–0.78	0.005
PTV	(Continuous, per 10 cc)	1.01	1.00–1.02	0.049
CBC D90, GyE	(Continuous)	2.13	1.54–3.06	<.001
Model 3 (AIC comparison)				
Baseline ALC	(Continuous)	0.48	0.28–0.78	0.004
PTV	(Continuous, per 10 cc)	1.01	1.00–1.02	0.022
CBC D90, GyE	(≤ 2.6 vs. > 2.6 GyE)	6.38	3.19–13.26	<.001

*The foreparts of parentheses were set as the reference group.
CBC, circulating blood cells; ALC, absolute lymphocyte count; PTV, planning target volume; D90, dose to 90% of volume; GyE, gray equivalent; AIC, Akaike information criterion.

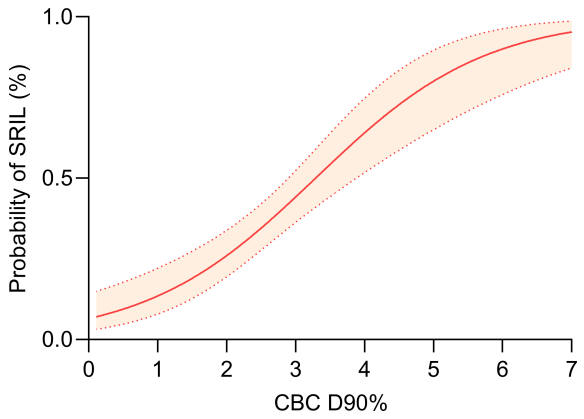

FIGURE 4
Dose-response relationship between dose to 90% of circulating blood cells and severe radiation-induced lymphopenia.

employed in HEDOS was the dose rates from beam-on-times during beam delivery. Therefore, dose criteria for CBCs could be considered when planning for patients scheduled to receive immunotherapy.

Proton beam therapy is advantageous over photon RT in reducing the low-dose radiation to out-of-field. Based on the aforementioned evidence of the dose-response relationship between the healthy organs and SRIL, proton beam therapy is considered to be a potential therapeutic tool for lymphocyte-sparing RT. PBPST alleviates the risk of SRIL by reducing the lung V5Gy compared with IMRT in patients with NSCLC (12). The clinical significance of proton beam therapy in reducing SRIL has also been explored in primary brain tumors and esophageal cancer (32–34). However, to the best of our knowledge, this is the first analysis determining the clinical significance of PBSPT when incorporated with the dose calculation of CBCs. PBPST could positively affect the dose distribution to CBCs compared with IMRT. Furthermore, FLASH RT with an ultra-high dose-rate could enhance the immune-related tumor response by minimizing radiation to CBCs and subsequently reducing SRIL.

This study has several limitations. First, this study was associated with inherent limitations owing to its retrospective design. Second, the limited number of patients in the PBSPT group might have led to an overestimation of the effect of PBSPT. However, the target volume or baseline ALC, which could affect the SRIL development, did not differ significantly. Other limitations related to HEDOS calculations are using a uniform blood path distribution for all patients, implying that we used same the blood flow rate and blood volume for all patients, as these values were unavailable and impossible to measure in this retrospective study. We did not consider the realistic time structure of the beam delivery of IMRT or PBSPT. As these beams consist of many beamlets with a high dose to a small irradiation area, the realistic beam may produce a few CBCs irradiated with very high dose rates, thereby changing the bDVH shapes. The impact of the realistic time structure on the dose to CBCs should be further investigated. Further analyses are required to develop a model for predicting healthy tissue complication probability for SRIL based on CBCs.

TABLE 5 Factors related to the dose to 90% of circulating blood cells.

Variables		Univariate analysis			Multivariate analysis		
		OR	95% CI	*p*-value	OR	95% CI	*p*-value
Sex	(Female vs. male)	1.00	0.51–2.00	0.996			
Age	(<65 vs. ≥ 65 years)	0.90	0.51–1.57	0.712			
Histology	(non-ADC vs. ADC)	0.67	0.38–1.18	0.165			
Clinical T-stage	(cT1–2 vs. cT3–4)	1.20	0.68–2.13	0.533			
Clinical N-stage	(cN2 vs. cN3)	0.97	0.54–1.75	0.927			
Baseline ALC	(Continuous)	1.15	0.80–1.67	0.443			
PTV (per 10 cc)	(Continuous)	1.03	1.02–1.04	<.001	1.03	1.02–1.05	<.001
Total prescribed dose	(>66 vs. ≤66 GyE)	1.15	0.45–3.10	0.771			
Treatment modality	(IMRT vs. PBSPT)	0.22	0.09–0.51	0.001	0.11	0.03–0.31	0.004

*The foreparts of parentheses were set as the reference group.
ADC, adenocarcinoma; ALC, absolute lymphocyte count; PTV, planning target volume; GyE, gray equivalent; IMRT, intensity-modulated radiotherapy; PBSPT, pencil-beam scanning proton therapy.

The occurrence of SRIL was associated with an increased risk of tumor progression and death in patients with NSCLC treated with CCRT. We proposed and clinically validated the significance of bDVH in predicting SRIL. CBC D90% > 2.6 GyE significantly increased the risk of SRIL, and PBPST could decrease CBC D90% compared to IMRT. This analysis should be further validated through randomized controlled trials comparing PBPST and IMRT, particularly providing evidence of lymphocyte-sparing from the sparing dose to CBCs in the setting of maintenance immunotherapy.

Data availability statement

The raw data supporting the conclusions of this article will be made available by the authors, without undue reservation.

Ethics statement

The studies involving human participants were reviewed and approved by Samsung medical center. Written informed consent for participation was not required for this study in accordance with the national legislation and the institutional requirements.

Author contributions

Conception, design, data collection, interpretation, and drafting of the manuscript were performed by NK, JS, and SA. Statistical analysis and editing of the manuscript were performed by NK and JS. All authors contributed to the article and approved the submitted version.

Funding

This work was supported by the National Research Foundation of Korea (NRF) grant funded by the Korean government (MSIT) (NRF-2021R1F1A1063383).

Conflict of interest

The authors declare that the research was conducted in the absence of any commercial or financial relationships that could be construed as a potential conflict of interest.

Publisher's note

Supplementary material

The Supplementary Material for this article can be found online at: https://www.frontiersin.org/articles/10.3389/fonc.2023.1119173/full#supplementary-material

References

1. Han Y. Current status of proton therapy techniques for lung cancer. *Radiat Oncol J* (2019) 37(4):232–48. doi: 10.3857/roj.2019.00633

2. Liao Z, Lee JJ, Komaki R, Gomez DR, O'Reilly MS, Fossella FV, et al. Bayesian Adaptive randomization trial of passive scattering proton therapy and intensity-modulated photon radiotherapy for locally advanced non-Small-Cell lung cancer. *J Clin Oncol* (2018) 36(18):1813–22. doi: 10.1200/jco.2017.74.0720

3. Kim N, Noh JM, Lee W, Park B, Pyo H. Clinical outcomes of pencil beam scanning proton therapy in locally advanced non-small cell lung cancer: Propensity score analysis. *Cancers (Basel)* (2021) 13(14):3497. doi: 10.3390/cancers13143497

4. Zou Z, Bowen SR, Thomas HMT, Sasidharan BK, Rengan R, Zeng J. Scanning beam proton therapy versus photon IMRT for stage III lung cancer: Comparison of dosimetry, toxicity, and outcomes. *Adv Radiat Oncol* (2020) 5(3):434–43. doi: 10.1016/j.adro.2020.03.001

5. Bae BK, Yang K, Noh JM, Pyo H, Ahn YC. Clinical outcomes following proton and photon stereotactic body radiation therapy for early-stage lung cancer. *Cancers (Basel)* (2022) 14(17):4152. doi: 10.3390/cancers14174152

6. Grossman SA, Ellsworth S, Campian J, Wild AT, Herman JM, Laheru D, et al. Survival in patients with severe lymphopenia following treatment with radiation and chemotherapy for newly diagnosed solid tumors. *J Natl Compr Canc Netw* (2015) 13 (10):1225–31. doi: 10.6004/jnccn.2015.0151

7. Formenti SC, Demaria S. Combining radiotherapy and cancer immunotherapy: a paradigm shift. *J Natl Cancer Inst* (2013) 105(4):256–65. doi: 10.1093/jnci/djs629

8. Hiam-Galvez KJ, Allen BM, Spitzer MH. Systemic immunity in cancer. *Nat Rev Cancer* (2021) 21(6):345–59. doi: 10.1038/s41568-021-00347-z

9. Grossman SA, Ye X, Lesser G, Sloan A, Carraway H, Desideri S, et al. Immunosuppression in patients with high-grade gliomas treated with radiation and temozolomide. *Clin Cancer Res* (2011) 17(16):5473–80. doi: 10.1158/1078-0432.Ccr-11-0774

10. Byun HK, Kim N, Yoon HI, Kang SG, Kim SH, Cho J, et al. Clinical predictors of radiation-induced lymphopenia in patients receiving chemoradiation for glioblastoma: Clinical usefulness of intensity-modulated radiotherapy in the immuno-oncology era. *Radiat Oncol* (2019) 14(1):51. doi: 10.1186/s13014-019-1256-6

11. Byun HK, Kim N, Park S, Seong J. Acute severe lymphopenia by radiotherapy is associated with reduced overall survival in hepatocellular carcinoma. *Strahlenther Onkol* (2019) 195(11):1007–17. doi: 10.1007/s00066-019-01462-5

12. Kim N, Myoung Noh J, Lee W, Park B, Park H, Young Park J, et al. Proton beam therapy reduces the risk of severe radiation-induced lymphopenia during chemoradiotherapy for locally advanced non-small cell lung cancer: A comparative analysis of proton versus photon therapy. *Radiother Oncol* (2021) 156:166–73. doi: 10.1016/j.radonc.2020.12.019

13. Shin J, Xing S, McCullum L, Hammi A, Pursley J, Correa CA, et al. HEDOS-a computational tool to assess radiation dose to circulating blood cells during external beam radiotherapy based on whole-body blood flow simulations. *Phys Med Biol* (2021) 66(16). doi: 10.1088/1361-6560/ac16ea

14. Xing S, Shin J, Pursley J, Correa-Alfonso CM, Depauw N, Domal S, et al. A dynamic blood flow model to compute absorbed dose to circulating blood and lymphocytes in liver external beam radiotherapy. *Phys Med Biol* (2022) 67(4). doi: 10.1088/1361-6560/ac4da4

15. Qian JM, Akama-Garren E, Shin J, Gunasti L, Bang A, Pike LRG, et al. Dosimetric modeling of lymphopenia in patients with metastatic cancer receiving palliative radiation and PD-1 immune checkpoint inhibitors. *Adv Radiat Oncol* (2022) 7(2):100880. doi: 10.1016/j.adro.2021.100880

16. Basic anatomical and physiological data for use in radiological protection: Reference values. a report of age- and gender-related differences in the anatomical and physiological characteristics of reference individuals. ICRP publication 89. *Ann ICRP* (2002) 32(3-4):5–265.

17. Upadhyay R, Venkatesulu BP, Giridhar P, Kim BK, Sharma A, Elghazawy H, et al. Risk and impact of radiation related lymphopenia in lung cancer: A systematic review and meta-analysis. *Radiother Oncol* (2021) 157:225–33. doi: 10.1016/j.radonc.2021.01.034

18. Cho Y, Kim Y, Chamseddine I, Lee WH, Kim HR, Lee IJ, et al. Lymphocyte dynamics during and after chemo-radiation correlate to dose and outcome in stage III NSCLC patients undergoing maintenance immunotherapy. *Radiother Oncol* (2022) 168:1–7. doi: 10.1016/j.radonc.2022.01.007

19. Cho Y, Park S, Byun HK, Lee CG, Cho J, Hong MH, et al. Impact of treatment-related lymphopenia on immunotherapy for advanced non-small cell lung cancer. *Int J Radiat Oncol Biol Phys* (2019) 105(5):1065–73. doi: 10.1016/j.ijrobp.2019.08.047

20. Abravan A, Faivre-Finn C, Kennedy J, McWilliam A, Van Herk M. Radiotherapy-related lymphopenia affects overall survival in patients with lung cancer. *J Thorac Oncol* (2020) 15(10):1624–35. doi: 10.1016/j.jtho.2020.06.008

21. Jing W, Xu T, Wu L, Lopez PB, Grassberger C, Ellsworth SG, et al. Severe radiation-induced lymphopenia attenuates the benefit of durvalumab after concurrent chemoradiotherapy for NSCLC. *JTO Clin Res Rep* (2022) 3(9):100391. doi: 10.1016/j.jtocrr.2022.100391

22. Friedes C, Chakrabarti T, Olson S, Prichett L, Brahmer JR, Forde PM, et al. Association of severe lymphopenia and disease progression in unresectable locally advanced non-small cell lung cancer treated with definitive chemoradiation and immunotherapy. *Lung Cancer* (2021) 154:36–43. doi: 10.1016/j.lungcan.2021.01.022

23. Chen D, Patel RR, Verma V, Ramapriyan R, Barsoumian HB, Cortez MA, et al. Interaction between lymphopenia, radiotherapy technique, dosimetry, and survival outcomes in lung cancer patients receiving combined immunotherapy and radiotherapy. *Radiother Oncol* (2020) 150:114–20. doi: 10.1016/j.radonc.2020.05.051

24. Golden EB, Apetoh L. Radiotherapy and immunogenic cell death. *Semin Radiat Oncol* (2015) 25(1):11–7. doi: 10.1016/j.semradonc.2014.07.005

25. Bremnes RM, Busund LT, Kilvær TL, Andersen S, Richardsen E, Paulsen EE, et al. The role of tumor-infiltrating lymphocytes in development, progression, and prognosis of non-small cell lung cancer. *J Thorac Oncol* (2016) 11(6):789–800. doi: 10.1016/j.jtho.2016.01.015

26. Eberst G, Vernerey D, Laheurte C, Meurisse A, Kaulek V, Cuche L, et al. Prognostic value of CD4+ T lymphopenia in non-small cell lung cancer. *BMC Cancer* (2022) 22(1):529. doi: 10.1186/s12885-022-09628-8

27. Tang C, Liao Z, Gomez D, Levy L, Zhuang Y, Gebremichael RA, et al. Lymphopenia association with gross tumor volume and lung V5 and its effects on non-small cell lung cancer patient outcomes. *Int J Radiat Oncol Biol Phys* (2014) 89(5):1084–91. doi: 10.1016/j.ijrobp.2014.04.025

28. Xie X, Lin SH, Welsh JW, Wei X, Jin H, Mohan R, et al. Radiation-induced lymphopenia during chemoradiation therapy for non-small cell lung cancer is linked with age, lung V5, and XRCC1 rs25487 genotypes in lymphocytes. *Radiother Oncol* (2021) 154:187–93. doi: 10.1016/j.radonc.2020.09.002

29. Joseph N, McWilliam A, Kennedy J, Haslett K, Mahil J, Gavarraju A, et al. Post-treatment lymphocytopaenia, integral body dose and overall survival in lung cancer patients treated with radical radiotherapy. *Radiother Oncol* (2019) 135:115–9. doi: 10.1016/j.radonc.2019.03.008

30. Chen F, Jin JY, Hui TSK, Jing H, Zhang H, Nong Y, et al. Radiation induced lymphopenia is associated with the effective dose to the circulating immune cells in breast cancer. *Front Oncol* (2022) 12:768956. doi: 10.3389/fonc.2022.768956

31. Xu C, Jin JY, Zhang M, Liu A, Wang J, Mohan R, et al. The impact of the effective dose to immune cells on lymphopenia and survival of esophageal cancer after chemoradiotherapy. *Radiother Oncol* (2020) 146:180–6. doi: 10.1016/j.radonc.2020.02.015

32. Mohan R, Liu AY, Brown PD, Mahajan A, Dinh J, Chung C, et al. Proton therapy reduces the likelihood of high-grade radiation-induced lymphopenia in glioblastoma patients: Phase II randomized study of protons vs photons. *Neuro Oncol* (2021) 23(2):284–94. doi: 10.1093/neuonc/noaa182

33. Ebrahimi S, Lim G, Liu A, Lin SH, Ellsworth SG, Grassberger C, et al. Radiation-induced lymphopenia risks of photon versus proton therapy for esophageal cancer patients. *Int J Part Ther* (2021) 8(2):17–27. doi: 10.14338/ijpt-20-00086

34. Routman DM, Garant A, Lester SC, Day CN, Harmsen WS, Sanheuza CT, et al. A comparison of grade 4 lymphopenia with proton versus photon radiation therapy for esophageal cancer. *Adv Radiat Oncol* (2019) 4(1):63–9. doi: 10.1016/j.adro.2018.09.004

frontiers | Frontiers in Immunology

TYPE Original Research
PUBLISHED 08 May 2023
DOI 10.3389/fimmu.2023.1066255

OPEN ACCESS

EDITED BY
Peter Sylvain Nicolas Van Rossum,
Amsterdam University Medical Center,
Netherlands

REVIEWED BY
Susannah Ellsworth,
University of Pittsburgh, United States
Dongjun Dai,
Zhejiang University, China

*CORRESPONDENCE
Zhiping Wang
707770685@qq.com
Qiwei Yao
yqwviva@126.com
Jiancheng Li
jianchengli_jack@126.com

†These authors have contributed equally to this work

RECEIVED 10 October 2022
ACCEPTED 24 April 2023
PUBLISHED 08 May 2023

CITATION
Qiu J, Lin H, Ke D, Yu Y, Xu J, Qiu H, Zheng Q, Li H, Zheng H, Liu L, Wang Z, Yao Q and Li J (2023) Higher radiation dose on immune cells is associated with radiation-induced lymphopenia and worse prognosis in patients with locally advanced esophageal squamous cell carcinoma. *Front. Immunol.* 14:1066255. doi: 10.3389/fimmu.2023.1066255

Higher radiation dose on immune cells is associated with radiation-induced lymphopenia and worse prognosis in patients with locally advanced esophageal squamous cell carcinoma

Jianjian Qiu, Hancui Lin, Dongmei Ke, Yilin Yu, Jiaying Xu, Hejin Qiu, Qunhao Zheng, Hui Li, Hongying Zheng, Lingyun Liu, Zhiping Wang*†, Qiwei Yao*† and Jiancheng Li*†

Clinical Oncology School of Fujian Medical University, Fujian Cancer Hospital, Fuzhou, China

Background: To explore the effective dose to immune cells (EDIC) for better prognosis while avoiding radiation-induced lymphopenia (RIL) in patients with locally advanced esophageal squamous cell carcinoma (ESCC).

Materials and methods: Overall, 381 patients with locally advanced ESCC receiving definitive radiotherapy with or without chemotherapy (dRT ± CT) between 2014 and 2020 were included in this study. The EDIC model was calculated by radiation fraction number and mean doses to the heart, lung, and integral body. The correlation between EDIC and clinical outcomes was analyzed using Cox proportional hazards regression, and risk factors for RIL were determined by logistic regression analysis.

Results: The median EDIC was 4.38 Gy. Multivariate analysis revealed that low-EDIC significantly improved the OS of patients when compared with high-EDIC (HR = 1.614, P = 0.003) and PFS (HR = 1.401, P = 0.022). Moreover, high-EDIC was associated with a higher incidence of grade 4 RIL (OR = 2.053, P = 0.007) than low-EDIC. In addition, we identified body mass index (BMI), tumor thickness, and nodal stage as independent prognostic factors of OS and PFS, while BMI (OR = 0.576, P = 0.046) and weight loss (OR = 2.214, P = 0.005) as independent risk factors of grade 4 RIL. In subgroup analyses, the good group had better clinical outcomes than the remaining two groups (P< 0.001).

Conclusion: This study demonstrated that EDIC significantly correlates with poor clinical outcomes and severe RIL. Optimizing treatment plans to decrease the radiation doses to immune cells is critical for improving the outcomes.

KEYWORDS

effective dose to immune cells (EDIC), esophageal carcinoma, radiation-induced lymphopenia (RIL), prognosis, radiotherapy

Introduction

Esophageal cancer (EC) is among the most common malignancies in China and worldwide, with 3 million deaths annually (1–3). However, most patients are diagnosed at an advanced stage due to a lack of effective screening methods for early-stage EC (4, 5). Radiotherapy is an essential treatment strategy for patients with locally advanced EC and there has been great progress in it. Nonetheless, the prognosis of locally advanced EC remains unsatisfactory (6), with a 5-year overall survival (OS) rate of 15%–25% worldwide (7). Fortunately, immunotherapy has shown enormous promise in clinical trials, and is used in clinical practice with a dramatically improved survival rate of patients with lung cancer and malignant melanoma (8–13). In addition, the development of monoclonal antibodies, anti-programmed death-1 (PD-1) and anti-programmed death-ligand 1 (PD-L1), has produced a significant therapeutic response in EC (14). Hence, radiotherapy can be combined with immunotherapy as a novel treatment strategy for patients with EC.

The immune system is crucial for promoting tumorigenesis. However, thoracic radiotherapy alters the immune system function and thus affects tumor control. On the one hand, it stimulates the immune system by releasing specific antigens and cascade reactions of atypical cytokine signals, thereby limiting tumor growth and metastasis (15). The abscopal effect, which is tumor shrinkage outside the radiation fields, has confirmed this theory observed in animal experiments and clinical practice (16–18). On the other hand, since lymphocytes are sensitive to radiation (19, 20), radiotherapy can suppress the immune function by killing them, thereby reducing the therapeutic effect. Moreover, previous studies revealed that radiation-induced lymphopenia (RIL) is associated with poor prognosis (19, 21). Additionally, increasing the radiation dose to the tumor increases the radiation dose to immune cells. To this end, a clinical trial considered the immune system as a risky organ to calculate the effective dose to immune cells (EDIC) and found that the radiation dose of the immune system was associated with OS and local tumor control (22). Consistently, another study of non-small cell lung cancer also proved the relationship between EDIC and the prognosis of patients (23). However, there are only a few studies on this aspect in esophageal squamous cell carcinoma (ESCC). Therefore, we aimed to apply a model to calculate the EDIC, and explore the relationship of EDIC with clinical outcomes and RIL in patients with locally advanced ESCC.

Abbreviations: EDIC, effective dose to immune cells; RIL, radiation-induced lymphopenia; ESCC, esophageal squamous cell carcinoma; BMI, body mass index; EC, esophageal cancer; PD-1, programmed death-1; PD-L1, programmed death-ligand 1; TNM, tumor-node-metastasis; IMRT, intensity-modulated radiation therapy; 3D-CRT, 3-dimensional conformal radiation therapy; GTV, gross tumor volume; CTV, clinical target volume; PTV, planning target volume; OARS, organs at risk; CBC, complete blood count; DVH, dose-volume histogram; MLD, mean lung dose; MHD, mean heart dose; MBD, mean body dose; CTCAE, common terminology criteria for adverse events; ROC, receiver operating characteristic curve; OS, overall survival; PFS, progression-free survival; HR, hazard ratio; OR, odds ratio; 95% CI, confidence interval; LRFS, local recurrence-free survival; SBRT, stereotactic body radiotherapy; and RT, radiotherapy.

Materials and methods

Study population

We included 381 patients with locally advanced ESCC who underwent definitive radiotherapy with/without chemotherapy at Fujian Medical University Cancer Hospital between 2014 and 2020 in this study. This study complied with the Declaration of Helsinki and was approved by the Institutional Ethics Committee. The inclusion criteria were as follows (1): Cytologically or pathologically confirmed ESCC (2), age > 18 years (3), treatment with definitive radiotherapy (≥ 50 Gy and ≥ 25 fractions) (4), no distinct metastasis or other malignancies (5), no surgery, and (6) available clinicopathologic and follow-up data. All patients were staged according to the 8th version of AJCC.

Treatments and follow-up

Several radiotherapy oncologists comprehensively evaluated the auxiliary examinations of patients before the initiation of the treatment, under the guidance of clinical practice guidelines. All patients underwent individualized thoracic radiotherapy with either intensity-modulated radiation therapy (IMRT) or 3-dimensional conformal radiation therapy (3D-CRT). The radiation dose prescriptions were 50–70 Gy in 25–34 fractions, five days per week. The gross tumor volume (GTV) included primary esophageal tumor and involved lymph nodes. Due to micrometastasis, the clinical target volume (CTV) included GTV of ≥ 3 cm in the upper and lower margin, and 0.5 cm in the lateral margin. Based on CTV, the planning target volume (PTV) expanded by a 0.5–1 cm margin. According to the 2019 esophageal carcinoma Guidelines of the National Comprehensive Cancer Network, the plans of all patients must meet the dose-volume limitations for organs at risk (OARS). All patients received 0–7 cycles of sequential or concurrent chemotherapy. Chemotherapy regimens included docetaxel, paclitaxel + nedaplatin, cisplatin, lobaplatin or carboplatin, and 5-fluorouracil + cisplatin. The patients were followed up every three months in the first year, every six months after the second year, and then annually. Follow-up was to monitor the patient's survival status and disease changes, and the median follow-up time was 21 months.

Data collection

We extracted clinical features, including gender, age, weight change, body mass index (BMI), chemotherapy regimens, chemotherapy cycles, tumor location, tumor length, tumor thickness, TNM stage, and complete blood count (CBC), from

electronic medical records. In this study, patients with a weight loss of 1 kg or more from their usual weight at diagnosis were defined as having lost weight (within 1 month). The Pinnacle system was used to obtain the dose-volume histogram (DVH) data of patients. Mean lung dose (MLD), mean heart dose (MHD), and mean body dose (MBD) were used to calculate the EDIC of the patient. In this study, the lymphocyte count was collected before and during radiotherapy (weekly). The minimum lymphocyte count during thoracic radiotherapy was defined as the lymphocyte nadir. The Common Terminology Criteria for Adverse Events (CTCAE) version 4.0 graded RIL.

Calculation of EDIC

EDIC estimates the dose to immune cells by using the radiation dose to circulation blood as a surrogate (22, 23). The circulation blood pool that is irradiated in radiotherapy includes the heart, lungs, and the large and small vessels/capillaries in the remaining organs. Additionally, the components were estimated from anatomy/physiology textbooks to estimate the percentage of cardiac output and blood volume for each component. The heart and lungs account for about 8% and 12% of the cardiac output, respectively. In addition, the blood volume in great vessels and small vessels account for 45% and 35% of cardiac output, respectively. The dose effectiveness factor for small vessels was 0.85. The final model was developed based on the following equation for patients undergoing ≥ 25 fractions of thoracic radiation:

$$EDIC = 0.12 \star MLD + 0.08 \star MHD + [0.45 + 0.35 \star 0.85 \star (n/45)^{1/2} \star MBD]$$

Statistical analysis

The primary endpoint was OS, which was defined from the date of pathological diagnosis to death due to any cause or last follow-up. The secondary endpoint was PFS, calculated from the date of pathological diagnosis to disease progression, death, or last follow-up. The Kaplan–Meier (KM) method was used to estimate the survival curves and univariate cox analysis to identify the crucial clinical factors that affect survival outcomes. The covariates with a P value< 0.05 in univariate analysis were incorporated into the multivariate analysis, which identified the independent prognostic factors. We evaluated the correlations among independent prognostic factors using Spearman correlation analysis. The logistic regression analysis was used to identify the potential risk factors with grade 4 RIL. The receiver operating characteristics (ROC) curve computed the optimal cut-off values of BMI, tumor length, tumor thickness, and EDIC. All statistical analyses were two-sided, and P value of < 0.05 was considered statistically significant. All statistical analyses were performed using SPSS software (version 25.0).

Results

Patient characteristics

In all, we included 381 patients in the final analysis and the clinical characteristics are summarized in Table 1. The median age of patients was 67 and 69.6% were males. Approximately 49.6% of patients experienced weight loss. Chemotherapy accounted for 75.1% and 56.4% of patients received concurrent chemoradiotherapy. Most common primary tumors were located in the upper (34.4%) and lower (48.3%) thorax. About 23.1% of the patients were at stage II, 29.4% were at stage III, and 47.5% at were stage IVA. The rates of grades 1, 2, 3, and 4 RIL were 1.3%, 15.0%, 62.2%, and 21.5%. The cut-off values for BMI, tumor length, tumor thickness, and EDIC were 19.03, 5.9 cm, 1.7 cm, and 4.78 Gy.

Prognostic factors of OS and PFS

The median OS and PFS were 21 months (range, 2.1–105.6 months) and 17.2 months (range, 1.2–101.4 months), respectively. Using univariate analysis, we identified BMI (P = 0.001), tumor location (P = 0.025), tumor length (P< 0.001), tumor thickness (P< 0.001), N stage (P = 0.001), TNM stage (P = 0.004), and EDIC (P< 0.001) as significant prognostic factors of a worse OS (Table 2). Of these, the multivariate analysis identified BMI (HR = 0.619, 95%CI, 0.452-0.848, p = 0.003), tumor thickness (HR = 1.859, 95% CI: 1.313–2.630, P< 0.001), N stage (HR = 1.534, 95% CI: 1.102–2.134, P = 0.011), and EDIC (HR = 1.614, 95% CI, 1.176–2.215, P = 0.003) as independent risk factors of OS. Additionally, univariate analysis recognized BMI (P = 0.001), tumor length (P< 0.001), tumor thickness (P< 0.001), N stage (P = 0.001), TNM stage (P< 0.001), and EDIC (p = 0.002) as significant prognostic factors of a worse PFS (Table 3). On multivariate analysis, BMI (HR = 0.667, 95% CI: 0.494–0.900, P = 0.008), tumor thickness (HR = 1.797, 95% CI: 1.282–2.517, P = 0.001), N stage (HR = 1.396, 95% CI: 1.021–1.910, P = 0.037), and EDIC (HR = 1.401, 95% CI: 1.050–1.869, P = 0.022) were identified as independent risk factors of PFS. After adjusting for other risk factors, EDIC was identified as a significant prognostic factor for both, OS and PFS. Spearman's analysis results showed that there is no correlation or weak correlation between the prognostic factors (correlation coefficient: 0.150 - 0.207). As shown in Figure 1, there were noteworthy differences in the OS and PFS in EDIC, BMI, tumor thickness, and N stage.

Further, to determine the association of EDIC with clinical outcomes, we divided EDIC into three categories according to cut-off values (< 4.19 Gy, 4.19–5.38 Gy, and ≥ 5.38 Gy) and equal study population (< 3.63 Gy, 3.63–5.35 Gy, and ≥ 5.35 Gy). The OS and PFS rates for EDIC divided into three groups based on the cut-off values are shown in Figure 2 (P< 0.001 and P = 0.0014). Patients with EDIC ≥ 5.38 Gy had significantly worse OS and PFS than those with EDIC< 4.19 Gy (P< 0.001 and P = 0.005). Comparisons between other groups were not statistically significant. The median OS for patients with EDIC ≥ 5.38 Gy and< 4.19 Gy were 23.6 and 51.3 months, respectively. The median PFS for patients

10.3389/fimmu.2023.1066255

TABLE 1 Patient clinical characteristics.

Characteristics		No.of patients (n = 381)
Age (years)		
	< 67	180 (47.2%)
	≥ 67	201 (52.8%)
Gender		
	Male	265 (69.6%)
	Female	116 (30.4%)
Weight loss		
	No	192 (50.4%)
	Yes	189 (49.6%)
BMI		
	< 19.03	100 (26.2%)
	≥ 19.03	281 (73.8%)
Radiotherapy		
	IMRT	299 (78.5%)
	3D-CRT	82 (21.5%)
Chemotherapy		
	concurrent chemotherapy	215 (56.4%)
	sequential chemotherapy	71(18.6%)
	without chemotherapy	95 (24.9%)
Chemotherapy regimen		
	paclitaxel + platinum	198(52.0%)
	5-fluorouraci + platinum	50(13.1%)
	docetaxel + platinum	38(10.0%)
	no	95 (24.9%)
Tumor location		
	Cervical	37 (9.7%)
	Upper thoracic	131 (34.4%)
	Middle thoracic	29 (7.6%)
	Lower thoracic	184 (48.3%)
Tumor length (cm)		
	< 5.9	209 (54.9%)
	≥ 5.9	172 (45.1%)
Tumor thickness (cm)		
	< 1.7	276 (72.4%)
	≥ 1.7	105 (27.6%)
T stage		
	T2	26 (6.8%)
	T3	188 (49.3%)
	T4	167 (43.8%)
N stage		
	N0	111 (29.1%)
	N1	165 (43.3%)
	N2	83 (21.8%)
	N3	22 (5.8%)
TNM stage		
	Stage II	88 (23.1%)
	Stage III	112 (29.4%)
	Stage IVA	181 (47.5%)
Radiation-induced lymphopenia		
	Grade 1	5 (1.3%)
	Grade 2	57 (15.0%)
	Grade 3	237 (62.2%)
	Grade 4	82 (21.5%)
EDIC		
	< 4.78	217 (57.0%)
	≥ 4.78	164 (43.0%)

BMI, body mass index; IMRT, intensity-modulated radiation therapy; 3D-CRT, 3-dimensional conformal radiation therapy; T, tumor; N, node; TNM, tumor-node-metastasis; EDIC, effective dose to the immune cell; RIL, radiation-induced lymphopenia.

with EDIC ≥ 5.38 Gy and< 4.19 Gy were 20.6 and 45.1 months, respectively. Furthermore, EDIC was divided into three groups according to the equal study population. The OS and PFS curves of the two EDICs are shown in Figure 3 (P = 0.001 and P = 0.0029). Patients with EDIC ≥ 5.35 Gy had significantly worse OS and PFS than those with EDIC< 3.63 Gy (P = 0.001 and P = 0.029). Both approaches showed a strong correlation of EDIC scores with OS and PFS.

Survival is stratified by EDIC, BMI, tumor thickness, and N stage

The EDIC, BMI, tumor thickness, and N stage were crucial prognostic factors for survival. Patients with EDIC ≥ 4.78 Gy, BMI< 19.03, tumor thickness ≥ 1.7 cm, and N2/N3 were considered to have one score. We observed that the lower the score, the worse the prognosis. Then, we divided the patients into three groups based on the independent prognostic factors: the poor group (0–1 scores), the intermediate group (2 scores), and the good group (≥ 3 scores). KM curves showed prominent differences in the OS (P<0.001) and PFS (P<0.001) among the three groups (Figure 4).

10.3389/fimmu.2023.1066255

TABLE 2 Univariate and multivariate cox regression analysis of patient clinical characteristics with overall survival.

Characteristics	Univariate analysis			Multivariate analysis		
	HR	95% CI	P value	HR	95% CI	P value
Age (years)						
≥ 67 vs< 67	1.343	0.998-1.808	0.052			
Gender						
Female vs Male	1.108	0.805-1.618	0.220			
Weight loss						
Yes vs No	1.247	0.930-1.673	0.141			
BMI						
≥ 19.03 vs< 19.03	0.586	0.432-0.797	0.001	0.619	0.452-0.848	0.003
Radiotherapy						
IMRT vs 3D-CRT	1.187	0.818-1.723	0.368			
Chemotherapy						
Concurrent vs sequential vs without	1.092	0.917-1.300	0.325			
Tumor location						
Cervical/Upper vs Middle/Lower	1.411	1.044-1.908	0.025	1.162	0.845-1.598	0.357
Tumor length (cm)						
≥ 5.9 vs< 5.9	1.921	1.428-2.585	< 0.001	1.296	0.920-1.825	0.138
Tumor thickness (cm)						
≥ 1.7 vs< 1.7	2.306	1.704-3.121	< 0.001	1.859	1.313-2.630	< 0.001
T stage						
T4 vs T2/T3	1.112	0.830-1.491	0.477			
N stage						
N2/N3 vs N0/N1	1.691	1.244-2.298	0.001	1.534	1.102-2.134	0.011
TNM stage						
Stage III/Stage IVA vs Stage II	1.818	1.207-2.741	0.004	1.173	0.752-1.830	0.482
EDIC						
≥ 4.78 vs< 4.78	1.879	1.398-2.524	< 0.001	1.614	1.176-2.215	0.003
RIL						
Grade 4 vs Grade ≤3	1.141	0.805-1.618	0.458			

HR, hazard ratio; CI, confidence interval; BMI, body mass index; IMRT, intensity-modulated radiation therapy; 3D-CRT, 3-dimensional conformal radiation therapy; T, tumor; N, node; TNM, tumor-node-metastasis; EDIC, effective dose to the immune cell; RIL, radiation-induced lymphopenia.

Risk factors of RIL

The lymphocyte count declined remarkably during thoracic radiotherapy, and the median lymphocyte nadir was $0.4*10^9$/L. Univariate logistic analysis showed that lower EDIC was associated with a higher lymphocyte count (P = 0.004). The multivariate logistic regression analysis revealed that EDIC was significantly correlated with RIL (OR, 2.053, 95% CI: 1.221–3.451, P = 0.007) after adjusting for other confounding variables. In addition, the BMI (P = 0.046) and weight loss (P = 0.005) were independent risk factors of RIL (Table 4).

Discussion

This study included 381 patients with locally advanced ESCC and revealed that EDIC is correlated with RIL during thoracic radiotherapy, and is an important prognostic factor for both, OS and PFS. These findings implicate that undue radiation doses to immune cells, especially lymphocytes, lead to severe lymphopenia and poor clinical outcomes.

Previous studies reported that high heart and lung radiation doses are significantly associated with decreased OS (24, 25). Someone argued that heart and lung toxicity leads to poor

10.3389/fimmu.2023.1066255

TABLE 3 Univariate and multivariate cox regression analysis of patient clinical characteristics with progression free-survival.

Characteristics	Univariate analysis			Multivariate analysis		
	HR	95% CI	P value	HR	95% CI	P value
Age (years)						
≥ 67 vs< 67	1.189	0.897-1.574	0.229			
Gender						
Female vs Male	1.091	0.935-1.274	0.268			
Weight loss						
Yes vs No	1.297	0.980-1.717	0.069			
BMI						
≥ 19.03 vs< 19.03	0.612	0.456-0.822	0.001	0.667	0.494-0.900	0.008
Radiotherapy						
IMRT vs 3D-CRT	1.023	0.714-1.466	0.902			
Chemotherapy						
Concurrent vs sequential vs without	1.034	0.875-1.223	0.692			
Tumor location						
Cervical/Upper vs Middle/Lower	1.261	0.949-1.676	0.110			
Tumor length (cm)						
≥ 5.9 vs< 5.9	1.841	1.389-2.441	< 0.001	1.238	0.893-1.718	0.201
Tumor thickness (cm)						
≥ 1.7 vs< 1.7	2.219	1.659-2.969	< 0.001	1.797	1.282-2.517	0.001
T stage						
T4 vs T2/T3	1.231	0.932-1.626	0.143			
N stage						
N2/N3 vs N0/N1	1.613	1.202-2.164	0.001	1.396	1.021-1.910	0.037
TNM stage						
Stage III/Stage IVA vs Stage II	2.038	1.365-3.042	< 0.001	1.421	0.923-2.186	0.110
EDIC						
≥ 4.78 vs< 4.78	1.566	1.182-2.075	0.002	1.401	1.050-1.869	0.022
RIL						
Grade 4 vs Grade ≤3	1.053	0.751-1.477	0.766			

HR, hazard ratio; CI, confidence interval; BMI, body mass index; IMRT, intensity-modulated radiation therapy; 3D-CRT, 3-dimensional conformal radiation therapy; T, tumor; N, node; TNM, tumor-node-metastasis; EDIC, effective dose to the immune cell; RIL, radiation-induced lymphopenia.

survival. However, according to the RTOG 0617 trial, the high-dose group had lower heart and lung toxicity than the low-dose group (22). Additionally, in multivariate cox analysis, MHD was significantly associated with local recurrence-free survival (LRFS), while MLD was important for PFS. This suggests that MHD and MLD were correlated with survival because of disease control or progression and not toxicity (22). Instead, MHD and MLD may be a surrogate for radiation dose to circulating lymphocytes in blood and are vital for tumor development. Therefore, the EDIC model was developed to predict the dose to circulating lymphocytes from the mean heart, lung, and body doses.

Circulating lymphocytes are among the most radiosensitive cells with a D50 (dose required for 50% pre-treatment lymphocyte cell death) of approximately 2 Gy. RIL is a common phenomenon observed during radiotherapy. The significance of EDIC for RIL in this study is consistent with previous findings (20) and can be explained by the principles of radiobiology. Moreover, several studies demonstrated that dosimetric factors, such as heart V50 and lung V5 in lung

10.3389/fimmu.2023.1066255

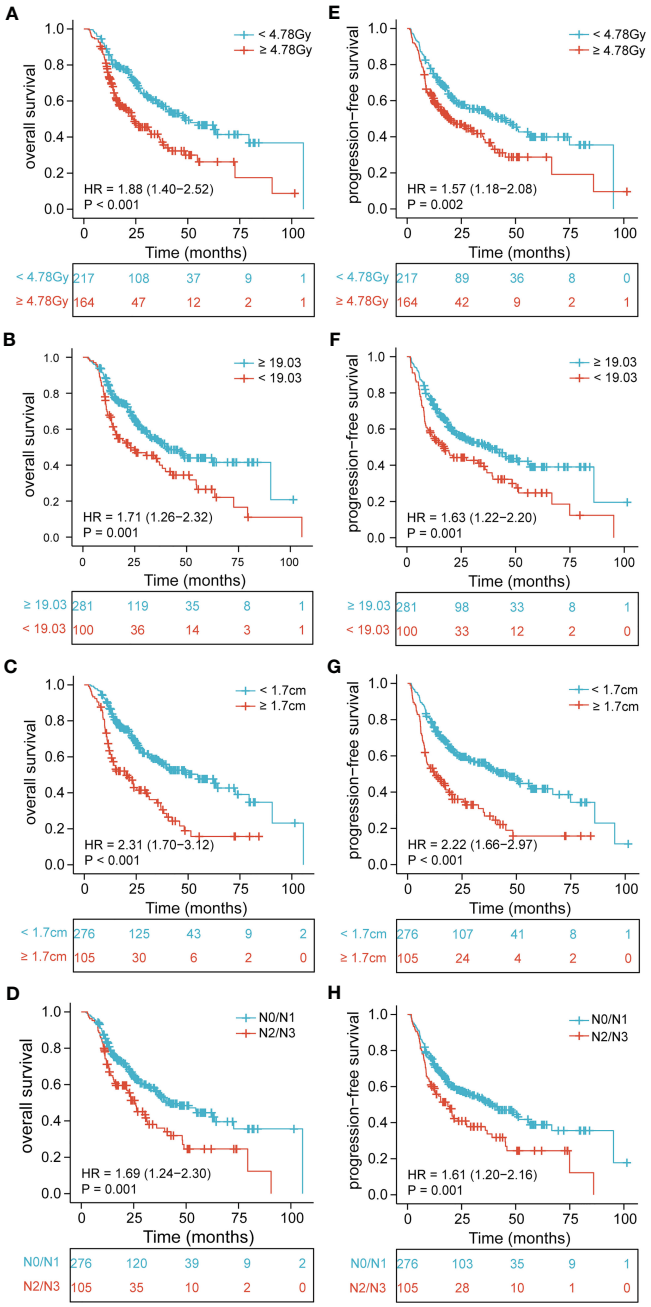

FIGURE 1
Kaplan-Meier curves of EDIC, BMI, tumor thickness, and N stage for all patients showing **(A–D)** overall survival (p< 0.001, p = 0.001, p< 0.001, p = 0.001, respectively); **(E–H)** progression-free survival (p = 0.002, p = 0.001, p< 0.001, p = 0.001, respectively). EDIC, effective dose to the immune cell; BMI, body mass index; HR, hazard ratio; N, node.

cancer and mean body dose in EC, are essential risk factors (19, 26, 27).

Radiotherapy causes immunosuppression by killing circulating lymphocytes in many solid tumor treatments. Thus, it could theoretically reduce the treatment efficacy and affect the prognosis, and is considered a negative prognostic factor in malignant solid tumors (19, 28). Nonetheless, the decrease in lymphocyte count after irradiation is not always associated with poor post-treatment survival outcomes. For instance, in a study of 395 EC patients, the 5-year OS difference between grade 4 and non-grade 4 lymphopenia was not statistically significant (29). Similarly, 83% of the patients with oropharyngeal cancer receiving definitive CRT at the MD Anderson Cancer Center had ≥ grade 3 and 25% had grade 4 lymphopenia, which did not affect the survival or local control outcomes (30). Similarly, Holub et al. did not find an association between post-treatment lymphopenia and survival outcomes (31). Likewise, we observed no difference in OS and PFS between grade 4 RIL compared with grades 1–3. The median survival of patients with grade 1–3 RIL was 6 months longer than those with grade 4 (36.8 vs. 30.4 months); however, the difference

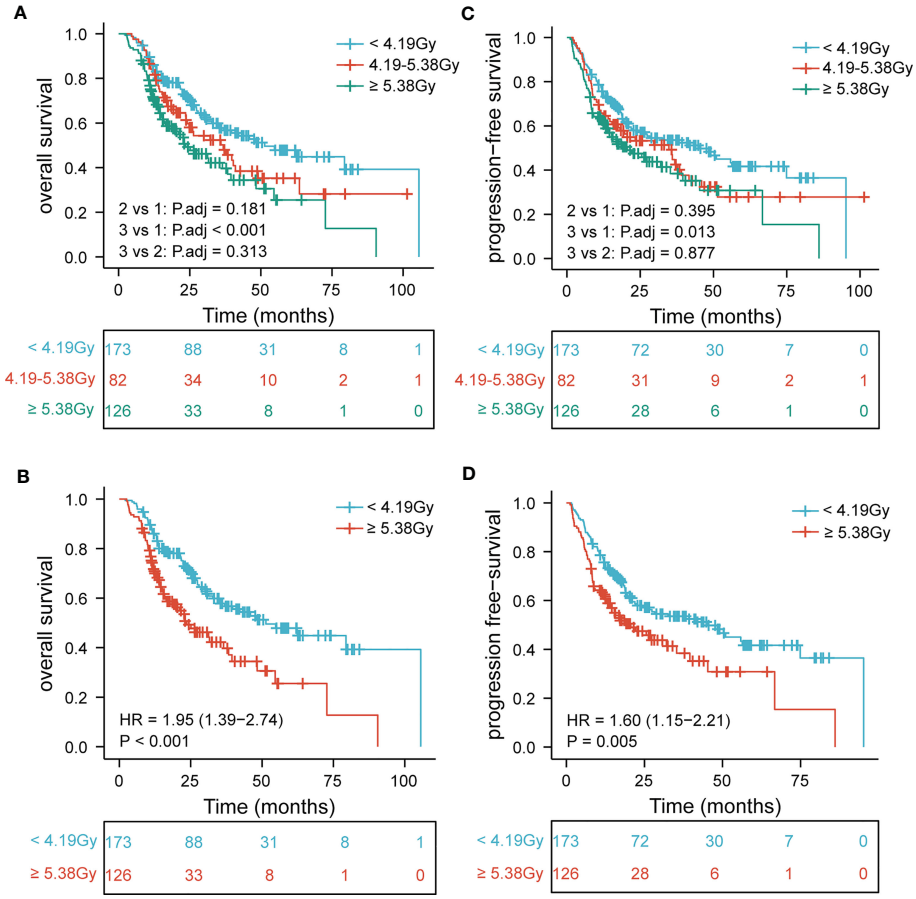

FIGURE 2
Patients are stratified by EDIC cut-off values. Kaplan-Meier curves for **(A)** overall survival by three categories; **(B)** overall survival first versus third; **(C)** progression-free survival by three categories; **(D)** progression-free survival first versus third. EDIC, effective dose to the immune cell; R, hazard ratio.

was not statistically significant. Therefore, the relationship between RIL and prognosis is unclear. Several reasons may account for the negative results in this study. Firstly, in addition to direct damage to lymphocytes by RT, lymphocytes infiltrating from peripheral blood after RT stimulation might also contribute to circulating lymphopenia. Second, the radiosensitivity of lymphocytes also represents the radiosensitivity of cancer cells, which predicts better survival (32). Third, there may be a bias in the lymphocyte nadir because more than half of the patients in this research received chemotherapy, which often has considerable hematological toxicity, especially for patients receiving concurrent chemoradiotherapy. Finally, since lymphocyte changes dynamically during radiotherapy, it is difficult to evaluate the immune status of patients using only the lymphocyte nadir, which results in negative results.

Our study confirmed the association between EDIC and RIL and revealed the impact of EDIC on the survival of patients with locally advanced ESCC. Consistently, previous studies demonstrated that high EDIC was an important risk factor for OS, PFS, and disease-free survival in lung cancer (23, 33). This may be due to the radiation-induced damage to immune cells, which are vital for limiting metastatic growth and maintaining the spreading cancer cells in an inert state (34–36). Tumor progression is the leading cause of death in patients with cancer. Although EDIC is an objective variable influenced by radiotherapy planning, its potential determinants, such as tumor size and N stage, were not considered, which may be related to clinical outcomes. The number of positive lymph nodes and tumor size are negatively associated with the survival of patients with EC (37). In addition, tumor size and N stage can affect the radiation area and dose during the development of radiotherapy schedules. Large GTV was a risk factor for worse OS and PFS in previous studies (38, 39). However, after adjusting for GTV size effects, a second study of RTOG0617 data revealed that EDIC was still substantially linked with OS and LPFS (22). Another study suggested that PTV did not correlate with OS or LPFS (23). Interestingly, spearman's analysis results showed that there is no correlation or weak correlation between EDIC and tumor thickness or N stage in this study. In all, the survival significance of EDIC may provide new insights into treatment schedule optimization in our daily practice.

The EDIC scoring is a powerful tool to assist clinicians in identifying high-risk patients for early intervention. It is a combined influence of beam-on time, radiation dose, and immune cell fractions. Hence, several approaches related to these factors can potentially decrease EDIC. Advanced radiotherapy techniques, such as high-dose, hypofractionated SBRT, and high-dose-rate FLASH

10.3389/fimmu.2023.1066255

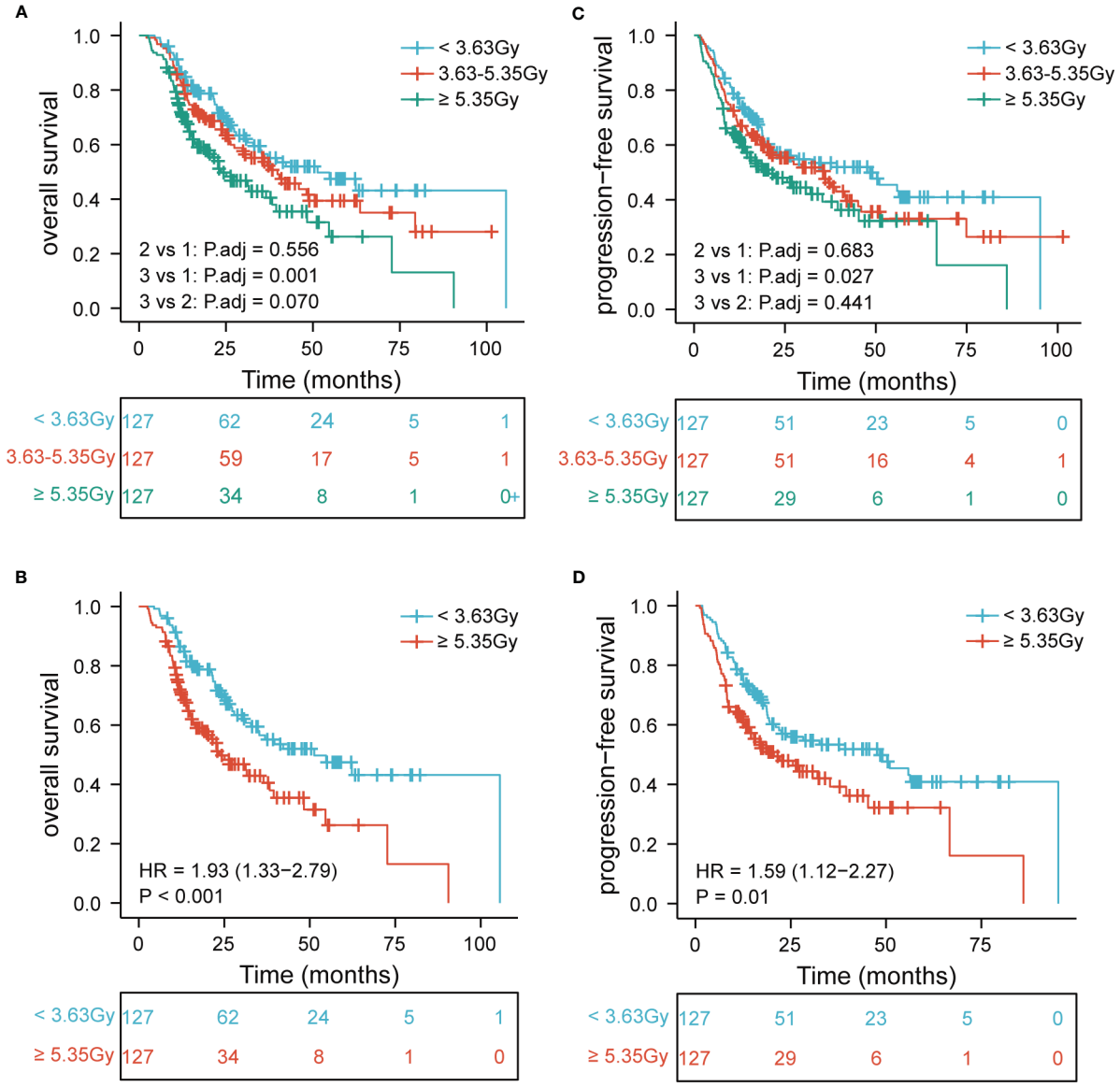

FIGURE 3
Patients are stratified by the equal study population. Kaplan-Meier curves for **(A)** overall survival by three categories; **(B)** overall survival first versus third; **(C)** progression-free survival by three categories; **(D)** progression-free survival first versus third. EDIC, effective dose to the immune cell; R, hazard ratio.

RT, reduce radiation delivery time thereby decreasing the circulating blood exposure (40). Moreover, proton beam therapy has better dose distribution and significantly lowers the dose in surrounding normal tissues than IMRT. Near the heart and lungs can drop the dose sharply (41). Of course, there are other advanced radiotherapy technologies, such as image-guided adaptive therapy and heavy ions therapy. From the perspective of clinicians, it is important to optimize planning by adjusting beam energy and direction and the number of beams before therapy. In addition, to accommodate anatomical changes and tumor regression, we may need to optimize the treatment plan again.

This study has certain limitations. Firstly, since it was a retrospective study, there was inevitable selection bias and did not consider all confounding factors, such as chemotherapy regimen, radiotherapy dose, and target volume size (such as GTV or PTV). Secondly, the EDIC equation only considered the estimate of circulating or resident immune cell pools in large organs within the radiation field, including the heart, lungs, liver, and kidneys. It did not incorporate the contributions of lymphatic vessels, lymph nodes, thymus, spleen, and bone marrow. Hence, it may not fully represent of the influence of radiation on the immune cells. Although the contribution of bone marrow to acute lymphopenia is small, it plays a role in lymphocyte recovery after treatment. The adult thymus is degenerated, hence its contribution to the associated lymphocyte pool is small. Additionally, due to anatomical location, the radiation dose to the spleen in thoracic radiotherapy is limited and has little effect on lymphopenia. Therefore, we need to refine the EDIC model by including

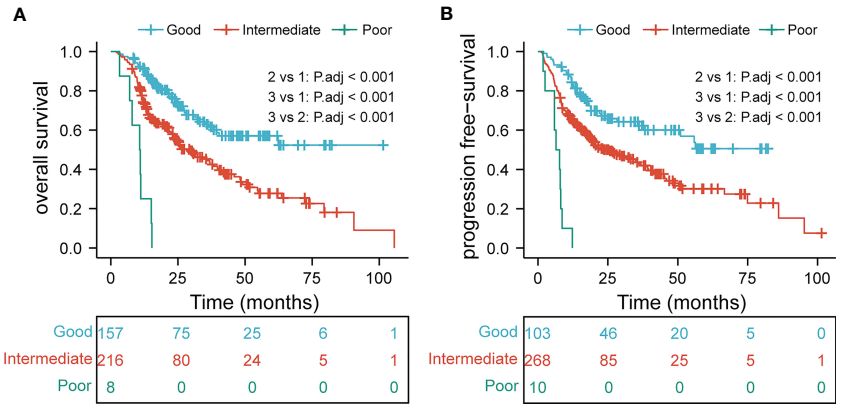

FIGURE 4
overall survival **(A)** and progression-free survival **(B)** in subgroup analysis based on multivariate analysis results.

TABLE 4 Univariate and multivariate logistic regression analysis for radiation-induced lymphopenia.

Characteristics	Univariate analysis			Multivariate analysis		
	OR	95% CI	P value	OR	95% CI	P value
Age (years)						
≥ 67 vs < 67	0.984	0.603-1.605	0.948			
Gender						
Female vs Male	1.074	0.629-1.835	0.794			
Weight loss						
Yes vs No	2.050	1.239-3.392	0.005	2.214	1.258-3.586	0.005
BMI						
≥ 19.03 vs < 19.03	0.494	0.293-0.831	0.008	0.576	0.335-0.989	0.046
Radiotherapy						
IMRT vs 3D-CRT	0.942	0.516-1.716	0.844			
Chemotherapy						
Concurrent vs sequential vs without	0.872	0.648-1.172	0.363			
Tumor location						
Cervical/Upper vs Middle/Lower	1.486	0.898-2.458	0.123			
Tumor length (cm)						
≥ 5.9 vs < 5.9	1.992	1.213-3.272	0.006	1.646	0.982-2.758	0.059
Tumor thickness (cm)						
≥ 1.7 vs < 1.7	1.293	0.760-2.200	0.343			
T stage						
T4 vs T2/T3	0.829	0.505-1.363	0.460			
N stage						
N2/N3 vs N0/N1	1.495	0.884-2.527	0.133			
TNM stage						

(Continued)

TABLE 4 Continued

Characteristics	Univariate analysis			Multivariate analysis		
	OR	95% CI	P value	OR	95% CI	P value
Stage III/Stage IVA vs Stage II	1.308	0.713-2.401	0.386			
EDIC						
≥ 4.78 vs < 4.78	2.089	1.273-3.428	0.004	2.053	1.221-3.451	0.007

OR, odds ratio; CI, confidence interval; BMI, body mass index; IMRT, intensity-modulated radiation therapy; 3D-CRT, 3-dimensional conformal radiation therapy; T, tumor; N, node; TNM, tumor-node-metastasis; EDIC, effective dose to the immune cell.

lymphoid structures and other related organs. Lastly, this is a single-center, small-sample study that needs to be validated by a prospective multicenter study with a larger sample size.

Conclusion

This study identified a correlation of EDIC with poor clinical outcomes and severe RIL, which indicates that high doses to the immune system were related to tumor progression and death. Hence, it is important to optimize treatment plans to decrease the radiation doses to immune cells for improving the clinical outcomes.

Data availability statement

The raw data supporting the conclusions of this article will be made available by the authors, without undue reservation.

Ethics statement

The studies involving human participants were reviewed and approved by the ethics committee of Fujian Medical University Cancer Hospital. The patients/participants provided their written informed consent to participate in this study.

Author contributions

QY, ZW and JQ designed this study. JQ, DK, YY, HQ, and JX contributed to data collection. HCL, HL, and QZ analyzed the data. JL and QY supervised the study. JQ, LL, HZ, and ZW wrote the manuscript. All authors contributed to the article and approved the submitted version.

Funding

This work was supported by the National Clinical Key Specialty Construction Program (Grant No. 2021), the Joint Funds for the Innovation of Science and Technology, Fujian province (Grant Nos. 2019Y9041), Fujian provincial Clinical Research Center for Cancer Radiotherapy and Immunotherapy (2020Y2012), and Fujian Clinical Research Center for Radiation and Therapy of Digestive, Respiratory and Genitourinary Malignancies(2021Y2014).

Acknowledgments

We thank the patients and their families, along with all the investigators. Thanks to the funding center for their support and Bullet Edits Limited for the linguistic editing and proofreading of the manuscript.

Conflict of interest

The authors declare that the research was conducted in the absence of any commercial or financial relationships that could be construed as a potential conflict of interest.

Publisher's note

Supplementary material

The Supplementary Material for this article can be found online at: https://www.frontiersin.org/articles/10.3389/fimmu.2023.1066255/full#supplementary-material

References

1. Siegel RL, Miller KD, Fuchs HE, Jemal A. Cancer statistics, 2022. *CA Cancer J Clin* (2022) 72(1):7–33. doi: 10.3322/caac.21708

2. Miller KD, Nogueira L, Devasia T, Mariotto AB, Yabroff KR, Jemal A, et al. Cancer treatment and survivorship statistics, 2022. *CA Cancer J Clin* (2022) 72(5):409–36. doi: 10.3322/caac.21731

3. Wang S, Zheng R, Arnold M, Abnet C, Zeng H, Zhang S, et al. Global and national trends in the age-specific sex ratio of esophageal cancer and gastric cancer by subtype. *Int J Cancer* (2022) 151(9):1447–61. doi: 10.1002/ijc.34158

4. Abbas G, Krasna M. Overview of esophageal cancer. *Ann Cardiothorac Surg* (2017) 6(2):131–6. doi: 10.21037/acs.2017.03.03

5. Smyth EC, Lagergren J, Fitzgerald RC, Lordick F, Shah MA, Lagergren P, et al. Oesophageal cancer. *Nat Rev Dis Primers 3 17048* (2017). doi: 10.1038/nrdp.2017.48

6. Antonia SJ, Villegas A, Daniel D, Vicente D, Murakami S, Hui R, et al. Overall survival with durvalumab after chemoradiotherapy in stage III NSCLC. *N Engl J Med* (2018) 379(24):2342–50. doi: 10.1056/NEJMoa1809697

7. Pennathur A, Gibson MK, Jobe BA, Luketich JD. Oesophageal carcinoma. *Lancet* (2013) 381(9864):400–12. doi: 10.1016/S0140-6736(12)60643-6

8. Guibert N, Mazieres J. Nivolumab for treating non-small cell lung cancer. *Expert Opin Biol Ther* (2015) 15(12):1789–97. doi: 10.1517/14712598.2015.1114097

9. Hodi FS, O'Day SJ, McDermott DF, Weber RW, Sosman JA, Haanen JB, et al. Improved survival with ipilimumab in patients with metastatic melanoma. *N Engl J Med* (2010) 363(8):711–23. doi: 10.1056/NEJMoa1003466

10. Weber J, Mandala M, Del Vecchio M, Gogas HJ, Arance AM, Cowey CL, et al. Adjuvant nivolumab versus ipilimumab in resected stage III or IV melanoma. *N Engl J Med* (2017) 377(19):1824–35. doi: 10.1056/NEJMoa1709030

11. Robert C, Schachter J, Long GV, Arance A, Grob JJ, Mortier L, et al. Pembrolizumab versus ipilimumab in advanced melanoma. *N Engl J Med* (2015) 372 (26):2521–32. doi: 10.1056/NEJMoa1503093

12. Reck M, Rodriguez-Abreu D, Robinson AG, Hui R, Csoszi T, Fulop A, et al. Pembrolizumab versus chemotherapy for PD-L1-Positive non-Small-Cell lung cancer. *N Engl J Med* (2016) 375(19):1823–33. doi: 10.1056/NEJMoa1606774

13. Rittmeyer A, Barlesi F, Waterkamp D, Park K, Ciardiello F, von Pawel J, et al. Atezolizumab versus docetaxel in patients with previously treated non-small-cell lung cancer (OAK): a phase 3, open-label, multicentre randomised controlled trial. *Lancet* (2017) 389(10066):255–65. doi: 10.1016/S0140-6736(16)32517-X

14. Kudo T, Hamamoto Y, Kato K, Ura T, Kojima T, Tsushima T, et al. Nivolumab treatment for oesophageal squamous-cell carcinoma: an open-label, multicentre, phase 2 trial. *Lancet Oncol* (2017) 18(5):631–9. doi: 10.1016/S1470-2045(17)30181-X

15. Formenti SC, Demaria S. Combining radiotherapy and cancer immunotherapy: a paradigm shift. *J Natl Cancer Inst* (2013) 105(4):256–65. doi: 10.1093/jnci/djs629

16. Lee Y, Auh SL, Wang Y, Burnette B, Wang Y, Meng Y, et al. Therapeutic effects of ablative radiation on local tumor require CD8+ T cells: changing strategies for cancer treatment. *Blood* (2009) 114(3):589–95. doi: 10.1182/blood-2009-02-206870

17. Vanpouille-Box C, Formenti SC, Demaria S. Toward precision radiotherapy for use with immune checkpoint blockers. *Clin Cancer Res* (2018) 24(2):259–65. doi: 10.1158/1078-0432.CCR-16-0037

18. Postow MA, Callahan MK, Barker CA, Yamada Y, Yuan J, Kitano S, et al. Immunologic correlates of the abscopal effect in a patient with melanoma. *N Engl J Med* (2012) 366(10):925–31. doi: 10.1056/NEJMoa1112824

19. Davuluri R, Jiang W, Fang P, Xu C, Komaki R, Gomez DR, et al. Lymphocyte nadir and esophageal cancer survival outcomes after chemoradiation therapy. *Int J Radiat Oncol Biol Phys* (2017) 99(1):128–35. doi: 10.1016/j.ijrobp.2017.05.037

20. Yovino S, Kleinberg L, Grossman SA, Narayanan M, Ford E. The etiology of treatment-related lymphopenia in patients with malignant gliomas: modeling radiation dose to circulating lymphocytes explains clinical observations and suggests methods of modifying the impact of radiation on immune cells. *Cancer Invest* (2013) 31(2):140–4. doi: 10.3109/07357907.2012.762780

21. Qian D, Wang Y, Zhao G, Cao F, Er P, Chen X, et al. Tumor remission and tumor-infiltrating lymphocytes during chemoradiation therapy: predictive and prognostic markers in locally advanced esophageal squamous cell carcinoma. *Int J Radiat Oncol Biol Phys* (2019) 105(2):319–28. doi: 10.1016/j.ijrobp.2019.06.079

22. Jin JY, Hu C, Xiao Y, Zhang H, Paulus R, Ellsworth SG, et al. Higher radiation dose to the immune cells correlates with worse tumor control and overall survival in patients with stage III NSCLC: a secondary analysis of RTOG0617. *Cancers (Basel)* (2021) 13(24). doi: 10.3390/cancers13246193

23. Ladbury CJ, Rusthoven CG, Camidge DR, Kavanagh BD, Nath SK. Impact of radiation dose to the host immune system on tumor control and survival for stage III non-small cell lung cancer treated with definitive radiation therapy. *Int J Radiat Oncol Biol Phys* (2019) 105(2):346–55. doi: 10.1016/j.ijrobp.2019.05.064

24. Tucker SL, Liu A, Gomez D, Tang LL, Allen P, Yang J, et al. Impact of heart and lung dose on early survival in patients with non-small cell lung cancer treated with chemoradiation. *Radiother Oncol* (2016) 119(3):495–500. doi: 10.1016/j.radonc.2016.04.025

25. Speirs CK, DeWees TA, Rehman S, Molotievschi A, Velez MA, Mullen D, et al. Heart dose is an independent dosimetric predictor of overall survival in locally advanced non-small cell lung cancer. *J Thorac Oncol* (2017) 12(2):293–301. doi: 10.1016/j.jtho.2016.09.134

26. Contreras JA, Lin AJ, Weiner A, Speirs C, Samson P, Mullen D, et al. Cardiac dose is associated with immunosuppression and poor survival in locally advanced non-small cell lung cancer. *Radiother Oncol* (2018) 128(3):498–504. doi: 10.1016/j.radonc.2018.05.017

27. Tang C, Liao Z, Gomez D, Levy L, Zhuang Y, Gebremichael RA, et al. Lymphopenia association with gross tumor volume and lung V5 and its effects on non-small cell lung cancer patient outcomes. *Int J Radiat Oncol Biol Phys* (2014) 89 (5):1084–91. doi: 10.1016/j.ijrobp.2014.04.025

28. Liu LT, Chen QY, Tang LQ, Guo SS, Guo L, Mo HY, et al. The prognostic value of treatment-related lymphopenia in nasopharyngeal carcinoma patients. *Cancer Res Treat* (2018) 50(1):19–29. doi: 10.4143/crt.2016.595

29. Zhang M, Oh P, Brady P, Ilson DH, Janjigian Y, Ku G, et al. Lack of validation of lymphopenia as a prognostic factor in esophageal cancer chemoradiation. *Int J Radiat OncologyBiologyPhysics* (2018) 102(3). doi: 10.1016/j.ijrobp.2018.07.456

30. Ng SP, Bahig H, Jethanandani A, Pollard C, Berends J, Sturgis EM, et al. Lymphopenia during radiotherapy in patients with oropharyngeal cancer. *Radiother Oncol* (2020) 145:95–100. doi: 10.1016/j.radonc.2019.12.023

31. Holub K, Vargas A, Biete A. Radiation-induced lymphopenia: the main aspects to consider in immunotherapy trials for endometrial and cervical cancer patients. *Clin Transl Oncol* (2020) 22(11):2040–8. doi: 10.1007/s12094-020-02345-3

32. Slonina D, Gasinska A. Intrinsic radiosensitivity of healthy donors and cancer patients as determined by the lymphocyte micronucleus assay. *Int J Radiat Biol* (1997) 72(6):693–701. doi: 10.1080/095530097142852

33. Yu Y, Fu P, Jin JY, Gao S, Wang W, Machtay M, et al. Impact of effective dose to immune cells (EDIC) on lymphocyte nadir and survival in limited-stage SCLC. *Radiother Oncol* (2021) 162:26–33. doi: 10.1016/j.radonc.2021.06.020

34. Kim K, Marquez-Palencia M, Malladi S. Metastatic latency, a veiled threat. *Front Immunol* (2019) 10:1836. doi: 10.3389/fimmu.2019.01836

35. Linde N, Fluegen G, Aguirre-Ghiso JA. The relationship between dormant cancer cells and their microenvironment. *Adv Cancer Res* (2016) 132:45–71. doi: 10.1016/bs.acr.2016.07.002

36. Baxevanis CN, Perez SA. Cancer dormancy: a regulatory role for endogenous immunity in establishing and maintaining the tumor dormant state. *Vaccines (Basel)* (2015) 3(3):597–619. doi: 10.3390/vaccines3030597

37. Rice TW, Patil DT, Blackstone EH. 8th edition AJCC/UICC staging of cancers of the esophagus and esophagogastric junction: application to clinical practice. *Ann Cardiothorac Surg* (2017) 6(2):119–30. doi: 10.21037/acs.2017.03.14

38. Kwint M, Stam B, Proust-Lima C, Philipps V, Hoekstra T, Aalbersberg E, et al. The prognostic value of volumetric changes of the primary tumor measured on cone beam-CT during radiotherapy for concurrent chemoradiation in NSCLC patients. *Radiother Oncol* (2020) 146:44–51. doi: 10.1016/j.radonc.2020.02.002

39. Nygard L, Vogelius IR, Fischer BM, Kjaer A, Langer SW, Aznar MC, et al. A competing risk model of first failure site after definitive chemoradiation therapy for locally advanced non-small cell lung cancer. *J Thorac Oncol* (2018) 13(4):559–67. doi: 10.1016/j.jtho.2017.12.011

40. Jin JY, Gu A, Wang W, Oleinick NL, Machtay M, Spring Kong FM. Ultra-high dose rate effect on circulating immune cells: a potential mechanism for FLASH effect? *Radiother Oncol* (2020) 149:55–62. doi: 10.1016/j.radonc.2020.04.054

41. Xi M, Xu C, Liao Z, Chang JY, Gomez DR, Jeter M, et al. Comparative outcomes after definitive chemoradiotherapy using proton beam therapy versus intensity modulated radiation therapy for esophageal cancer: a retrospective, single-institutional analysis. *Int J Radiat Oncol Biol Phys* (2017) 99(3):667–76. doi: 10.1016/j.ijrobp.2017.06.2450

frontiers | Frontiers in Oncology

TYPE Original Research
PUBLISHED 12 May 2023
DOI 10.3389/fonc.2023.1076428

OPEN ACCESS

EDITED BY
Deniz Yuce,
Hacettepe University, Türkiye

REVIEWED BY
Qiliang Peng,
Second Affiliated Hospital of Soochow University, China
Guler Yavas,
Başkent University, Türkiye

*CORRESPONDENCE
Jian He
hejian62@163.com

†These authors have contributed equally to this work and share first authorship

RECEIVED 21 October 2022
ACCEPTED 26 April 2023
PUBLISHED 12 May 2023

CITATION
Chen J, Huang W, Xu X, Fan S, Zhang Q, Li X, Zeng Z and He J (2023) Prognostic implications of systemic immune-inflammation index in patients with bone metastases from hepatocellular carcinoma treated with radiotherapy. *Front. Oncol.* 13:1076428. doi: 10.3389/fonc.2023.1076428

Prognostic implications of systemic immune-inflammation index in patients with bone metastases from hepatocellular carcinoma treated with radiotherapy

Jingyao Chen[1†], Wenhan Huang[1†], Xiaohong Xu[1†], Shaonan Fan[1], Qi Zhang[1], Xuan Li[2], Zhaochong Zeng[1] and Jian He[1*]

[1]Department of Radiation Oncology, Zhongshan Hospital, Fudan University, Shanghai, China, [2]Jinshan Hospital Center for Tumor Diagnosis & Therapy, Jinshan Hospital, Fudan University Shanghai Medical School, Shanghai, China

Background: Previous studies have shown that systemic inflammation indicators could predict the survival outcomes of patients with malignant tumors receiving various treatments. Radiotherapy, as a crucial treatment modality, effectively alleviates discomfort in patients with bone metastasis (BM) and greatly improves the quality of life for them. This study aimed to investigate the prognostic value of systemic inflammation index in hepatocellular carcinoma (HCC) patients with BM treated with radiotherapy.

Methods: We retrospectively analyzed clinical data collected from HCC patients with BM who received radiotherapy in our institution between January 2017 and December 2021. The pre-treatment neutrophil-to-lymphocyte ratio (NLR), platelet-to-lymphocyte ratio (PLR), and systemic immune-inflammation index (SII) were derived to determine their relationship with overall survival (OS) and progression-free survival (PFS), using the Kaplan-Meier survival curves. The optimal cut-off value of the systemic inflammation indicators for predicting prognosis was assessed by receiver operating characteristic (ROC) curves. Univariate and multivariate analyses were performed to ultimately evaluate the factors associated with survival.

Results: The study included 239 patients with a median 14-month follow-up. The median OS was 18 months (95% confidence interval [CI] = 12.0-24.0) and the median PFS was 8.5 months (95% CI = 6.5-9.5). The optimal cut-off values for the patients were determined by ROC curve analysis as follows: SII =395.05, NLR=5.43 and PLR = 108.23. The area under the receiver operating characteristic curve values for SII, NLR and PLR in disease control prediction were 0.750, 0.665 and 0.676, respectively. Elevated systemic immune-inflammation index (SII>395.05) and higher NLR (NLR>5.43) were independently associated with poor OS and PFS. In multivariate analysis, Child-Pugh class (P = 0.038), intrahepatic tumor controlled (P = 0.019), SII (P = 0.001)

and NLR (P = 0.007) were independent prognostic factors of OS and Child-Pugh class (P = 0.042), SII (P < 0.001) and NLR (P = 0.002) were independently correlated with PFS.

Conclusion: NLR and SII were associated with poor prognosis in HCC patients with BM receiving radiotherapy and might be considered reliable and independent prognostic biomarkers for HCC patients with BM.

KEYWORDS

hepatocellular carcinoma, bone metastasis, radiotherapy, systemic immune-inflammation index, prognostic value

Introduction

Hepatocellular carcinoma (HCC), one of the most common cancers worldwide, is an aggressive tumor, which is prone to extrahepatic metastasis that occurs in 25.5-38.5% of patients (1–3). In recent years, with the continuous prolongation of the survival period of liver cancer and the gradual progression of imaging diagnosis technology, the positive diagnosis rate of bone metastasis (BM) among HCC patients has increased significantly (4–8). Those patients often suffer pain, pathological fractures, spinal cord compression, hypercalcemia and other skeletal-related events (SRE), seriously damaging their quality of life (9). Thus, having a method for determining the survival in HCC patients with BM can us anticipate the development of detrimental symptoms stated above and prepare treatments preemptively to help mitigate them.

Recently, accumulating studies have confirmed that peripheral blood markers have prognostic significance in patients with malignant tumors (10–15). NLR, defined as neutrophil-to-lymphocyte count ratio, and PLR, defined as platelet-to-lymphocyte count ratio, are proved to be applicable biomarkers for patient prognostic evaluation and therapeutic decision-making (16, 17). SII is a comprehensive parameter, defined as the absolute platelet count multiplied by the neutrophil-to-lymphocyte count ratio (18, 19). The NLR, PLR, and SII are sensitive inflammatory markers in peripheral blood that can predict poor outcomes and prognosis for HCC patients who underwent surgical resection (20–22), liver transplantation (23, 24), stereotactic ablative radiation therapy (25), transarterial chemoembolization (26) or sorafenib treatment (27).

However, there are still much to learn about the prognostic potential of systemic inflammation biomarkers on HCC patients treated with palliative radiation therapy for bone metastases. Therefore, investigating the clinical significance of systemic Immune-Inflammation markers in those patients can further deepen our understanding of tumor inflammation and help us manage the wellbeing of our patients better.

In this retrospective study, our main purpose is to investigate the prognostic value of inflammatory indexes (NLR, PLR, and SII) before radiotherapy for predicting survival outcomes in HCC patients with BM.

Materials and methods

Patients

Patients who were diagnosed with HCC with bone metastases between January 2017 and December 2021 and received radiotherapy for bone metastases at Zhongshan Hospital, Fudan University were retrospectively identified. The eligibility criteria were as follows: (1) Clinical diagnosis or pathologically confirmed hepatocellular carcinoma and no coinciding other malignancy; (2) Computed tomography (CT), magnetic resonance imaging (MRI), or bone scan evidence of bone metastasis at the index site; (3) Child-Turcotte-Pugh (CTP) class A or B liver function; (4) over the age of 18. The exclusion criteria were as follows: (1) pregnant or lactating women; (2) combined with other serious complications; (3) with serious infection or bleeding disease; (4) using immunosuppressive or anti-inflammatory drugs before treatment; (5) incomplete or absent follow-up. Ethics approval for the use of human subjects was obtained from the research ethics committee of Zhongshan Hospital, and informed consent was obtained from each patient.

Data collection

Demographic information and tumor variables of all patients were collected, including gender, age, Eastern Cooperative Oncology Group performance status (ECOG PS), HCC etiologic history, liver functionality, sites and number of bone metastases, other distant metastatic sites, serum ALP and AFP and blood cell counts. Among them, blood information such as platelet(P), neutrophil (N), and lymphocyte (L) were collected from reports of routine blood samples performed within one week before the radiotherapy for bone metastases.

Treatment and follow-up

The treatments were administrated as described previously according to our institutional protocol (28). All patients underwent external beam radiotherapy with linear accelerator beam energies ranging from 6–15 megavolts (MV). Each radiation dose was administered using the ONCOR Avant-Garde Linear Accelerator (Siemens Medical Solutions, Inc. Oncology Care Systems Group). The types and modalities of radiation therapy were chosen based on the location and size of the lesions as well as the general condition of the patients. The bone metastatic lesions were scheduled the full radiation dosage at 28-60 Gy in 5-30 fractions.

All patients were assessed *via* blood examination, CT, MRI, and bone scan at 1 to 3 months after radiotherapy completion and every 3 months thereafter. Survival data was followed up by telephone and email 3-monthly until December 2021 to understand the patient's survival status, tumor recurrence, or time to metastasis. Overall survival (OS) was defined as the time from the initiation of radiotherapy for bone metastases to death or the last follow-up, and progression-free survival (PFS) was calculated from the time from the first day of radiotherapy for bone metastases to recurrence and deterioration, death, or final follow-up.

Statistical analysis

The SII, NLR, and PLR were calculated as follows: SII = P ×N/L, NLR = N/L, and PLR = P/L. All statistical analyses were performed using SPSS version 26.0 (IBM, Armonk, NY, USA). The continuous variables were presented as the median ± interquartile range (IQR). The categorical variables were described by numbers and percentages. Patient characteristics were examined using the $\chi 2$ test or Fisher exact test. OS and PFS were assessed with the Kaplan-Meier to analyze the survival probability, and Log–rank test was used to calculate the significance of differences. Cox proportional hazard model was applied for the univariate and multivariate analyses to calculate the hazard ratios (HRs) and 95% confidence intervals on survival outcomes. Variables with P values <0.1 in univariable analyses were selected for multivariable analyses. Receiver operating characteristic (ROC) curve analysis was performed to determine the optimal cut-off values of serum biomarkers in predicting patient survival based on the Youden index. The area under the curve (AUC) was calculated to evaluate the discriminatory power. A two-tailed P value less than 0.05 was considered statistically significant in the study.

Results

Patient characteristics

The clinical characteristics of all patients are shown in Table 1, who were diagnosed with HCC with bone metastases between January 2017 and December 2021 in Zhongshan Hospital, Fudan University (Shanghai, China). A total of 239 patients with a median age of 58 years were retrospectively identified; 89.1% were male (213/239) and 23.6% were female (26/239). Among them, 96.7% (231/239) had an ECOG PS score of 0–1, 77.8% (186/239) were positive for hepatitis B virus, and 3.8% (9/239) for hepatitis C virus, 95.8% (229/239) and 4.2% (10/239) patients were Child-Pugh class A and B, respectively. There were 20.5% (49/239) patients diagnosed with bone metastases at the same time of diagnosis of HCC. The median radiation dose was 40 Gy (IQR, 30-45 Gy), delivered in 10-20 fractions. In addition to bone metastases, 46% of patients (110/239) had other sites of distant metastases, such as lung and adrenal gland. The blood characteristics of all patients are shown in Table 2. The median SII, NLR, and PLR were 705.05(IQR, 298.28-783.23), 4.73 (IQR, 2.38-6.00) and 163.56 (IQR, 95.12-196.67).

Sites of bone metastases and number of lesions

In 239 patients, a total of 389 bone metastatic sites were identified. Sites of bone metastases for all patients were shown in Figure 1. The most common site of bone metastases was the spine (66%), followed by ribs (32%) and pelvis (29%). One hundred fifty-two patients (64%) had a single bone metastatic site, while the other patients (36%) had more than one bone lesion.

Optimal cut-off analysis

The optimal cut-off values for the patients were determined by ROC curve analysis (Figure 2) as follows: SII =395.05, NLR=5.43 and PLR = 108.23. In disease control prediction, the area under the receiver operating characteristic curve values for SII, NLR, and PLR were 0.750, 0.665 and 0.676, respectively. Consequently, patients were stratified into two groups (low and high groups) based on the optimal cut-off value of each index.

Overall survival analysis

The median follow-up duration was 14 months. The median overall survival was 18 months (95%CI, 12.0-24.0). The 1-,2-,3-year OS rate was 58.9%, 44.6%, 42.1%, respectively.

Compared with the low SII group, the high SII group had inferior survival outcomes. The median OS of the low SII group was statistically higher than that of the high SII group (NR vs. 16 months, P = 0.015; Figure 3A). The median OS of the low NLR group was 29 months, significantly higher than the 9 months of the high NLR group (P = 0.011; Figure 3B). However, there was no significant difference between low PLR and high PLR group (P=0.083; Figure 3C).

A total of 24 variables were applied for univariate Cox regression analysis, and P-values less than 0.1 were included in the multivariable analysis. For OS, univariate analysis indicated that ECOG performance status (P = 0.018), Child-Pugh class (P < 0.001), multiple intrahepatic tumors (P = 0.086), intrahepatic tumor controlled (P = 0.034), AFP level (P < 0.001), ALP level (P = 0.001), ALT level (P = 0.011), AST level (P = 0.007), SII (P =0.018), NLR (P = 0.014), and PLR (P = 0.092) were statistical prognostic factors. Multivariate analysis determined that Child-Pugh class (P = 0.038), intrahepatic tumor controlled (P =

TABLE 1 Patient and treatment characteristics.

Variable	n or median	% or IQR range
Age, years	58	50-66
Sex		
Female	26	10.9%
Male	213	89.1%
ECOG performance status		
0-1	231	96.7%
≥2	8	3.3%
Etiology		
B-viral	186	77.8%
C-viral	9	3.8%
Non-B, non-C	44	18.4%
Child-Pugh class		
A	229	95.8%
B	10	4.2%
Recurrent HCC	49	20.5%
Number of intrahepatic tumors		
single	130	54.4%
multiple	109	45.6%
Size of intrahepatic tumors (cm)		
≤5	112	46.9%
>5	127	53.1%
Intrahepatic control		
controlled	150	62.8%
uncontrolled	89	37.2%
Extraosseous metastases		
absent	129	54.0%
present	110	46.0%
Lymph node metastasis		
absent	148	61.9%
present	91	38.1%
Vascular tumor thrombus		
absent	134	56.1%
present	105	43.9%
Number of BMs		
single	124	51.9%
multiple	115	48.1%
Radiation dose, Gy	40	30-45
Fraction number	11	10-20
BED10, Gy	50.7	39.0-58.5

ECOG, Eastern Cooperative Oncology Group; HCC, hepatocellular carcinoma; BM, bone metastasis; BED10, biological effective dose calculated using $\alpha/\beta = 10$.

0.019), SII (P = 0.001) and NLR (P = 0.007) were independent prognostic factors (Table 3).

Progression-free survival analysis

The median progression-free survival was 8.5 months (95%CI, 6.5-9.5). The 1- and 2-year PFS rate was 36.8% and 21.2%, respectively.

Regarding survival outcomes of different groups, the median PFS of the low SII group was statistically higher than that of the high SII group (21 vs. 6 months, P < 0.001; Figure 4A). The median PFS of the low NLR group was 11.5 months, which was significantly extended than the 4.5 months of the high NLR group (P < 0.001; Figure 4B). The median PFS of the low PLR group was 13 months, significantly higher than the 6.5 months of the high PLR group (P < 0.001; Figure 4C).

The result of the univariate analysis revealed that ECOG performance status (P = 0.052), etiology (P = 0.028), Child-Pugh class (P = 0.007), intrahepatic tumor controlled (P = 0.014), extraosseous metastases (P = 0.008), multiple bone metastases (P = 0.099), AFP level (P = 0.011), ALT level (P = 0.089), SII (P < 0.001), NLR (P < 0.001), and PLR (P < 0.001) were significant risk factors for PFS. Multivariate analysis determined that Child-Pugh class (P = 0.042), SII (P < 0.001) and NLR (P = 0.002) were independently associated with PFS (Table 4).

Discussion

High NLR, PLR, and SII have been associated with poor survival in individuals with several solid tumors, including lung cancer, gastric cancer, colorectal cancer, and pancreatic cancer (12, 18, 29). High NLR and PLR correspond to worse OS and PFS in geriatric patients with HCC who underwent resection (29, 30). An elevated NLR and PLR independently predicted higher mortality in NSCLC patients treated with immunotherapy (11). NLR is an objective and valuable inflammatory marker that can predict survival outcomes and liver toxicity in HCC patients treated with SBRT. Likewise, post-PLR ≥263.0 was a prognostic factor of inferior PFS and OS in small hepatocellular carcinoma patients treated with SBRT (31). SII could be considered a combination of NLR and PLR and thus might be a better predictive biomarker, which has been proven to be an independent predictor in patients with HCC who received sequential therapy with sorafenib and regorafenib (32). In a meta-analysis comprising 2796 HCC patients, the results revealed that elevated pre-treatment SII was related to lower OS (HR:1.54, P < 0.001) and earlier time to recurrence (HR:1.77, P < 0.001) (33).

TABLE 2 Blood characteristics.

Variable	n or median	% or IQR range
AFP level		
≤400 ng/mL	159	66.50%
>400 ng/mL	80	33.50%
ALP level		
≤150 U/L	149	62.30%
>150 U/L	90	37.30%
γ-GT level		
≤75 U/L	113	47.30%
>75 U/L	126	52.70%
ALT level		
≤40 U/L	147	61.50%
>40 U/L	92	38.50%
AST level		
≤40 U/L	123	51.50%
>40 U/L	116	48.50%
HGB(g/L)	128.69	114.50-144.50
WBC(10^9/L)	10.3	3.96-7.23
PLT(10^9/L)	154.45	93.5-194.00
Neutrophil(10^9/L)	4.14	2.60-5.10
Lymphocyte(10^9/L)	1.16	0.70-1.50
SII	705.05	298.28-783.23
NLR	4.73	2.38-6.00
PLR	163.56	95.12-196.67

AFP, alpha-fetoprotein; ALP, alkaline phosphatase; γ-GT, gamma-glutamyl transferase; ALT, alanine aminotransferase; AST, aspartate aminotransferase; HGB, hemoglobin; WBC, white blood cell; PLT, platelet; SII, system immune-inflammation index; NLR, neutrophil-to-lymphocyte ratio; PLR, platelet-to-lymphocyte ratio; IQR, interquartile range.

While previous studies have mainly focused on HCC patients receiving various other treatments, there are few reports on the prognostic role of these indicators in HCC patients with BM receiving radiotherapy. The development of bone metastasis is considered a multi-step process, including the displacement of cancer cells from the primary site, vascular invasion, distal capillary migration and attachment to bone, recruitment of inflammatory factors, and adjacent tissue invasion. Among them, systemic inflammation is an important accelerator in the proliferation, invasion, and metastasis of tumor cells. It plays an essential role in the tumor microenvironment, thus influencing cancer development and therapeutic response (34, 35). As one of the most common palliative treatments for patients with bone metastasis, radiotherapy is a crucial treatment modality, effectively alleviating discomfort and greatly improving quality of life (36). Previous studies revealed that systemic inflammation would inevitably impact radiotherapy's efficacy (37, 38). In this study, we evaluated the association between several immune inflammatory parameters (NLR, PLR, SII) and clinical outcomes in HCC patients with BM. We demonstrated that NLR and SII were independently associated with survival outcomes in patients after radiotherapy. The optimal predictive potential of these biomarkers was determined based on the ROC curve, and the patients were divided into high- and low-value groups. Patients with NLR> 5.43 or SII >395.05 have poorer clinical outcomes. In the multivariate cox regression analyses, the results revealed that SII independently predicted OS (HR, 2.539; 95% CI, 1.439–4.481; P = 0.001) and PFS (HR, 2.726; 95% CI, 1.557-4.773; P < 0.001). NLR independently predicted OS (HR, 1.771; 95% CI, 1.171-2.679; P = 0.007) and PFS (HR, 1.942; 95% CI, 1.268-2.973; P = 0.002).

The molecular mechanisms of the prognostic significance of NLR, PLR, and SII for cancer patients may correlate with the function of platelets, neutrophils, and lymphocytes, reflecting inflammatory response and immune dysfunction. Beyond hemostasis and thrombosis, blood platelets also play a part in numerous pathways pivotal for cancer progression and metastasis. Research indicated that platelets can protect tumor cells from shear forces and assault of NK cells, and communicate with multiple growth factors, chemokines, inflammatory factors, and other immune cells, thereby inducing tumor cells proliferation and distant extravasation (39). Neutrophils, considered essential for the immune surveillance of tumor cells, exert multifaceted and sometimes opposing roles during cancer initiation, progression and dissemination (40). Neutrophils may be reprogrammed into a cancer-promoting state in the cancer microenvironment. They could produce some granule proteins (MMP-9 and ARG-1), subsequently degrading the extracellular matrix, and suppressing antigen-presentation and T lymphocyte activation, thereby resulting in immune escape, prompting cancer cells evasion and decreasing sensitivity to radiation treatment (41, 42). It is well established that as one of the most vital cells of the immune system, lymphocytes play a crucial role in tumorigenesis, cancer progression, metastatic seeding, and therapy resistance. Lymphocytes can directly interact with circulating tumor cells through the FAS-FASL axis or immune-checkpoint molecules, such as PD1-PDL1 and CTLA 4, which will induce immunosuppressive responses, leading to enhanced survival of the tumor cells (43, 44). Together with those findings, we can better understand the interactive functions of the immune inflammatory biomarkers with cancer progression and therapeutic response.

We considered several limitations to this study as follows. Firstly, this was a real-world retrospective study from only a single center, with a small sample size, and existing unavoidable in presence of objective biases. Therefore, it is reasonable to conduct additional large-scale and muti-center studies to validate the prognostic potential of immune-inflammatory indicators. Secondly, there were measurement biases because peripheral blood cell counts were performed only once. Inflammatory indicators in the peripheral blood can be influenced by infections, cirrhosis-associated hypersplenism, or medications including steroid. Lastly, HCC patients with bone metastases often sought treatment until significant symptoms had occurred, so we are unable to identify the exact number of patients with bone metastases who exhibited minor or no symptoms.

In conclusion, NLR and SII were associated with poor prognosis in HCC patients with BM receiving radiotherapy and might be considered reliable and independent prognostic biomarkers for HCC patients with BM. Furthermore, the systemic

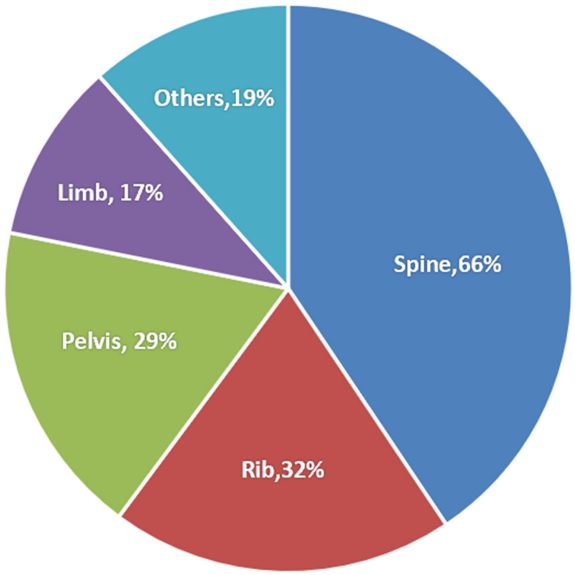

FIGURE 1
Sites of bone metastases in all patients.

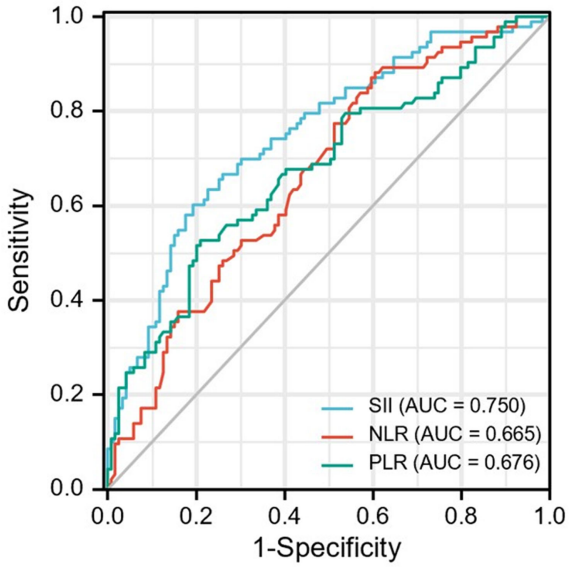

FIGURE 2
ROC curve analysis for optimal cut-off value of SII, NLR and PLR. ROC, receiver operating characteristic; SII, systemic immune-inflammation index; NLR, neutrophil-to-lymphocyte ratio; PLR, platelet-to-lymphocyte ratio.

TABLE 3 Univariate and multivariate cox proportional hazards analysis for overall survival.

Variable	Univariate analysis		Multivariate analysis	
	HR (95%CI)	*P* value	HR (95%CI)	*P* value
Age, years (>50)	0.950(0.492-1.833)	0.877		
Sex(male)	1.144(0.717-1.826)	0.573		
ECOG performance status≥2	3.417(1.233-9.465)	0.018	1.432(0.240-8.537)	0.693
Etiology(B-viral or C-viral)	1.071(0.624-1.838)	0.803		

(Continued)

TABLE 3 Continued

Variable	Univariate analysis		Multivariate analysis	
	HR (95%CI)	*P* value	HR (95%CI)	*P* value
Child-Pugh class(B)	5.584(2.639-11.818)	<0.001	4.659(1.090-19.910)	0.038
Recurrent HCC	0.809(0.449-1.456)	0.809		
Multiple intrahepatic tumors	1.435(0.951-2.165)	0.086	1.006(0.678-1.492)	0.978
Size of intrahepatic tumors (>5cm)	1.098(0.727-1.658)	0.656		
Intrahepatic uncontrolled	1.615(1.037-2.516)	0.034	1.651(1.088-2.504)	0.019
Extraosseous metastases	1.069(0.707-1.616)	0.751		
Lymph node metastasis	1.315(0.863-2.006)	0.203		
Vascular tumor thrombus	0.846(0.555-1.290)	0.438		
Multiple bone metastases	1.129(0.748-1.704)	0.564		
AFP level>400 ng/mL	2.619(1.705-4.022)	<0.001	1.354(0.864-2.122)	0.186
ALP level>150 U/L	2.042(1.348-3.091)	0.001	1.369(0.869-2.156)	0.175
γ-GT level>75 U/L	1.405(0.930-2.123)	0.107		
ALT level>40 U/L	1.721(1.134-2.611)	0.011	1.308(0.750-2.281)	0.344
AST level>40 U/L	1.765(1.166-2.670)	0.007	0.763(0.437-1.332)	0.341
Fraction number	1.012(0.978-1.048)	0.491		
Fraction dose, Gy	0.898(0.723-1.116)	0.333		
BED10, Gy	0.999(0.984-1.016)	0.946		
SII>395.05	1.712(1.095-2.676)	0.018	2.539(1.439-4.481)	0.001
NLR>5.43	1.780(1.121-2.825)	0.014	1.771(1.171-2.679)	0.007
PLR>108.23	1.468(0.940-2.293)	0.092	0.923(0.558-1.528)	0.755

ECOG, Eastern Cooperative Oncology Group; HCC, hepatocellular carcinoma; AFP, alpha-fetoprotein; ALP, alkaline phosphatase; γ-GT, gamma-glutamyl transferase; ALT, alanine aminotransferase; AST, aspartate aminotransferase; BED_{10}, biological effective dose calculated using $\alpha/\beta = 10$; SII, system immune-inflammation index; NLR, neutrophil-to-lymphocyte ratio; PLR, platelet-to-lymphocyte ratio.

TABLE 4 Univariate and multivariate cox proportional hazards analysis for progression-free survival.

Variable	Univariate analysis		Multivariate analysis	
	HR (95%CI)	*P* value	HR (95%CI)	*P* value
Age, years (>50)	0.890(0.605-1.309)	0.555		
Sex(male)	1.008(0.567-1.792)	0.977		
ECOG performance status≥2	2.713(0.990-7.437)	0.052	2.213(0.421-11.624)	0.348
Etiology(B-viral or C-viral)	0.631(0.419-0.952)	0.028	0.995(0.653-1.517)	0.981
Child-Pugh class(B)	3.138(1.360-7.241)	0.007	4.174(1.052-16.563)	0.042
Recurrent HCC	1.402(0.920-2.136)	0.116		
Multiple intrahepatic tumors	0.924(0.649-1.316)	0.662		
Size of intrahepatic tumors (>5cm)	1.151(0.812-1.632)	0.431		
Intrahepatic uncontrolled	1.593(1.100-2.305)	0.014	1.359(0.894-2.066)	0.152
Extraosseous metastases	1.603(1.129-2.276)	0.008	1.477(0.990-2.206)	0.056
Lymph node metastasis	1.277(0.894-1.825)	0.179		
Vascular tumor thrombus	0.916(0.644-1.303)	0.627		

(Continued)

TABLE 4 Continued

Variable	Univariate analysis		Multivariate analysis	
	HR (95%CI)	*P* value	HR (95%CI)	*P* value
Multiple bone metastases	1.341(0.946-1.902)	0.099	1.217(0.814-1.818)	0.339
AFP level>400 ng/mL	1.656(1.124-2.440)	0.011	1.382(0.878-2.176)	0.162
ALP level>150 U/L	1.219(0.841-1.767)	0.295		
γ-GT level>75 U/L	1.209(0.854-1.714)	0.285		
ALT level>40 U/L	1.369(0.953-1.965)	0.089	1.067(0.695-1.637)	0.768
AST level>40 U/L	1.080(0.760-1.536)	0.667		
Fraction number	0.990(0.960-1.020)	0.497		
Fraction dose, Gy	1.095(0.936-1.281)	0.257		
BED10, Gy	1.003(0.990-1.017)	0.612		
SII>395.05	3.687(2.373-5.730)	<0.001	2.726(1.557-4.773)	<0.001
NLR>5.43	2.746(1.891-3.987)	<0.001	1.942(1.268-2.973)	0.002
PLR>108.23	2.216(1.470-3.341)	<0.001	0.897(0.544-1.478)	0.669

ECOG, Eastern Cooperative Oncology Group; HCC, hepatocellular carcinoma; AFP, alpha-fetoprotein; ALP, alkaline phosphatase; γ-GT, gamma-glutamyl transferase; ALT, alanine aminotransferase; AST, aspartate aminotransferase; BED_{10}, biological effective dose calculated using $\alpha/\beta = 10$; SII, system immune-inflammation index; NLR, neutrophil-to-lymphocyte ratio; PLR, platelet-to-lymphocyte ratio.

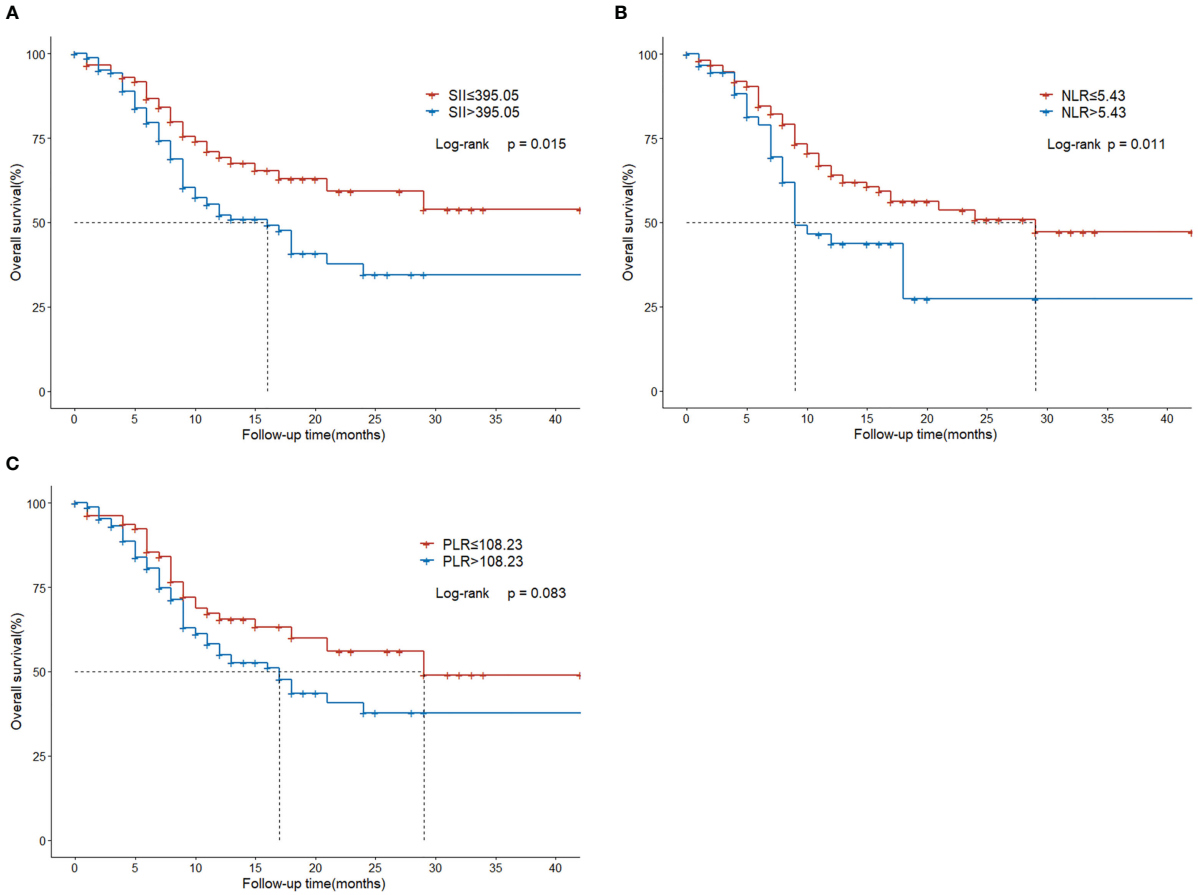

FIGURE 3
Overall survival in HCC patients with BM treated with radiotherapy based on their systemic immune-inflammation index **(A)** and neutrophil-to-lymphocyte ratio **(B)** and platelet-to-lymphocyte ratio **(C)**.

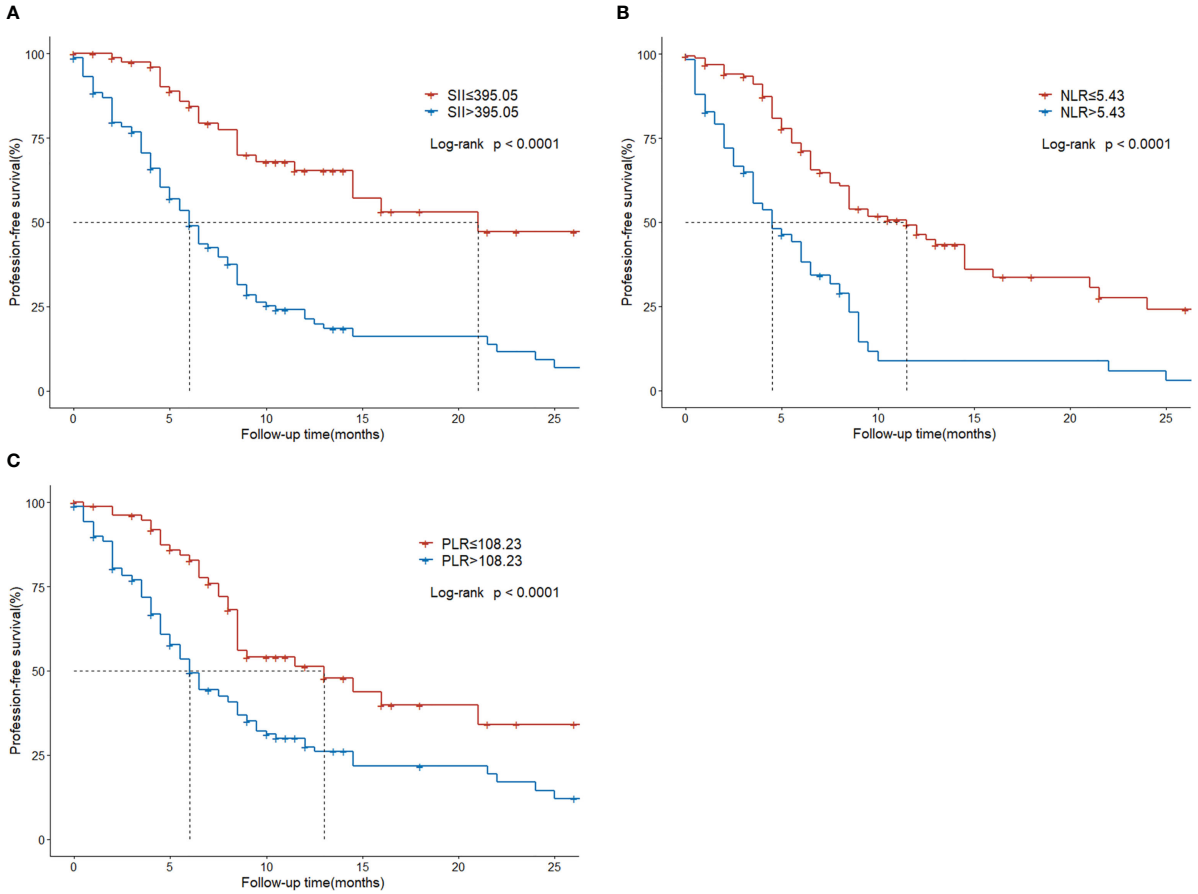

FIGURE 4
Progression-free survival in HCC patients with BM treated with radiotherapy based on their systemic immune-inflammation index **(A)** and neutrophil-to-lymphocyte ratio **(B)** and platelet-to-lymphocyte ratio **(C)**.

inflammation indexes are convenient and readily available during routine clinical practice, adding no additional financial burden to patients, so they are worthy of widespread use in clinical practice.

Data availability statement

The original contributions presented in the study are included in the article. Further inquiries can be directed to the corresponding authors.

Ethics statement

The protocol was approved by the Ethics Committee of Zhongshan Hospital, and the requirement of informed consent was waived by the Institutional Review Board since this was a retrospective analysis.

Author contributions

JC, ZZ and JH designed the study. WH, XX and XL collected the data. JC, SF and QZ contributed to the data statistical analyses and wrote the manuscript. All authors contributed to the article and approved the submitted version.

Funding

The research was supported by the major project in the basic research field of Shanghai Science and Technology Innovation Action Plan [22JC1402300].

Acknowledgments

The authors would like to thank all the patients who participated in this study.

Conflict of interest

The authors declare that the research was conducted in the absence of any commercial or financial relationships that could be construed as a potential conflict of interest.

Publisher's note

References

1. Toyoda H, Kumada T, Kiriyama S, Sone Y, Tanikawa M, Hisanaga Y, et al. Changes in the characteristics and survival rate of hepatocellular carcinoma from 1976 to 2000: analysis of 1365 patients in a single institution in Japan. *Cancer* (2004) 100 (11):2415–21. doi: 10.1002/cncr.20289

2. Ho CL, Chen S, Yeung DW, Cheng TK. Dual-tracer Pet/Ct imaging in evaluation of metastatic hepatocellular carcinoma. *J Nucl Med* (2007) 48(6):902–9. doi: 10.2967/jnumed.106.036673

3. Uchino K, Tateishi R, Shiina S, Kanda M, Masuzaki R, Kondo Y, et al. Hepatocellular carcinoma with extrahepatic metastasis: clinical features and prognostic factors. *Cancer* (2011) 117(19):4475–83. doi: 10.1002/cncr.25960

4. He J, Zeng ZC, Tang ZY, Fan J, Zhou J, Zeng MS, et al. Clinical features and prognostic factors in patients with bone metastases from hepatocellular carcinoma receiving external beam radiotherapy. *Cancer* (2009) 115(12):2710–20. doi: 10.1002/cncr.24300

5. Harding JJ, Abu-Zeinah G, Chou JF, Owen DH, Ly M, Lowery MA, et al. Frequency, morbidity, and mortality of bone metastases in advanced hepatocellular carcinoma. *J Natl Compr Canc Netw* (2018) 16(1):50–8. doi: 10.6004/jnccn.2017.7024

6. Hu C, Yang J, Huang Z, Liu C, Lin Y, Tong Y, et al. Diagnostic and prognostic nomograms for bone metastasis in hepatocellular carcinoma. *BMC Cancer* (2020) 20 (1):494. doi: 10.1186/s12885-020-06995-y

7. Huang Z, Wen J, Wang Y, Han S, Li Z, Hu X, et al. Bone metastasis of hepatocellular carcinoma: facts and hopes from clinical and translational perspectives. *Front Med* (2022) 16(4):551–73. doi: 10.1007/s11684-022-0928-z

8. Yuan X, Zhuang M, Zhu X, Cheng D, Liu J, Sun D, et al. Emerging perspectives of bone metastasis in hepatocellular carcinoma. *Front Oncol* (2022) 12:943866. doi: 10.3389/fonc.2022.943866

9. Oldenburger E, Brown S, Willmann J, van der Velden JM, Spalek M, van der Linden YM, et al. Estro acrop guidelines for external beam radiotherapy of patients with complicated bone metastases. *Radiother Oncol* (2022) 173:240–53. doi: 10.1016/j.radonc.2022.06.002

10. Yang L, He W, Kong P, Jiang C, Yang Q, Xie Q, et al. Clinical baseline and prognostic difference of platelet lymphocyte ratio (Plr) in right-sided and let-sided colon cancers. *BMC Cancer* (2017) 17(1):873. doi: 10.1186/s12885-017-3862-8

11. Diem S, Schmid S, Krapf M, Flatz L, Born D, Jochum W, et al. Neutrophil-to-Lymphocyte ratio (Nlr) and platelet-to-Lymphocyte ratio (Plr) as prognostic markers in patients with non-small cell lung cancer (Nsclc) treated with nivolumab. *Lung Cancer* (2017) 111:176–81. doi: 10.1016/j.lungcan.2017.07.024

12. Fu X, Li T, Dai Y, Li J. Preoperative systemic inflammation score (Sis) is superior to neutrophil to lymphocyte ratio (Nlr) as a predicting indicator in patients with esophageal squamous cell carcinoma. *BMC Cancer* (2019) 19(1):721. doi: 10.1186/s12885-019-5940-6

13. Tang X, Cao Y, Liu J, Wang S, Yang Y, Du P. Diagnostic value of inflammatory factors in pathology of bladder cancer patients. *Front Mol Biosci* (2020) 7:575483. doi: 10.3389/fmolb.2020.575483

14. Wang C, Zhao K, Hu S, Huang Y, Ma L, Song Y, et al. A predictive model for treatment response in patients with locally advanced esophageal squamous cell carcinoma after concurrent chemoradiotherapy: based on suvmean and nlr. *BMC Cancer* (2020) 20(1):544. doi: 10.1186/s12885-020-07040-8

15. Ruan GT, Ge YZ, Xie HL, Hu CL, Zhang Q, Zhang X, et al. Association between systemic inflammation and malnutrition with survival in patients with cancer sarcopenia-a prospective multicenter study. *Front Nutr* (2022) 8:811288. doi: 10.3389/fnut.2021.811288

16. Prabawa IPY, Bhargah A, Liwang F, Tandio DA, Tandio AL, Lestari AAW, et al. Pretreatment neutrophil-to-Lymphocyte ratio (Nlr) and platelet-to-Lymphocyte ratio (Plr) as a predictive value of hematological markers in cervical cancer. *Asian Pac J Cancer Prev* (2019) 20(3):863–8. doi: 10.31557/APJCP.2019.20.3.863

17. Lou C, Jin F, Zhao Q, Qi H. Correlation of serum nlr, plr and halp with efficacy of neoadjuvant chemotherapy and prognosis of triple-negative breast cancer. *Am J Transl Res* (2022) 14(5):3240–6.

18. Murthy P, Zenati MS, Al Abbas AI, Rieser CJ, Bahary N, Lotze MT, et al. Prognostic value of the systemic immune-inflammation index (Sii) after neoadjuvant therapy for patients with resected pancreatic cancer. *Ann Surg Oncol* (2020) 27(3):898–906. doi: 10.1245/s10434-019-08094-0

19. Ruiz-Ranz M, Lequerica-Fernandez P, Rodriguez-Santamarta T, Suarez-Sanchez FJ, Lopez-Pintor RM, Garcia-Pedrero JM, et al. Prognostic implications of preoperative systemic inflammatory markers in oral squamous cell carcinoma, and correlations with the local immune tumor microenvironment. *Front Immunol* (2022) 13:941351. doi: 10.3389/fimmu.2022.941351

20. Qu Z, Lu YJ, Feng JW, Chen YX, Shi LQ, Chen J, et al. Preoperative prognostic nutritional index and neutrophil-to-Lymphocyte ratio predict survival outcomes of patients with hepatocellular carcinoma after curative resection. *Front Oncol* (2021) 11:823054. doi: 10.3389/fonc.2021.823054

21. Wu W, Wang Q, Han D, Li J, Nie Y, Guo D, et al. Prognostic value of preoperative inflammatory markers in patients with hepatocellular carcinoma who underwent curative resection. *Cancer Cell Int* (2021) 21(1):500. doi: 10.1186/s12935-021-02204-3

22. Ji F, Liang Y, Fu SJ, Guo ZY, Shu M, Shen SL, et al. A novel and accurate predictor of survival for patients with hepatocellular carcinoma after surgical resection: the neutrophil to lymphocyte ratio (Nlr) combined with the aspartate Aminotransferase/Platelet count ratio index (Apri). *BMC Cancer* (2016) 16:137. doi: 10.1186/s12885-016-2189-1

23. Motomura T, Shirabe K, Mano Y, Muto J, Toshima T, Umemoto Y, et al. Neutrophil-lymphocyte ratio reflects hepatocellular carcinoma recurrence after liver transplantation *Via* inflammatory microenvironment. *J Hepatol* (2013) 58(1):58–64. doi: 10.1016/j.jhep.2012.08.017

24. Kong W, Qu E, Sheng N, Zhang J, Li X, Zheng J, et al. Prognostic significance of inflammation-based score in patients with hepatocellular carcinoma after liver transplantation. *Eur J Gastroenterol Hepatol* (2021) 33(1S Suppl 1):e282–e9. doi: 10.1097/MEG.0000000000002037

25. Wang S, Deng Y, Yu X, Zhang XW, Huo CL, Sun ZG, et al. Prognostic significance of preoperative systemic inflammatory biomarkers in patients with hepatocellular carcinoma after microwave ablation and establishment of a nomogram. *Sci Rep* (2021) 11(1):13814. doi: 10.1038/s41598-021-93289-3

26. Wang H, Lin C, Fan W, Zhang J, Zhang Y, Yao W, et al. Dynamic changes in the neutrophil-to-Lymphocyte ratio predict the prognosis of patients with hepatocellular carcinoma undergoing transarterial chemoembolization. *Cancer Manag Res* (2020) 12:3433–44. doi: 10.2147/CMAR.S245396

27. Sprinzl MF, Kirstein MM, Koch S, Seib ML, Weinmann-Menke J, Lang H, et al. Improved prediction of survival by a risk factor-integrating inflammatory score in sorafenib-treated hepatocellular carcinoma. *Liver Cancer* (2019) 8(5):387–402. doi: 10.1159/000492628

28. He J, Shi S, Ye L, Ma G, Pan X, Huang Y, et al. A randomized trial of conventional fraction versus hypofraction radiotherapy for bone metastases from hepatocellular carcinoma. *J Cancer* (2019) 10(17):4031–7. doi: 10.7150/jca.28674

29. Wang W, Tong Y, Sun S, Tan Y, Shan Z, Sun F, et al. Predictive value of nlr and plr in response to preoperative chemotherapy and prognosis in locally advanced gastric cancer. *Front Oncol* (2022) 12:936206. doi: 10.3389/fonc.2022.936206

30. Safcak D, Drazilova S, Gazda J, Andrasina I, Adamcova-Selcanova S, Balazova L, et al. Inflammatory indexes as prognostic factors of survival in geriatric patients with hepatocellular carcinoma: a case control study of eight Slovak centers. *J Clin Med* (2022) 11(14):4183. doi: 10.3390/jcm11144183

31. Zhuang Y, Yuan BY, Hu Y, Chen GW, Zhang L, Zhao XM, et al. Pre/Post-treatment dynamic of inflammatory markers has prognostic value in patients with small hepatocellular carcinoma managed by stereotactic body radiation therapy. *Cancer Manag Res* (2019) 11:10929–37. doi: 10.2147/CMAR.S231901

32. Hong YM, Yoon KT, Cho M. Systemic immune-inflammation index predicts prognosis of sequential therapy with sorafenib and regorafenib in hepatocellular carcinoma. *BMC Cancer* (2021) 21(1):569. doi: 10.1186/s12885-021-08124-9

33. Wang B, Huang Y, Lin T. Prognostic impact of elevated pre-treatment systemic immune-inflammation index (Sii) in hepatocellular carcinoma: a meta-analysis. *Med (Baltimore)* (2020) 99(1):e18571. doi: 10.1097/MD.0000000000018571

34. Diakos CI, Charles KA, McMillan DC, Clarke SJ. Cancer-related inflammation and treatment effectiveness. *Lancet Oncol* (2014) 15(11):e493–503. doi: 10.1016/S1470-2045(14)70263-3

35. Sas Z, Cendrowicz E, Weinhauser I, Rygiel TP. Tumor microenvironment of hepatocellular carcinoma: challenges and opportunities for new treatment options. *Int J Mol Sci* (2022) 23(7):3778. doi: 10.3390/ijms23073778

36. Meyer J, Singal AG. Stereotactic ablative radiotherapy for hepatocellular carcinoma: history, current status, and opportunities. *Liver Transpl* (2018) 24 (3):420–7. doi: 10.1002/lt.24991

37. Shaverdian N, Veruttipong D, Wang J, Schaue D, Kupelian P, Lee P. Pretreatment immune parameters predict for overall survival and toxicity in early-

stage non-Small-Cell lung cancer patients treated with stereotactic body radiation therapy. *Clin Lung Cancer* (2016) 17(1):39–46. doi: 10.1016/j.cllc.2015.07.007

38. Chen DJ, Qin HY, Deng GC, Wang Q, Wang HY, Liu XJ. Pre-radiotherapy systemic immune inflammation index associated with overall survival in patients with advanced egfr mutant non-small cell lung cancer receiving thoracic radiotherapy. *Clin Transl Oncol* (2022) 25(1):226–35. doi: 10.1007/s12094-022-02936-2

39. Schlesinger M. Role of platelets and platelet receptors in cancer metastasis. *J Hematol Oncol* (2018) 11(1):125. doi: 10.1186/s13045-018-0669-2

40. Coffelt SB, Wellenstein MD, de Visser KE. Neutrophils in cancer: neutral no more. *Nat Rev Cancer* (2016) 16(7):431–46. doi: 10.1038/nrc.2016.52

41. Christoffersson G, Vagesjo E, Vandooren J, Liden M, Massena S, Reinert RB, et al. Vegf-a recruits a proangiogenic mmp-9-Delivering neutrophil subset that induces angiogenesis in transplanted hypoxic tissue. *Blood* (2012) 120(23):4653–62. doi: 10.1182/blood-2012-04-421040

42. Xiong S, Dong L, Cheng L. Neutrophils in cancer carcinogenesis and metastasis. *J Hematol Oncol* (2021) 14(1):173. doi: 10.1186/s13045-021-01187-y

43. Gruber I, Landenberger N, Staebler A, Hahn M, Wallwiener D, Fehm T. Relationship between circulating tumor cells and peripheral T-cells in patients with primary breast cancer. *Anticancer Res* (2013) 33(5):2233–8.

44. Arnoletti JP, Reza J, Rosales A, Monreal A, Fanaian N, Whisner S, et al. Pancreatic ductal adenocarcinoma (Pdac) circulating tumor cells influence myeloid cell differentiation to support their survival and immunoresistance in portal vein circulation. *PloS One* (2022) 17(3):e0265725. doi: 10.1371/journal.pone.0265725

frontiers | Frontiers in Oncology

TYPE Original Research
PUBLISHED 16 June 2023
DOI 10.3389/fonc.2023.1186479

OPEN ACCESS

EDITED BY
David Azria,
Université de Montpellier, France

REVIEWED BY
Fernanda Herrera,
Centre Hospitalier Universitaire Vaudois (CHUV), Switzerland
Pervin Hurmuz,
Hacettepe University, Türkiye

*CORRESPONDENCE
Jonathan Khalifa
khalifa.jonathan@iuct-oncopole.fr

RECEIVED 14 March 2023
ACCEPTED 30 May 2023
PUBLISHED 16 June 2023

CITATION
Pasquier C, Chaltiel L, Massabeau C, Rabeau A, Lebas L, Lusque A, Texier J-S, Moyal EC-J, Mazières J and Khalifa J (2023) Impact of radiation on host immune system in patients treated with chemoradiotherapy and durvalumab consolidation for unresectable locally advanced non-small cell lung cancer. *Front. Oncol.* 13:1186479. doi: 10.3389/fonc.2023.1186479

Impact of radiation on host immune system in patients treated with chemoradiotherapy and durvalumab consolidation for unresectable locally advanced non-small cell lung cancer

Corentin Pasquier[1], Léonor Chaltiel[2], Carole Massabeau[1], Audrey Rabeau[3], Louisiane Lebas[4], Amélie Lusque[2], Jean-Sébastien Texier[5], Elizabeth Cohen-Jonathan Moyal[1,6,7], Julien Mazières[3,6] and Jonathan Khalifa[1,6,7]*

[1]Department of Radiation Oncology, Institut Claudius Regaud/Institut Universitaire du Cancer de Toulouse-Oncopole, Toulouse, France, [2]Department of Biostatistics, Institut Claudius Regaud/Institut Universitaire du Cancer de Toulouse-Oncopole, Toulouse, France, [3]Department of Thoracic Oncology, Centre Hospitalier Universitaire de Toulouse, Hôpital Larrey, Toulouse, France, [4]Department of Pulmonology, Centre Hospitalier Intercommunal des Vallées de l'Ariège (CHIVA), Saint-Jean-de-Verges, France, [5]Department of Nuclear Medicine, Institut Claudius Regaud/Institut Universitaire du Cancer de Toulouse-Oncopole, Toulouse, France, [6]Université de Toulouse III Paul Sabatier, Toulouse, France, [7]Institut National de la Santé et de la Recherche Médicale U1037, Centre de Recherche contre le Cancer de Toulouse, Toulouse, France

Background: The optimal modalities of radiotherapy when combining concurrent chemoradiation (CCRT) and immunotherapy (IO) for locally advanced non-small cell lung cancer (LA-NSCLC) remain to be determined. The aim of this study was to investigate the impact of radiation on different immune structures and immune cells in patients treated with CCRT followed by durvalumab.

Material and methods: Clinicopathologic data, pre- and post-treatment blood counts, and dosimetric data were collected in patients treated with CCRT and durvalumab consolidation for LA-NSCLC. Patients were divided into two groups according to the inclusion (NILN-R+) or not (NILN-R–) of at least one non-involved tumor-draining lymph node (NITDLN) in the clinical target volume (CTV). Progression-free survival (PFS) and overall survival (OS) were estimated by the Kaplan–Meier method.

Results: Fifty patients were included with a median follow-up of 23.2 months (95% CI 18.3–35.2). Two-year PFS and 2-year OS were 52.2% (95% CI 35.8–66.3) and 66.2% (95% CI 46.5–80.1), respectively. In univariable analysis, NILN-R+ (hazard ratio (HR) 2.60, p = 0.028), estimated dose of radiation to immune cells (EDRIC) >6.3 Gy (HR 3.19, p = 0.049), and lymphopenia ≤ 500/mm^3 at IO initiation (HR 2.69, p = 0.021) were correlated with poorer PFS; lymphopenia ≤

500/mm^3 was also associated with poorer OS (HR 3.46, p = 0.024). In multivariable analysis, NILN-R+ was the strongest factor associated with PFS (HR 3.15, p = 0.017).

Conclusion: The inclusion of at least one NITDLN station within the CTV was an independent factor for poorer PFS in the context of CCRT and durvalumab for LA-NSCLC. The optimal sparing of immune structures might help in achieving better synergy between radiotherapy and immunotherapy in this indication.

KEYWORDS

radiotherapy, immunotherapy, non-small cell lung cancer (NSCLC), tumor-draining lymph nodes (TDLN), EDRIC, lymphopenia, elective node irradiation

Introduction

The most important improvement in patients with unresectable stage III non-small cell lung cancer (NSCLC) was recently obtained by the addition of consolidation immunotherapy (durvalumab) to concurrent chemoradiation (CCRT), which now constitutes the standard of care (1, 2). However, the optimal radiation therapy regimen in the context of immunotherapy remains to be determined.

One of the immunosuppressive effects of radiotherapy is the direct depletion of circulating lymphocytes or progenitors in lymphoid organs (3–5). Before the era of immunotherapy (IO), several studies highlighted the detrimental impact of lymphopenia on patients treated by CCRT for unresectable LA-NSCLC (5–8). Several models have been proposed to estimate the dose delivered to circulating immune cells. Jin et al. developed a three-step model to calculate the estimated dose of radiation to immune cells (EDRIC) during thoracic radiotherapy, assuming the following: a) the dose to circulating immune cells including rapidly circulating ones in the heart, lung, and blood vessels and slowly circulating ones in the lymphatic system and blood reservoirs (a portion of veins/capillaries) is a surrogate for the EDRIC; b) at each fraction, the radiation dose is uniformly delivered to all cells for rapidly circulating ones and only to those in the irradiated volume for slowly circulating cells. In this model, the blood dose relating to the contribution of a given organ is approximated by its mean organ dose, the percentage of cardiac output, the percentage of blood volume it receives, the time for one blood circulation, the irradiation time, and the number of fractions. Second, the equivalent uniform dose (EUD) is determined from a blood dose/volume histogram (percentage of blood volume irradiated at a given dose). Third, the EDRIC is the sum of the EUDs of each organ. In summary, the EDRIC can be approximated as a function of the mean heart dose, the mean lung dose, the mean body dose, and the number of fractions (9). In a secondary analysis of the RTOG 0617 trial, they showed that a higher EDRIC was significantly associated with poorer outcomes (10). The model was adjusted and externally validated in a retrospective cohort of stage III NSCLC following definitive CCRT (11). In addition, EDRIC was negatively associated with lymphocyte and neutrophil counts. More recently, the impact of lymphopenia (12–14) and EDRIC (15) on outcomes has been suggested in the context of durvalumab consolidation.

As the tumor-draining lymph nodes (TDLNs) are the main sites of lymphocyte priming, their sparing in the context of radiotherapy and IO should be addressed. In the context of high dose per fraction, preclinical models have established the deleterious effect of TDLN irradiation on the radiation-induced anti-tumor immune response, whether or not it is associated with immune checkpoint inhibitors (16–18). However, the impact of radiation dose on non-involved tumor-draining lymph nodes (NITDLNs) as well as other "immune" organs at risk (iOARs), such as bone marrow, spleen, and immune cells in the context of conventionally fractionated CCRT and durvalumab consolidation for stage III NSCLC, remains to be established.

Therefore, the aim of this study was to assess the impact of radiation on different immune structures including NITDLNs and iOARs with regard to clinical outcomes in a cohort of patients treated by CCRT followed by durvalumab.

Materials and methods

Study population

Between January 2015 and March 2022, patients with unresectable LA-NSCLC who underwent platinum-based CCRT followed by durvalumab consolidation were retrospectively analyzed through the electronic database of a Comprehensive Cancer Center (xxx). Inclusion criteria were as follows: 1) histologically documented NSCLC; 2) imaging evaluation including at least computed tomography (CT) of the chest, abdomen, and pelvis and/or F-18 fluorodeoxyglucose positron emission tomography/computed tomography (^{18}F FDG-PET/CT) and brain CT or magnetic resonance imaging (MRI); 3) diagnosis of unresectable locally advanced disease; 4) treatment with platinum-based CCRT (at least two cycles concurrent with radiotherapy) and initiation of durvalumab consolidation therapy (10 mg/kg every 2 weeks or 1,500 mg every 4 weeks) if no disease progression after CCRT; 5) complete blood counts accessible at baseline and follow-up. Patients who underwent sequential chemoradiotherapy were excluded.

This study was approved by the institutional review boards of our institution. Patients received a letter detailing the aim of the study and the use of data collection and could refuse inclusion at any time, but informed consent was not necessary because of the retrospective nature of the study.

Data collection

Demographics

Patient characteristics such as age, WHO performance status, clinical staging (TNM), histology, PD-L1 expression, and mutational status were collected. Standardized uptake value (SUV) max and SUV peak were evaluated from ^{18}F FDG-PET/CT of eligible patients by a single physician.

Radiotherapy data

Treatment was delivered by intensity-modulated radiation therapy (IMRT) with volumetric modulated arc therapy (VMAT), and motion was managed by using 4D-CT and motion-adapted gross tumor volume (GTV) in all patients. Target volumes for the whole cohort were based on the European guidelines (19–21). The lung window setting on planning CT scan was used to delineate the GTV of the primary tumor. Depending on the histology, a 5–8-mm expansion was made and edited accounting for the surrounding anatomy to create the clinical target volume (CTV) of the primary tumor. Lymph nodes were included in target volumes in the event of enlarged and/or FDG-avid nodes (21). Nodal CTV was defined as the whole lymph node station(s) of the involved node(s). A 5-mm margin was applied around the CTV to create the planning target volume (PTV) in all patients. Patients were treated with curative intent radiotherapy, most commonly to 66 Gy in 2-Gy fractions, prescribed on the median of the PTV.

NITDLNs were retrospectively segmented in eligible patients by a single physician. Lymph node stations were defined according to the Japan Lung Cancer Society atlas (22). TDLNs were defined according to the topography of the primary tumor (23–25): stations 10/11R, 7, 4R, and 2R for right upper lobe tumors; stations 10/11R, 8, 7, 4R, and 2R for middle lobe or right lower lobe tumors; stations 10/11L, 7, 2L, 4L, 5, and 6 for left upper lobe tumors; stations 10/11L, 7, 2L, 4L, 5, 6, and 8 for left lower lobe tumors.

Patients were divided into two groups: 1) patients with at least one NITDLN station included in the CTV (radiation to non-involved lymph node (NILN-R+)) and 2) patients with no NITDLN station included in the CTV (NILN-R−).

In addition, we retrospectively delineated the thoracic vertebrae from T1 to T12 and the spleen on planning CT scans.

All dosimetric parameters were extracted from dose–volume histograms available in our planning system (Eclipse®, Varian, Palo Alto, CA, USA).

Biological data

White blood cell (WBC) count, absolute lymphocyte count (ALC), absolute neutrophil count (ANC), and neutrophil-to-lymphocyte ratio (NLR) were collected from complete blood count before treatment, at the end of CCRT and the initiation of consolidative immunotherapy (durvalumab). ALC nadir was also reported. Lymphopenia was graded according to the Common Terminology Criteria for Adverse Events (CTCAE v5.0). A cutoff of 500/mm^3 was chosen as clinically relevant in this cohort.

The lymphocyte variation rate (LVR) from baseline to the end of CCRT was calculated according to the following equation:

$$\frac{(ALC\ \ end\ \ CCRT - ALC\ \ baseline)}{ALC\ \ baseline} \times 100.$$

Calculation of EDRIC

EDRIC was calculated by using dosimetric data including mean heart dose (MHD), mean lung dose (MLD), mean body dose (MBD), and the number of fractions as reported by Ladbury et al. (11):

$$EDRIC = 0.12 \times MLD + 0.08 \times MHD + \left[0.45 + 0.35 \times 0.85 \times \left(\frac{\#of\ \ fractions}{45}\right)^{1/2}\right] \times MBD\,.$$

With the use of data from Jin et al. and Ladbury et al. (10, 11), the 6.3-Gy cutoff was used to split the cohort into two groups.

Outcomes and follow-up

Overall survival (OS) was defined as the time from initiation of durvalumab to death or the last follow-up (censored data). Progression-free survival (PFS) was defined as the time from initiation of durvalumab to progression or death. Patients still alive and without recurrence were censored at the last follow-up. Time to local recurrence (TLR) was defined as the time from initiation of durvalumab to local recurrence. Patients who did not experience local recurrence as the first event were censored at the date of the first event (distant recurrence or death) or the last follow-up.

Controlled disease after CCRT was confirmed by CT in all patients. During consolidation IO, patients were monitored by full-body CT scan and clinical examination every 3 months. At the end of durvalumab or after confirmation of the first disease progression, follow-up was at the discretion of the treating oncologist.

Tumor response was evaluated according to the Response Evaluation Criteria in Solid Tumors (RECIST), version 1.1 (26).

Statistical analysis

Data were summarized by frequency and percentage for qualitative variables and by median and range for continuous variables. Groups were compared by using the chi-square or Fisher's exact test for qualitative variables and the Kruskal–Wallis test for continuous variables. Correlations between continuous variables were calculated with Spearman's coefficient.

All survival times were estimated by the Kaplan–Meier method with 95% confidence intervals (CIs). In univariable analyses, p-

values were calculated by using the Cox proportional hazards model for continuous variables and the log-rank test for qualitative variables, and hazard ratios (HRs) with 95% confidence intervals were estimated with the Cox proportional hazards model for each variable. Cox proportional hazards model was also used to perform multivariable analyses. HRs with 95% confidence intervals were estimated for each variable.

All statistical tests were two-sided, and p-values<0.05 were considered significant. No adjustment was made for multiple comparisons. Statistical analyses were conducted by using Stata® version 16.

Results

Patient characteristics

In total, 50 patients were included. The baseline and treatment characteristics of the population are summarized in Table 1. Of the patients, 52% (n = 26/50) had adenocarcinoma histology, and 72% (n = 36) had stage IIIA or IIIB disease. PD-L1 expression was ≥1% in 37 patients. Most patients were treated with carboplatin-based concurrent chemoradiotherapy (58%, n = 29), and the median number of cycles of chemotherapy was 4 (range, 3–6). All patients were treated with IMRT and image-guided radiation therapy (IGRT). The median dose to the PTV was 66 Gy (55–66 Gy) with a median dose per fraction of 2 Gy (2–2.75 Gy). Eleven patients (22%) had NILN-R+. The median number of irradiated non-involved station(s) was 1 (1–3), and the most common stations targeted were 7, 4, and 2. Forty-two patients (84%) had a partial response at the end of CCRT. All patients received durvalumab as consolidative radiotherapy, and it was started at a median time of 34 days from the end of CCRT.

Dosimetric data

In the whole cohort, the median total PTV was 326 cm^3 (114.1–1,284 cm^3); mean heart, lung PTV, and body dose were 9.4 Gy (0.8–

TABLE 1 Patients characteristics.

Baseline characteristics		Total / N =50	NILN-R- n = 39	NILN-R+ n = 11	p-value
Age at initial diagnosis	Median, years (Range)	61,5 (36 – 75)	61 (36-73)	68 (49-75)	0.497
Sex	Male Female	38 (76%) 12 (24%)	30 (77%) 9 (23%)	8 (73%) 3 (27%)	1
Smoking history	Current Former Never	12 (24%) 36 (72%) 2 (4%)	9 (23%) 29 (74%) 1 (3%)	3 (27%) 7 (64%) 1 (9%)	0.438
History of previous neoplasia	Yes No	10 (20%) 40 (80%)	8 (20%) 31 (80%)	2 (18%) 9 (82%)	1
ECOG PS	0 1	18 (36%) 32 (64%)	14 (36%) 25 (64%)	4 (36%) 7 (64%)	1
Tumor histology	Adenocarcinoma Squamous cell Other	26 (52%) 21 (42%) 3 (6%)	21 (54%) 15 (39%) 3 (7%)	5 (46%) 6 (54%) 0	0.769
PDL1 Expression	< 1% ≥ 1% Unknown	6 (12%) 37 (74%) 7 (14%)	5 (13%) 28 (72%) 6 (15%)	1 (9%) 9 (82%) 1 (9%)	1
Overall stage (AJCC 8th)	II IIIA IIIB IIIC	3 (6%) 19 (38%) 17 (34%) 11 (22%)	2 (5%) 12 (31%) 15 (39%) 10 (25%)	1 (9%) 7 (64%) 2 (18%) 1 (9%)	0.186
Chemotherapy regimen	Carboplatin + Vinorelbine Cisplatin + Vinorelbine Carboplatin + Pemetrexed Cisplatin + Pemetrexed	28 (56%) 19 (38%) 1 (2%) 2 (4%)	21 (54%) 16 (41%) 1 (2%) 1 (2%)	3 (27%) 7 (64%) 1 (9%) 0	0.529
Radiation total dose and regimen	66 Gy / 33 fx 64 Gy / 32 fx 62 Gy / 31 fx 60 Gy / 30 fx 55 Gy / 20 fx	34 (68%) 5 (10%) 1 (2%) 8 (16%) 2 (4%)	28 (72%) 3 (7%) 1 (3%) 6 (15%) 1 (3%)	6 (55%) 2 (18%) 0 (0%) 2 (18%) 1 (9%)	0.297
Duration of CCRT	Median, days (range)	86 (52 – 147)	85 (52 – 147)	92 (71 – 130)	0.468
Time interval between CCRT and durvalumab initiation	Median, days (range)	34 (6 – 81)	34 (13 – 81)	34 (6 – 54)	0.504
Response to CCRT	Stable disease Partial response	8 (16%) 42 (84%)	6 (15%) 33 (85%)	2 (18%) 9 (82%)	1

CCRT, concurrent chemoradiotherapy.

17.9), 12.2 Gy (5.6–19.2), and 7.1 Gy (2.7–12), respectively. Median EDRIC was 7.6 Gy (2.8–11.6). Of the patients, 72% (36/50) had EDRIC > 6.3 Gy. Forty-two patients (84%) had NITDLNs available for dosimetric analysis because eight patients in the NILN-R– group had all the TDLNs involved. The median mean dose to NITDLNs was 40.4 Gy (25.8–64.3) in the NILN-R+ group *vs.* 23.2 Gy (3.1–58.9) in the NILN-R– group (p = 0.002).

Dosimetric data are summarized in Table 2.

Biological data

Median ALC at baseline, at the end of CCRT, and IO initiation was 1,715/mm^3 (628–3,060), 495/mm^3 (130–1,500), and 705/mm^3 (175–1,960), respectively. Median NLR at baseline, at the end of CCRT, and IO initiation was 2.75 (0.9–10.5), 5.46 (2–24.6), and 4.28 (1.4–16.2), respectively. Eleven patients (22%) experienced lymphopenia ≤ 500/mm3 at IO initiation. Median nadir lymphopenia was 480/mm3 (130–1,215). Twenty-seven (54%) patients experienced grade 3 or 4 (G3/4) lymphopenia. The median LVR was −71.7% (−84.6%; −26.7%). No clinical/dosimetric difference was found between patients with ALC ≤ 500/mm^3 and patients with ALC > 500 mm^3 at IO initiation. Patients with ALC ≤ 500/mm^3 at IO initiation had significantly lower ALC at baseline and the end of CCRT when compared to patients with ALC >500 mm^3, but both groups had a similar LVR (Supplementary Table 1). Similarly, no clinical/dosimetric difference was found between patients with grade 1/2 lymphopenia at nadir and patients with grade 3/4 lymphopenia.

Spearman's correlation was weak between the LVR and any clinical/dosimetric relevant variables (Supplementary Table 2). There was no association between the LVR and the number of concurrent chemotherapy cures (LVR of −71.7% (−84.6; −26.7) versus −71.7% (−84.3; −42.2) for 1–2 versus 3 cures, respectively)

TABLE 2 Dosimetric data.

Dosimetric parameters	Total (N = 50)	NILN-R- (N=39)	NILN-R+ (N=11)	p-value
Volume of PTV (median, cm^3) (range)	326 (114.1 – 1284)	352.2 (114.1 – 1284)	305.8 (203.3 – 698)	0.824
Volume of tumor GTV (median, cm3), (range)	52.0 (0.4 - 837.5)	47.5 (0.4 – 837.5)	60.3 (2.4 – 266.5)	0.7
Mean heart dose (median, Gy) (range)	9.4 (0.8 – 17.9)	8.2 (0.8 – 17.9)	10.7 (1.7 – 15)	0.787
Mean lung dose (lung minus PTV) (median, Gy) (range)	12.2 (5.6 – 19.2)	12.6 (5.6 – 19.2)	11.2 (8.4 – 16.4)	0.218
Mean spleen dose (median, Gy) (range)	0.3 (0 – 2.8)	0.3 (0 – 2.8)	0.3 (0.1 – 1.7)	0.911
Mean dose to T1-T12 (median, Gy) (range)	11.1 (2.8 – 22.6)	11.4 (2.8 – 22.5)	10.9 (5.4 – 16.3)	0.386
Mean body dose (median, Gy) (range)	7.1 (2.7 – 12)	7.3 (2.7 – 12)	6.2 (3.9 – 10.5)	0.467
EDRIC (median, Gy) (range)	7.6 (2.8 – 11.6)	7.8 (2.8 – 11.6)	6.8 (4.2 – 10.6)	0.355
EDRIC ≤ 6.3 Gy (n, %) > 6.3 Gy (n, %)	14 (28%) 36 (72%)	10 (26%) 29 (74%)	4 (36%) 7 (64%)	0.475
Volume NITDLN (median, cm^3) (range)	26.5 (0 – 132.1)	26.3 (0 – 132.1)	31 (6.5 – 90.5)	0.297
Dose NITDLN	*Total (N =41)*	*NILN-R- (N=31)*	*NILN-R+ (N=11)*	*p-value*
Mean dose Gy (median, Gy) (range)	28.9 (3.1 – 64.3)	23.2 (3.1 – 58.9)	40.4 (25.9 – 64.3)	0.002
V10Gy %, (range)	76.4 (2.7 – 100)	74.2 (2.7 – 100.0)	89.9 (43.8 – 100.0)	0.112
V20Gy %, (range)	59.3 (0.0 – 100)	51.7 (0.0 – 100.0)	76 (42 – 100.0)	0.014
V30Gy %, (range)	40.3 (0.0 – 100)	36.4 (0.0 – 99.8)	66.7 (34.4 – 100)	0.006
V40Gy %, (range)	31.1 (0.0 – 100)	18.9 (0.0 – 98.4)	57 (19.8 – 100)	0.001
V50Gy %, (range)	20.1 (0.0 – 100)	13.5 (0.0 – 92.7)	49.2 (13.2 – 100)	0.001

NILN-R+, inclusion of at least one non-involved tumor draining lymph node; NITDLN, non-involved tumor draining lymph node; EDRIC, estimated dose to immune cells; ALC, absolute lymphocyte count.

nor between the LVR and the total prescribed dose (LVR of −71.7% (−84.3; −29.5) versus −71.7% (−84.6; −26.7) for dose< 66 Gy versus dose of 66 Gy, respectively).

Survival outcomes

The median follow-up time was 23.2 months (95% CI 18.3–35.2 months).

Fourteen patients (28%) had died at the cutoff date for analysis. The median OS was not reached, and the 2-year OS was 66.2% (95% CI 46.5–80.1). In univariable analysis, previous history of neoplasia (HR 4.44, 95% CI 1.27–15.5, p = 0.011) and lymphopenia ≤ 500/mm^3 at IO initiation (HR 3.46, 95% CI 1.10–10.87, p = 0.024) were significantly associated with poor OS. In multivariable analysis, the results were similar, but the associations were not significant (Table 3).

At the time of analysis, 24 patients experienced disease progression or death. The median PFS was 31.4 months (95% CI 14.0–not reached). NILN-R+ (HR 2.60, 95% CI 1.08–6.27, p = 0.028), G3/4 lymphopenia at nadir (HR 2.73, 95% CI 1.09–6.82, p = 0.026), lymphopenia ≤ 500/mm^3 at IO initiation (HR 2.69, 95% CI 1.12–6.46, p = 0.021), and EDRIC > 6.3 Gy (HR 3.19, 95% CI 0.94–10.82, p = 0.049) were associated with worse PFS in univariable analysis (Figure 1). In the univariable Cox regression model for continuous variables, tumor SUVmax (HR 1.04, 95% CI 1.00–1.08, p = 0.030), ALC at IO initiation (HR 0.85, 95% CI 0.72–1.00, p = 0.047), and nadir ALC (HR 0.79, 95% CI 0.63–0.99, p = 0.038) were significantly associated with PFS. The multivariable analysis, including NILN-R+, lymphopenia ≤ 500/mm^3 at IO initiation, EDRIC > 6.3 Gy, and SUVmax, revealed that NILN-R+ was the strongest factor associated with PFS (HR 3.15, 95% CI 1.23–8.10, p = 0.017). SUVmax was still a prognostic factor (p = 0.038), and there was a trend toward worse PFS with EDRIC > 6.3 Gy (HR 3.03, 95% CI 0.83–11.00, p = 0.093) (Table 4).

The association between PD-L1 status and OS or PFS was not tested owing to the small number of PD-L1-negative patients (n = 6).

Toxicity

At the end of CCRT, 96% had experienced at least one adverse event of any cause and grade, and 20% (10/50) had grade 3 toxicity. The most common grade 3 adverse event was hematologic toxicity (90%, 9/10), and one patient experienced grade 3 esophagitis. Immune-related adverse events (iRAEs) occurred in 66% (33/50) of patients. No grade 4 or 5 iRAE was reported. Five patients (15.2%) experienced grade 3 iRAE: three cases of musculoskeletal toxicity and two cases of skin toxicity (rash). No grade 3 pneumonitis adverse event occurred in the cohort.

Discussion

In this retrospective study, we evaluated the impact of radiation on the immune system, in the context of CCRT followed by durvalumab for stage III NSCLC. One of the main findings is the negative effect of the prophylactic radiation of at least one NITDLN station(s) (NILN-R+). To our knowledge, this is the first study to demonstrate the deleterious impact of radiation on NITDLNs on outcomes in the era of durvalumab after CCRT in NSCLC. Indeed, radiation to NITDLNs was an independent factor for worse PFS in our cohort.

Before the era of durvalumab, involved-field radiotherapy (IFRT) in patients treated with conformational 3D radiotherapy (3D-CRT) was shown to be non-inferior to prophylactic irradiation of all NITDLN stations, known as “elective nodal irradiation” (ENI), in terms of loco-regional recurrence (27–30). In a recent randomized trial, Nestle et al. compared two target volume delineation strategies: one strategy based upon ^{18}F FDG-PET/CT only versus another combining ^{18}F FDG-PET/CT and CT data plus ENI. This trial was the first to show the non-inferiority of reducing target volumes and avoiding ENI based on modern molecular imaging staging (31). Moreover, the risk of locoregional progression was lower in the ^{18}F FDG-PET/CT-based target group (14% *vs.* 29% at 1 year, HR 0.57; per protocol analysis).

However, it was shown that incidental dose to NITDLNs is high when using IFRT with the 3D-CRT technique, as most of the uninvolved nodal stations receive more than 40 Gy (32). Since the implementation of IMRT, there has been no formal comparison of ENI *vs.* IFRT. In the study by Nestle et al., as many as 50% of patients were treated with IMRT (31). In our cohort of IMRT-only treatment, a subgroup of patients had at least one NITDLN station included in the CTV (e.g., in the event of NITDLNs between two involved nodal stations). Most of them had only one station included (64%), and the most common stations targeted were stations 2, 4, and 7. Whether or not this strategy is safe in the context of IMRT and consolidation IO remained to be established; herein, we showed that NILN-R+ was associated with worse outcomes.

These findings are in line with a disturbance of the anti-tumor immune response due to prophylactic nodal irradiation. Several preclinical data from TDLN irradiation support these findings. First, some studies highlighted the key role of TDLNs in the anti-tumor immune response (33, 34). Indeed, Dammeijer et al. demonstrated that in the context of immune checkpoint inhibitors, TDLNs contribute to the anti-tumor effects by generating progenitor-exhausted T cells that seed the tumor (33). Furthermore, they showed that PD-1/PD-L1 interactions in TDLN, but not in the tumor, correlate with prognosis in melanoma patients. Marciscano et al. underlined the fact that irradiation of TDLNs restrained the adaptive immune response when stereotactic radiation and immunotherapy were associated (16). A decrease in tumor-infiltrating immune cell density such as CD8+ T cells and attenuation of chemokines associated with T-cell chemoattraction could explain this phenomenon. Similarly, Buchwald et al. found a proliferation of tumor-specific CD8+ T cells in TDLNs following tumor radiotherapy without treatment of lymph nodes (17). More recently, Darragh et al. showed that ENI to a dose of 8 Gy × 3 could disrupt the local and systemic anti-tumor response following combined primary head and neck tumor radiation (3 × 8 Gy) and immunotherapy (anti-CD25) mainly through a decrease in tumor

10.3389/fonc.2023.1186479

TABLE 3 Univariable and multivariable analyses for overall survival.

Variable		Univariable		Multivariable	
		HR (95% CI)	p-Value	HR (95% CI)	p-Value
Sex	Male	1			
	Female	0.51 (0.11–2.29)	0.371		
ECOG PS	0	1			
	1	1.40 (0.44–4.50)	0.569		
Smoking history	Former smoker	1			
	Current smoker	1.55 (0.51–4.66)	0.436		
History of previous neoplasia	No	1		1	
	Yes	4.44 (1.27–15.50)	0.011	3.0 (0.75–11.95)	0.119
Histology	Squamous cell	1			
	Adenocarcinoma	0.42 (0.15–1.20)	*0.096*		
Overall stage (AJCC 8th)	II/IIIA/IIIB	1			
	IIIC	2.07 (0.61–7.01)	0.230		
Radiation total dose	<66 Gy	1			
	66 Gy	0.86 (0.27–2.79)	0.807		
NILN-R+	No	1			
	Yes	0.95 (0.21–4.29)	0.943		
Response to CCRT	Partial response	1			
	Stable disease	1.83 (0.57–5.86)	0.303		
Grade lymphopenia (nadir)	1/2	1			
	3/4	2.54 (0.80–8.01)	0.103		
Lymphopenia at IO initiation	>500/mm^3	1			
	≤500/mm^3	3.46 (1.10–10.87)	0.024	2.38 (0.66–8.56)	0.183
EDRIC	≤6.3 Gy	1			
	>6.3 Gy	2.79 (0.61–12.73)	0.168		
Age*		1.07 (0.99–1.15)	*0.093*		
SUVmax*		1.03 (0.99–1.08)	0.154		
Duration of CCRT (days)*		1.00 (0.98–1.03)	0.746		
PTV*		1.18 (0.98–1.41)	*0.073*		
Mean NITDLN dose*		1.01 (0.96–1.06)	0.708		
Days from CCRT to IO*		0.99 (0.95–1.04)	0.803		
ALC at IO initiation*		0.81 (0.63–1.04)	0.095		
Nadir lymphopenia (/mm^3)*		0.72 (0.51–1.02)	*0.062*		
NLR at baseline*		0.98 (0.76–1.27)	0.877		
NLR at end of CCRT*		1.09 (0.97–1.22)	0.143		
NLR at IO initiation*		1.12 (0.95–1.33)	0.173		

NILN-R+, inclusion of at least one non-involved tumor-draining lymph node; NITDLN, non-involved tumor-draining lymph node; CCRT, concurrent chemoradiotherapy; IO, immunotherapy; EDRIC, estimated dose to immune cells; ALC, absolute lymphocyte count; NLR, neutrophil-to-lymphocyte ratio; ECOG PS, Eastern Cooperative Oncology Group Performance Status; AJCC, American Joint Committee on Cancer; PTV, planning target volume; SUV, standardized uptake value.
*Continuous variables.

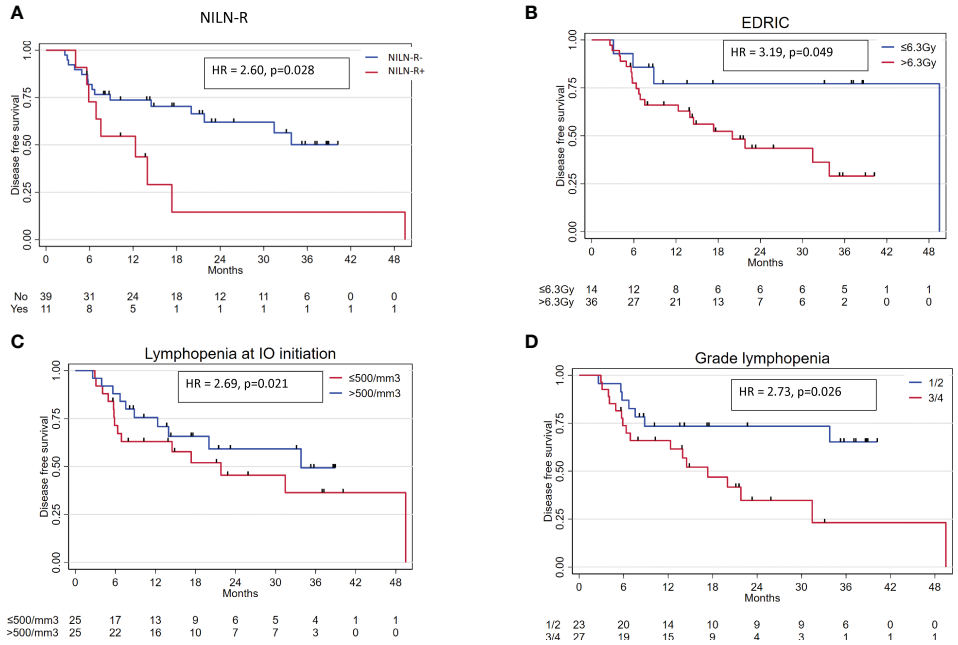

FIGURE 1
Main variables associated with PFS in univariable analysis. **(A)** NILN-R. **(B)** EDRIC. **(C)** Lymphopenia at IO initiation. **(D)** Grade of lymphopenia at nadir. NILN-R+, inclusion of at least one non-involved tumor-draining lymph node; IO, immunotherapy; EDRIC, estimated dose to immune cells; PFS, progression-free survival.

antigen-specific T-cell priming in TDLNs and consequently decrease in circulating antigen-specific T cells (both CD4+ and CD8+) and infiltration into the tumor microenvironment (18).

All this evidence suggests that ENI is probably not the optimal strategy when combining radiotherapy and IO. While the PACIFIC trial in NSCLC is the only phase III trial to have shown a benefit of the adjunction of immune checkpoint inhibitors (ICIs) to chemoradiotherapy for locally advanced disease, the JAVELIN trial and the PEMBRORAD trial in locally advanced head and neck cancer assessing the adjunction of avelumab and pembrolizumab to chemoradiotherapy, respectively, failed to demonstrate any improvement in outcome (35, 36), nor did the KEYNOTE-412 with pembrolizumab in head and neck cancer (NCT03040999) and the CALLA trial with durvalumab in cervical cancer (NCT03830866), according to recent unpublished data (37, 38). One of the key differences between the PACIFIC trial and the other negative trials is the absence of extended ENI in the former, while it was systematically used in the latter. Therefore, the sparing of uninvolved TDLNs during the planning of radiotherapy in the context of immunotherapy could be a promising approach to optimize such a therapeutic association, along with other approaches such as margin reduction, hypofractionation, or alternative radiotherapy techniques including FLASH radiotherapy (39).

We also performed an exploratory analysis to establish a dose cutoff that should not be exceeded in NITDLN. In univariable analysis, no dose cutoff to NITDLNs was correlated with outcomes, possibly due to the lack of power in our study. Interestingly, we found that the median (incidental) dose to NITDLNs in the NILN-R− group was 23.2 Gy. This dose obtained with IMRT is lower than the incidental dose delivered to NITDLNs (approximately 40 Gy) with 3D-CRT (32). This finding underlines the fact that IMRT can achieve better TDLN radiation dose-sparing in order to obtain a stronger synergic effect when combined with IO.

Moreover, our analysis of a modern homogeneous cohort treated with CCRT and consolidation IO seems to confirm the benefit of dose reduction to circulating immune cells as suggested by Ladbury et al. in the pre-immunotherapy era (11). At the 6.3-Gy cutoff, EDRIC was a prognostic factor for PFS (≤6.3 *vs.* >6.3 Gy, p = 0.049) in univariable analysis. In multivariable analysis, there was only a trend for significance (EDRIC > 6.3 Gy: HR 3.03, p = 0.093). In addition, a recent retrospective study found similar results in a cohort of 100 patients with locally advanced NSCLC treated with IO consolidation (15). Nevertheless, McCall et al. used the equation developed by Jin et al. by considering uniform body volume between patients (10, 15), while we used the model developed by Ladbury et al. with the incorporation of MBD instead of integral total dose divided by 62×10^3. The exploration of ALC at three different times was necessary to better appreciate our EDRIC data. We found that ALC ≤ 500/mm^3 at durvalumab initiation was a poor prognostic factor for PFS in univariable analysis (HR 2.69, 95% CI 1.12–6.46, p = 0.021). Nadir ALC was also an important prognostic factor, as patients who did not experience G3/4 lymphopenia had better PFS. These results are consistent with the findings from Friedes et al. (14). Nonetheless, except for age, baseline ALC, and ALC at the end of CCRT, no clinical/dosimetric data were associated with lymphopenia ≤ 500/mm^3 at IO initiation in our cohort, and no clinical/dosimetric correlation could be established with the LVR. Especially, neither NILN-R+ nor EDRIC was associated with lymphopenia in this cohort, perhaps because we did not consider the dose to large vessels in the model. Indeed, Cho

10.3389/fonc.2023.1186479

TABLE 4 Univariable and multivariable analyses for progression-free survival.

Variable		Univariable		Multivariable	
		HR (95% CI)	p-Value	HR (95% CI)	p-Value
Sex	Male	1			
	Female	1.25 (0.49–3.17)	0.642		
ECOG PS	0	1			
	1	2.04 (0.80–5.18)	0.127		
Smoking history	Former smoker	1			
	Current smoker	1.78 (0.72–4.38)	0.205		
History of previous neoplasia	No	1			
	Yes	1.76 (0.64–4.89)	0.269		
Histology	Squamous cell	1			
	Adenocarcinoma	0.77 (0.33–1.78)	0.540		
Overall stage (AJCC 8th)	II/IIIA/IIIB	1			
	IIIC	2.24 (0.90–5.57)	*0.076*		
Radiation total dose	<66 Gy	1			
	66 Gy	0.74 (0.31–1.77)	0.500		
NILN-R+	No	1			
	Yes	2.60 (1.08–6.27)	0.028	3.15 (1.23–8.10)	0.017
Response to CCRT	Partial response	1			
	Stable disease	1.53 (0.57–4.14)	0.398		
Grade lymphopenia (nadir)	1/2	1			
	3/4	2.73 (1.09–6.82)	0.026		
Lymphopenia at IO initiation	>500/mm^3	1			
	≤500/mm^3	2.69 (1.12–6.46)	0.021	1.93 (0.77–4.83)	0.158
EDRIC	≤6.3 Gy	1			
	>6.3 Gy	3.19 (0.94–10.82)	0.049	3.03 (0.83–11.0)	*0.093*
Age*		1.04 (0.98–1.09)	0.182		
SUVmax*		1.04 (1.00–1.08)	0.030	1.05 (1.00–1.09)	0.038
Duration CCRT (days)*		1.01 (0.99–1.03)	0.350		
PTV*		1.06 (0.92–1.23)	0.426		
Mean NITDLN dose*		1.02 (0.99–1.06)	0.125		
Days from CCRT to IO*		0.99 (0.96–1.02)	0.507		
ALC at IO initiation*		0.85 (0.72–1.00)	0.047		
Nadir lymphopenia (/mm^3)*		0.79 (0.63–0.99)	0.038		
NLR at baseline*		1.14 (0.93–1.39)	0.200		
NLR at end of CCRT		1.06 (0.98–1.14)	0.155		
NLR at IO initiation		1.06 (0.94–1.20)	0.346		

NILN-R+, inclusion of at least one non-involved tumor-draining lymph node; NITDLN, non-involved tumor-draining lymph node; CCRT, concurrent chemoradiotherapy; IO, immunotherapy; EDRIC, estimated dose to immune cells; ALC, absolute lymphocyte count; ECOG PS, Eastern Cooperative Oncology Group Performance Status; NLR, neutrophil-to-lymphocyte ratio; AJCC, American Joint Committee on Cancer; PTV, planning target volume; SUV, standardized uptake value.
*Continuous variables.

et al. found a correlation between dose to large vessels and lymphopenia (13). Moreover, the monitoring of tumor-specific subpopulations of lymphocytes could not be assessed. For these reasons, we cannot rule out that the impact of radiation to NITDLNs on the outcome is correlated with circulating tumor-specific lymphocytes *via* a decrease in tumor antigen-specific T-cell priming.

We also explored the impact of radiation dose on other iOARs on outcomes. Dose to thoracic vertebrae was not associated with worse outcomes or lymphopenia. Doses to the spleen were very low in our cohort, so no correlation could be established.

This study has some limitations mainly due to its retrospective nature and its small cohort size. Multiple comparisons have been performed, which can inflate the alpha risk and the likelihood of type I error. However, due to the exploratory nature of our study, no adjustments were made for multiple comparisons, and all p-values and confidence intervals were shown to allow readers to interpret the results themselves according to the number of tests performed. Therefore, our results are exploratory and need to be confirmed in a larger cohort. However, notably, the single-center design guaranteed homogeneity in radiotherapy techniques and follow-up.

Conclusion

In conclusion, we found that prophylactic irradiation of at least one NITDLN was a strong independent factor for worse PFS in patients treated with consolidation immunotherapy following CCRT for locally advanced NSCLC. Moreover, we confirmed the impact of lymphopenia and irradiation of immune cells (EDRIC) on outcomes in this population. These findings lend weight to the idea that modern radiotherapy techniques should spare host immune structures and especially NITDLNs when combining radiotherapy and immunotherapy for locally advanced disease.

Data availability statement

The raw data supporting the conclusions of this article will be made available by the authors, without undue reservation.

Ethics statement

The studies involving human participants were reviewed and approved by Institutional review boards of Toulouse Cancer Institute. Written informed consent for participation was not required for this study in accordance with the national legislation and the institutional requirements.

Author contributions

Conceptualization, JK and CP; methodology, JK and CP; formal analysis, CP, LC, AL, and JK; investigation, all; data curation, CP; writing—original draft, CP and JK; writing—review and editing, all; supervision, JK. All authors contributed to the article and approved the submitted version.

Conflict of interest

The authors declare that the research was conducted in the absence of any commercial or financial relationships that could be construed as a potential conflict of interest.

Publisher's note

Supplementary material

The Supplementary Material for this article can be found online at: https://www.frontiersin.org/articles/10.3389/fonc.2023.1186479/full#supplementary-material

References

1. Antonia SJ, Villegas A, Daniel D, Vicente D, Murakami S, Hui R, et al. Overall survival with durvalumab after chemoradiotherapy in stage III NSCLC. *N Engl J Med* (2018) 379:2342–50. doi: 10.1056/NEJMoa1809697

2. Spigel DR, Faivre-Finn C, Gray JE, Vicente D, Planchard D, Paz-Ares L, et al. Five-year survival outcomes from the PACIFIC trial: durvalumab after chemoradiotherapy in stage III non-small-cell lung cancer. *J Clin Oncol* (2022). doi: 10.1200/JCO.21.01308

3. Trowell OA. The sensitivity of lymphocytes to ionising radiation. *J Pathol Bacteriol* (1952) 64:687–704. doi: 10.1002/path.1700640403

4. Chadha AS, Liu G, Chen HC, Das P, Minsky BD, Mahmood U, et al. Does unintentional splenic radiation predict outcomes after pancreatic cancer radiation therapy? *Int J Radiat Oncol Biol Phys* (2017) 97:323–32. doi: 10.1016/J.IJROBP.2016.10.046

5. Abravan A, Faivre-Finn C, Kennedy J, McWilliam A, van Herk M. Radiotherapy-related lymphopenia affects overall survival in patients with lung cancer. *J Thorac Oncol* (2020) 15:1624–35. doi: 10.1016/J.JTHO.2020.06.008

6. Damen PJJ, Kroese TE, van Hillegersberg R, Schuit E, Peters M, Verhoeff JJC, et al. The influence of severe radiation-induced lymphopenia on overall survival in solid tumors: a systematic review and meta-analysis. *Int J Radiat Oncol Biol Phys* (2021) 111:936–48. doi: 10.1016/J.IJROBP.2021.07.1695

7. Campian JL, Ye X, Brock M, Grossman SA. Treatment-related lymphopenia in patients with stage III non-small-cell lung cancer. *Cancer Invest* (2013) 31:183–8. doi: 10.3109/07357907.2013.767342

8. Tang C, Liao Z, Gomez D, Levy L, Zhuang Y, Gebremichael RA, et al. Lymphopenia association with gross tumor volume and lung V5 and its effects on non-small cell lung cancer patient outcomes. *Int J Radiat Oncol Biol Phys* (2014) 89:1084–91. doi: 10.1016/J.IJROBP.2014.04.025

9. Jin JY, Hu C, Xiao Y, Zhang H, Ellsworth S, Schild SE, et al. Higher radiation dose to immune system is correlated with poorer survival in patients with stage III non–small cell lung cancer: a secondary study of a phase 3 cooperative group trial (NRG oncology RTOG 0617). *Int J Radiat Oncol* (2017) 99:S151–2. doi: 10.1016/j.ijrobp.2017.06.351

10. Jin JY, Hu C, Xiao Y, Zhang H, Paulus R, Ellsworth SG, et al. Higher radiation dose to the immune cells correlates with worse tumor control and overall survival in patients with stage III NSCLC: a secondary analysis of RTOG0617. *Cancers (Basel)* (2021) 13. doi: 10.3390/CANCERS13246193

11. Ladbury CJ, Rusthoven CG, Camidge DR, Kavanagh BD, Nath SK. Impact of radiation dose to the host immune system on tumor control and survival for stage III non-small cell lung cancer treated with definitive radiation therapy. *Int J Radiat Oncol Biol Phys* (2019) 105:346–55. doi: 10.1016/J.IJROBP.2019.05.064

12. Thor M, Shepherd AF, Preeshagul I, Offin M, Gelblum DY, Wu AJ, et al. Pre-treatment immune status predicts disease control in NSCLCs treated with chemoradiation and durvalumab. *Radiother Oncol* (2022) 167:158–64. doi: 10.1016/J.RADONC.2021.12.016

13. Cho Y, Kim Y, Chamseddine I, Lee WH, Kim HR, Lee IJ, et al. Lymphocyte dynamics during and after chemo-radiation correlate to dose and outcome in stage III NSCLC patients undergoing maintenance immunotherapy. *Radiother Oncol* (2022) 168:1–7. doi: 10.1016/J.RADONC.2022.01.007

14. Friedes C, Chakrabarti T, Olson S, Prichett L, Brahmer JR, Forde PJ, et al. Association of severe lymphopenia and disease progression in unresectable locally advanced non-small cell lung cancer treated with definitive chemoradiation and immunotherapy. *Lung Cancer* (2021) 154:36–43. doi: 10.1016/J.LUNGCAN.2021.01.022

15. McCall NS, McGinnis HS, Janopaul-Naylor JR, Kesarwala AH, Tian S, Stokes WA, et al. Impact of radiation dose to the immune cells in unresectable or stage III non-small cell lung cancer in the durvalumab era. *Radiother Oncol* (2022) 174:133–40. doi: 10.1016/J.RADONC.2022.07.015

16. Marciscano AE, Ghasemzadeh A, Nirschl TR, Theodros D, Kochel CM, Francica BJ, et al. Elective nodal irradiation attenuates the combinatorial efficacy of stereotactic radiation therapy and immunotherapy. *Clin Cancer Res* (2018) 24:5058–71. doi: 10.1158/1078-0432.CCR-17-3427

17. Buchwald ZS, Nasti TH, Lee J, Eberhardt CS, Wieland A, Im SJ, et al. Tumor-draining lymph node is important for a robust abscopal effect stimulated by radiotherapy. *J Immunother Cancer* (2020) 8. doi: 10.1136/jitc-2020-000867

18. Darragh LB, Gadwa J, Pham TT, Van Court B, Neupert B, Olimpo NA, et al. Elective nodal irradiation mitigates local and systemic immunity generated by combination radiation and immunotherapy in head and neck tumors. *Nat Commun* (2022) 13:7015. doi: 10.1038/S41467-022-34676-W

19. De Ruysscher D, Faivre-Finn C, Moeller D, Nestle U, Hurkmans CW, Le Péchoux C, et al. European Organization for research and treatment of cancer (EORTC) recommendations for planning and delivery of high-dose, high precision radiotherapy for lung cancer. *Radiother Oncol* (2017) 124:1–10. doi: 10.1016/J.RADONC.2017.06.003

20. Nestle U, Le Pechoux C, De Ruysscher D. Evolving target volume concepts in locally advanced non-small cell lung cancer. *Transl Lung Cancer Res* (2021) 10:1999–2010. doi: 10.21037/TLCR-20-805

21. Nestle U, De Ruysscher D, Ricardi U, Geets X, Belderbos J, Pöttgen C, et al. ESTRO ACROP guidelines for target volume definition in the treatment of locally advanced non-small cell lung cancer. *Radiother Oncol* (2018). doi: 10.1016/j.radonc.2018.02.023

22. Itazawa T, Tamaki Y, Komiyama T, Nishimura Y, Nakayama Y, Ito H, et al. The Japan lung cancer society-Japanese society for radiation oncology consensus-based computed tomographic atlas for defining regional lymph node stations in radiotherapy for lung cancer. *J Radiat Res* (2017) 58:86–105. doi: 10.1093/JRR/RRW076

23. Ichinose Y, Kato H, Koike T, Tsuchiya R, Fujisawa T, Shimizu N, et al. Completely resected stage IIIA non-small cell lung cancer: the significance of primary tumor location and N2 station. *J Thorac Cardiovasc Surg* (2001) 122:803–8. doi: 10.1067/MTC.2001.116473

24. Kim AW. Lymph node drainage patterns and micrometastasis in lung cancer. *Semin Thorac Cardiovasc Surg* (2009) 21:298–308. doi: 10.1053/J.SEMTCVS.2009.11.001

25. Watanabe Y, Shimizu J, Tsubota M, Iwa T. Mediastinal spread of metastatic lymph nodes in bronchogenic carcinoma. mediastinal nodal metastases in lung cancer. *Chest* (1990) 97:1059–65. doi: 10.1378/CHEST.97.5.1059

26. Eisenhauer EA, Therasse P, Bogaerts J, Schwartz LH, Sargent D, Ford R, et al. New response evaluation criteria in solid tumours: revised RECIST guideline (version 1.1). *Eur J Cancer* (2009) 45:228–47. doi: 10.1016/j.ejca.2008.10.026

27. Chen M, Bao Y, Ma HL, Hu X, Wang J, Wang Y, et al. Involved-field radiotherapy versus elective nodal irradiation in combination with concurrent chemotherapy for locally advanced non-small cell lung cancer: a prospective randomized study. *BioMed Res Int* (2013) 2013. doi: 10.1155/2013/371819

28. Yuan S, Sun X, Li M, Yu J, Ren R, Yu Y, et al. A randomized study of involved-field irradiation versus elective nodal irradiation in combination with concurrent chemotherapy for inoperable stage III nonsmall cell lung cancer. *Am J Clin Oncol* (2007) 30:239–44. doi: 10.1097/01.COC.0000256691.27796.24

29. Yang K, Cao F, Wang J, Liu L, Zhang T, Wu G. Improved local control without elective nodal radiotherapy in patients with unresectable NSCLC treated by 3D-CRT. *Front Med China* (2007) 1:381–5. doi: 10.1007/S11684-007-0074-7

30. Li R, Yu L, Lin S, Wang L, Dong X, Yu L, et al. Involved field radiotherapy (IFRT) versus elective nodal irradiation (ENI) for locally advanced non-small cell lung cancer: a meta-analysis of incidence of elective nodal failure (ENF). *Radiat Oncol* (2016) 11. doi: 10.1186/S13014-016-0698-3

31. Nestle U, Schimek-Jasch T, Kremp S, Schaefer-Schuler A, Mix M, Küsters A, et al. Imaging-based target volume reduction in chemoradiotherapy for locally advanced non-small-cell lung cancer (PET-plan): a multicentre, open-label, randomised, controlled trial. *Lancet Oncol* (2020) 21:581–92. doi: 10.1016/S1470-2045(20)30013-9

32. Kimura T, Togami T, Nishiyama Y, Ohkawa M, Takashima H. Impact of incidental irradiation on clinically uninvolved nodal regions in patients with advanced non-small-cell lung cancer treated with involved-field radiation therapy: does incidental irradiation contribute to the low incidence of elective nodal failure? *Int J Radiat Oncol Biol Phys* (2010) 77:337–43. doi: 10.1016/J.IJROBP.2009.05.039

33. Dammeijer F, van Gulijk M, Mulder EE, Lukkes M, Klaase L, van den Bosch T, et al. The PD-1/PD-L1-Checkpoint restrains T cell immunity in tumor-draining lymph nodes. *Cancer Cell* (2020) 38:685–700.e8. doi: 10.1016/J.CCELL.2020.09.001

34. Fransen MF, Schoonderwoerd M, Knopf P, Camps MG, Hawinkels LJ, Kneilling M, et al. Tumor-draining lymph nodes are pivotal in PD-1/PD-L1 checkpoint therapy. *JCI Insight* (2018) 3. doi: 10.1172/JCI.INSIGHT.124507

35. Lee NY, Ferris RL, Psyrri A, Haddad RI, Tahara M, Bourhis J, et al. Avelumab plus standard-of-care chemoradiotherapy versus chemoradiotherapy alone in patients with locally advanced squamous cell carcinoma of the head and neck: a randomised, double-blind, placebo-controlled, multicentre, phase 3 trial. *Lancet Oncol* (2021) 22:450–62. doi: 10.1016/S1470-2045(20)30737-3

36. Tao Y, Biau J, Sun XS, Sire C, Martin L, Alfonsi M, et al. Pembrolizumab versus cetuximab, concurrent with radiotherapy in patients with locally advanced squamous cell carcinoma of head and neck unfit for cisplatin (GORTEC 2015-01 PembroRad): a multicenter, randomized, phase 2 trial. *Ann Oncol* (2022). doi: 10.1016/J.ANNONC.2022.10.006

37. *Update on CALLA phase III trial of concurrent use of imfinzi and chemoradiotherapy in locally advanced cervical cancer* . Available at: https://www.astrazeneca.com/media-centre/press-releases/2022/update-on-calla-phase-iii-trial-for-imfinzi.html (Accessed July 31, 2022).

38. *Primary results of the phase III KEYNOTE-412 study: pembrolizumab (pembro) with chemoradiation therapy (CRT) vs placebo plus CRT for locally advanc.| OncologyPRO* . Available at: https://oncologypro.esmo.org/meeting-resources/esmo-congress/primary-results-of-the-phase-iii-keynote-412-study-pembrolizumab-pembro-with-chemoradiation-therapy-crt-vs-placebo-plus-crt-for-locally-advanc (Accessed December 12, 2022).

39. Khalifa J, Mazieres J, Gomez-Roca C, Ayyoub M, Moyal ECJ. Radiotherapy in the era of immunotherapy with a focus on non-Small-Cell lung cancer: time to revisit ancient dogmas? *Front Oncol* (2021) 11:662236. doi: 10.3389/FONC.2021.662236

frontiers | Frontiers in Oncology

TYPE Review
PUBLISHED 03 August 2023
DOI 10.3389/fonc.2023.1201500

OPEN ACCESS

EDITED BY
Timothy James Kinsella,
Brown University, United States

REVIEWED BY
Franz Rödel,
University Hospital Frankfurt, Germany
Gianluca Ferini,
Rem Radiotherapy, Italy

*CORRESPONDENCE
Harald Paganetti
hpaganetti@mgh.harvard.edu

RECEIVED 06 April 2023
ACCEPTED 17 July 2023
PUBLISHED 03 August 2023

CITATION
Paganetti H (2023) A review on lymphocyte radiosensitivity and its impact on radiotherapy.
Front. Oncol. 13:1201500.
doi: 10.3389/fonc.2023.1201500

A review on lymphocyte radiosensitivity and its impact on radiotherapy

Harald Paganetti[1,2]*

[1]Department of Radiation Oncology, Massachusetts General Hospital, Boston MA, United States, [2]Harvard Medical School, Boston MA, United States

It is well known that radiation therapy causes lymphopenia in patients and that this is correlated with a negative outcome. The mechanism is not well understood because radiation can have both immunostimulatory and immunosuppressive effects. How tumor dose conformation, dose fractionation, and selective lymph node irradiation in radiation therapy does affect lymphopenia and immune response is an active area of research. In addition, understanding the impact of radiation on the immune system is important for the design and interpretation of clinical trials combining radiation with immune checkpoint inhibitors, both in terms of radiation dose and treatment schedules. Although only a few percent of the total lymphocyte population are circulating, it has been speculated that their increased radiosensitivity may contribute to, or even be the primary cause of, lymphopenia. This review summarizes published data on lymphocyte radiosensitivity based on human, small animal, and *in vitro* studies. The data indicate differences in radiosensitivity among lymphocyte subpopulations that affect their relative contribution and thus the dynamics of the immune response. In general, B cells appear to be more radiosensitive than T cells and NK cells appear to be the most resistant. However, the reported dose-response data suggest that in the context of lymphopenia in patients, aspects other than cell death must also be considered. Not only absolute lymphocyte counts, but also lymphocyte diversity and activity are likely to be affected by radiation. Taken together, the reviewed data suggest that it is unlikely that radiation-induced cell death in lymphocytes is the sole factor in radiation-induced lymphopenia.

KEYWORDS

lymphopenia, lymphocytes, radiotherapy, radiosensitivity, blood dose

1 Introduction

Radiation-induced lymphopenia (RIL) has long been observed in radiation therapy patients (1–3) and develops in up to ~70% of patients undergoing external beam radiation therapy (4–8). High-grade RIL has been shown to correlate with poor overall survival, disease recurrence, and metastasis rates (9). A correlation between lymphopenia and dose

to circulating lymphocytes has been demonstrated (e.g., (6, 8, 10–13). Therefore, it has been speculated that lymphopenia is caused by an increased radiosensitivity of circulating lymphocytes (7) and the large volume of blood irradiated during radiotherapy.

Treatment delivery techniques differ in the distribution of the low dose bath outside of the planned treatment volume and in the duration of treatment in a fraction (10, 14, 15) resulting in different dose distributions experienced by circulating lymphocytes (6, 16–19). In a study of esophageal cancer, 35% of patients had grade 4 RIL when treated with concurrent chemotherapy and either intensity-modulated photon (IMRT) or proton therapy, which was correlated with overall survival (20). Due to the lower integral dose, patients treated with protons had 70% less grade 4 RIL compared to IMRT. However, this was not confirmed in a study of 150 oropharyngeal cancer patients (21) and in locally advanced non-small cell lung cancer (NSCLC) treated with either IMRT or proton therapy (15). Dose to lymphocytes is also influenced by patient specific factors such as baseline levels of absolute counts and lymphocyte subpopulations, which are known to differ between patient groups (22), as well as fractionation and dose rate (18, 23–27). Consequently, lymphocyte sparing radiation therapy has been proposed (8, 28). Smaller target volumes and hypo-fractionated regimens may be associated with higher post-treatment lymphocyte counts. For example, during a 30-fraction treatment with 2 Gy/fraction to a target volume of 8 cm in diameter, 95% of the circulating blood receives doses greater than 0.5 Gy, with a mean dose to the circulating blood greater than 2 Gy (8). Larger field sizes increased chromosomal aberrations in circulating lymphocytes in a prospective series of lung cancer patients treated with carbon-ion therapy (29) and were associated with lower post-treatment lymphocyte counts in lung cancer treated with protons (15). There have been several other studies of field size effects on lymphopenia in solid tumors (5, 30, 31).

Although the amount of circulating blood plays a role, considering that only a few percent of the total lymphocyte population is circulating, compared to those residing in organs or lymph nodes, is not clear whether RIL is simply caused by radiation-induced depletion of circulating lymphocytes. Radiation has deleterious effects not only on circulating lymphocytes but also on tumor-infiltrating lymphocytes and lymphocytes residing in structures such as the bone marrow (32), spleen (33), and lymph nodes (34). Lymphopenia has been shown to correlate strongly with dose to the spleen (33, 35–37). The capillaries in the spleen are permeable, resulting in high transit times for lymphocytes in the spleen, which in turn results in significant dose to lymphocytes in treatments involving the spleen. By assessing chromosome aberrations in lymphocytes in breast cancer patients, it has been shown that the number of lymph nodes in the field plays a significant role (34). A correlation with bone marrow dose has also been shown by several investigators (32, 38–41), but not by Saito et al. (36). Lymphopenia has also been associated with lymph node irradiation in prostate radiation therapy (42) and breast radiation therapy (43). Consequently, dose constraints to lymphoid organs have been proposed to mitigate lymphopenia (44). Reduced total counts as well as counts in lymphocyte subpopulations were reported for colorectal cancer patients (45) and liver SBRT patients (46).

The interaction of radiation with the immune system is complex (47). Radiation therapy can have both immune-stimulatory (18, 48–52) and immune-suppressive (5) effects. Radiation can promote the release of damage-associated molecular patterns (DAMPs) and tumor antigens via immunogenic cell death, activate the production of type I interferon (IFN) and IFN-stimulated genes via DNA damage that is sensed via the cGAS/STING pathway, and activate antigen-presenting cells, including dendritic cells (DCs) and macrophages (53). Antigen-presenting cells travel through lymphatic vessels to the draining lymph nodes (for instance) where they present antigens to naïve lymphocytes initiating their differentiation into effector and memory cells. Activated lymphocytes returnvia the blood to the tumor site where they recognize tumor antigens and carry out various effector functions. Radiation can also suppress the immune response via IFN-mediated upregulation of immune checkpoint molecules (e.g., PD-L1) (54) and by inducing immune-suppressive populations including myeloid-derived suppressor cells. Additionally, radiation can also directly kill immune cells and thereby modulate the immune response.

While some patients respond favorably to immunotherapy, many develop progressive disease (55). This has led to interest in combining immunotherapy with radiation (56–62). Synergistic combinations of radiation and immunotherapy have shown promise (62–66) as they help to overcome the immunosuppressive tumor microenvironment and thus enhance the therapeutic effect of radiation (67, 68). The optimal sequencing of radiation with immunotherapy (18, 69–72) as well as the best radiation modality for combination therapies (6, 16, 17, 73–76) are being studied extensively. It has even been suggested that low dose whole-body irradiation may improve outcome after subsequent treatment regimens due to radiation induced antigen release (52). Furthermore, pre-clinical data suggest that nodal irradiation may attenuate the combinatorial efficacy of immunotherapy-radiation combination regimens (77). There are numerous clinical trials combining radiation with immunotherapy (78).

While radiation-induced cell death is not the only key parameter when optimizing radiation treatments in this context, it certainly has a profound impact. Section 2 summarizes the published methods for estimating the dose delivered to circulating lymphocytes during radiation therapy. In section 3, studies assessing the radiation sensitivity of lymphocytes are reviewed.

2 Estimating the dose to the blood and to circulating lymphocytes in radiation therapy

Under the assumption that the dose to circulating blood is a surrogate for the dose to circulating lymphocytes, several efforts have been made to estimate the blood dose from radiation exposure. To estimate the cumulative blood dose from whole-body irradiation, Molloy et al. developed a blood perfusion model in

which the circulation was modeled in a sinusoidal motion between the upper and lower body without regard to individual organs (79). The blood volume was divided into discrete voxels and a statistical dispersion was introduced to reflect the inhomogeneous blood flow in the body. The treatment beam was simulated assuming a time-dependent dose cloud depending on the field size and machine motion.

Yovino et al. (7) calculated the dose to circulating blood for a high-grade glioma patient as a function of dose rate and photon treatment technique. The model uses the three-dimensional dose distributions in the brain and calculates the dose to the blood passing through the radiation field by assuming that 16% of the cardiac output enters the brain with a total blood volume of 5 l and a blood flow velocity of 10 mm/sec. The model includes several simplifications, such as uniformly distributed blood flow without whole-body blood flow dynamics. Another assumption is that blood does not re-enter the treatment field during the duration of a single beam and/or segment. Between beams and between treatment fractions, the cumulative dose was calculated by convolution of the blood dose histograms. The simulations predicted that a single fraction of radiation would deliver 0.5 Gy to 5% of the circulating cells. After 30 fractions, 99% of the circulating blood had received ≥0.5 Gy. Target volume and field size were the most important parameters. This model was also used by Wild et al. (8) who came to similar conclusions.

Basler et al. (80) used dose-volume histograms for liver treatments to estimate the dose to circulating lymphocytes in VMAT. A mean hepatic blood flow velocity of 10 mm/s with a total body blood volume of 5 l was considered. Cardiac output was set at 5 l/min with a circulation time of 60 s for the total blood volume. The model assumes that regional hepatic blood flow is comparable in the different liver segments. Full blood mixing in between fields or fractions was considered and the probability of re-entering a specific liver segment and treatment field was calculated based on the cardiac output and relative volumes of the liver segments. The results show that the dose to the circulating lymphocytes was mainly influenced by the beam-on time and the target volume.

Jin et al. (81) used a similar approach as Yovino et al. to calculate the dose to the blood using a blood flow network consisting of the lungs, heart, large vessels, and body mass. The blood dose and blood volume contributing to each of these compartments during a single fraction were estimated and converted to an equivalent uniform dose, with the total effective blood dose being the sum of the contributions from all irradiated organs. The model was applied to lung treatments, taking into account mean lung dose, mean heart dose, and the integral dose. Blood dose was correlated with radiation-induced lymphopenia. This model was subsequently applied in other studies that demonstrated a correlation between blood dose and lymphopenia in non-small cell lung cancer (82), esophageal cancer (83, 84), and breast cancer (11), especially when the blood dose was above 4 Gy (84).

The dose to the blood was also estimated to analyze the transcriptional response of genes over time in blood samples after irradiation *in vivo* (85, 86). Considering that most of the blood is irradiated during a 2-min treatment time, the authors determined the mean blood dose as a function of the mean dose to the irradiated volume, the irradiated blood volume, and the body blood volume.

Shin et al. developed a compartmental model that considers blood flow throughout the human body based on compartments defined by the ICRP (International Commission on Radiological Protection) (23). The algorithm assumes a dynamic model describing the spatio-temporal distribution of blood particles (BPs) in organs throughout the body using a discrete-time Markov process. Blood transit times were modeled using ICRP reference mean transit time distributions assuming a Weibull distribution. This was then convolved with the time-dependent radiation field delivery. The simulations revealed different dose levels to the circulating blood for brain irradiation compared to liver irradiation even for similar field sizes due to the different blood flow characteristics of the two organs. The authors also showed that the blood dose-volume histogram is highly sensitive to changes in the treatment time, indicating that dynamic modeling of blood flow and radiation delivery is necessary to evaluate dose to the circulating blood.

To add another level of complexity and accuracy, blood dose algorithms have been developed that explicitly consider venous and arterial vascular trees to account for inhomogeneous organ dose distributions and blood flow dynamics. Hammi et al. (87) developed an intracranial blood flow model based on the major cerebral vasculature extracted from patient MRI data and extended with a network of generic brain vessels. The brain model contains more than 1000 vascular pathways. To determine the dose to the circulating blood, Monte Carlo simulations track the propagation of each individual blood particle through the brain and the time-dependent radiation field delivery. The mean dose to the blood pool was estimated after fractions of proton and photon therapy and showed that the fraction of blood volume receiving any dose after the first fraction was significantly lower for proton therapy. Higher dose rates effectively reduced the fraction of blood irradiated to low doses but increased the amount of blood receiving high doses. The model was also applied by Qian et al. (13), who showed that the treatment dose to the whole body, bone, and large blood vessels as well as the modeled dose to circulating lymphocytes were correlated with lymphopenia.

The internal vasculature of the adult liver, including hepatic arterial, hepatic venous, and hepatic portal venous vessel trees, was created within individual lobes of the ICRP adult female and male livers by Correa-Alfonso et al. (88). For each iteration of the algorithm, pressure, blood flow, and vessel radii within each tree were updated as each new vessel was created and connected to a viable bifurcation site. Liver models were created with virtual vasculature of ~6000 non-intersecting straight cylinders representing the circulations of the vascular tree. To combine the vascular trees with a dynamic dose delivery model, the trees were translated into centerlines that can be deformed to account for patient specific organ contours and for BPs entering the liver. An explicit simulation was implemented to track BPs along different vascular pathways through the liver (24). The dosimetric impact of treatment modality, delivery time, and fractionation on circulating blood cells was quantified showing that doses are highly sensitive to

the beam-on time and demonstrating the trade-off between low dose to a large fraction of blood cells and high dose to a small fraction of blood cells. It was concluded that proton treatments are not necessarily advantageous in terms of dose to the blood even though they are associated with a lower integral dose because of the importance of the beam-on time. Similar vascular tree models have been developed for the brain (89) and lung (90). Such organ-specific vasculature models can be combined with a Markov chain approach to link them to whole body blood flow based on reference values for cardiac output and organ blood volumes (23, 24).

These blood dose models have been used to demonstrate how the dose to the patient's circulating blood depends not only on hemodynamic data but also on treatment modality, beam delivery parameters such as field size, treatment time, fractionation, and dose. While they have been able to show trends in RIL, their main weakness is that the results from blood dose simulations do not necessarily translate directly to doses to circulating lymphocytes, which may have different transition and flow parameters than the blood. Unfortunately, these are more complex and not as well-known (91, 92).

Jin et al. (93) developed a lymphocyte trafficking model that is an extension of an algorithm discussed previously (21). The framework considers 5 compartments of the immune system, i.e. the circulating blood, the bone marrow, specific lymphatic organs such as spleen, lymph nodes/vessels, and other lymphatic tissues in non-lymphatic organs such as gut, lung, liver and skin. Circulating and noncirculating lymphocytes are considered separately. The model also incorporates lymphocyte radiosensitivity and reproductivity. The authors assume that lymphocytes in the blood circulate at a higher rate than the blood. Clinical beam delivery times were not taken into account as the irradiation time was assumed to be equal to the blood circulation time, and all organs were treated as homogeneous.

To study the interaction between immunotherapy and radiotherapy, Friedrich et al. introduced a biophysical model of lymphocyte trafficking that takes into account primary and distal tumor masses, immune cell kinetics targeting tumor cells, and immune cell replenishment after radiation (94). Model parameters were derived from mouse data. The model suggests that the immune response is stronger when checkpoint inhibitors are administered at the time of radiation or shortly thereafter. It predicts that there is a window for radiotherapy that optimally balances radiogenic immune response and depletion of the immune cell pool.

In order to understand the impact of high-dose rate irradiation on the dose to the circulating blood and lymphocytes an algorithmic model was developed by Cucinotta and Smirnova (95). The model also incorporates a one-target-one-hit model of radiation-induced damage as a basis to consider the response of blood lymphocytes to the radiation exposure. It considers time-dependent dose delivery, radiosensitivity and concentration of lymphocytes, as well as blood flow characteristics through the blood circulatory system including the total blood volume and heart rate. The model confirms that the level of surviving blood lymphocytes increases as the dose rate increases.

3 Radiosensitivity of lymphocytes

Monocytes and macrophages isolated from peripheral blood cells are highly radioresistant (96, 97). Monocytes do not express proteins required for non-homologous end-joining and are impaired in base excision repair, which is likely to limit repair especially at higher doses (98). When monocytes proliferate into macrophages and dendritic cells, proteins are upregulated that make these cells repair competent. Dendritic cells are thought to be highly resistant to radiation-induced apoptosis (99). However, the irradiation of dendritic cells may impair their ability to stimulate T cells (100).

Peripheral blood lymphocytes are primed to undergo apoptosis (101). While most mammalian cells are radioresistant at rest and radiosensitive during proliferation, the opposite is true for circulating lymphocytes. Even a small amount of DNA damage appears to be sufficient to activate a DNA damage response and apoptosis (102). Damage to peripheral lymphocytes (e.g., chromosome aberrations) has been used as bio-dosimeters to predict late radiation toxicity in radiation therapy patients (103).

The literature discussed in the following sections is not always consistent in terms of notation. Naïve T cells can be categorized into helper T_h cells (CD3+, CD4+) and cytotoxic T_{cyt} cells (CD3+, CD8+) with regulatory T_{reg} cells (CD4+ CD25+, Foxp3+) as a subset of T_h cells. Categorization can also be done into naïve, effector T_{eff} (CD25+), and memory T cells (effector memory T_{EM} (CD45RO+, CD25-, CCR7-) and central memory T_{CM} (CD45RO+, CD25+, CCR7+)). Naïve B cells (CD27-) and B cells (CD19+, CD20+) can also play an immune-suppressive role, for example by blocking the T_{cyt} cell response. Naïve NK cells (CD16-) can become effector, regulatory, and memory NK cells (CD16+, CD56+, CD3-). NKT cells are a subset of T cells that express both CD3+ and CD56+.

3.1 Lymphocyte radiosensitivity studies in humans

The results of *in vivo* radiosensitivity studies in patients with qualitative or quantitative information are summarized in Tables 1A, B with the latter showing estimated alpha values [Gy^{-1}] for a linear dose-response curve ($\exp(-\alpha D)$). A rather comprehensive study of lymphocyte radiosensitivity was performed by Trowell et al. already in 1952 (110). After whole-body irradiation, lymphocytes were counted in lymph nodes. In addition, lymph nodes and blood samples were irradiated *in vitro*. In 1975, Heier et al. (1) analyzed early and late T cell and B cell counts in patients with seminoma testis. B cells seemed to be more radiosensitive. They also concluded that B cells recovered more rapidly than T cells after the irradiation of the iliac and paraaortic lymph nodes and that irradiation of the thymus did not alter lymphocyte recovery.

Lymphocyte radiosensitivity *in vivo* was evaluated by Clave et al. (105) based on whole-body irradiation of patients prior to bone marrow transplantation. Lymphocyte subpopulations were counted after irradiation at 2 Gy/fraction. B cells were the most

TABLE 1A Ranking of lymphocyte radiosensitivity based on lymphocyte depletion in patients.

Radiosensitivity Ranking	Dose Range	Time	Reference
B > T	40 Gy (20 fractions)	12 d – 10 y	(1)
CD4+ > CD8+	Therapeutic		(104)
B > T > NK, CD34+	0-2 Gy	6 h	(105)
B > T_h; T_{cyt} > NK	50 Gy (25 fractions)	5 w	(106)
B > T; T_{naive} > T_{memory}	26 Gy (13 fractions)	11 d – 4 m	(107)
CD4+ > CD8+ > pre-curser NK > NK, T_{reg}	50-60 Gy (3-5 fractions)		(46)
CD4+ > CD8+	50-60 Gy (5-10 fractions)		(108)
B > T, NK	12 Gy (6 fractions)		(97)

TABLE 1B Estimated alpha values (in Gy^{-1}) for a linear dose-response curve exp(-aD) based on lymphocyte depletion in patients (fits performed using LMfit in python).

T_h	T_{cyt}	B	NK	Peripheral lymphocytes	Reference
0.45 +/- 0.02	0.46 +/- 0.03	0.67 +/- 0.03	0.37 +/- 0.03		(106)
				0.40 (0.08 – 2.0)	(93)
				0.58 (0.28 – 1.23)	(118)

sensitive, followed by T cells (CD4+, CD8+) and NK cells. CD34+ progenitor cells appeared to be highly radioresistant. Note that the easurements include circulating lymphocytes while also irradiating lymphatic vessels. A similar study by Girinsky et al. found no statistically significant difference in radiosensitivity between T cells and B cells (111). Lymphocyte depletion and recovery for different subpopulations has also been studied for low dose whole body irradiation from the Chernobyl accident and in atomic bomb survivors (112).

B cells were the most sensitive and NK cells the least sensitive lymphocyte fraction in cancer patients receiving pelvic radiation therapy (106). No significant differences between T_h cells and T_{cyt} cells were reported. The counts of the lymphocyte subpopulation as a function of total body dose can be translated into alpha values in a linear dose-response curve. Belka et al. (107) evaluated lymphocyte subpopulations after radiation therapy and found that B cells and T cells seemed to be most affected. Recovery of CD8+ cells was significantly faster than that of CD4+ cells, and naïve cells were generally more sensitive than memory cells. Lymphocytes were still unable to respond adequately to antigen stimulation even after recovery of the population.

A comprehensive assessment of circulating immune cell populations in response to stereotactic body radiation therapy in patients with liver cancer was performed by Gustafson et al. (46). They found a severe decrease (~50%) in T cells in liver SBRT patients, even in the absence of bone marrow or nodes in the field, with CD4+ cells being most affected, while CD8+ cells showed no significant differences compared to pre-treatment levels. More specifically, within the CD4+ compartment, T_{reg} cells were not affected. SBRT did not appear to affect mature NK cells (CD16+) but did affect pre-cursor cells (CD16-). McGee et al. analyzed the blood of 31 patients after stereotactic ablation radiation therapy (113). They showed that the effect of radiation on T cells and NK cells depends on the treatment site. Therapy of parenchymal sites induced a systemic immune response (i.e., a decrease in NK cells and an increase in memory CD4+ and CD8+ T cells). This was not seen in non-parenchymal sites (bone and brain).

Zhao et al. (108) analyzed lymphocyte subpopulations after SBRT of early-stage lung cancer. The number and relative percentage of CD4+ T cells were significantly decreased, whereas the number of CD8+ T cells was less affected as their relative percentage was almost unchanged. This decreasing ratio of CD4+/CD8+ T cells was also observed by Yang et al. (104) in head and neck cancer patients. The change in the ratio could not be explained by the small difference in radiosensitivities of CD4+ T cells and CD8+ T cells but was presumably caused by radiation-induced priming and mobilization of CD8+ T cells compensating for the loss of CD8+ T cells. Lymphocyte subpopulations in patients after radiation therapy have also been studied in other sites, such as in prostate cancer (42, 114–116) and in breast cancer (117, 118), demonstrating radiosensitivity of B cells in particular.

Heylmann et al. (97) analyzed T cells and monocytes after treatment in leukemia patients receiving whole body irradiation (6 times 2 Gy). Monocytes showed high radioresistance, and the difference in the lower response between T cells and NK cells was not statistically significant. Three patients who received 12 Gy in 3 days (2 times 2 Gy per day) were analyzed. Analysis of γH2AX foci indicated efficient elimination of damaged B cells during treatment. In NK cells (CD56+), DNA damage accumulated in the surviving NK after repeated irradiation. Whether these cells later undergo apoptotic death or survive in the presence of DNA damage was unclear.

Assuming an exponential dose response relationship, the alpha value of circulating lymphocytes has also been deduced indirectly in patients. A lymphocyte trafficking model was fitted to 51 patients with abdominal cancer treated with radiotherapy (93). The patient specific α values had a median of 0.40 Gy^{-1} (range 0.08 – 2.0 Gy^{-1}). Similarly, for hepatocellular carcinoma the dose to circulating lymphocytes was estimated using a dynamic blood circulation model (23) and combined with the observed lymphocyte depletion in patients, empirically accounting for both cell death and lymphocyte replenishment. The *in vivo* derived patient-specific α had a median value of 0.58 Gy^{-1} (range 0.28 - 1.23 Gy^{-1}) (109).

Schaue et al. (119) isolated lymphocytes from colorectal and prostate cancer patients before, during, and one week after chemoradiation therapy. In most patients, they found an increase of T_{reg} cells as well as CD8+ cells after radiation which was more pronounced in colorectal patients. A relative resistance of T_{reg} could have negative consequences in radiation therapy of their tumor protective role as compared to the immune stimulatory role of more radiosensitive T_{cyt} cells and T_h cells. However, radiation can also reduce protein expression and reduce functionality of T_{reg} cells (120).

3.2 Lymphocyte radiosensitivity studies in mice

Results from preclinical studies of *in vivo* radiosensitivity with qualitative or quantitative information are summarized in Tables 2A, B and include fitting of exponential dose-response curves where possible (Figure 1).

Anderson et al. (121) investigated the effect of radiation on lymphocyte migration. Activated thoracic duct lymphocytes from CBA inbred mice were used as a surrogate for T cells (80-85% T cells, 15-20% B cells) and those from athymic (nude, nu/nu) mice were used as a surrogate for B cells (97%). B cells were highly radiosensitive compared to T cells and activated T cells were more radioresistant than their resting counterparts. In another study, T cells were shown to be more radioresistant than B cells in the spleen of C3Hf mice (122). After whole-body irradiation, T and B cells were analyzed after 3 days. At low doses (0.47 Gy), the number of T and B cells in the spleen was significantly higher compared to unirradiated control mice.

That B cells are more radiosensitive than T cells was also observed after whole-body irradiation with doses of 0.5-15 Gy (123). Mice were sacrificed and thymus, spleen, mesenteric lymph nodes, femur, tibia and fibula were removed, and peripheral blood was analyzed after 6 days. The authors also studied recovery of T and B cell populations after 6 Gy and showed that cells in the thymus and spleen recovered more rapidly than those in the lymph nodes and in the bone marrow. Hochman et al. (140) reported the relative resistance of NK cells in the spleen of (C57BL/6 x C3H/He) F mice and the temporary cessation of progenitor activity. Sado et al. (124) showed that cells from C3H mice were more radioresistant compared to BALB/c, C57BL/6, and B10.BR mice. After whole-body irradiation, T cells were analyzed in the spleen after 3 days. CD8+ T cells were slightly more radiosensitive than CD4+ T cells.

Harrington et al. (125) irradiated C57Bl/6 mice with doses of 0-7 Gy (whole-body) and analyzed splenic T cells (CD4+ and CD8+), B cells, and NK cells after 1, 4, and 7 days after irradiation. They observed a 7-fold enrichment of NK cells and a 3-fold enrichment of T CD4+ cells, while the proportion of CD8+ cells was unchanged and B cells decreased. While radiation may reduce the total number of lymphocytes, the spleen may be enriched when comparing subpopulations. B cells were most sensitive to radiation, followed by CD8+, CD4+, and NK cells. In a study by Chambers et al. (126) on lymphocyte subpopulations after whole-body irradiation of mice, the total number of peripheral lymphocytes decreased as a function of dose and the lymphocyte distribution changed. Relative to the total number of lymphocytes, CD8+ increased slightly on day 1 and then decreased, while CD4+ increased 2-fold on day 4 after 7 Gy. The relative contribution of NK cells increased 9-fold at day 4 at 7 Gy, while the relative number of B cells decreased at all dose levels, e.g., by half at 1 Gy. This indicated radioresistance of NK cells relative to CD4+, CD8+, and B cells.

Mice were exposed to a whole-body dose of 3 Gy of protons and ^{60}Co X-rays by Kajioka et al. (127) and acute effects on the immune system were assessed. Overall, B cells were the most sensitive cell population, while T cells were moderately sensitive and NK cells were the most resistant cell population. Within the T cell population, T_h cells were more resistant than T_{cyt} cells. This was also true for the splenic lymphocyte population. B cells had the most rapid recovery and recovered completely in the spleen but not in circulating lymphocytes. Grayson et al. (128) found that naive T cells were more sensitive than their memory counterparts (CD8+) after whole body irradiation of mice at 2-6 Gy. Lymphocytes were isolated from the spleen, lymph nodes, bone marrow, and peripheral blood. In a dose-dependent manner, memory CD8+ T cells were enriched in the spleen, increasing from 20% of the total CD8+ population in untreated mice to 76% after 6 Gy. Garg et al. (129) analyzed immune cell populations in the intestinal mucosa after whole body irradiation of mice and found that B cells were more sensitive compared to T cells.

In another study of apoptosis in mouse spleen cells, animals were sacrificed 4 h, 1, 3 or 7 days after irradiation (130). The authors analyzed T_h, T_{cyt}, T_{reg}, NK, B, and CD8+CD44+ memory T cells. Low dose radiation decreased apoptosis compared to the control. In terms of apoptosis at 4h, CD8+ and B cells were more resistant to low doses but were very sensitive to 2 Gy, while NK cells and T_{reg} were much more resistant to higher doses. B cells were the most sensitive, followed by T_{cyt}, T_h, T_{reg}, and NK cells. Analysis of subpopulations after 7 days showed that T_{cyt} cells started to regenerate earlier than T_h cells.

In a series of investigations, Qu et al. compared the radiosensitivity of CD4+CD25^{high} Foxp3+ T_{reg} cells and CD4+CD25- T cells in mice after 2 Gy (131) and 5 Gy (132) whole-body irradiation. *In vivo* depletion showed an increased sensitivity of CD8+ compared to CD4+, while the level of CD4+CD25^{high} T_{reg} increased. For both spleen and lymph nodes, the radiosensitivity of CD8+ was higher than CD4+, followed by

TABLE 2A Ranking of lymphocyte radiosensitivity based on lymphocyte depletion in mice.

Radiosensitivity Ranking	Dose Range	Time	Reference
B > T; resting T > activated T	0 - 10 Gy	4 d	(121)
B > T	0 - 100 Gy	3 d	(122)
B > T	0.5 - 15 Gy	6 d	(123)
CD8+ > CD4+	0 - 10 Gy	3 d	(124)
B > CD8+ > CD4+ > NK	0 - 7 Gy	1, 4, 7 d	(125)
B > CD8+ > CD4+ > NK	1 - 7 Gy	1, 4, 7 d	(126)
B > T > NK; CD4+ > CD8+	3 Gy		(127)
T_{naive} > T_{memory} (CD8+)	2 - 6 Gy	4 - 60 d	(128)
B > T (CD4+)	8 Gy	4 h - 12 d	(129)
Spleen; B > CD8+ > CD4+ > T_{reg} > NK	0.01 - 2 Gy	4 h - 7 d	(130)
Total, spleen, lymph nodes: CD8+ > CD4+ > T_{reg}	2, 5 Gy	0.5, 5, 15 d	(131, 132)
T_{reg} > T_{mem}	1.25 Gy		(52)
CD8+ T; $CD44^{lo}$ T_{naive} > $CD44^{hi}$ T (NKT and T_{mem})	10 Gy	24, 48, 72, 120 h	(133)
T_{reg} radioresistant	0 - 20 Gy		(134)
Spleen; CD4+ > T_{reg}	2 Gy	4 h – 11 d	(135)
T_{naive} > CD8 T_{EM} > CD8 T_{cm}	0 - 4 Gy	72 h	(136)
Cardiac: B > CD8+ > CD4+; Spleen: B > CD8+ = CD4+	2 Gy/day		(137)
CD8+ circulating > CD8+ infiltrating CD8+ nodes, spleen > CD8+ gut	0 - 20 Gy	24 h	(138)
Circulating > Splenic	6, 12 Gy	1, 4, 7 d	(139)

TABLE 2B Estimated alpha values (in Gy^{-1}) for a linear dose-response curve exp(-aD) based on lymphocyte depletion in mice (fits were performed using LMfit in python and include only data points ≤ 3 Gy).

T_h	T_{cyt}	T	T_{reg}	B	NK	Spleen	T	Ref.
		0.65+/-0.01		1.31+/-0.07			4 d	(121)
		0.17+/-0.03		0.54+/-0.02			3 d	(122)
0.43+/-0.01	0.53+/-0.01						3 d	(124)
0.32+/-0.01	0.44+/-0.01			0.68+/-0.02	0.18+/-0.04		4 d	(125)
0.82+/-0.06	0.97+/-0.03		0.74+/-0.10	0.42+/-0.22	0.32+/-0.25	1.00+/-0.15	4 h	(130)
0.51+/-0.04	0.69+/-0.02		0.34+/-0.05	0.83+/-0.01	0.55+/-0.04	0.69+/-0.01	1 d	(130)
0.66+/-0.09	0.73+/-0.05		0.35+/-0.11	0.75+/-0.01	0.44+/-0.09	0.72+/-0.06	3 d	(130)

T_{reg} cells. In the thymus, the levels of CD4+CD8+ decreased. However, the newly developed T_{reg} cells in the thymus were less sensitive to radiation than other thymocytes. The function of Treg cells was impaired after 5 Gy radiation but not after 2 Gy, suggesting a threshold effect.

Assessing lymphocyte populations after low-dose total body irradiation in mice, Liu et al. found significant decrease in the T_{reg} cell population (52), but an increase in memory T cells (CD4+/CD8+). Despite increased radiosensitivity, T_{cyt} cells were activated in mice after fractionated low-dose exposure (0.2 Gy), which was not previously observed for T_h cells (141). Spleen cells were analyzed after whole body irradiation of mice with 10 Gy in another report (133). Analysis was performed at 24, 48, 72, and 120 h. CD4+ T cells were significantly more resistant than CD8+ T cells, and $CD44^{high}$ T cells, including NKT cells and memory T cells, were significantly more resistant than $CD44^{low}$ (naive) T cells. Furthermore, the effect of radiation on naturally occurring T_{reg} cells was investigated in a mouse model (134). The number of T_{reg} cells increased after irradiation as they appeared to be more radioresistant compared to other lymphocytes. Their functional integrity was also unaffected. However, this

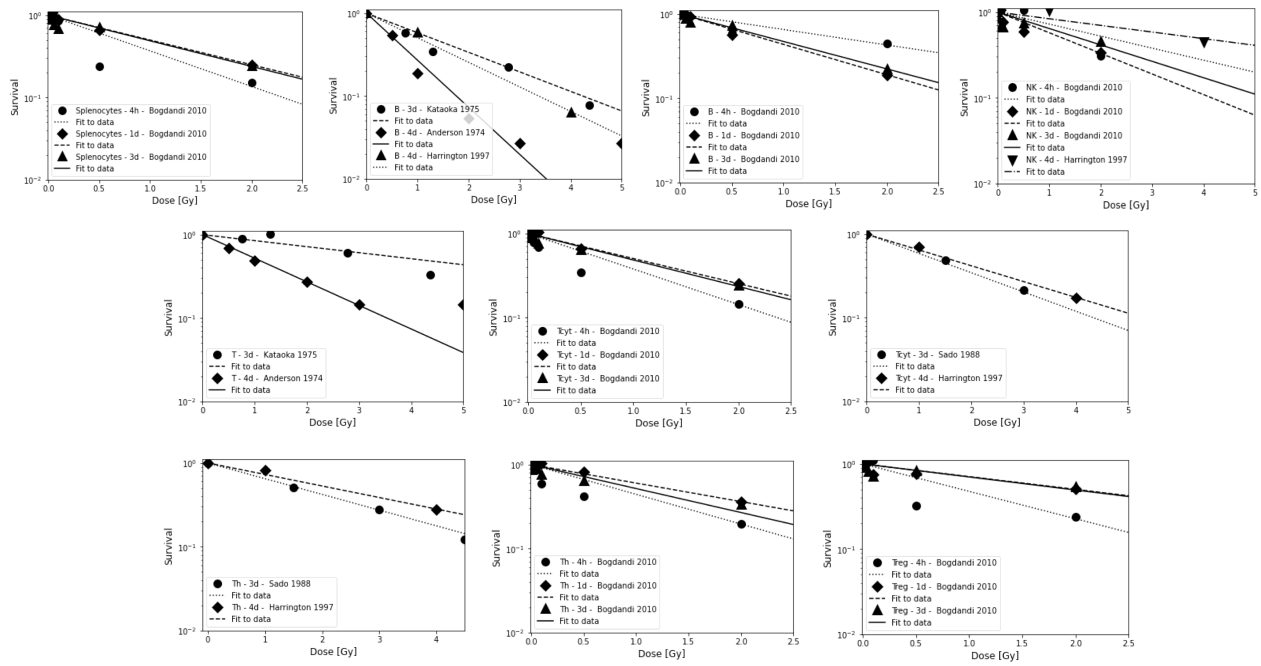

FIGURE 1
Radiosensitivity of lymphocyte sub-populations in mice for studies shown in Table 2B. First row: Splenocytes, B cells, and NK cells. Second row: Combined T cells and T_{cyt} cells. Third row: T_h cells and T_{reg} cells. Data points are shown up to 5 Gy but alpha value fits were only done for data points ≤3 Gy because lymphocytes will not receive more than the prescription dose in a single fraction in radiation therapy, and because the majority of the dose-response data show a more shallow slope and a saturation at higher doses. The data points were extracted from the published figures (using plotdigitizer (plotdigitizer.com)). Experimental error bars are not shown but are included in the fits (performed using LMfit in python).

observation could also be caused by radiation-induced T_{reg} cell activation.

Balogh et al. (135) irradiated C57Bl/6 mice with 2 Gy (whole body) and analyzed changes in lymphocyte fractions isolated from the spleen. T_{reg} cells were less prone to apoptosis than other lymphocytes after *in vivo* irradiation. The results showed a greater decrease in CD4+ numbers compared to T_{reg} cells that were not only less susceptible to radiation-induced apoptosis but also recovered faster than CD4 +Foxp3- cells. However, irradiated T_{reg} cells were functionally compromised with a reduced suppressive capacity (~2.5 fold). In addition, radiation increased the proliferation rate of surviving CD4+ cells. In a study by Pugh et al. (136), mice were irradiated *in vivo* at doses up to 4 Gy and splenocytes as well as peripheral lymphocytes were analyzed at 3, 12, 17, and 24 h. CD8 T_{EM} cells were more resistant and naive T cells more sensitive. CD8 T_{CM} cells were significantly more resistant *in vivo* than *in vitro*. The authors hypothesize that this may be due to the genome-wide chromatin structure that governs early DSB binding and survival. Chromatin remodeling occurs during the differentiation of naive T cells to memory T cells.

In T cell recovery after low-dose whole body irradiation of female C57BL/6 mice, CD4+ T cell reconstitution was delayed more than that of CD8+ T cells (142). Venkatesulu et al. showed lymphopenia after heart (2 Gy per day for 5 days) and spleen (1 Gy per day for 5 days) irradiation of female BALB/c mice *in vivo* (137). B cells were most sensitive in both cohorts. For cardiac irradiation this was followed by CD8+, while CD4+ depletion was moderate in comparison. For splenic irradiation there was no significant difference between CD8+ and CD4+. Radio-resistance of splenic lymphocytes compared to circulating lymphocytes has also been shown in a C57BL/6J mouse model after studying partial body irradiation with and without lymph node involvement (139). The authors also investigated the effect of different field sizes using a small animal image-guided irradiation device.

A study by Arina et al. (138) in which mice were irradiated with a whole-body dose of 8 Gy showed a dose-dependent loss of circulating CD8+ T lymphocytes, but not of tumor-infiltrating CD8+ T cells after 24 h. The authors also quantified the sensitivity of parenchymal CD8+ in various organs. Within certain solid organs there was a higher radio-resistance compared to T cells in circulation and in lymphoid organs. Lymph nodes and spleen had the most radiosensitive CD8+ T cells, while CD8+ T cells in the intestine were the most radioresistant. They hypothesized that the higher radioresistance of parenchymal CD8+ T cells from non-lymphoid compared to lymphoid solid organs is due to the presence of tissue resident memory cells. In tissues harboring the most radioresistant CD8+ T cells (intraepithelial and tumor), not only cells with the standard memory T cells but all CD8+ T cells were similarly radioresistant. In contrast, memory T cells in the liver were more radiosensitive than other T cells.

3.3 *In vitro* lymphocyte radiosensitivity studies

Results from *in vitro* radiosensitivity studies with qualitative or quantitative information are summarized in Tables 3A, B

TABLE 3A Ranking of lymphocyte radiosensitivity based on *in vitro* studies.

Radiosensitivity Ranking	Dose Range	Time	Reference
B > T	0 - 10 Gy	24, 48, 72, 96 h	(143)
B > T	0 - 4 Gy	96 h	(144)
NK = T	0 - 30 Gy	4 h	(145)
NK (CD56+, CD16+) > NK (CD56+)	0 - 30 Gy	3, 48 h	(146)
CD4+ = CD8+	0 - 5 Gy		(147)
T; patient variation			(148)
NK > CD8+, B > CD4+	15 Gy	48 h	(149)
B > CD4+ > CD8+ > NK	2 Gy	24 h	(150)
CD8+ > CD4+	2, 9 Gy	48 h	(151)
CD8+ > CD4+	0 - 2 Gy	48 h	(152)
NK > CD8+ > B > CD4+	0 - 1.5 Gy	44 h, 68 h	(153)
B > CD8+ > CD4+; T_h (male) > T_h (female)	0 - 2 Gy	18 h	(154)
CD34+CD38- stem > CD34+CD38+ differentiated	5 Gy	4 h, 16 h	(155)
Peripheral lymphocytes	0 – 15 Gy	4, 24, 48, 72 h	(156)
Peripheral lymphocytes	0 - 8 Gy	24, 48, 72 h	(157)
CD34+CD38- stem > CD34+CD38+ progenitors	3 Gy	0.5 – 6h	(158)
T_{reg} (CD4+CD25+) > T (CD4+CD25-)	0 - 2 Gy		(159)
B > CD8+ > CD4+	0 - 8 Gy	24, 48, 72 h	(160)
NK (CD56+, CD16+) = NK (CD56+)	0 - 80 Gy	2 – 72 h	(161)
T(non-prof) > T(prof); CD34+(non-prof) = CD34+(prof); T_h > T_{cyt} > CD34	0 – 2 Gy	6 – 48 h	(96)
NK > B > T	0 – 60 Gy	24, 48, 72 h	(162)
protons vs. photons	0 - 4 Gy	1 h, 4 h	(75)
CD4+ > T_{reg}	0, 10 Gy	48 h	(120)
T(non-prof) > B > T > NK > CD34; T_h > T_{reg} > T_{cyt}	0 – 8 Gy	1 – 24 h	(97)
CD4+CD25- T > CD4+CD25^{high} Foxp3+ T_{reg}	5 Gy	12 h	(131, 132)
CD8+ > CD4+; T_{CM}, T_{naive} > T_{EM}	1 - 10 Gy	3 - 24 h	(136)

TABLE 3B Estimated alpha values (in Gy^{-1}) for a linear dose-response curve exp(-aD) based on in vitro measurements (fits were performed using LMfit in python and include only data points ≤ 3 Gy).

T_p	T	T_{cyt}	T_h	T_{reg}	Time	Reference
	0.00 +/- 0.02				24 h	(143)
	0.11 +/- 0.02				48 h	(143)
	0.26 +/- 0.05				72 h	(143)
	0.45 +/- 0.03				96 h	(143)
	0.77					(163)
	0.65					(163)
	0.05 +/- 0.01				24 h	(162)
	0.34 +/- 0.03				72 h	(162)

(Continued)

TABLE 3B Continued

T_p	T	T_{cyt}	T_h	T_{reg}	Time	Reference
		0.61 +/- 0.05	0.68 +/- 0.02			(147)
		0.21 +/- 0.01	0.15 +/- 0.02		48 h	(152)
		0.56 +/- 0.04	0.17 +/- 0.01		44 h	(153)
		0.08 +/- 0.01	0.04 +/- 0.01		18 h	(154)
		0.22 +/- 0.05	0.43 +/- 0.08	0.30 +/- 0.04	24 h	(97)
0.18 +/- 0.03		0.36 +/- 0.03	0.44 +/- 0.06		24 h	(96) unstim
0.25 +/- 0.02		0.10 +/- 0.01	0.13 +/- 0.01		24 h	(96) stim.

T_{CM} CD4+	T_{EM} CD4+	T_{naive} CD4+	T_{CM} CD8+	T_{EM} CD8+	T_{naive} CD8+	Time	Reference
0.69 +/- 0.17	0.76 +/- 0.14	2.14 +/- 0.07	0.85 +/- 0.03	0.32 +/- 0.01	1.84 +/- 0.07	72 h	(136)

B	NK	General Peripheral Lymphocytes	Time	Reference
0.26 +/- 0.06			24 h	(143)
0.53 +/- 0.10			48 h	(143)
0.66 +/- 0.10			72 h	(143)
1.15 +/- 0.13			96 h	(143)
0.17 +/- 0.01			18 h	(154)
0.34 +/- 0.07	0.31 +/- 0.04		24 h	(97)
0.12 +/- 0.01	0.17 +/- 0.01	0.14 +/- 0.01	24 h	(162)
0.31 +/- 0.05	0.65 +/- 0.07	0.49 +/- 0.02	72 h	(162)
	0.08 +/- 0.01		18 h	(161)
		0.72 +/- 0.04		(147)
		0.18 +/- 0.01	48 h	(152)
		0.01 +/- 0.01	4 h	(156)
		0.18 +/- 0.01	24 h	(156)
		0.30 +/- 0.02	48 h	(156)
		0.50 +/- 0.04	72 h	(156)
		0.06 +/- 0.01	24 h	(157)
		0.11 +/- 0.01	48 h	(157)
		0.15 +/- 0.01	72 h	(157)
		0.05 +/- 0.01	24 h	(160)
		0.15 +/- 0.02	48 h	(160)
		0.26 +/- 0.04	72 h	(160)
		0.37 +/- 0.04	24 h	(96) unstim
		0.12 +/- 0.01	24 h	(96) stim.
		0.08 +/- 0.02	4 h	(75) X-rays
		0.32 +/- 0.04	4 h	(75) protons
		0.45 [0.05-1.2]		(148)

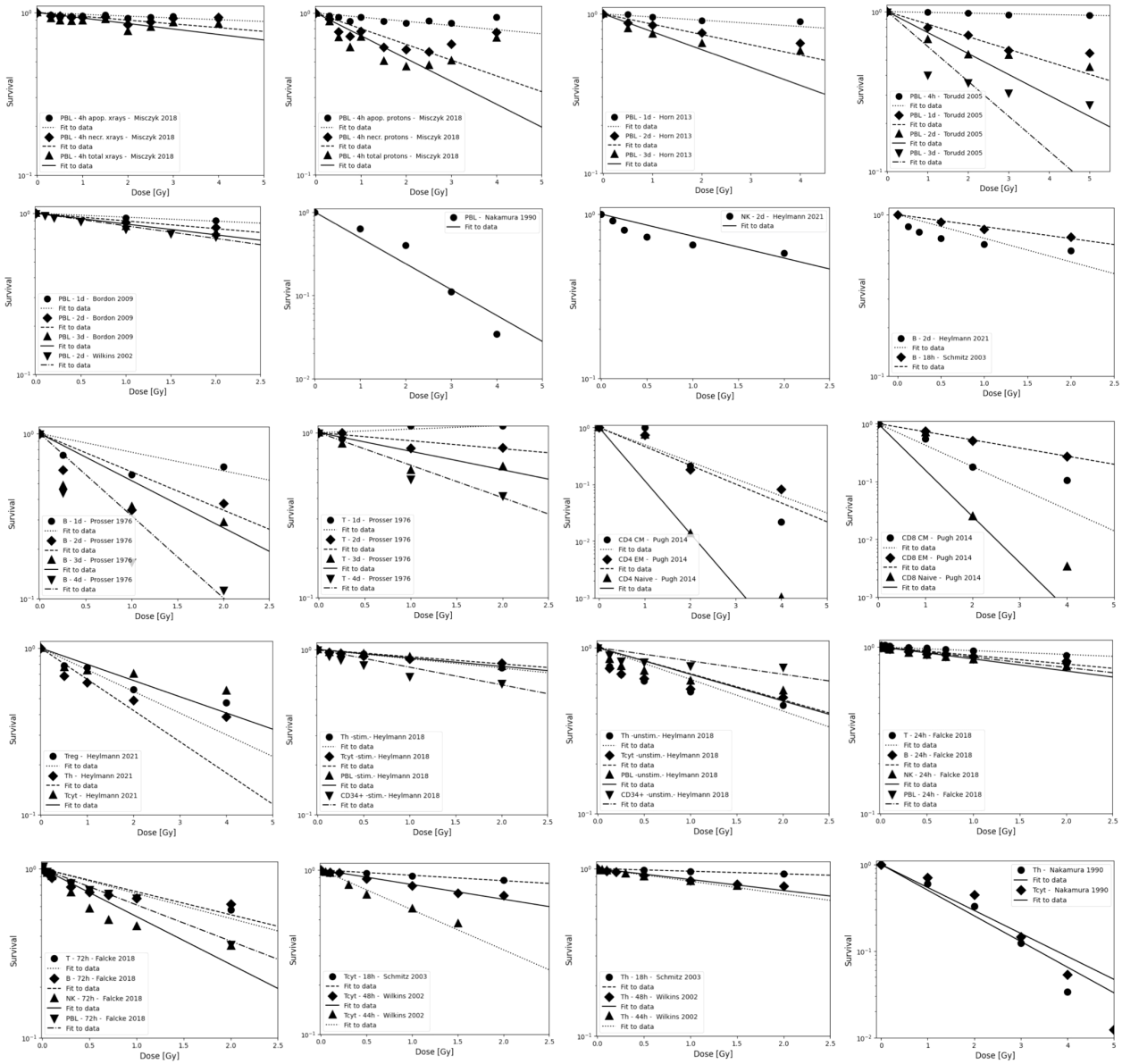

FIGURE 2
Radiosensitivity of peripheral lymphocytes, NK cells, T cells, and B cells. Data are grouped to illustrate both, differences between experiments as well as differences between subpopulations. Data points are shown up to 5 Gy but alpha values fits include only data points ≤ 3 Gy because lymphocytes will not receive more than the prescription dose in a single fraction in radiation therapy, and because the majority of the dose-response data show a more shallow slope and a saturation at higher doses. The data points were extracted from the published figures (using plotdigitizer (plotdigitizer.com)). Experimental error bars are not shown but are included in the fits (performed using LMfit in python).

andinclude fitting exponential dose response curves where possible (Figure 2).

The survival of unstimulated T and B cells from a healthy donor was evaluated in 1-day intervals up to 4 days after irradiation with doses up to 10 Gy by Prosser et al. (143). They observed a higher radiosensitivity of B cells compared to T cells. Cole et al. measured T cell survival in blood from 9 donors and T cell lines (163). The *in vitro* survival of human peripheral blood lymphocytes and thymocytes (T cell progenitors) was also measured after 4 days in a study by Kwan and Norman in healthy volunteers (144). B cells appeared to be slightly more radiosensitive than T cells. The authors concluded that there are subpopulations of T and B cells with different radiosensitivities, resulting in a biphasic survival curve for T cells. Brovall et al. (164) studied NK cell activity in the peripheral blood of healthy adults. While activity was lost at 30 Gy, it was enhanced at lower doses (5 to 20 Gy, depending on the donor). This suggests that radiation affects the cytotoxic function of NK cells before death or apoptosis is observed. Zarcone et al. (145) investigated the effect of radiation on different NK cell activities. The cytotoxic functions of NK and T cells showed identical sensitivity to radiation. Similarly, Rana et al. (146) investigated cytotoxic activities of NK cells as a function of dose up to 30 Gy and showed that CD16+ were the most radiosensitive.

Nakamura et al. (147) investigated the radiosensitivity of proliferating T_h and T_{cyt} lymphocytes *in vitro* using a colony formation assay. This particular study is often cited when discussing lymphopenia and its relationship to lymphocyte radiosensitivity. Strikingly, the measured cell survival curves follow a linear-quadratic dose-response fitted by the linear quadratic model (PBL: α=0.29+/-0.01; β=0.14+/-0.01; CD4+ α=0.32+/-0.01; β=0.13+/-0.01; CD8+ α=0.19+/-0.03; β=0.14 +/-0.01), whereas in the majority of *in vitro* studies reviewed, the response curves show either an exponential or upward-sloping curve and a decrease in response (saturation) at higher doses.

Using blood from cancer patients and healthy individuals, Geara et al. analyzed the radiosensitivity of peripheral T lymphocytes *in vitro* and demonstrated a significant variation among individuals (148). Patient-specific α values were fitted with a median of 0.45 Gy^{-1} (range 0.05 - 1.20 Gy^{-1}). Seki et al. (149) showed that CD8+ T cells were more susceptible to interphase death than CD4+ T cells and NK cells were the most radiosensitive. Philippe et al. (150) assessed apoptosis after 24 h *in vitro*. B cells showed more apoptotic cells than T cells. Among T cells, T_h cells were the most sensitive, followed by T_{cyt} cells. NK cells were the most resistant. Spontaneous apoptosis in immune subsets of *in vitro* cultured cells correlated with differences in radiation induced apoptosis. Radojcic and Crompton used peripheral lymphocytes from three donors to assess the age dependence of CD4+ and CD8+ cell apoptosis at 2 and 9 Gy and suggested that radiosensitivity may be higher in younger individuals (151). CD8+ were more sensitive than CD4+.

Wilkins et al. studied the apoptotic response in lymphocytes using blood from healthy volunteers. One study focused only on CD8+ and CD4+ cells (152). CD8+ T cells were more sensitive to radiation-induced apoptosis than CD4+ at doses up to 2 Gy at 48 h. The authors state that the relative amounts of CD4+ and CD8+ in the combined culture likely influenced the observed apoptosis due to changes in the production of specific cytokines in the cell culture. A second study examined B cells, NK cells, and CD4+ and CD8+ T-cells at 44 h and 68 h after exposure to up to 1.5 Gy (153). Although B cells showed the highest radiation-induced apoptotic response at 1 Gy, CD8+ T-cells appeared to be the most sensitive based on their low spontaneous apoptotic fraction. At 48 h, the radiation-induced apoptosis of the cell subpopulations decreased in the order of NK cells, CD8+ T cells, B cells and CD4+ T cells, although the differences were not significant. Again, lymphocytes in isolation appeared to be more responsive to radiation than those cultured in the presence of other lymphocytes.

In a study of spontaneous and radiation-induced apoptosis of human lymphocytes *in vitro*, lymphocytes from females were less radiosensitive compared to those from males and radiosensitivity seemed to increase with age (154). T_{cyt} cells were more sensitive than T_h cells. Hayashi et al. (155) investigated radiation-induced apoptosis of stem/progenitor cells in human umbilical cord blood. The CD34 +/CD38− stem cell population was more sensitive to radiation-induced apoptosis, compared to more differentiated CD34+/CD38+ and CD34−/CD38+ cells. Human lymphocytes were irradiated *in vitro* with doses up to 15 Gy by Torudd et al. (156). Apoptosis was assessed at 4, 24, 48, and 72 hours. There was very little effect at the early time point at 4 hours. In the context of establishing a predictor of patient's response based on individual lymphocyte radiosensitivity, Bordon et al. (157) evaluated how radiation induced apoptosis correlates with late toxicity and patient's radiosensitivity in cervical cancer. Radiation-induced apoptosis was analyzed at 24, 48, and 72 hours.

Milyavsky et al. (158) reported that human hematopoietic stem cells (CD34+) exhibited delayed DNA double-strand break rejoining, persistent γH2AX foci, and increased apoptosis after irradiation compared to progenitor cells. Cao et al. (159) compared the radiosensitivity of T_{reg} cells (CD4+CD25+) and effector T cells (CD4 +CD25-) *in vitro* using lymphocytes from healthy individuals and hepatocellular carcinoma patients. In the range of 0-2 Gy, Treg cells were more radiosensitive than effector T cells, the opposite trend compared to a previous *in vivo* study (135). T_{reg} cell functionality was moderately affected in Cao et al. (165) using *in vitro* cultured and *in vitro* irradiated T_{reg} cells, showing a dose-dependent reduction in T_{reg} cell proliferation as well as an alteration in phenotype.

In another study of peripheral lymphocytes from healthy donors, radiation-induced apoptosis *in vitro* was not apparent until 24 h after exposure when data were analyzed at 24, 48, and 72 h (160). Radiosensitivity was highest for B cells, followed by T_{cyt} cells, and T_h cells, but the trend was reversed for B cells and T_{cyt} cells after 48h and 4 Gy. Hietanen et al. (161) applied single and fractionated doses to enriched NK cell populations. Cell survival was reported from 2 to 72 h and for doses up to 80 Gy. The response based on the reported α values was very similar for CD16+ and general CD56+ cells at 18 h at doses up to 40 Gy.

A review of the radiosensitivity of human and murine peripheral blood lymphocytes concluded that stem cells, T_h cells, T_{cyt} cells, monocytes, neutrophils and, to a high degree, B cells exhibit a radiosensitive phenotype, whereas T_{reg} cells, macrophages, dendritic cells and NK cells appear to be more radioresistant (166). The same authors studied stimulated (proliferating) and unstimulated (non-proliferating) peripheral lymphocytes in the blood from healthy volunteers (96). Unstimulated peripheral lymphocytes contained mainly T cells arrested in G0/G1. Upon stimulation of the CD3 T-cell receptor and the CD28 co-receptor with anti-CD3 and anti-CD28, respectively, the cells begin to proliferate. Lymphocytes were shown to be highly radiosensitive but stimulation induced radioresistance in several T cell subsets, with the exception of CD34+ cells which did not become radioresistant when stimulated to proliferate. There was no difference in repair between stimulated and unstimulated cells, i.e., the difference in radiosensitivity was likely caused by the induced DNA damage. The investigators found that most of the cells underwent apoptosis with only a small fraction of necrosis, with data collected between 6 and 48 hours after irradiation. It was concluded that T cells and B cells are highly sensitive and undergo apoptosis at doses as low as 0.125 Gy with no apparent threshold and a saturation of ~50% at about 1-2 Gy. Sensitivity was highest for non-proliferating T cells followed by B cells, and NK cells. However, while non-proliferating T and B cells were sensitive, they had a high repair capacity, which was also the case for CD34+. There was no significant difference in radiosensitivity between the non-proliferating T cell subcategories. The same authors then measured the *in vitro* dose response of blood cells from healthy volunteers (97). The analysis included unstimulated T cells (T_{reg}, T_h, T_{cyt}) purified with magnetic beads as well as unstimulated B cells, and NK cells obtained from peripheral blood. Doses ranging from 0.5 to 8 Gy were administered. T_h cells were the most sensitive (30% apoptosis

level at 0.5 Gy, while T_{reg}, NK and B cells showed values around 20–25%). The authors point out that absolute numbers may be associated with uncertainties because there may be early apoptotic events that have been fragmented, or late apoptotic events that have not yet materialized at the time of the assay.

Apoptotic cells may lose membrane integrity and become secondary necrotic cells that retain immune activation properties. Falcke et al. (162) studied lymphocyte cell death by apoptosis, primary necrosis, and secondary necrosis (late apoptotic). They found that B cells and NK cells died mainly by apoptosis (secondary necrosis), whereas T cells showed significant primary and secondary necrotic cells. NK cells were the most sensitive to radiation, followed by B cells and T cells. The researchers also analyzed cell viability. In an *in vitro* study of human peripheral lymphocytes, necrosis was more frequent than apoptosis, especially with proton irradiation (75). This may indicate a mechanistic difference in lymphocyte damage when comparing photon and proton radiation (75, 167). The accumulation of radiation-induced repair protein foci differed after proton versus X-ray irradiation (168). Annexin V labeling was performed 1 h and 4 h after irradiation with doses of 0-4 Gy (75). Alpha values for peripheral lymphocytes differed between X-rays and protons as well as between apoptosis and necrosis (apoptosis X-rays: α=0.02+/-0.01 Gy^{-1}; apoptosis protons: α=0.03+/-0.01 Gy^{-1}; necrosis X-rays: α=0.04 +/-0.01 Gy^{-1}; necrosis protons: α=0.15+/-0.03 Gy^{-1}).

Using blood from healthy volunteers Beauford et al. (120) found that T_h cells were more radiosensitive than T_{reg} cells. Although T_{reg} cells appeared to be more resistant, radiation caused a decreased Foxp3 expression as well as decreased expression of CD25 and CTLA-4, resulting in a reduced ability to suppress CD8+ T cell proliferation. Vandevoorde et al. (169) compared the dose response of CD34+ cells and umbilical cord T cells from newborns and adults. Naïve and memory T cells were analyzed *in vitro* 0.5 h after irradiation with low doses (100-200 mGy). Newborn peripheral T lymphocytes were significantly more radiosensitive than adult peripheral T lymphocytes. This may be due to immunophenotypic changes of T lymphocytes with age.

De Kruyff et al. (170) analyzed the functional behavior of lymph node T cells in mouse cell cultures as a function of dose. Specifically, the authors evaluated the helper activity of CD4+ T cells in terms of their ability to induce immunoglobin synthesis (IgG, IgM, and IgE synthesis) in B cells. The capacity for IgG synthesis was not affected, while that for IgE (which depends on IL-4 and IL-5) was significantly reduced. Thus, IL-4 in T_h cells appears to be sensitive to radiation, causing T cell functions to show large variations in radiosensitivity. Pugh et al. (136) measured the radiosensitivity of naïve lymphocytes, effective memory cells (CD8, T_{EM}), and central memory cells (T_{CM}) from mice *in vitro*. There was no significant difference in radiosensitivity between T cell subsets. However, CD8 T_{EM} cells were more radioresistant and showed less interphase death than T_{CM} cells or naïve T cells. CD4 T cells were more radioresistant than CD8 T cells. This pattern was extended to both CD4 naïve T cells and T_{CM} cell subsets. It was unclear whether the enhanced radioresistance of T_{reg} cells could fully account for the enhanced radioresistance of any specific CD4 subset.

Qu et al. compared the radiosensitivity of CD4+$CD25^{high}$ Foxp3+ T_{reg} cells and CD4+CD25- T cells *in vitro* showing higher sensitivity for CD4+CD25- T cells than for CD4+$CD25^{high}$ T_{reg} cells at 2 Gy (131) and 5 Gy (132), respectively. They reported that more dead cells were observed in the T_{eff} cell population than in the T_{reg} cell pool, which correlated with a higher levels of anti-apoptotic protein expression in T_{reg} cells. They also found that the T_{eff} cell suppressive capacity of the *in vitro* irradiated T_{reg} cells was only moderately affected by radiation. The evaluation was performed 2 weeks after irradiation.

4 Summary and discussion

The radiosensitivity of lymphocytes has been evaluated in a variety of ways, including studies in humans, pre-clinical studies, and *in vitro* clonogenic cell survival assays. The available data published in the open literature have been reviewed in this work. Interpretation of experimental data is often difficult. For example, *in vitro* measurements must be corrected for spontaneous apoptosis, which is particularly relevant for B cells. In addition, data from *in vivo* studies have to take into account that a part of the lympho-hematopoietic system has been irradiated, allowing for lymphocyte redistribution from non-irradiated areas. Expression changes may also occur.

Studies based on lymphocyte depletion in patients consistently suggest that B cells are the most radiosensitive, followed by T cells and NK cells, with helper T cells (CD4+) being more radiosensitive than cytotoxic T cells (CD8+). The preclinical studies support this difference between B and T cells. Preclinical studies also suggest that circulating lymphocytes appear to be more radiosensitive than non-circulating lymphocytes and tumor infiltrating T lymphocytes. In addition, parenchymal T cells from non-lymphoid solid organs appear to be more radioresistant than those from lymphoid solid organs. The obtained average dose-response alpha values derived from lymphocyte depletion in mice are ~0.8 Gy^{-1}, ~0.6 Gy^{-1}, and ~0.4 Gy^{-1}, for B cells, T cells, and NK cells, respectively (for doses up to 3 Gy, after 4 hours to 4 days). For splenocytes, an average value of ~0.8 Gy^{-1} was extracted. There is some indication that naïve lymphocytes, which make up more than 50% of the lymphocyte population (depending on age, health status, and other factors) are more radiosensitive.

The reported *in vitro* data are less consistent than the *in vivo* results, but generally show the same ranking of radiosensitivity (B > T (CD8+) > T(CD4+) > NK) with response differences that are smaller than *in vivo*, i.e., average alpha values of ~0.4 Gy^{-1}, ~0.3 Gy^{-1}, and ~0.3 Gy^{-1} for B cells, T cells, and NK cells, respectively (for doses up to 3 Gy, after 4 hours to 4 days). One report shows significantly higher radiosensitivity for memory T cells. The fitted alpha values depend on the chosen dose range as most measured cell survival curves show a decreasing slope with increasing dose, i.e., a saturation typically starting already between 0.5 and 2 Gy. There is also a strong time dependence. Although radiation-induced apoptosis is measurable early after exposure, it continues to increase up to and beyond 48 hours, resulting in steeper dose-response curves. Many clinical studies on radiation-induced lymphopenia point out the importance of the dose to the circulating lymphocytes and refer to the high radiosensitivity of lymphocytes, often citing a single study (147). This widely cited study reports higher radiosensitivity than other studies and appears to be the only one showing a linear-quadratic dose response curve.

To assess the dose-response of lymphocytes *in vivo* for lymphopenia studies in patients, it is necessary to estimate the dose to lymphocytes. This work also reviews methods to estimate dose to the blood. While

various models have been proposed to estimate the dose to the blood (based on reasonably well-known organ transit times of the blood), the dose to circulating lymphocytes is related but not identical to the blood dose. In addition to the recirculation of lymphocytes between blood and secondary lymphoid tissues, several factors cause lymphocyte transit times to be, on average, to be much longer than blood transit times. Lymphocytes often attach and detach from endothelial cells and radiation may cause upregulation of adhesion molecules that alter leucocyte adhesion to endothelial cells (171), which may increase mean transit times and thus dose to lymphocytes. In addition, they may have to deform to squeeze through capillaries because their size is much larger (~6 μm) than, for example, platelets (172, 173). In particular, pulmonary capillaries are thought to be slightly smaller than the diameter of lymphocytes (173). In the liver, a relatively low average velocity of T cells has been reported because they might be crawling on the endothelial wall of the sinusoids instead of flowing with the blood. This could reduce the average velocity to ~6-7 μm/min. Thus, CD8 T cells can super-diffuse in the liver for almost 20 minutes (172). It is therefore likely that the dose to the blood, while a potential surrogate for the dose to lymphocytes, does not accurately predict the correct dose experienced by circulating lymphocytes. Research efforts are underway to explicitly model lymphocyte trafficking rather than relying on the use of blood dose as a surrogate for dose to circulating lymphocytes (91, 92, 174).

While lymphocyte radiosensitivity is likely to play an important role in lymphopenia, radiation-induced effects such as cell survival or cell motility on lymphocytes are not necessarily robust predictors of immune suppression. Radiation also affects lymphocyte infiltration into tumors and tumor sensitization, increases antigen release, and other mechanisms (175). Zhao et al. (176) investigated lymphopenia in SBRT for early-stage lung cancer patients and concluded that lymphocyte radiosensitivity alone cannot explain lymphopenia without considering lymphocyte recovery times. The number of circulating lymphocytes might also decrease due to inflammation caused by low-dose baths in secondary irradiated organs during radiation therapy. In contrast to naïve adaptive lymphocytes which frequently migrate between secondary lymphoid organs, tissue-resident lymphocytes generally do not recirculate through the blood (177), but are also irradiated. The circulatory behavior of lymphocytes and their lymph node transit times also differs among lymphocytes subpopulations (178, 179), e.g., CD4+ seem to recirculate more rapidly compared to CD8+. In addition, radiation likely affects lymphocyte migration, for instance, through radiation-induced changes in sphingosine-1-phosphate (180). Lymphocyte depletion is also likely related to indirect mechanisms, such as radiation-induced expression of TNF-α which has a cytotoxic effect on lymphocytes (107, 181, 182). In addition, lymphocyte function appears to be affected at lower doses than cell survival in both *in vitro* and clinical studies (183–185).

5 Conclusions

The reported data suggest differences in radiation sensitivity among lymphocytes subpopulations, which may affect their relative contribution and thus the dynamics of the immune response. The data reviewed here show low dose (< 3Gy) radiosensitivity of lymphocytes in the same order of magnitude as normal fibroblasts (186). In general, B cells appear to be more radiosensitive than T cells, and NK cells appear to be the most resistant. Patient variability is likely to be of the same order of magnitude as the differences between subpopulations. Because tumor-infiltrating lymphocytes appear to be quite radioresistant, differences in radiosensitivity between circulating lymphocytes and lymphocytes in lymphoid organs may have implications for lymphopenia and thus for considerations of dose prescription and dose scheduling in radiation therapy as well as for fractionation and scheduling of therapies involving both radiation and immune checkpoint inhibitors. An important aspect is also the influence of radiation dose distribution, delivery time and beam arrangement, which has been discussed in the context of highly conformal radiotherapy and its positive effect on lymphopenia (114, 187).

It remains an open question whether the observed effects of radiation on lymphocyte counts in patients are indeed mainly due to the radiation sensitivity of circulating lymphocytes. To answer this question, it is necessary to consider not only the dose to different lymphocyte compartments in the field (e.g., the lymphatic system), but also radiation effects on lymphocyte trafficking and residence times (91, 92). Certainly, data on cell death don't fully capture radiation-induced effects on lymphocyte functionality (135). This review outlines areas where additional research is needed to mechanistically explain radiation induced lymphopenia in patients and its correlation with treatment outcome.

Author contributions

The author confirms being the sole contributor of this work and has approved it for publication.

Funding

This work was supported by the National Institute of Health/ National Cancer Institute: P01 CA261669 and R01 CA248901.

Acknowledgments

The author wishes to thank Ryan J Park, MD PhD, Massachusetts General Hospital, for reviewing general statements about lymphocytes and the immune system.

Conflict of interest

The author declares that the research was conducted in the absence of any commercial or financial relationships that could be construed as a potential conflict of interest.

Publisher's note

References

1. Heier HE, Christensen I, Froland SS, Engeset A. Early and late effects of irradiation for seminoma testis on the number of blood lymphocytes and their B and T subpopulations. *Lymphology* (1975) 8:69–74.

2. Weeke E. The development of lymphopenia in uremic patients undergoing extracorporeal irradiation of the blood with portable beta units. *Radiat Res* (1973) 56:554–9. doi: 10.2307/3573724

3. MacLennan IC, Kay HE. Analysis of treatment in childhood leukemia. IV. The critical association between dose fractionation and immunosuppression induced by cranial irradiation. *Cancer* (1978) 41:108–11. doi: 10.1002/1097-0142(197801)41:1<108::AID-CNCR2820410116>3.0.CO;2-Z

4. Grossman SA, Ellsworth S, Campian J, Wild AT, Herman JM, Laheru D, et al. Survival in patients with severe lymphopenia following treatment with radiation and chemotherapy for newly diagnosed solid tumors. *J Natl Compr Cancer Network JNCCN* (2015) 13:1225–31. doi: 10.6004/jnccn.2015.0151

5. Ellsworth SG. Field size effects on the risk and severity of treatment-induced lymphopenia in patients undergoing radiation therapy for solid tumors. *Adv Radiat Oncol* (2018) 3:512–9. doi: 10.1016/j.adro.2018.08.014

6. Fang P, Shiraishi Y, Verma V, Jiang W, Song J, Hobbs BP, et al. Lymphocyte-Sparing effect of proton therapy in patients with esophageal cancer treated with definitive chemoradiation. *Int J Part Ther* (2018) 4:23–32. doi: 10.14338/IJPT-17-00033.1

7. Yovino S, Kleinberg L, Grossman SA, Narayanan M, Ford E. The etiology of treatment-related lymphopenia in patients with malignant gliomas: modeling radiation dose to circulating lymphocytes explains clinical observations and suggests methods of modifying the impact of radiation on immune cells. *Cancer Invest* (2013) 31:140–4. doi: 10.3109/07357907.2012.762780

8. Wild AT, Herman JM, Dholakia AS, Moningi S, Lu Y, Rosati LM, et al. Lymphocyte-Sparing effect of stereotactic body radiation therapy in patients with unresectable pancreatic cancer. *Int Jornal Radiat Oncol Biol Phys* (2016) 94:571–9. doi: 10.1016/j.ijrobp.2015.11.026

9. Damen PJJ, Kroese TE, van Hillegersberg R, Schuit E, Peters M, Verhoeff JJC, et al. The influence of severe radiation-induced lymphopenia on overall survival in solid tumors: A systematic review and meta-analysis. *Int J Radiat Oncol Biol Phys* (2021) 111:936–48. doi: 10.1016/j.ijrobp.2021.07.1695

10. Shiraishi Y, Fang P, Xu C, Song J, Krishnan S, Koay EJ, et al. Severe lymphopenia during neoadjuvant chemoradiation for esophageal cancer: A propensity matched analysis of the relative risk of proton versus photon-based radiation therapy. *Radiother Oncol* (2018) 128:154–60. doi: 10.1016/j.radonc.2017.11.028

11. Chen F, Jin JY, Hui TSK, Jing H, Zhang H, Nong Y, et al. Radiation induced lymphopenia is associated with the effective dose to the circulating immune cells in breast cancer. *Front Oncol* (2022) 12:768956. doi: 10.3389/fonc.2022.768956

12. Monti S, Xu T, Liao Z, Mohan R, Cella L, Palma G. On the interplay between dosiomics and genomics in radiation-induced lymphopenia of lung cancer patients. *Radiother Oncol* (2022) 167:219–25. doi: 10.1016/j.radonc.2021.12.038

13. Qian JM, Akama-Garren E, Shin J, Gunasti L, Bang A, Pike LRG, et al. Dosimetric modeling of lymphopenia in patients with metastatic cancer receiving palliative radiation and PD-1 immune checkpoint inhibitors. *Adv Radiat Oncol* (2022) 7:100880. doi: 10.1016/j.adro.2021.100880

14. Correia D, Terribilini D, Zepter S, Pica A, Bizzocchi N, Volken W, et al. Whole-ventricular irradiation for intracranial germ cell tumors: Dosimetric comparison of pencil beam scanned protons, intensity-modulated radiotherapy and volumetric-modulated arc therapy. *Clin Transl Radiat Oncol* (2019) 15:53–61. doi: 10.1016/j.ctro.2019.01.002

15. Tang C, Liao Z, Gomez D, Levy L, Zhuang Y, Gebremichael RA, et al. Lymphopenia association with gross tumor volume and lung V5 and its effects on non-small cell lung cancer patient outcomes. *Int J Radiat Oncol Biol Phys* (2014) 89:1084–91. doi: 10.1016/j.ijrobp.2014.04.025

16. Helm A, Ebner DK, Tinganelli W, Simoniello P, Bisio A, Marchesano V, et al. Combining heavy-ion therapy with immunotherapy: An update on recent developments. *Int J Particle Ther* (2018) 5:84–93. doi: 10.14338/IJPT-18-00024.1

17. Gameiro SR, Malamas AS, Bernstein MB, Tsang KY, Vassantachart A, Sahoo N, et al. Tumor cells surviving exposure to proton or photon radiation share a common immunogenic modulation signature, rendering them more sensitive to T cell-mediated killing. *Int J Radiat Oncol Biol Phys* (2016) 95:120–30. doi: 10.1016/j.ijrobp.2016.02.022

18. Ko EC, Benjamin KT, Formenti SC. Generating antitumor immunity by targeted radiation therapy: Role of dose and fractionation. *Adv Radiat Oncol* (2018) 3:486–93. doi: 10.1016/j.adro.2018.08.021

19. Routman DM, Garant A, Lester SC, Day CN, Harmsen WS, Sanheuza CT, et al. A comparison of grade 4 lymphopenia with proton versus photon radiation therapy for esophageal cancer. *Adv Radiat Oncol* (2019) 4:63–9. doi: 10.1016/j.adro.2018.09.004

20. Davuluri R, Jiang W, Fang P, Xu C, Komaki R, Gomez DR, et al. Lymphocyte nadir and esophageal cancer survival outcomes after chemoradiation therapy. *Int J Radiat Oncol Biol Phys* (2017) 99:128–35. doi: 10.1016/j.ijrobp.2017.05.037

21. Jensen GL, Blanchard P, Gunn GB, Garden AS, David Fuller C, Sturgis EM, et al. Prognostic impact of leukocyte counts before and during radiotherapy for oropharyngeal cancer. *Clin Transl Radiat Oncol* (2017) 7:28–35. doi: 10.1016/j.ctro.2017.09.008

22. Abdullah M, Chai PS, Chong MY, Tohit ER, Ramasamy R, Pei CP, et al. Gender effect on in *vitro* lymphocyte subset levels of healthy individuals. *Cell Immunol* (2012) 272:214–9. doi: 10.1016/j.cellimm.2011.10.009

23. Shin J, Xing S, McCullum L, Hammi A, Pursley J, Correa CA, et al. HEDOS-a computational tool to assess radiation dose to circulating blood cells during external beam radiotherapy based on whole-body blood flow simulations. *Phys Med Biol* (2021) 66:164001. doi: 10.1088/1361-6560/ac16ea

24. Xing S, Shin J, Pursley J, Correa-Alfonso CM, Depauw N, Domal S, et al. A dynamic blood flow model to compute absorbed dose to circulating blood and lymphocytes in liver external beam radiotherapy. *Phys Med Biol* (2022) 67:045010. doi: 10.1088/1361-6560/ac4da4

25. Plowman PN. The effects of conventionally fractionated, extended portal radiotherapy on the human peripheral blood count. *Int J Radiat Oncol Biol Phys* (1983) 9:829–39. doi: 10.1016/0360-3016(83)90008-1

26. Crocenzi T, Cottam B, Newell P, Wolf RF, Hansen PD, Hammill C, et al. A hypofractionated radiation regimen avoids the lymphopenia associated with neoadjuvant chemoradiation therapy of borderline resectable and locally advanced pancreatic adenocarcinoma. *J Immunother Cancer* (2016) 4:45. doi: 10.1186/s40425-016-0149-6

27. Dewan MZ, Galloway AE, Kawashima N, Dewyngaert JK, Babb JS, Formenti SC, et al. Fractionated but not single-dose radiotherapy induces an immune-mediated abscopal effect when combined with anti-CTLA-4 antibody. *Clin Cancer Res* (2009) 15:5379–88. doi: 10.1158/1078-0432.CCR-09-0265

28. Lambin P, Lieverse RIY, Eckert F, Marcus D, Oberije C, van der Wiel AMA, et al. Lymphocyte-sparing radiotherapy: The rationale for protecting lymphocyte-rich organs when combining radiotherapy with immunotherapy. *Semin Radiat Oncol* (2020) 30:187–93. doi: 10.1016/j.semradonc.2019.12.003

29. Lee R, Yamada S, Yamamoto N, Miyamoto T, Ando K, Durante M, et al. Chromosomal aberrations in lymphocytes of lung cancer patients treated with carbon ions. *J Radiat Res* (2004) 45:195–9. doi: 10.1269/jrr.45.195

30. Rudra S, Hui C, Rao YJ, Samson P, Lin AJ, Chang X, et al. Effect of radiation treatment volume reduction on lymphopenia in patients receiving chemoradiotherapy for glioblastoma. *Int J Radiat Oncol Biol Phys* (2018) 101:217–25. doi: 10.1016/j.ijrobp.2018.01.069

31. Yang L, Xu Z, Ma L, Liu Q, Chang ATY, Wang Q, et al. Early onset of severe lymphopenia during definitive radiotherapy correlates with mean body dose and predicts poor survival in cervical cancer. *Cancer biomark* (2022) 34:149–59. doi: 10.3233/CBM-210292

32. Zhang BZ, Li Y, Xu LM, Chai YL, Qu C, Cao YJ, et al. The relationship between the radiation dose of pelvic-bone marrow and lymphocytic toxicity in concurrent chemoradiotherapy for cervical cancer. *Radiat Oncol* (2023) 18:12. doi: 10.1186/s13014-023-02205-8

33. Liu J, Zhao Q, Deng W, Lu J, Xu X, Wang R, et al. Radiation-related lymphopenia is associated with spleen irradiation dose during radiotherapy in patients with hepatocellular carcinoma. *Radiat Oncol* (2017) 12:90. doi: 10.1186/s13014-017-0824-x

34. d'Alesio V, Pacelli R, Durante M, Canale Cama G, Cella L, Gialanella G, et al. Lymph nodes in the irradiated field influence the yield of radiation-induced chromosomal aberrations in lymphocytes from breast cancer patients. *Int J Radiat Oncol Biol Phys* (2003) 57:732–8. doi: 10.1016/S0360-3016(03)00664-3

35. Chadha AS, Liu G, Chen HC, Das P, Minsky BD, Mahmood U, et al. Does unintentional splenic radiation predict outcomes after pancreatic cancer radiation therapy? *Int J Radiat Oncol Biol Phys* (2017) 97:323–32. doi: 10.1016/j.ijrobp.2016.10.046

36. Saito T, Toya R, Yoshida N, Shono T, Matsuyama T, Ninomura S, et al. Spleen dose-volume parameters as a predictor of treatment-related lymphopenia during definitive chemoradiotherapy for esophageal cancer. *In Vivo* (2018) 32:1519–25. doi: 10.21873/invivo.11409

37. Yalamanchali A, Zhang H, Huang KC, Mohan R, Lin SH, Zhu C, et al. Patient-specific lymphocyte loss kinetics as biomarker of spleen dose in patients undergoing radiation therapy for upper abdominal malignancies. *Adv Radiat Oncol* (2021) 6:100545. doi: 10.1016/j.adro.2020.08.002

38. Xu H, You G, Zhang M, Song T, Zhang H, Yang J, et al. Association of pre-surgery to pre-radiotherapy lymphocyte counts ratio with disease-free survival in rectal cancer patients receiving neoadjuvant concurrent chemoradiotherapy. *World J Surg Oncol* (2019) 17:199. doi: 10.1186/s12957-019-1747-9

39. Anderson JL, Newman NB, Anderson C, Sherry AD, Yock AD, Osmundson EC. Mean cardiopulmonary dose and vertebral marrow dose differentially predict lineage-specific leukopenia kinetics during radiotherapy for esophageal cancer. *Radiother Oncol* (2020) 152:169–76. doi: 10.1016/j.radonc.2019.12.008

40. Qing H, Chuanshu C, Weijian Z, Shaobin Z, Jing L. Low-dose range of pelvic irradiation leads to acute hematological toxicity in early-stage cervical cancer with

intermediate risk factors by postoperative intensity-modulated radiotherapy. *Eur J gynaecological Oncol* (2019) 40:437–42. doi: 10.12892/ejgo4654.2019

41. Sini C, Fiorino C, Perna L, Noris Chiorda B, Deantoni CL, Bianchi M, et al. Dose-volume effects for pelvic bone marrow in predicting hematological toxicity in prostate cancer radiotherapy with pelvic node irradiation. *Radiother Oncol* (2016) 118:79–84. doi: 10.1016/j.radonc.2015.11.020

42. Eckert F, Schaedle P, Zips D, Schmid-Horch B, Rammensee HG, Gani C, et al. Impact of curative radiotherapy on the immune status of patients with localized prostate cancer. *Oncoimmunology* (2018) 7:e1496881. doi: 10.1080/2162402X.2018.1496881

43. Standish LJ, Torkelson C, Hamill FA, Yim D, Hill-Force A, Fitzpatrick A, et al. Immune defects in breast cancer patients after radiotherapy. *J Soc Integr Oncol* (2008) 6:110–21.

44. Venkatesulu B, Giridhar P, Pujari L, Chou B, Lee JH, Block AM, et al. Lymphocyte sparing normal tissue effects in the clinic (LymphoTEC): A systematic review of dose constraint considerations to mitigate radiation-related lymphopenia in the era of immunotherapy. *Radiother Oncol* (2022) 177:81–94. doi: 10.1016/j.radonc.2022.10.019

45. Waidhauser J, Nerlinger P, Arndt TT, Schiele S, Sommer F, Wolf S, et al. Alterations of circulating lymphocyte subsets in patients with colorectal carcinoma. *Cancer Immunol Immunother* (2022) 71:1937–47. doi: 10.1007/s00262-021-03127-8

46. Gustafson MP, Bornschlegl S, Park SS, Gastineau DA, Roberts LR, Dietz AB, et al. Comprehensive assessment of circulating immune cell populations in response to stereotactic body radiation therapy in patients with liver cancer. *Adv Radiat Oncol* (2017) 2:540–7. doi: 10.1016/j.adro.2017.08.003

47. Kaur P, Asea A. Radiation-induced effects and the immune system in cancer. *Front Oncol* (2012) 2:191. doi: 10.3389/fonc.2012.00191

48. Ahmed MM, Hodge JW, Guha C, Bernhard EJ, Vikram B, Coleman CN. Harnessing the potential of radiation-induced immune modulation for cancer therapy. *Cancer Immunol Res* (2013) 1:280–4. doi: 10.1158/2326-6066.CIR-13-0141

49. Demaria S, Ng B, Devitt ML, Babb JS, Kawashima N, Liebes L, et al. Ionizing radiation inhibition of distant untreated tumors (abscopal effect) is immune mediated. *Int J Radiat Oncol Biol Phys* (2004) 58:862–70. doi: 10.1016/j.ijrobp.2003.09.012

50. Rubner Y, Wunderlich R, Ruhle PF, Kulzer L, Werthmoller N, Frey B, et al. How does ionizing irradiation contribute to the induction of anti-tumor immunity? *Front Oncol* (2012) 2:75. doi: 10.3389/fonc.2012.00075

51. Park B, Yee C, Lee KM. The effect of radiation on the immune response to cancers. *Int J Mol Sci* (2014) 15:927–43. doi: 10.3390/ijms15010927

52. Liu R, Xiong S, Zhang L, Chu Y. Enhancement of antitumor immunity by low-dose total body irradiationis associated with selectively decreasing the proportion and number of T regulatory cells. *Cell Mol Immunol* (2010) 7:157–62. doi: 10.1038/cmi.2009.117

53. Storozynsky Q, Hitt MM. The impact of radiation-induced DNA damage on cGAS-STING-mediated immune responses to cancer. *Int J Mol Sci* (2020) 21:8877. doi: 10.3390/ijms21228877

54. Tuomela K, Mukherjee D, Ambrose AR, Harikrishnan A, Mole H, Hurlstone A, et al. Radiotherapy transiently reduces the sensitivity of cancer cells to lymphocyte cytotoxicity. *Proc Natl Acad Sci USA* (2022) 119:e2111900119. doi: 10.1073/pnas.2111900119

55. Abdel-Rahman O. Nonconventional patterns of benefit of solid tumors treated with PD-(L)1 inhibitors: a systematic review. *Immunotherapy* (2017) 9:995–1004. doi: 10.2217/imt-2017-0074

56. Kalbasi A, June CH, Haas N, Vapiwala N. Radiation and immunotherapy: a synergistic combination. *J Clin Invest* (2013) 123:2756–63. doi: 10.1172/JCI69219

57. Salama AK, Postow MA, Salama JK. Irradiation and immunotherapy: From concept to the clinic. *Cancer* (2016) 122:1659–71. doi: 10.1002/cncr.29889

58. Seyedin SN, Schoenhals JE, Lee DA, Cortez MA, Wang X, Niknam S, et al. Strategies for combining immunotherapy with radiation for anticancer therapy. *Immunotherapy* (2015) 7:967–80. doi: 10.2217/imt.15.65

59. Durante M, Reppingen N, Held KD. Immunologically augmented cancer treatment using modern radiotherapy. *Trends Mol Med* (2013) 19:565–82. doi: 10.1016/j.molmed.2013.05.007

60. Levy A, Chargari C, Cheminant M, Simon N, Bourgier C, Deutsch E. Radiation therapy and immunotherapy: implications for a combined cancer treatment. *Crit Rev oncology/hematol* (2013) 85:278–87. doi: 10.1016/j.critrevonc.2012.09.001

61. Wang Y, Deng W, Li N, Sharma A, Jiang W, Lin SH. Combining immunotherapy and radiotherapy for cancer treatment: Current challenges and future directions. *Frotiers Pharmacol* (2018) 9:185. doi: 10.3389/fphar.2018.00185

62. Vatner RE, Cooper BT, Vanpouille-Box C, Demaria S, Formenti SC. Combinations of immunotherapy and radiation in cancer therapy. *Front Oncol* (2014) 4:325. doi: 10.3389/fonc.2014.00325

63. Barker CA, Postow MA. Combinations of radiation therapy and immunotherapy for melanoma: a review of clinical outcomes. *Int J Radiat Oncol Biol Phys* (2014) 88:986–97. doi: 10.1016/j.ijrobp.2013.08.035

64. Tang C, Wang X, Soh H, Seyedin S, Cortez MA, Krishnan S, et al. Combining radiation and immunotherapy: a new systemic therapy for solid tumors? *Cancer Immunol Res* (2014) 2:831–8. doi: 10.1158/2326-6066.CIR-14-0069

65. Patel MA, Kim JE, Ruzevick J, Li G, Lim M. The future of glioblastoma therapy: synergism of standard of care and immunotherapy. *Cancers* (2014) 6:1953–85. doi: 10.3390/cancers6041953

66. Matsumura S, Wang B, Kawashima N, Braunstein S, Badura M, Cameron TO, et al. Radiation-induced CXCL16 release by breast cancer cells attracts effector T cells. *J Immunol* (2008) 181:3099–107. doi: 10.4049/jimmunol.181.5.3099

67. Demaria S, Pilones KA, Vanpouille-Box C, Golden EB, Formenti SC. The optimal partnership of radiation and immunotherapy: from preclinical studies to clinical translation. *Radiat Res* (2014) 182:170–81. doi: 10.1667/RR13500.1

68. Bhattacharyya T, Purushothaman K, Puthiyottil SS, Bhattacharjee A, Muttah G. Immunological interactions in radiotherapy-opening a new window of opportunity. *Ann Transl Med* (2016) 4:51. doi: 10.3978/j.issn.2305-5839.2015.10.44

69. Young KH, Baird JR, Savage T, Cottam B, Friedman D, Bambina S, et al. Optimizing timing of immunotherapy improves control of tumors by hypofractionated radiation therapy. *PloS One* (2016) 11:e0157164. doi: 10.1371/journal.pone.0157164

70. Verma V, Cushman TR, Tang C, Welsh JW. Toxicity of radiation and immunotherapy combinations. *Adv Radiat Oncol* (2018) 3:506–11. doi: 10.1016/j.adro.2018.08.003

71. Gunderson AJ, Young KH. Exploring optimal sequencing of radiation and immunotherapy combinations. *Adv Radiat Oncol* (2018) 3:494–505. doi: 10.1016/j.adro.2018.07.005

72. Pike LRG, Bang A, Mahal BA, Taylor A, Krishnan M, Spektor A, et al. The impact of radiation therapy on lymphocyte count and survival in metastatic cancer patients receiving PD-1 immune checkpoint inhibitors. *Int J Radiat Oncol Biol Phys* (2019) 103:142–51. doi: 10.1016/j.ijrobp.2018.09.010

73. Lee HJJr., Zeng J, Rengan R. Proton beam therapy and immunotherapy: an emerging partnership for immune activation in non-small cell lung cancer. *Transl Lung Cancer Res* (2018) 7:180–8. doi: 10.21037/tlcr.2018.03.28

74. Tsuboi K. Advantages and limitations in the use of combination therapies with charged particle radiation therapy. *Int J Particle Ther* (2018) 5:122–32. doi: 10.14338/IJPT-18-00019.1

75. Miszczyk J, Rawojc K, Panek A, Borkowska A, Prasanna PGS, Ahmed MM, et al. Do protons and X-rays induce cell-killing in human peripheral blood lymphocytes by different mechanisms? *Clin Transl Radiat Oncol* (2018) 9:23–9. doi: 10.1016/j.ctro.2018.01.004

76. Ebner DK, Tinganelli W, Helm A, Bisio A, Yamada S, Kamada T, et al. The immunoregulatory potential of particle radiation in cancer therapy. *Front Immunol* (2017) 8:99. doi: 10.3389/fimmu.2017.00099

77. Marciscano AE, Ghasemzadeh A, Nirschl TR, Theodros D, Kochel CM, Francica BJ, et al. Elective nodal irradiation attenuates the combinatorial efficacy of stereotactic radiation therapy and immunotherapy. *Clin Cancer Res* (2018) 24:5058–71. doi: 10.1158/1078-0432.CCR-17-3427

78. Crittenden M, Kohrt H, Levy R, Jones J, Camphausen K, Dicker A, et al. Current clinical trials testing combinations of immunotherapy and radiation. *Semin Radiat Oncol* (2015) 25:54–64. doi: 10.1016/j.semradonc.2014.07.003

79. Molloy JA. Statistical analysis of dose heterogeneity in circulating blood: implications for sequential methods of total body irradiation. *Med Phys* (2010) 37:5568–78. doi: 10.1118/1.3495816

80. Basler L, Andratschke N, Ehrbar S, Guckenberger M, Tanadini-Lang S. Modelling the immunosuppressive effect of liver SBRT by simulating the dose to circulating lymphocytes: an in-silico planning study. *Radiat Oncol* (2018) 13:10. doi: 10.1186/s13014-018-0952-y

81. Jin JY, Hu C, Xiao Y, Zhang H, Paulus R, Ellsworth SG, et al. Higher radiation dose to the immune cells correlates with worse tumor control and overall survival in patients with stage III NSCLC: A secondary analysis of RTOG0617. *Cancers* (2021) 13:6193. doi: 10.3390/cancers13246193

82. Ladbury CJ, Rusthoven CG, Camidge DR, Kavanagh BD, Nath SK. Impact of radiation dose to the host immune system on tumor control and survival for stage III non-small cell lung cancer treated with definitive radiation therapy. *Int J Radiat Oncol Biol Phys* (2019) 105:346–55. doi: 10.1016/j.ijrobp.2019.05.064

83. So TH, Chan SK, Chan WL, Choi H, Chiang CL, Lee V, et al. Lymphopenia and radiation dose to circulating lymphocytes with neoadjuvant chemoradiation in esophageal squamous cell carcinoma. *Adv Radiat Oncol* (2020) 5:880–8. doi: 10.1016/j.adro.2020.03.021

84. Xu C, Jin JY, Zhang M, Liu A, Wang J, Mohan R, et al. The impact of the effective dose to immune cells on lymphopenia and survival of esophageal cancer after chemoradiotherapy. *Radiother Oncol* (2020) 146:180–6. doi: 10.1016/j.radonc.2020.02.015

85. Cruz-Garcia L, Nasser F, O'Brien G, Grepl J, Vinnikov V, Starenkiy V, et al. Transcriptional dynamics of DNA damage responsive genes in circulating leukocytes during radiotherapy. *Cancers* (2022) 14:2649. doi: 10.3390/cancers14112649

86. O'Brien G, Cruz-Garcia L, Majewski M, Grepl J, Abend M, Port M, et al. FDXR is a biomarker of radiation exposure in vivo. *Sci Rep* (2018) 8:684. doi: 10.1038/s41598-017-19043-w

87. Hammi A, Paganetti H, Grassberger C. 4D blood flow model for dose calculation to circulating blood and lymphocytes. *Phys Med Biol* (2020) 65:055008. doi: 10.1088/1361-6560/ab6c41

88. Correa-Alfonso CM, Withrow JD, Domal SJ, Xing S, Shin J, Grassberger C, et al. A mesh-based model of liver vasculature: implications for improved radiation

dosimetry to liver parenchyma for radiopharmaceuticals. *EJNMMI Phys* (2022) 9:28. doi: 10.1186/s40658-022-00456-0

89. Correa-Alfonso CM, Withrow JD, Domal SJ, President B, Dawson R, McCullum L, et al. Intra-brain vascular models within the ICRP mesh-type adult reference phantoms for applications to internal dosimetry. *Phys Med Biol* (2023) 68:105001. doi: 10.1088/1361-6560/acc926

90. Withrow JD, Pathak SP, Correa-Alfonso CM, Dawson RJ, Domal SJ, Beekman C, et al. Heart and lung vascular models within the adult mesh-type reference computational phantoms for applications to internal dosimetry. . *Med Phys* (2023) 50:e533.

91. Ganusov VV, Auerbach J. Mathematical modeling reveals kinetics of lymphocyte recirculation in the whole organism. *PloS Comput Biol* (2014) 10: e1003586. doi: 10.1371/journal.pcbi.1003586

92. McDaniel MM, Ganusov VV. Estimating residence times of lymphocytes in ovine lymph nodes. *Front Immunol* (2019) 10:1492. doi: 10.3389/fimmu.2019.01492

93. Jin J-Y, Mereniuk T, Yalamanchali A, Wang W, Machtay M, Spring, Kong F-M, et al. A framework for modeling radiation induced lymphopenia in radiotherapy. *Radiother Oncol* (2020) 144:105–13. doi: 10.1016/j.radonc.2019.11.014

94. Friedrich T, Scholz M, Durante M. A predictive biophysical model of the combined action of radiation therapy and immunotherapy of cancer. *Int J Radiat Oncol Biol Phys* (2022) 113:872–84. doi: 10.1016/j.ijrobp.2022.03.030

95. Cucinotta FA, Smirnova OA. Effects of flash radiotherapy on blood lymphocytes in humans and small laboratory animals. *Radiat Res* (2023) 199:240–51. doi: 10.1667/RADE-22-00093.1

96. Heylmann D, Badura J, Becker H, Fahrer J, Kaina B. Sensitivity of CD3/CD28-stimulated versus non-stimulated lymphocytes to ionizing radiation and genotoxic anticancer drugs: key role of ATM in the differential radiation response. *Cell Death Dis* (2018) 9:1053. doi: 10.1038/s41419-018-1095-7

97. Heylmann D, Ponath V, Kindler T, Kaina B. Comparison of DNA repair and radiosensitivity of different blood cell populations. *Sci Rep* (2021) 11:2478. doi: 10.1038/s41598-021-81058-1

98. Bauer M, Goldstein M, Christmann M, Becker H, Heylmann D, Kaina B. Human monocytes are severely impaired in base and DNA double-strand break repair that renders them vulnerable to oxidative stress. *Proc Natl Acad Sci U.S.A.* (2011) 108:21105–10. doi: 10.1073/pnas.1111919109

99. Konig L, Hommertgen A, Orschiedt L, Horner-Rieber J, Brons S, Huber PE, et al. Influence of photon, proton and carbon ion irradiation on differentiation, maturation and functionality of dendritic cells. *Front Biosci (Schol Ed)* (2022) 14:2. doi: 10.31083/j.fbs1401002

100. Merrick A, Errington F, Milward K, O'Donnell D, Harrington K, Bateman A, et al. Immunosuppressive effects of radiation on human dendritic cells: reduced IL-12 production on activation and impairment of naive T-cell priming. *Br J Cancer* (2005) 92:1450–8. doi: 10.1038/sj.bjc.6602518

101. Rathmell JC, Thompson CB. Pathways of apoptosis in lymphocyte development, homeostasis, and disease. *Cell* (2002) 109 Suppl:S97–107. doi: 10.1016/S0092-8674(02)00704-3

102. Belka C, Heinrich V, Marini P, Faltin H, Schulze-Osthoff K, Bamberg M, et al. Ionizing radiation and the activation of caspase-8 in highly apoptosis-sensitive lymphoma cells. *Int J Radiat Biol* (1999) 75:1257–64. doi: 10.1080/095530099139412

103. Vinnikov V, Hande MP, Wilkins R, Wojcik A, Zubizarreta E, Belyakov O. Prediction of the acute or late radiation toxicity effects in radiotherapy patients using ex vivo induced biodosimetric markers: A review. *J Pers Med* (2020) 10:285. doi: 10.3390/jpm10040285

104. Yang SJ, Rafla S, Youssef E, Selim H, Salloum N, Chuang JY. Changes in T-cell subsets after radiation therapy. *Radiology* (1988) 168:537–40. doi: 10.1148/radiology.168.2.3260678

105. Clave E, Socie G, Cosset JM, Chaillet MP, Tartour E, Girinsky T, et al. Multicolor flow cytometry analysis of blood cell subsets in patients given total body irradiation before bone marrow transplantation. *Int J Radiat Oncol Biol Phys* (1995) 33:881–6. doi: 10.1016/0360-3016(95)00213-6

106. Louagie H, Van Eijkeren M, Philippe J, Thierens H, de Ridder L. Changes in peripheral blood lymphocyte subsets in patients undergoing radiotherapy. *Int J Radiat Biol* (1999) 75:767–71. doi: 10.1080/095530099140113

107. Belka C, Ottinger H, Kreuzfelder E, Weinmann M, Lindemann M, Lepple-Wienhues A, et al. Impact of localized radiotherapy on blood immune cells counts and function in humans. *Radiother Oncol* (1999) 50:199–204. doi: 10.1016/S0167-8140(98)00130-3

108. Zhao Q, Li T, Chen G, Zeng Z, He J. Prognosis and risk factors of radiation-induced lymphopenia in early-stage lung cancer treated with stereotactic body radiation therapy. *Front Oncol* (2019) 9:1488. doi: 10.3389/fonc.2019.01488

109. McCullum L, Shin J, Xing S, Beekman C, Schuemann J, Hong T, et al. Predicting severity of radiation induced lymphopenia in individual proton therapy patients for varying dose rate and fractionation using dynamic 4D blood flow simulations. *Int Jornal Radiat Oncol Biol Phys press* (2023) 116:1226–33. doi: 10.1016/j.ijrobp.2023.01.054

110. Trowell OA. The sensitivity of lymphocytes to ionising radiation. *J Pathol Bacteriol* (1952) 64:687–704. doi: 10.1002/path.1700640403

111. Girinsky T, Socie G, Cosset JM, Malaise EP. Blood lymphocyte subsets after the first fraction in patients given hyperfractionated total body irradiation for bone marrow transplantation. *Br J Cancer* (1991) 63:646–7. doi: 10.1038/bjc.1991.148

112. Akiyama M. Late effects of radiation on the human immune system: an overview of immune response among the atomic-bomb survivors. *Int J Radiat Biol* (1995) 68:497–508. doi: 10.1080/09553009514551491

113. McGee HM, Daly ME, Azghadi S, Stewart SL, Oesterich L, Schlom J, et al. Stereotactic ablative radiation therapy induces systemic differences in peripheral blood immunophenotype dependent on irradiated site. *Int J Radiat Oncol Biol Phys* (2018) 101:1259–70. doi: 10.1016/j.ijrobp.2018.04.038

114. D'Auria F, Statuto T, Rago L, Montagna A, Castaldo G, Schiro I, et al. Modulation of peripheral immune cell subpopulations after rapidArc/moderate hypofractionated radiotherapy for localized prostate cancer: findings and comparison with 3D conformal/conventional fractionation treatment. *Front Oncol* (2022) 12:829812. doi: 10.3389/fonc.2022.829812

115. Yang ZR, Zhao N, Meng J, Shi ZL, Li BX, Wu XW, et al. Peripheral lymphocyte subset variation predicts prostate cancer carbon ion radiotherapy outcomes. *Oncotarget* (2016) 7:26422–35. doi: 10.18632/oncotarget.8389

116. Sage EK, Schmid TE, Geinitz H, Gehrmann M, Sedelmayr M, Duma MN, et al. Effects of definitive and salvage radiotherapy on the distribution of lymphocyte subpopulations in prostate cancer patients. *Strahlenther Onkol* (2017) 193:648–55. doi: 10.1007/s00066-017-1144-7

117. Sage EK, Schmid TE, Sedelmayr M, Gehrmann M, Geinitz H, Duma MN, et al. Comparative analysis of the effects of radiotherapy versus radiotherapy after adjuvant chemotherapy on the composition of lymphocyte subpopulations in breast cancer patients. *Radiother Oncol* (2016) 118:176–80. doi: 10.1016/j.radonc.2015.11.016

118. Yuan C, Wang Q. Comparative analysis of the effect of different radiotherapy regimes on lymphocyte and its subpopulations in breast cancer patients. *Clin Trans Oncol* (2018) 20:1219–25. doi: 10.1007/s12094-018-1851-2

119. Schaue D, Comin-Anduix B, Ribas A, Zhang L, Goodglick L, Sayre JW, et al. T-cell responses to survivin in cancer patients undergoing radiation therapy. *Clin Cancer Res* (2008) 14:4883–90. doi: 10.1158/1078-0432.CCR-07-4462

120. Beauford SS, Kumari A, Garnett-Benson C. Ionizing radiation modulates the phenotype and function of human CD4+ induced regulatory T cells. *BMC Immunol* (2020) 21:18. doi: 10.1186/s12865-020-00349-w

121. Anderson RE, Sprent J, Miller JF. Radiosensitivity of T and B lymphocytes. I. Effect of irradiation on cell migration. *Eur J Immunol* (1974) 4:199–203. doi: 10.1002/eji.1830040309

122. Kataoka Y, Sado T. The radiosensitivity of T and B lymphocytes in mice. *Immunology* (1975) 29:121–30.

123. Durum SK, Gengozian N. The comparative radiosensitivity of T and B lymphocytes. *Int J Radiat Biol Relat Stud Phys Chem Med* (1978) 34:1–15. doi: 10.1080/09553007814550581

124. Sado T, Kamisaku H, Ikarashi Y, Kubo E. Immediate and long-term effects of radiation on the immune system of specific-pathogen-free mice. *Int J Radiat Biol Relat Stud Phys Chem Med* (1988) 53:177–87. doi: 10.1080/09553008814550531

125. Harrington NP, Chambers KA, Ross WM, Filion LG. Radiation damage and immune suppression in splenic mononuclear cell populations. *Clin Exp Immunol* (1997) 107:417–24. doi: 10.1111/j.1365-2249.1997.272-ce1158.x

126. Chambers KA, Harrington NP, Ross WM, Filion LG. Relative alterations in blood mononuclear cell populations reflect radiation injury in mice. *Cytometry* (1998) 31:45–52. doi: 10.1002/(SICI)1097-0320(19980101)31:1<45::AID-CYTO6>3.0.CO;2-I

127. Kajioka EH, A. ML, Li J, Mao XW, Moyers MF, Nelson GA, et al. Acute effects of whole-ody proton irradiation on the immune system of the mouse. *Radiat Res* (2000) 153:587–94. doi: 10.1667/0033-7587(2000)153[0587:AEOWBP]2.0.CO;2

128. Grayson JM, Harrington LE, Lanier JG, Wherry EJ, Ahmed R. Differential sensitivity of naive and memory CD8+ T cells to apoptosis in vivo. *J Immunol* (2002) 169:3760–70. doi: 10.4049/jimmunol.169.7.3760

129. Garg S, Boerma M, Wang J, Fu Q, Loose DS, Kumar KS, et al. Influence of sublethal total-body irradiation on immune cell populations in the intestinal mucosa. *Radiat Res* (2010) 173:469–78. doi: 10.1667/RR1742.1

130. Bogdandi EN, Balogh A, Felgyinszki N, Szatmari T, Persa E, Hildebrandt G, et al. Effects of low-dose radiation on the immune system of mice after total-body irradiation. *Radiat Res* (2010) 174:480–9. doi: 10.1667/RR2160.1

131. Qu Y, Zhang B, Liu S, Zhang A, Wu T, Zhao Y. 2-Gy whole-body irradiation significantly alters the balance of CD4+ CD25- T effector cells and CD4+ CD25+ Foxp3 + T regulatory cells in mice. *Cell Mol Immunol* (2010) 7:419–27. doi: 10.1038/cmi.2010.45

132. Qu Y, Jin S, Zhang A, Zhang B, Shi X, Wang J, et al. Gamma-ray resistance of regulatory CD4+CD25+Foxp3+ T cells in mice. *Radiat Res* (2010) 173:148–57. doi: 10.1667/RR0978.1

133. Yao Z, Jones J, Kohrt H, Strober S. Selective resistance of CD44hi T cells to p53-dependent cell death results in persistence of immunologic memory after total body irradiation. *J Immunol* (2011) 187:4100–8. doi: 10.4049/jimmunol.1101141

134. Kachikwu EL, Iwamoto KS, Liao YP, DeMarco JJ, Agazaryan N, Economou JS, et al. Radiation enhances regulatory T cell representation. *Int J Radiat Oncol Biol Phys* (2011) 81:1128–35. doi: 10.1016/j.ijrobp.2010.09.034

135. Balogh A, Persa E, Bogdandi EN, Benedek A, Hegyesi H, Safrany G, et al. The effect of ionizing radiation on the homeostasis and functional integrity of murine splenic regulatory T cells. *Inflammation Res* (2013) 62:201–12. doi: 10.1007/s00011-012-0567-y

136. Pugh JL, Sukhina AS, Seed TM, Manley NR, Sempowski GD, van den Brink MR, et al. Histone deacetylation critically determines T cell subset radiosensitivity. *J Immunol* (2014) 193:1451–8. doi: 10.4049/jimmunol.1400434

137. Venkatesulu BP, Sharma A, Pollard-Larkin JM, Sadagopan R, Symons J, Neri S, et al. Ultra high dose rate (35 Gy/sec) radiation does not spare the normal tissue in cardiac and splenic models of lymphopenia and gastrointestinal syndrome. *Sci Rep* (2019) 9:17180. doi: 10.1038/s41598-019-53562-y

138. Arina A, Beckett M, Fernandez C, Zheng W, Pitroda S, Chmura SJ, et al. Tumor-reprogrammed resident T cells resist radiation to control tumors. *Nat Commun* (2019) 10:3959. doi: 10.1038/s41467-019-11906-2

139. Telarovic I, Yong CSM, Guckenberger M, Unkelbach J, Pruschy M. Radiation-induced lymphopenia does not impact treatment efficacy in a mouse tumor model. *Neoplasia* (2022) 31:100812. doi: 10.1016/j.neo.2022.100812

140. Hochman PS, Cudkowicz G, Dausset J. Decline of natural killer cell activity in sublethally irradiated mice. *J Natl Cancer Inst* (1978) 61:265–8. doi: 10.1093/jnci/61.1.265

141. Pandey R, Shankar BS, Sharma D, Sainis KB. Low dose radiation induced immunomodulation: effect on macrophages and CD8+ T cells. *Int J Radiat Biol* (2005) 81:801–12. doi: 10.1080/09553000500531886

142. Zheng X, Guo Y, Wang L, Zhang H, Wang S, Wang L, et al. Recovery profiles of T-cell subsets following low-dose total body irradiation and improvement with cinnamon. *Int J Radiat Oncol Biol Phys* (2015) 93:1118–26. doi: 10.1016/j.ijrobp.2015.08.034

143. Prosser JS. Survival of human T and B lymphocytes after X-irradiation. *Int J Radiat Biol Relat Stud Phys Chem Med* (1976) 30:459–65. doi: 10.1080/09553007614551271

144. Kwan DK, Norman A. Radiosensitivity of human lymphocytes and thymocytes. *Radiat Res* (1977) 69:143–51. doi: 10.2307/3574524

145. Zarcone D, Tilden AB, Lane VG, Grossi CE. Radiation sensitivity of resting and activated nonspecific cytotoxic cells of T lineage and NK lineage. *Blood* (1989) 73:1615–21. doi: 10.1182/blood.V73.6.1615.1615

146. Rana R, Vitale M, Mazzotti G, Manzoli L, Papa S. Radiosensitivity of human natural killer cells: binding and cytotoxic activities of natural killer cell subsets. *Radiat Res* (1990) 124:96–102. doi: 10.2307/3577701

147. Nakamura N, Kusunoki Y, Akiyama M. Radiosensitivity of CD4 or CD8 positive human T-lymphocytes by an in *vitro* colony formation assay. *Radiat Res* (1990) 123:224–7. doi: 10.2307/3577549

148. Geara FB, Peters LJ, Ang KK, Wike JL, Sivon SS, Guttenberger R, et al. Intrinsic radiosensitivity of normal human fibroblasts and lymphocytes after high- and low-dose-rate irradiation. *Cancer Res* (1992) 52:6348–52.

149. Seki H, Iwai K, Kanegane H, Konno A, Ohta K, Ohta K, et al. Differential protective action of cytokines on radiation-induced apoptosis of peripheral lymphocyte subpopulations. *Cell Immunol* (1995) 163:30–6. doi: 10.1006/cimm.1995.1095

150. Philippe J, Louagie H, Thierens H, Vral A, Cornelissen M, De Ridder L. Quantification of apoptosis in lymphocyte subsets and effect of apoptosis on apparent expression of membrane antigens. *Cytometry* (1997) 29:242–9. doi: 10.1002/(SICI)1097-0320(19971101)29:3<242::AID-CYTO7>3.0.CO;2-D

151. Radojcic M, Crompton NEA. Age dependence of T-lymphocyte apoptosis induced by high-energy proton exposure. *Radiat Environ Biophys* (2001) 40:131–5. doi: 10.1007/s004110100093

152. Wilkins RC, Kutzner BC, Truong M, McLean JR. The effect of the ratio of CD4 + to CD8+ T-cells on radiation-induced apoptosis in human lymphocyte subpopulations. *Int J Radiat Biol* (2002) 78:681–8. doi: 10.1080/09553000210144475

153. Wilkins RC, Wilkinson D, Maharaj HP, Bellier PV, Cybulski MB, McLean JR. Differential apoptotic response to ionizing radiation in subpopulations of human white blood cells. *Mutat Res* (2002) 513:27–36. doi: 10.1016/S1383-5718(01)00290-X

154. Schmitz A, Bayer J, Dechamps N, Thomas G. Intrinsic susceptibility to radiation-induced apoptosis of human lymphocyte subpopulations. *Int J Radiat Oncol Biol Phys* (2003) 57:769–78. doi: 10.1016/S0360-3016(03)00637-0

155. Hayashi T, Hayashi I, Shinohara T, Morishita Y, Nagamura H, Kusunoki Y, et al. Radiation-induced apoptosis of stem/progenitor cells in human umbilical cord blood is associated with alterations in reactive oxygen and intracellular pH. *Mutat Res* (2004) 556:83–91. doi: 10.1016/j.mrfmmm.2004.07.002

156. Torudd J, Protopopova M, Sarimov R, Nygren J, Eriksson S, Markova E, et al. Dose-response for radiation-induced apoptosis, residual 53BP1 foci and DNA-loop relaxation in human lymphocytes. *Int J Radiat Biol* (2005) 81:125–38. doi: 10.1080/09553000500077211

157. Bordon E, Henriquez Hernandez LA, Lara PC, Pinar B, Fontes F, Rodriguez Gallego C, et al. Prediction of clinical toxicity in localized cervical carcinoma by radio-induced apoptosis study in peripheral blood lymphocytes (PBLs). *Radiat Oncol* (2009) 4:58. doi: 10.1186/1748-717X-4-58

158. Milyavsky M, Gan OI, Trottier M, Komosa M, Tabach O, Notta F, et al. A distinctive DNA damage response in human hematopoietic stem cells reveals an apoptosis-independent role for p53 in self-renewal. *Cell Stem Cell* (2010) 7:186–97. doi: 10.1016/j.stem.2010.05.016

159. Cao M, Cabrera R, Xu Y, Liu C, Nelson D. Different radiosensitivity of CD4(+) CD25(+) regulatory T cells and effector T cells to low dose gamma irradiation in vitro. *Int J Radiat Biol* (2011) 87:71–80. doi: 10.3109/09553002.2010.518208

160. Horn S, Barnard S, Brady D, Prise KM, Rothkamm K. Combined analysis of gamma-H2AX/53BP1 foci and caspase activation in lymphocyte subsets detects recent and more remote radiation exposures. *Radiat Res* (2013) 180:603–9. doi: 10.1667/RR13342.1

161. Hietanen T, Pitkanen M, Kapanen M, Kellokumpu-Lehtinen PL. Effects of single and fractionated irradiation on natural killer cell populations: Radiobiological characteristics of viability and cytotoxicity in vitro. *Anticancer Res* (2015) 35:5193–200.

162. Falcke SE, Ruhle PF, Deloch L, Fietkau R, Frey B, Gaipl US. Clinically relevant radiation exposure differentially impacts forms of cell death in human cells of the innate and adaptive immune system. *Int J Mol Sci* (2018) 19:3574. doi: 10.3390/ijms19113574

163. Cole J, Arlett CF, Green MH, Harcourt SA, Priestley A, Henderson L, et al. Comparative human cellular radiosensitivity: II. The survival following gamma-irradiation of unstimulated (G0) T-lymphocytes, T-lymphocyte lines, lymphoblastoid cell lines and fibroblasts from normal donors, from ataxia-telangiectasia patients and from ataxia-telangiectasia heterozygotes. *Int J Radiat Biol* (1988) 54:929–43. doi: 10.1080/09553008814552331

164. Brovall C, Schacter B. Radiation sensitivity of human natural killer cell activity: control by X-linked genes. *J Immunol* (1981) 126:2236–9. doi: 10.4049/jimmunol.126.6.2236

165. Cao M, Cabrera R, Xu Y, Liu C, Nelson D. Gamma irradiation alters the phenotype and function of CD4+CD25+ regulatory T cells. *Cell Biol Int* (2009) 33:565–71. doi: 10.1016/j.cellbi.2009.02.007

166. Heylmann D, Rodel F, Kindler T, Kaina B. Radiation sensitivity of human and murine peripheral blood lymphocytes, stem and progenitor cells. *Biochim Biophys Acta* (2014) 1846:121–9. doi: 10.1016/j.bbcan.2014.04.009

167. Miszczyk J, Rawojc K, Panek A, Swakon J, Prasanna PG, Rydygier M. Response of human lymphocytes to proton radiation of 60 MeV compared to 250 kV X-rays by the cytokinesis-block micronucleus assay. *Radiother Oncol* (2015) 115:128–34. doi: 10.1016/j.radonc.2015.03.003

168. Panek A, Miszczyk J. ATM and RAD51 repair pathways in human lymphocytes irradiated with 70 MeV therapeutic proton beam. *Radiat Res* (2022) 197:396–402. doi: 10.1667/RADE-21-00109.1

169. Vandevoorde C, Vral A, Vandekerckhove B, Philippe J, Thierens H. Radiation sensitivity of human CD34(+) cells versus peripheral blood T lymphocytes of newborns and adults: DNA repair and mutagenic effects. *Radiat Res* (2016) 185:580–90. doi: 10.1667/RR14109.1

170. DeKruyff RH, Fang Y, Umetsu DT. IL-4-based helper activity of CD4+ T cells is radiation sensitive. *Cell Immunol* (1995) 160:248–56. doi: 10.1016/0008-8749(95)80035-H

171. Eckert D, Rapp F, Tsedeke AT, Molendowska J, Lehn R, Langhans M, et al. ROS- and radiation source-dependent modulation of leukocyte adhesion to primary microvascular endothelial cells. *Cells* (2021) 11:72. doi: 10.3390/cells11010072

172. Rajakaruna H, O'Connor JH, Cockburn IA, Ganusov VV. Liver environment-imposed constraints diversify movement strategies of liver-localized CD8 T cells. *J Immunol* (2022) 208:1292–304. doi: 10.4049/jimmunol.2100842

173. Downey GP, Doherty DE, Schwab B3rd, Elson EL, Henson PM, Worthen GS. Retention of leukocytes in capillaries: role of cell size and deformability. *J Appl Physiol (1985)* (1990) 69:1767–78. doi: 10.1152/jappl.1990.69.5.1767

174. Pham TN, Coupey J, Candeias SM, Ivanova V, Valable S, Thariat J, et al. Beyond lymphopenia, unraveling radiation-induced leucocyte subpopulation kinetics and mechanisms through modeling approaches. *J Exp Clin Cancer Res CR* (2023) 42:50. doi: 10.1186/s13046-023-02621-4

175. Spiotto M, Fu YX, Weichselbaum RR. The intersection of radiotherapy and immunotherapy: mechanisms and clinical implications. *Sci Immunol* (2016) 1:1226–33. doi: 10.1126/sciimmunol.aag1266

176. Zhao Q, Li T, Du S, He J, Zeng Z. Shortened radiation time promotes recovery from radiation-induced lymphopenia in early-stage non-small cell lung cancer patients treated with stereotactic body radiation therapy. *Technol Cancer Res Treat* (2022) 21:15330338221112287. doi: 10.1177/15330338221112287

177. Chou C, Li MO. Tissue-resident lymphocytes across innate and adaptive lineages. *Front Immunol* (2018) 9:2104. doi: 10.3389/fimmu.2018.02104

178. Tong AA, Forestell B, Murphy DV, Nair A, Allen F, Myers J, et al. Regulatory T cells differ from conventional CD4(+) T cells in their recirculatory behavior and lymph node transit times. *Immunol Cell Biol* (2019) 97:787–98. doi: 10.1111/imcb.12276

179. Mandl JN, Liou R, Klauschen F, Vrisekoop N, Monteiro JP, Yates AJ, et al. Quantification of lymph node transit times reveals differences in antigen surveillance strategies of naive CD4+ and CD8+ T cells. *Proc Natl Acad Sci U.S.A.* (2012) 109:18036–41. doi: 10.1073/pnas.1211717109

180. Tse BCY, Ireland RA, Lee JY, Marsh-Wakefield F, Kok LF, Don AS, et al. Exposure to systemic immunosuppressive ultraviolet radiation alters T cell recirculation through sphingosine-1-phosphate. *J Immunol* (2021) 207:2278–87. doi: 10.4049/jimmunol.2001261

181. Galdiero M, Cipollaro de l'Ero G, Folgore A, Cappello M, Giobbe A, Sasso FS. Effects of irradiation doses on alterations in cytokine release by monocytes and lymphocytes. *J Med* (1994) 25:23–40.

182. Krivenko SI, Dryk SI, Komarovskaya ME, Karkanitsa LV. Ionizing radiation increases TNF/cachectin production by human peripheral blood mononuclear cells in vitro. *Int J Hematol* (1992) 55:127–30.

183. Yamazaki H, Yoshioka Y, Inoue T, Tanaka E, Nishikubo M, Sato T, et al. Changes in natural killer cell activity by external radiotherapy and/or brachytherapy. *Oncol Rep* (2002) 9:359–63. doi: 10.3892/or.9.2.359

184. McGinnes K, Florence J, Penny R. The effect of radiotherapy on the natural killer (NK)-cell activity of cancer patients. *J Clin Immunol* (1987) 7:210–7. doi: 10.1007/BF00915726

185. Mozaffari F, Lindemalm C, Choudhury A, Granstam-Bjorneklett H, Helander I, Lekander M, et al. NK-cell and T-cell functions in patients with breast cancer: effects of surgery and adjuvant chemo- and radiotherapy. *Br J Cancer* (2007) 97:105–11. doi: 10.1038/sj.bjc.6603840

186. Marchese MJ, Zaider M, Hall EJ. Potentially lethal damage repair in human cells. *Radiother Oncol* (1987) 9:57–65. doi: 10.1016/S0167-8140(87)80219-0

187. Kim N, Noh JM, Lee W, Park B, Park H, Park JY, et al. Proton beam therapy reduces the risk of severe radiation-induced lymphopenia during chemoradiotherapy for locally advanced non-small cell lung cancer: A comparative analysis of proton versus photon therapy. *Radiother Oncol* (2021) 156:166–73. doi: 10.1016/j.radonc.2020.12.019

frontiers | Frontiers in Oncology

TYPE Original Research
PUBLISHED 09 November 2023
DOI 10.3389/fonc.2023.1278723

OPEN ACCESS

EDITED BY
Andrea Riccardo Filippi,
University of Pavia, Italy

REVIEWED BY
Jianyang Wang,
Chinese Academy of Medical Sciences and Peking Union Medical College, China
Prashanth Giridhar,
Tata Memorial Centre, India

*CORRESPONDENCE
Peter S. N. van Rossum
p.s.n.vanrossum@amsterdamumc.nl

RECEIVED 16 August 2023
ACCEPTED 23 October 2023
PUBLISHED 09 November 2023

CITATION
van Rossum PSN, Juan-Cruz C, Stam B, Rossi MMG, Lin SH, Abravan A, Belderbos JSA and Sonke J-J (2023) Severe radiation-induced lymphopenia during concurrent chemoradiotherapy for stage III non-small cell lung cancer: external validation of two prediction models.
Front. Oncol. 13:1278723.
doi: 10.3389/fonc.2023.1278723

Severe radiation-induced lymphopenia during concurrent chemoradiotherapy for stage III non-small cell lung cancer: external validation of two prediction models

Peter S. N. van Rossum[1,2]*, Celia Juan-Cruz[1], Barbara Stam[1], Maddalena M. G. Rossi[1], Steven H. Lin[3], Azadeh Abravan[4,5], José S. A. Belderbos[1] and Jan-Jakob Sonke[1]

[1]Department of Radiation Oncology, Netherlands Cancer Institute-Antoni van Leeuwenhoek Hospital, Amsterdam, Netherlands, [2]Department of Radiation Oncology, Amsterdam University Medical Centers (UMC), Amsterdam, Netherlands, [3]Department of Radiation Oncology, The University of Texas MD Anderson Cancer Center, Houston, TX, United States, [4]Division of Cancer Sciences, School of Medical Sciences, Faculty of Biology, Medicine and Health, The University of Manchester, Manchester, United Kingdom, [5]Department of Radiotherapy Related Research, The Christie National Health Service (NHS) Foundation Trust, Manchester, United Kingdom

Background: Severe radiation-induced lymphopenia (RIL) in patients undergoing chemoradiotherapy (CRT) for non-small cell lung cancer (NSCLC) is associated with decreased immunotherapy efficacy and survival. At The Christie and MD Anderson Cancer Center (MDACC), prediction models for lymphopenia were developed in lung and esophageal cancer patients, respectively. The aim of this study was to externally validate both models in patients with stage III NSCLC.

Methods: Patients who underwent concurrent CRT for stage III NSCLC in 2019–2021 were studied. Outcomes were grade ≥3 and grade 4 lymphopenia during CRT. The Christie model predictors for grade ≥3 lymphopenia included age, baseline lymphocyte count, radiotherapy duration, chemotherapy, mean heart and lung doses, and thoracic vertebrae V20Gy. MDACC predictors for grade 4 lymphopenia were age, baseline lymphocyte count, planning target volume (PTV), and BMI. The external performance of both models was assessed.

Results: Among 100 patients, 78 patients (78%) developed grade ≥3 lymphopenia, with grade 4 lymphopenia in 17 (17%). For predicting grade ≥3 lymphopenia, the Christie and MDACC models yielded *c*-statistics of 0.77 and 0.79, respectively. For predicting grade 4 lymphopenia, *c*-statistics were 0.69 and 0.80, respectively. Calibration for the Christie and MDACC models demonstrated moderate and good agreement, respectively.

Conclusion: The PTV-based MDACC prediction model for severe RIL demonstrated superior external performance in NSCLC patients compared to the dosimetry-based Christie model. As such, the MDACC model can aid in identifying patients at high risk for severe lymphopenia. However, to optimize radiotherapy planning, further improvement and external validation of dosimetry-based models is desired.

KEYWORDS

lung cancer, radiotherapy, chemoradiotherapy, lymphopenia, hematologic toxicity

Introduction

Non-small cell lung cancer (NSCLC) accounts for approximately 85% of all lung cancer cases and presents as locally advanced (stage III) disease in approximately one-fifth of patients (1, 2). Since the early 1990s, the standard treatment for patients with unresectable stage III NSCLC has consisted of radiotherapy in combination with concurrent platinum-based chemotherapy (3, 4). After a few years, consolidative immunotherapy (i.e., durvalumab) after concurrent chemoradiotherapy (CRT) became the new standard of care in this setting as the PACIFIC trial demonstrated a sustained survival benefit (5, 6). By blocking PD-L1, durvalumab allows the patient's vital T-lymphocytes to recognize and kill tumor cells.

As these important anti-tumor lymphocytes are the most radiosensitive cells of the hematopoietic system, many get killed during radiotherapy, which puts patients at risk of radiation-induced lymphopenia (RIL) (7). With growing interest in this topic driven by the emergence of immunotherapy, in recent years, several studies demonstrated an independent association between lymphopenia and detrimental survival in NSCLC (8–12). In addition, two recent studies in NSCLC patients observed that severe lymphopenia before the initiation of immunotherapy was associated with worse progression-free and overall survival outcomes (13, 14).

The apparent impact of lymphopenia on the efficacy of consolidative immunotherapy and survival provides a strong incentive to identify patients at high risk of severe lymphopenia who could potentially benefit from lymphopenia-mitigating strategies. Thus, before starting CRT, accurate prediction of the individual risk of developing severe lymphopenia during CRT would be of interest. One such elaborate model predicting grade ≥3 lymphopenia originated from The Christie (Manchester, UK) and was developed in 901 lung cancer patients, of whom 227 patients received concurrent CRT for NSCLC (11). External validation of the Christie model in 305 patients with esophageal cancer yielded a satisfactory *c*-statistic of 0.78 (11). A more simple prediction model (i.e., not requiring any dosimetric parameters) predicting grade 4 lymphopenia originated from MD Anderson Cancer Center (MDACC, Houston, Texas, USA) and was developed in 860 patients with esophageal cancer (15). External validation of the MDACC model in 219 patients with esophageal cancer in another country yielded a satisfactory *c*-statistic of 0.80 (16).

The Christie experience (11) suggested that a prediction model for lymphopenia developed in lung cancer could be used interchangeably in esophageal cancer. Although validated in other esophageal cancer cohorts, the MDACC model (15) has not yet been validated in patients with lung cancer. Therefore, the aim of this study was to externally validate and compare both the Christie and MDACC model for predicting grade ≥3 and grade 4 RIL during concurrent CRT in patients with stage III NSCLC.

Methods

This single-center retrospective cohort study was approved by the institutional review board and the need for informed consent was waived. All patients had an institutional opt-out option upon first consultation in case they wished their data would not be used for research purposes. Reporting of this study was performed in accordance with the "Transparent Reporting of a Multivariable Prediction Model for Individual Prognosis or Diagnosis" (TRIPOD) guidelines (17).

Study population

Consecutive patients who underwent concurrent CRT for stage III NSCLC at our comprehensive cancer center between February 2019 and November 2021 were eligible for inclusion. Patients who opted out for consenting to use their data for research were excluded. Some patients were treated at a satellite location of our hospital where no routine determination of absolute lymphocyte counts (ALCs) was performed and these patients were therefore excluded. In addition, patients were excluded in case a baseline ALC or ALC beyond the first 3 weeks of CCRT was lacking or in case therapy was discontinued in the first 2 weeks for issues unrelated to lymphopenia. Finally, a patient with an active hematologic malignancy (and associated high baseline ALC) was excluded. A detailed comparison of the inclusion and exclusion criteria of the development cohorts (11, 15) and the current validation cohort is provided in Supplementary Table 1.

Treatment

Chemotherapy consisted of cisplatin 6 mg/m^2 in 24 administrations (five times per week) and was administered as a bolus injection, 1–2 h before radiotherapy (18). All patients were treated with hypofractionated radiotherapy (24 × 2.75 Gy) up to 70 Gy ($EQD2_{10}$) to the primary tumor and up to 60 Gy ($EQD2_{10}$; 24 × 2.42 Gy) to the involved lymph nodes. Photon-based intensity-modulated radiotherapy was used in all patients and the two dose levels were achieved using a simultaneous integrated boost technique (19). A 4D-CT scan with intravenous contrast was acquired, from which a 3D-midposition-CT scan (MidP) was reconstructed. An ^{18}F-FDG PET-CT scan was registered to the MidP to guide gross tumor volume (GTV) delineation of the primary tumor and pathologic lymph nodes in all patients. No CTV concept was applied. Subsequently, the GTVs were expanded to a planning target volume (PTV) using individualized margins according to the peak-to-peak respiratory amplitude movement of the primary tumor and lymph nodes.

Predictors

The refined dosimetry-based Christie model predictors for grade ≥3 lymphopenia included higher age, lower baseline ALC, longer duration of radiotherapy, higher mean heart and lung doses, and higher thoracic vertebrae V20Gy (i.e., volume of thoracic vertebrae receiving ≥20 Gy) (11). In the more simple PTV-based MDACC model, predictors for grade 4 lymphopenia consisted of higher age, lower baseline ALC, and higher PTV in interaction with a lower body mass index (BMI) (15). For the current study, all of these predictors were collected from our institutional database in addition to other baseline characteristics (i.e., gender, year of treatment start, histology, tumor location, and clinical stage).

The original Christie prediction model (11) is defined by the following logistic regression formula, where p describes the individual risk to develop grade ≥3 lymphopenia:

$$\begin{aligned}\log\left(\frac{p}{1-p}\right) = {} & -4.654 + 0.019{*}Age - 0.544{*}Baseline\_ALC \\ & + 0.435{*}chemotherapy[0 = \text{no}; 1 = \text{yes}] \\ & + 0.090{*}Radiotherapy\_duration \\ & + 0.028{*}Mean\_heart\_dose \\ & + 0.046{*}Mean\_lung\_dose \\ & + 0.014{*}Vertebrae\_V20Gy\,.\end{aligned}$$

The original MDACC prediction model (15) for the prediction of grade 4 lymphopenia is defined as follows:

$$\begin{aligned}\log\left(\frac{p}{1-p}\right) = {} & -22.845 + 0.021{*}Age - 1.019{*}Baseline\_ALC \\ & + 0.516{*}BMI + 3.579{*}\log(PTV) \\ & - 0.086{*}BMI{*}\log(PTV) + 0.949{*}Photons[0 \\ & = \text{no, Protons}; 1 = \text{yes, Photons}]\,.\end{aligned}$$

Outcomes

ALC was routinely measured mostly twice per week (but at least once weekly) during concurrent CRT as part of routine blood examinations to evaluate hematologic and renal chemotherapy toxicity. The frequency of blood examinations in The Christie and MDACC cohorts was generally less and details are provided in Supplementary Table 1. The lowest measured ALC during CRT on a per-patient basis was defined as the nadir. The primary outcomes of grade ≥3 and grade 4 lymphopenia were defined as ALC nadirs during CRT of <0.5 and <0.2 K/μL, respectively, in accordance with the Common Terminology Criteria for Adverse Events (version 5). The studied outcome measure consisted of the external model performance in terms of discrimination and calibration of the Christie and MDACC models to predict the risk of grade ≥3 and grade 4 lymphopenia.

Statistical analysis

A table with baseline characteristics was constructed. Univariable logistic regression analyses were performed to explore the crude associations of (baseline) variables with grade ≥3 and grade 4 lymphopenia. Next, for each patient, the individual predicted probabilities of grade ≥3 and grade 4 lymphopenia according to the Christie and MDACC prediction models were calculated. The discriminatory model performances were assessed by calculating external *c*-statistics and by plotting ROC curves. External model calibration performances (i.e., the agreements between predicted and observed proportions of grade ≥3 or grade 4 lymphopenia) were visually assessed in calibration plots using 3 equally sized risk groups (i.e., tertiles of predicted risks).

In case of miscalibration due to a different *a priori* risk (i.e., incidences) of grade ≥3 or grade 4 lymphopenia in the current cohort compared to the original Christie and MDACC development cohorts, the intercept was updated for each model and each outcome. This intercept was updated in such way that the sum of predicted probabilities was equal to the observed number of events (20). Model coefficients were not updated. Analyses were performed using SPSS version 27.0 (IBM Corp., Armonk, NY) and R version 3.5.1 ("rms" package). A p-value<0.05 was considered statistically significant.

10.3389/fonc.2023.1278723

TABLE 1 Baseline characteristics of 100 included patients.

	n (%)
Age (years)*	66.1 ± 8.4
Male gender	55 (55%)
BMI (kg/m^2)*	25.3 ± 4.5
Year of treatment start	
2019	30 (30%)
2020	38 (38%)
2021	32 (32%)
Histology	
Adenocarcinoma	48 (48%)
Squamous cell carcinoma	35 (35%)
Other (large cell)	17 (17%)
Primary tumor lateralization	
Left sided	40 (40%)
Right sided	59 (59%)
Missing	1 (1%)
Primary tumor location	
Upper lobe	67 (67%)
Middle lobe	4 (4%)
Lower lobe	25 (25%)
Trachea/main bronchus	3 (3%)
Missing	1 (1%)
Clinical T-stage	
cT1	20 (20%)
cT2	18 (18%)
cT3	12 (12%)
cT4	50 (50%)
Clinical N-stage	
cN0	11 (11%)
cN1	5 (5%)
cN2	60 (60%)
cN3	24 (24%)
Overall clinical stage	
IIIA	46 (46%)
IIIB	39 (39%)
IIIC	15 (15%)
Baseline ALC (K/μL)†	1.71 [1.18–2.19]
PTV (mL)†	0.337 [0.204–0.503]
Mean heart dose (Gy)†	4.34 [1.93–8.62]
Mean lung dose (Gy)†	11.1 [9.16–13.2]
Thoracic vertebrae V20Gy (%)†	23.5 [14.8–32.4]

*Expressed as mean ± SD. †Expressed as median [IQR]. ALC, Absolute lymphocyte count; BMI, Body mass index; PTV, Planning target volume.

Results

From a total of 148 identified patients who underwent concurrent CRT for stage III NSCLC in the study period, 100 patients were eligible for analysis. The 48 patients were excluded because of the opt-out procedure (n = 3), concurrent CRT was administered at the satellite location of our hospital with no routine ALC values available (n = 16), baseline ALC values were missing (n = 24), ALC values beyond 3 weeks after start of treatment were missing (n = 2), therapy was discontinued early due to a severe COVID-19 infection or unexpected sudden death (n = 2), or an active hematologic malignancy was present (n = 1).

The majority of the 100 included patients were male (55%) and were diagnosed with a clinical T4 (50%) and/or N2–3 (84%) lung cancer. The predominant histologic tumor types were adenocarcinoma (48%) and squamous cell carcinoma (35%), and the primary tumor was mostly located in an upper lobe (67%). Baseline patient-, tumor-, and treatment-related characteristics are presented in Table 1.

The course of ALC values over the time of treatment showed an overall declining trend and is illustrated in Figure 1. The median duration of treatment was 32 days [IQR: 31–33]. The ALC nadir was observed at a median of 30 days [IQR: 25–31] after the start of concurrent CRT, generally corresponding to the fifth week of treatment. Grade ≥3 lymphopenia during concurrent CRT occurred in 78 patients (78%), and among those patients, grade 4 lymphopenia was observed in 17 (17% of total).

Explorative logistic regression analysis for grade ≥3 and grade 4 lymphopenia is presented in Table 2. Significant univariable associations were observed for baseline ALC and PTV with both grade ≥3 and grade 4 lymphopenia. For the 78 patients with versus 22 patients without grade ≥3 lymphopenia, median baseline ALC was 1.53 [IQR: 1.13–1.93] versus 2.36 [IQR: 1.93–2.62] K/μL, respectively, and median PTV was 392 [IQR: 237–522] versus 203 [132–347] mL, respectively. For the 17 patients with versus 83 patients without grade 4 lymphopenia, median baseline ALC was 1.37 [IQR: 1.02–1.73] versus 1.83 [IQR: 1.24–2.33] K/μL, respectively, and median PTV was 499 [IQR: 325–718] versus 296 [IQR: 190–496] mL, respectively. In addition, right-sided tumor lateralization and mean lung dose appeared significantly associated with grade ≥3 lymphopenia.

For prediction of grade ≥3 lymphopenia, application of the Christie and MDACC models yielded c-statistics of 0.77 (95% CI: 0.65–0.89) and 0.79 (95% CI: 0.67–0.91), respectively (Figure 2A). For prediction of grade 4 lymphopenia, the Christie and MDACC models yielded c-statistics of 0.69 (95% CI: 0.57–0.81) and 0.80 (95% CI: 0.70–0.89), respectively (Figure 2B).

10.3389/fonc.2023.1278723

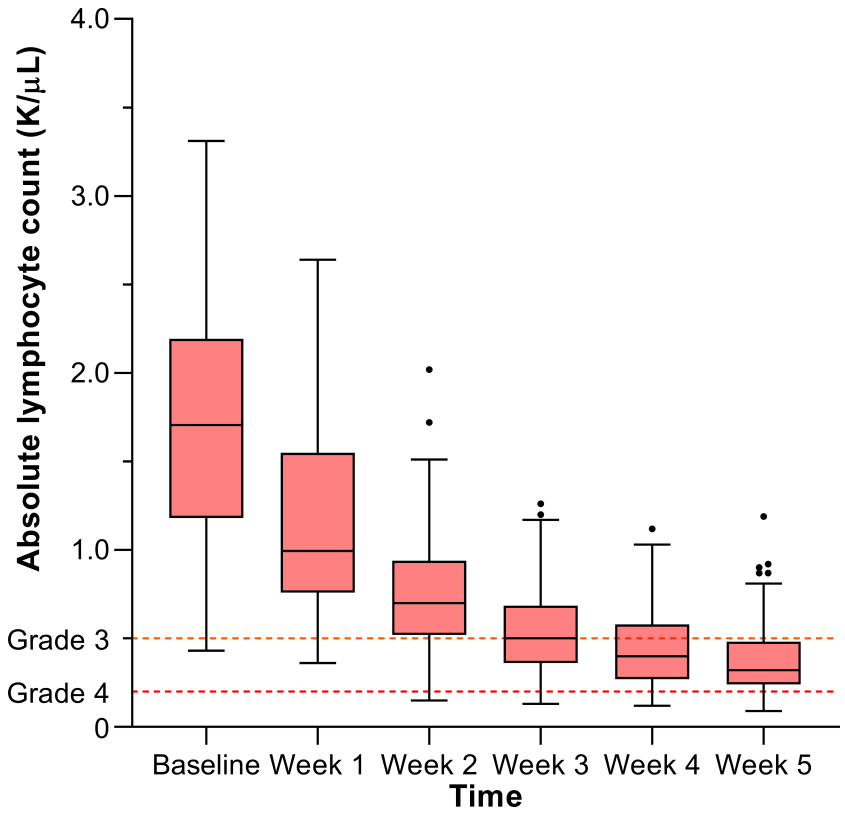

FIGURE 1
Lymphocyte counts over the course of treatment.

TABLE 2 Exploratory univariable logistic regression analyses for grade ≥3 and grade 4 lymphopenia.

	Grade ≥3 lymphopenia		Grade 4 lymphopenia	
	OR (95% CI)	*p*-value	OR (95% CI)	*p*-value
Age (years)	1.04 (0.98–1.10)	0.170	1.00 (0.94–1.07)	0.988
Male gender	1.64 (0.63–4.24)	0.311	2.23 (0.72–6.90)	0.163
BMI (kg/m^2)	1.01 (0.91–1.12)	0.910	0.95 (0.84–1.07)	0.388
Histology				
Adenocarcinoma	Ref		Ref	
Squamous cell carcinoma	1.44 (0.48–4.35)	0.521	1.74 (0.56–5.34)	0.337
Other (large cell)	0.71 (0.21–2.47)	0.594	0.78 (0.15–4.19)	0.773
Right-sided tumor lateralization	4.46 (1.61–12.3)	0.004*	0.96 (0.33–2.78)	0.943
Primary tumor location				
Upper lobe	Ref		Ref	
Other	2.66 (0.82–8.64)	0.103	1.13 (0.38–3.38)	0.825
Clinical T-stage				
cT1–2	Ref		Ref	
cT3–4	1.49 (0.57–3.88)	0.416	1.15 (0.39–3.42)	0.801

(Continued)

TABLE 2 Continued

	Grade ≥3 lymphopenia		Grade 4 lymphopenia	
	OR (95% CI)	*p*-value	OR (95% CI)	*p*-value
Clinical N-stage				
cN0–1	Ref		Ref	
cN2–3	2.55 (0.81–8.05)	0.110	0.87 (0.22–3.45)	0.839
Overall clinical stage				
IIIA	Ref		Ref	
IIIB-C	3.25 (1.19–8.88)	0.022*	1.27 (0.44–3.65)	0.662
Baseline ALC (K/μL)	0.24 (0.11–0.53)	0.001*	0.25 (0.09–0.69)	0.007*
Log(PTV) [mL]	4.53 (1.83–11.3)	0.001*	5.86 (1.83–18.7)	0.003*
Mean heart dose (Gy)	1.08 (0.96–1.20)	0.195	1.01 (0.92–1.11)	0.853
Mean lung dose (Gy)	1.22 (1.05–1.40)	0.008*	1.10 (0.94–1.28)	0.226
Thoracic vertebrae V20Gy (%)	1.04 (0.99–1.08)	0.088	1.02 (0.98–1.06)	0.381
Radiotherapy duration (days)	0.86 (0.63–1.16)	0.857	0.94 (0.66–1.33)	0.713

*Statistically significant univariable association with the outcome. ALC, Absolute lymphocyte count; BMI, Body mass index; CI, Confidence interval; OR, Odds ratio; PTV, Planning target volume.

Application of the Christie model for predicting grade ≥3 lymphopenia resulted in an uncorrected calibration in which the predicted risk consistently underestimated the observed risk. Therefore, the model was updated by intercept correction to take into account the higher *a priori* risk of grade ≥3 lymphopenia in the current cohort compared with the development cohort (i.e., 78% versus 55% (11); Supplementary Figures 1A, B). In contrast, the MDACC prediction model for predicting grade 4 lymphopenia resulted in an uncorrected calibration in which the predicted risk consistently overestimated the observed risk. Therefore, the model was updated by intercept correction to take into account the lower *a priori* risk of grade 4 lymphopenia in the current cohort compared with the development cohort (i.e., 17% versus 37% (15); Supplementary Figures 1C, D). Separately, the intercept of the Christie model (developed for predicting 55% grade ≥3 lymphopenia (11)) was also adjusted to the currently observed incidence of grade 4 lymphopenia (17%), and the intercept of the MDACC model (developed for predicting 37% grade 4 lymphopenia (15)) was similarly adjusted to the observed incidence of grade ≥3 lymphopenia.

The resulting agreement between predicted and observed risks (i.e., calibration performance) of the models was visually assessed (Figure 3). For predicting grade ≥3 lymphopenia, the Christie and MDACC models demonstrated moderate and good agreement, respectively (Figure 3A). For predicting grade 4 lymphopenia, the Christie and MDACC models demonstrated moderate and excellent agreement, respectively (Figure 3B).

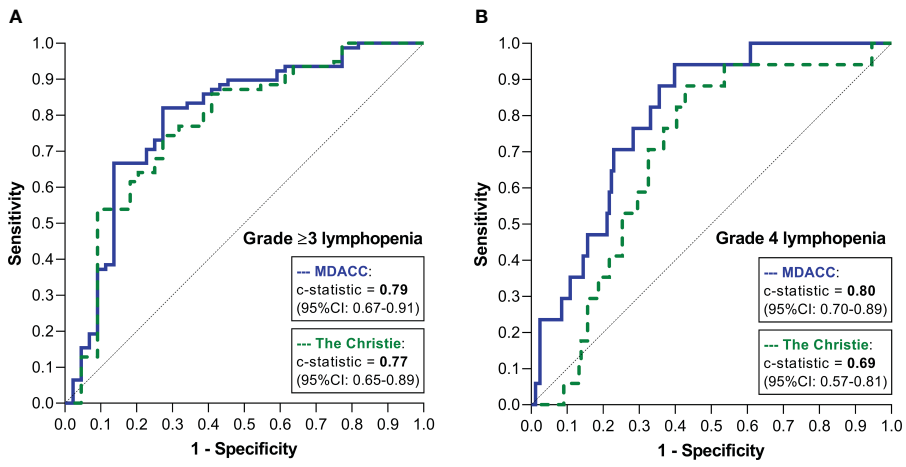

FIGURE 2
ROC curves demonstrating the discriminatory performances of the two models for predicting grade ≥3 lymphopenia **(A)** and grade 4 lymphopenia **(B)**.

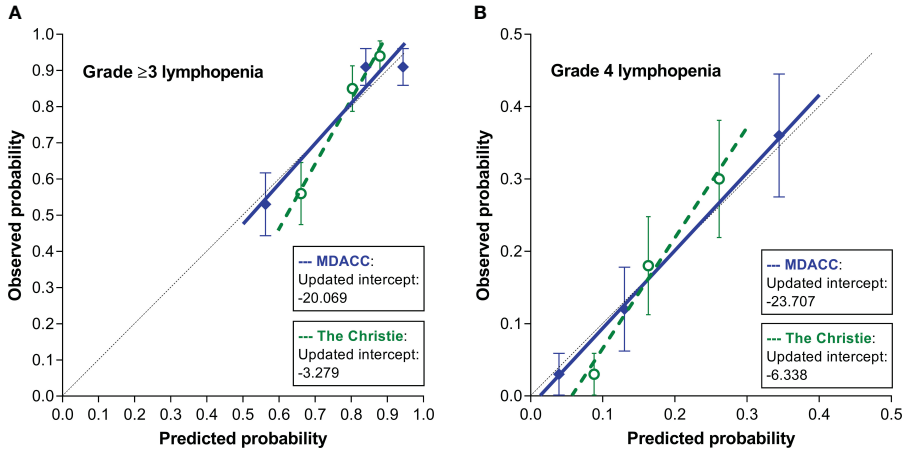

FIGURE 3
Calibration plots demonstrating the agreement between the predicted risks by the 2 models and the observed risks of grade ≥3 lymphopenia **(A)** and grade 4 lymphopenia **(B)**.

Discussion

This study demonstrated that the majority (78%) of patients with stage III NSCLC experience grade ≥3 lymphopenia during concurrent CRT, and in 17% of patients, the ALC drops as low as<0.2 K/mL (i.e., grade 4). The performance of the simple PTV-based MDACC prediction model for severe RIL (15) in our current external cohort appeared superior in terms of discrimination and calibration in comparison to the more refined dosimetry-based Christie model (11). In fact, the MDACC prediction model developed in esophageal cancer for grade 4 RIL (15) demonstrated good external performance in our setting of concurrent CRT for patients with stage III NSCLC with a *c*-statistic of 0.80 and excellent calibration. In addition, after intercept adjustment to the *a priori* risk, the MDACC model appeared capable of satisfactorily distinguishing patients who will experience grade ≥3 lymphopenia versus those who will not with a *c*-statistic of 0.79 and good calibration. The herein reported external model performance (in another center in another country) suggests good overall generalizability of the model.

As the MDACC lymphopenia model developed and validated in esophageal cancer appeared compatible in lung cancer, the model could potentially serve as a generalized thoracic cancer risk tool for predicting severe lymphopenia. Similarly, the Christie lymphopenia model developed in lung cancer was previously validated in a cohort of esophageal cancer as well with satisfactory results (11). As such, these current and previous findings can help encourage increased collaboration of investigators and clinicians in the fields of esophageal cancer and lung cancer to jointly elucidate the impact of lymphopenia, improve risk prediction, and study strategies to mitigate the lymphopenia risk.

Because the simple PTV-based MDACC model does not contain dosimetric variables, the model cannot aid in optimizing radiotherapy planning parameters for lymphopenia mitigation. For the important goal of lymphopenia mitigation by adjusting radiotherapy plans, refined dosimetry-based prediction models such as the Christie model are required. However, this study demonstrates that applying such a complex dosimetry-based model in an external setting carries more risk of suboptimal performance (i.e., appears less robust across varying disease sites, lymphopenia outcome definitions, and care settings). Therefore, for moving forward with radiotherapy planning optimization aimed at reducing the risk of severe lymphopenia, further improvement and external validation of dosimetry-based models is desired.

The initial poor calibration of the prediction models is explained by the lower incidence of grade 4 lymphopenia in the current lung cancer cohort (13%) in comparison with the esophageal cancer cohorts from MDACC used for development (37%) (15), and our higher incidence of grade ≥3 lymphopenia (78%) in comparison to the Christie development cohort (55%) (11). After intercept correction to adjust for this varying incidence, the calibration of the MDACC model in our external lung cancer cohort was good to excellent, revealing that the same predictors in esophageal cancer hold their predictive value in lung cancer.

The relatively high incidence of grade 4 lymphopenia in esophageal cancer has been confirmed in multiple series (16, 21–23), and is attributed to the major collateral irradiation of large pools of lymphocytes (e.g., heart, lungs, and aorta) in typical esophageal cancer radiotherapy fields (7, 22). Besides the major role of blood pool irradiation, the risk and depth of RIL may also be affected (to a lesser extent) by irradiation of the spinal column that contains a significant portion of the hematopoietic potential in adults and replenishes the circulating lymphocyte pool (7, 22). The statistical power of lymphopenia risk modeling in esophageal cancer is strengthened by the high number of events, but limited by the relatively small variation in tumor location and thus in dosimetric parameters. In contrast, risk modeling in lung cancer is hampered by the lower incidence of grade 4 lymphopenia, but strengthened by the larger variation in dosimetric parameters by greater tumor location variability. Therefore, combining knowledge and data from both esophageal and lung cancer populations carries the potential to overcome current limitations.

Although the typical depletion of lymphocytes over the course of treatment is typical for radiotherapy-only as well as CRT cohorts, the addition of chemotherapy does result in an even lower ALC nadir (24). A study comparing different doublet platinum-based chemotherapy regimens (i.e., cisplatin-etoposide, cisplatin-docetaxel, carboplatin-paclitaxel, and carboplatin-docetaxel) found an equal 88%–89% grade ≥3 lymphopenia rate for each regimen (25). Since reported incidence rates of grade ≥3 lymphopenia in stage III NSCLC patients undergoing 3-weekly doublet platinum-based chemotherapy vary from 49% to 89% (7, 9–11, 22, 25), the incidence in the current study of 78% does not appear different with our daily low-dose cisplatin regimen.

Before commencing treatment, the MDACC prediction model allows the identification of individual patients at high risk for severe lymphopenia. These patients may benefit from lymphopenia-mitigating strategies. Examples of such strategies include further hypofractionation, sparing lymphocyte-rich organs in radiation treatment planning, or reducing PTV by minimizing radiotherapy margins through modern daily online adaptive radiotherapy (e.g., using MR-linac) (7, 11, 26). In addition, a significant lymphocyte-sparing effect of proton beam therapy, through decreasing the integral body dose, has been convincingly demonstrated in esophageal cancer and more recently also in lung cancer (7, 11, 12, 26–28). In the recent systematic review-based LymphoTEC initiative, dose constraints were described that can be used in clinical practice and future studies to limit the risk of RIL and possibly improve oncologic outcomes (29). Experimental attempts to attenuate lymphopenia included isolating lymphocytes before treatment with reinfusion upon treatment completion (which appeared feasible and safe, but not effective) (30), or administering interleukins (e.g., IL-2, IL-7, and IL-15) essential for lymphocyte proliferation and survival with promising results in pilot studies (31).

Besides inherent shortcomings resulting from the retrospective design of the current study, some other limitations require mention. First, no causal inferences can be made between predictors and the outcome of severe lymphopenia since this was no intervention study. The observational design allows for concluding strong associations only. Second, a larger sample size could have increased the precision of estimations and may have allowed for further model improvements. Third, in the analyses on the performance of the Christie model for predicting grade 4 lymphopenia and the MDACC for grade ≥3 lymphopenia, the studied outcome was (intentionally) defined differently from how it was defined in the original publications. Intercept corrections were applied to adjust for the large differences in *a priori* risks between grade ≥3 and grade 4 lymphopenia, but model coefficients were kept the same. This approach assumed that the relative contribution of predictors would be similar for grade ≥3 and grade 4 lymphopenia, but this assumption might not completely hold. However, this method was chosen because further model updates (e.g., adjusting model coefficients) would imply developing a new prediction model, which, in turn, would require another internal and external validation. Fourth, the survival impact of lymphopenia was not studied here as follow-up was too short for this recent cohort. This study is strengthened by the homogeneous study cohort and the frequent (i.e., twice-weekly) determination of ALC values with only very few missing values.

In conclusion, 78% and 17% of patients with stage III NSCLC who undergo concurrent CRT develop grade ≥3 and grade 4 lymphopenia, respectively. The simple PTV-based MDACC prediction model (15) for grade 4 lymphopenia developed in patients with esophageal cancer demonstrated good external performance in the setting of lung cancer, and outperformed the more refined dosimetry-based Christie prediction model (11). Good to excellent discriminative ability and agreement between predicted and observed risk were observed. Before treatment, the MDACC model can identify thoracic cancer patients at high risk of severe lymphopenia who might benefit most from lymphopenia-mitigating strategies, which may ultimately improve survival. To optimize radiotherapy planning with the purpose of reducing the risk of severe lymphopenia, further improvement and external validation of dosimetry-based models (such as the Christie model) is desired.

Data availability statement

The raw data supporting the conclusions of this article will be made available upon request, without undue reservation.

Ethics statement

The studies involving humans were approved by Netherlands Cancer Institute Institutional Review Board. The studies were conducted in accordance with the local legislation and institutional requirements. Retrospective data collection. Nothing was asked from the patients. Data was handled anonymously.

Author contributions

PR: Conceptualization, Data curation, Formal Analysis, Investigation, Methodology, Project administration, Validation, Visualization, Writing – original draft. CJ-C: Data curation, Investigation, Methodology, Writing – review & editing. BS: Data curation, Investigation, Methodology, Writing – review & editing. MR: Data curation, Investigation, Writing – review & editing. SL: Investigation, Methodology, Validation, Writing – review & editing. AA: Investigation, Methodology, Validation, Writing – review & editing. JB: Data curation, Formal Analysis, Investigation, Methodology, Supervision, Writing – review & editing. J-JS: Conceptualization, Formal Analysis, Investigation, Methodology, Supervision, Validation, Writing – review & editing.

Funding

The author(s) declare that no financial support was received for the research, authorship, and/or publication of this article.

Conflict of interest

The authors declare that the research was conducted in the absence of any commercial or financial relationships that could be construed as a potential conflict of interest.

The author(s) declared that they were an editorial board member of Frontiers, at the time of submission. This had no impact on the peer review process and the final decision.

Publisher's note

All claims expressed in this article are solely those of the authors and do not necessarily represent those of their affiliated organizations, or those of the publisher, the editors and the reviewers. Any product that may be evaluated in this article, or claim that may be made by its manufacturer, is not guaranteed or endorsed by the publisher.

Supplementary material

The Supplementary Material for this article can be found online at: https://www.frontiersin.org/articles/10.3389/fonc.2023.1278723/full#supplementary-material

SUPPLEMENTARY FIGURE 1
Calibration plots of the Christie model for predicting grade ≥3 lymphopenia before **(A)** and after **(B)** correcting the model intercept to match the a-priori risk of 78%. Calibration plots of the MDACC model for predicting grade 4 lymphopenia before **(C)** and after **(D)** correcting the model intercept to match the a-priori risk of 17%.

References

1. Jemal A, Bray F, Center MM, Ferlay J, Ward E, Forman D. Global cancer statistics. *CA Cancer J Clin* (2011) 61:69–90. doi: 10.3322/caac.20107

2. Evers J, de Jaeger K, Hendriks LEL, van der Sangen M, Terhaard C, Siesling S, et al. Trends and variations in treatment of stage I-III non-small cell lung cancer from 2008 to 2018: A nationwide population-based study from the Netherlands. *Lung Cancer* (2021) 155:103–13. doi: 10.1016/j.lungcan.2021.03.013

3. Dillman RO, Herndon J, Seagren SL, Eaton WL JR, Green MR. Improved survival in stage III non-small-cell lung cancer: seven-year follow-up of cancer and leukemia group B (CALGB) 8433 trial. *J Natl Cancer Inst* (1996) 88:1210–5. doi: 10.1093/jnci/88.17.1210

4. Hung M, Wu Y, Chen Y. Efficacy of chemoradiotherapy versus radiation alone in patients with inoperable locally advanced non-small-cell lung cancer: a meta-analysis and systematic review. *Med (Baltimore)* (2019) 98:e16167. doi: 10.1097/MD.0000000000016167

5. Antonia SJ, Villegas A, Daniel D, Vicente D, Murakami S, Hui R, et al. Durvalumab after chemoradiotherapy in stage III non-small-cell lung cancer. *N Engl J Med* (2017) 377:1919–29. doi: 10.1056/NEJMoa1709937

6. Faivre-Finn C, Vicente D, Kurata T, Planchard D, Paz-Ares L, Vansteenkiste JF, et al. Four-year survival with durvalumab after chemoradiotherapy in stage III NSCLC-an update from the PACIFIC trial. *J Thorac Oncol* (2021) 16:860–7. doi: 10.1016/j.jtho.2020.12.015

7. Venkatesulu BP, Mallick S, Lin SH, Krishnan S. A systematic review of the influence of radiation-induced lymphopenia on survival outcomes in solid tumors. *Crit Rev Oncol Hematol* (2018) 123:42–51. doi: 10.1016/j.critrevonc.2018.01.003

8. Damen PJJ, Kroese TE, van Hillegersberg R, Schuit E, Peters M, Verhoeff JJC, et al. The influence of severe radiation-induced lymphopenia on overall survival in solid tumors: a systematic review and meta-analysis. *Int J Radiat Oncol Biol Phys* (2021) 111:936–48. doi: 10.1016/j.ijrobp.2021.07.1695

9. Campian JL, Ye X, Brock M, Grossman SA. Treatment-related lymphopenia in patients with stage III non-small-cell lung cancer. *Cancer Invest* (2013) 31:183–8. doi: 10.3109/07357907.2013.767342

10. Zhao Q, Chen G, Ye L, Shi S, Du S, Zeng Z, et al. Treatment-duration is related to changes in peripheral lymphocyte counts during definitive radiotherapy for unresectable stage III NSCLC. *Radiat Oncol* (2019) 14:86. doi: 10.1186/s13014-019-1287-z

11. Abravan A, Faivre-Finn C, Kennedy J, McWilliam A, van Herk M. Radiotherapy-related lymphopenia affects overall survival in patients with lung cancer. *J Thorac Oncol* (2020) 15:1624–35. doi: 10.1016/j.jtho.2020.06.008

12. Kim N, Myoung Noh J, Lee W, Park B, Park H, Young Park J, et al. Proton beam therapy reduces the risk of severe radiation-induced lymphopenia during chemoradiotherapy for locally advanced non-small cell lung cancer: A comparative analysis of proton versus photon therapy. *Radiother Oncol* (2021) 156:166–73. doi: 10.1016/j.radonc.2020.12.019

13. Friedes C, Chakrabarti T, Olson S, Prichett L, Brahmer JR, Forde PM, et al. Association of severe lymphopenia and disease progression in unresectable locally advanced non-small cell lung cancer treated with definitive chemoradiation and immunotherapy. *Lung Cancer* (2021) 154:36–43. doi: 10.1016/j.lungcan.2021.01.022

14. Pike LRG, Bang A, Mahal BA, Taylor A, Krishnan M, Spektor A, et al. The impact of radiation therapy on lymphocyte count and survival in metastatic cancer patients receiving PD-1 immune checkpoint inhibitors. *Int J Radiat Oncol Biol Phys* (2019) 103:142–51. doi: 10.1016/j.ijrobp.2018.09.010

15. van Rossum PSN, Deng W, Routman DM, Liu AY, Xu C, Shiraishi Y, et al. Prediction of severe lymphopenia during chemoradiation therapy for esophageal cancer: development and validation of a pretreatment nomogram. *Pract Radiat Oncol* (2020) 10:e16-26. doi: 10.1016/j.prro.2019.07.010

16. Kroese TE, Jairam J, Ruurda JP, Lin SH, Mohan R, Mook S, et al. Severe lymphopenia acquired during chemoradiotherapy for esophageal cancer: Incidence and external validation of a prediction model. *Radiother Oncol* (2021) 163:192–8. doi: 10.1016/j.radonc.2021.08.009

17. Moons KG, Altman DG, Reitsma JB, Ioannidis JPA, Macaskill P, Steyerberg EW, et al. Transparent Reporting of a multivariable prediction model for Individual Prognosis Or Diagnosis (TRIPOD): explanation and elaboration. *Ann Intern Med* (2015) 162:1. doi: 10.7326/M14-0698

18. Belderbos J, Uitterhoeve L, van Zandwijk N, Belderbos H, Rodrigus P, van de Vaart P, et al. Randomised trial of sequential versus concurrent chemo-radiotherapy in patients with inoperable non-small cell lung cancer (EORTC 08972-22973). *Eur J Cancer* (2007) 43:114–21. doi: 10.1016/j.ejca.2006.09.005

19. van Diessen JNA, Kwint M, Sonke J-J, Walraven I, Stam B, de Langen AJ, et al. Safety and efficacy of reduced dose and margins to involved lymph node metastases in locally advanced NSCLC patients. *Radiother Oncol* (2020) 143:66–72. doi: 10.1016/j.radonc.2019.07.028

20. Steyerberg E. *Validation and updating of clinical prediction models: Why and how*? London: Springer Nature (2019).

21. Deng W, Xu C, Liu A, van Rossum PSN, Deng W, Liao Z, et al. The relationship of lymphocyte recovery and prognosis of esophageal cancer patients with severe radiation-induced lymphopenia after chemoradiation therapy. *Radiother Oncol* (2019) 133:9–15. doi: 10.1016/j.radonc.2018.12.002

22. Zhang E, Deng M, Egleston B, Wong JK, Su S, Denlinger C, et al. Dose to heart, spine, aorta, and body predict for severe lymphopenia and poor survival in patients undergoing chemoradiation for esophageal cancer. *Int J Radiat Oncol Biol Physics* (2019) 105:E206–7. doi: 10.1016/j.ijrobp.2019.06.2041

23. Xu H, Lin M, Hu Y, Zhang L, Li Q, Zhu J, et al. Lymphopenia during definitive chemoradiotherapy in esophageal squamous cell carcinoma: association with dosimetric parameters and patient outcomes. *Oncologist* (2021) 26:e425-34. doi: 10.1002/onco.13533

24. Tang C, Liao Z, Gomez D, Levy L, Zhuang Y, Gebremichael RA, et al. Lymphopenia association with gross tumor volume and lung V5 and its effects on non-small cell lung cancer patient outcomes. *Int J Radiat Oncol Biol Phys* (2014) 89:1084–91. doi: 10.1016/j.ijrobp.2014.04.025

25. Tang C, Lee MS, Gomez D, Levy LB, Zhuang Y, et al. Effects of chemotherapy regimen and radiation modality on hematologic toxicities in patients receiving definitive platinum-based doublet chemoradiation for non-small cell lung cancer. *Am J Clin Oncol* (2017) 40:625–30. doi: 10.1097/COC.0000000000000206

26. Bainbridge HE, Menten MJ, Fast MF, Nill S, Oelfke U, McDonald F, et al. Treating locally advanced lung cancer with a 1.5T MR-Linac - Effects of the magnetic field and irradiation geometry on conventionally fractionated and isotoxic dose-escalated radiotherapy. *Radiother Oncol* (2017) 125:280–5. doi: 10.1016/j.radonc.2017.09.009

27. Shiraishi Y, Fang P, Xu C, Song J, Krishnan S, Koay EJ, et al. Severe lymphopenia during neoadjuvant chemoradiation for esophageal cancer: A propensity matched analysis of the relative risk of proton versus photon-based radiation therapy. *Radiother Oncol* (2018) 128:154–60. doi: 10.1016/j.radonc.2017.11.028

28. Routman DM, Garant A, Lester SC, Day CN, Harmsen WS, Sanheuza CT, et al. A comparison of grade 4 lymphopenia with proton versus photon radiation therapy for esophageal cancer. *Adv Radiat Oncol* (2019) 4:63–9. doi: 10.1016/j.adro.2018.09.004

29. Venkatesulu B, Giridhar P, Pujari L, Chou B, Lee JH, Block AM, et al. Lymphocyte sparing normal tissue effects in the clinic (LymphoTEC): a systematic review of dose constraint considerations to mitigate radiation-related lymphopenia in the era of immunotherapy. *Radiother Oncol* (2022) 177:81–94. doi: 10.1016/j.radonc.2022.10.019

30. Campian JL, Ye X, Gladstone DE, Ambady P, Nirschl TR, Borrello I, et al. Pre-radiation lymphocyte harvesting and post-radiation reinfusion in patients with newly diagnosed high grade gliomas. *J Neurooncol* (2015) 124:307–16. doi: 10.1007/s11060-015-1841-y

31. Ménétrier-Caux C, Ray-Coquard I, Blay J, Caux C. Lymphopenia in Cancer Patients and its Effects on Response to Immunotherapy: an opportunity for combination with Cytokines? *J Immunother Cancer* (2019) 7:85. doi: 10.1186/s40425-019-0549-5

frontiers | Frontiers in Oncology

TYPE Systematic Review
PUBLISHED 01 December 2023
DOI 10.3389/fonc.2023.1287555

OPEN ACCESS

EDITED BY
Peter Sylvain Nicolas van Rossum,
Amsterdam University Medical Center,
Netherlands

REVIEWED BY
Pim Damen,
Erasmus Medical Center, Netherlands
Bhanu Prasad Venkatesulu,
Loyola University Chicago, United States

*CORRESPONDENCE
Shanqing Li
shanqingli_pumc@21cn.com

RECEIVED 01 September 2023
ACCEPTED 07 November 2023
PUBLISHED 01 December 2023

CITATION
Zhang Y, Huang C and Li S (2023) Influence of treatment-related lymphopenia on the efficacy of immune checkpoint inhibitors in lung cancer: a meta-analysis. *Front. Oncol.* 13:1287555. doi: 10.3389/fonc.2023.1287555

Influence of treatment-related lymphopenia on the efficacy of immune checkpoint inhibitors in lung cancer: a meta-analysis

Ye Zhang, Cheng Huang and Shanqing Li*

Department of Thoracic Surgery, Peking Union Medical College Hospital, Peking Union Medical College and Chinese Academy of Medical Sciences, Beijing, China

Background: Treatment-related lymphopenia (TRL) is common in patients with lung cancer, particularly in those with radiotherapy. However, the influence of TRL on the efficacy of immune checkpoint inhibitors (ICIs) for patients with lung cancer remains poorly understood. We performed a systematic review and meta-analysis to investigate the influence of TRL on survival of lung cancer patients on ICIs.

Methods: In order to accomplish the aim of the meta-analysis, a comprehensive search was conducted on databases including PubMed, Embase, Cochrane Library, and the Web of Science to identify observational studies with longitudinal follow-up. The Cochrane Q test was employed to evaluate heterogeneity among the included studies, while the I^2 statistic was estimated. Random-effects models were utilized to merge the results, considering the potential impact of heterogeneity.

Results: Ten cohort studies with 1130 lung cancer patients who were treated with ICIs were included. Among them, 427 (37.8%) had TRL. Pooled results showed that compared to patients without TRL, patients with TRL were associated with poor progression-free survival (hazard ratio [HR]: 2.05, 95% confidence interval [CI]: 1.62 to 2.60, $p < 0.001$; $I^2 = 22\%$) and overall survival (HR: 2.69, 95% CI: 2.10 to 3.43, $p < 0.001$; $I^2 = 0\%$). Sensitivity analysis limited to patients with non-small cell lung cancer showed similar results (HR: 2.66 and 2.62, both $p < 0.05$). Moreover, subgroup analyses according to the diagnostic criteria of TRL, regression analysis model (univariate or multivariate), and indications of ICIs (for locally advanced or advanced lung cancer) showed consistent results (p for subgroup difference all > 0.05).

Conclusion: TRL was associated with poor survival of lung cancer patients who were treated with ICIs.

KEYWORDS

lung cancer, lymphopenia, immunotherapy, survival, meta-analysis

Introduction

Lung cancer is a prevalent malignancy affecting the global population (1). According to the global cancer statistics in 2020, lung cancer constituted 11.4% of all cancer cases and accounted for 18.0% of cancer-related fatalities worldwide (2). Histologically, lung cancer can be categorized as non-small cell lung cancer (NSCLC) and small cell lung cancer (SCLC), with therapeutic interventions primarily encompassing surgery, radiation therapy, chemotherapy, and targeted drug therapy (3, 4). A growing body of research underscores the significance of the immune system in cancer surveillance and anti-tumor activity (5, 6). Recent evidence has emphasized the significant role of immune checkpoint inhibitors (ICIs) as efficacious anticancer agents through the inhibition of programmed death-ligand 1 (PD-L1), programmed death 1 (PD-1), or cytotoxic t-lymphocyte-associated protein 4 (CTLA-4) receptors, thereby augmenting the cytotoxicity of T lymphocytes towards tumor cells (7). The overall effectiveness and safety of immunotherapy utilizing ICIs have been generally demonstrated in patients afflicted with metastatic and locally advanced non-small cell lung cancer (NSCLC) (8), as well as small cell lung cancer (SCLC) (9). However, subsequent observations suggest that the therapeutic response to ICIs may vary in individual patients with lung cancer (10). Accordingly, uncovering of the clinical factors that are related to the efficacy of ICIs in patients with lung cancer is of great clinical significance.

Lymphopenia is a prevalent occurrence in cancer patients, primarily attributed to the administration of anticancer treatments such as radiotherapy and chemotherapy, referred to as treatment-related lymphopenia (TRL) (11, 12). A recent meta-analysis encompassing 14 studies revealed that the average occurrence of severe lymphopenia (defined as an absolute lymphocyte count [ALC] < 500/ul) in lung cancer patients undergoing radiotherapy was 64.2% (13). Although sever TRL has been related to poor prognosis in patients with various solid tumors including lung cancer in early studies, patients with concurrent ICIs were rarely included in these studies (14). The potential impact of TRL on the effectiveness of ICIs, specifically by reducing the active T lymphocytes, has been postulated (15). However, the precise effect of TRL on the efficacy of ICIs in individuals with lung cancer has yet to be fully elucidated. Consequently, we conducted a comprehensive review and meta-analysis to examine the influence of TRL on the survival outcomes of lung cancer patients undergoing ICIs treatment.

Materials and methods

The study adhered to the Preferred Reporting Items for Systematic Reviews and Meta-Analyses statement (16, 17) and the Cochrane Handbook (18) throughout the stages of planning, conducting, and reporting.

Inclusion and exclusion criteria of studies

The development of inclusion criteria adhered to the PICOS recommendations and aligned with the objective of the meta-analysis.

P (patients): Patients with pathologically confirmed diagnosis of lung cancer who were treated with ICIs.

I (exposure): Patients with TRL at the initiation or during ICIs treatment. Diagnostic criteria and cutoffs for defining TRL were consistent with those of the original studies. We included studies of patients with lymphopenia related to any anticancer treatment, not limited to those of patients received radiation only.

C (control): Patients without TRL.

O (outcomes): The study compared the progression-free survival (PFS) and/or overall survival (OS) outcomes between individuals with and without TRL. In essence, PFS denotes the time from the initiation of treatment to the occurrence of disease recurrence or progression, while OS represents the time from the initiation of treatment to the patient's eventual demise.

S (study design): This study incorporated longitudinal follow-up studies, such as cohort and nested case-control studies, along with *post-hoc* analyses of clinical trials. Excluded from the meta-analysis were reviews, editorials, meta-analyses, preclinical studies, and studies that did not involve patients with lung cancer or with ICIs, failed to evaluate TRL, or did not report the survival outcomes of interest during follow-up. In cases where there was an overlap in patient populations, the study with the largest sample size was included in the meta-analysis.

Search of databases

A comprehensive search was conducted in electronic databases, namely PubMed, Embase, Cochrane Library, and Web of Science, encompassing the period from inception to July 10, 2023. The search strategy employed relevant terms pertaining to the subject matter of our investigation, aiming to identify studies published within this timeframe, which included: (1) "lymphopenia" OR "lymphocytopenia"; (2) "lung cancer"; and (3) "immunotherapy" OR "immune checkpoint inhibitor" OR "PD-1" OR "PD-L1" OR "CTLA-4" OR "programmed death 1" OR "programmed death ligand 1" OR "pembrolizumab" OR "atezolizumab" OR "nivolumab" OR "ipilimumab" OR "durvalumab" OR "tremelimumab" OR "camrelizumab" OR "tislelizumab" OR "sintilimab" OR "cemiplimab" OR "toripalimab" OR "lambrolizumab" OR "pidilizumab" OR "avelumab". Only studies that met the criteria of being published as full-length articles in English and appearing in peer-reviewed journals were included in our analysis. Additionally, during our manual screening process, we thoroughly examined the references cited in relevant original and review articles to identify any potentially relevant studies.

Data extraction and quality evaluation

Two authors independently performed literature searches, data collection, and assessments of study quality. In cases where discrepancies emerged, a third author was consulted for deliberation, leading to a consensus. The analysis of studies encompassed the gathering of data related to study information, design characteristics, patient diagnosis, demographic factors, medications for immunotherapy, definition of TRL, number of patients with TRL, median follow-up durations, outcomes reported, and variables adjusted for the evaluation of the association between TRL and survival of lung cancer patients on ICIs. The quality of the study was assessed using the Newcastle-Ottawa Scale (NOS) (19), which evaluates participant selection, group comparability, and outcome validity. The scale consisted of nine stars, with a greater number of stars indicating a study of higher quality.

Statistics

Hazard ratios (HRs) and their corresponding 95% confidence intervals (CIs) were utilized as the variables to assess the relationship between TRL and the survival of lung cancer patients receiving immune ICIs. To stabilize and normalize the variance, a logarithmical transformation was applied to the HR and its corresponding standard error in each study (20). The Cochrane Q test and the I^2 statistic (21) were employed to estimate between-study heterogeneity. A value of I^2 greater than 50% indicates the presence of significant heterogeneity among the studies. The random-effects model was utilized to combine the findings, as it has been recognized to account for potential heterogeneity (18). Sensitivity analysis limited to patients with NSCLC was performed. Additionally, subgroup analysis was conducted to explore the influence of cutoffs for TRL, different regression analysis model (univariate or multivariate), and indications of ICIs (for locally advanced or advanced lung cancer) on the outcomes. The cutoffs for defining overall TRL (<1000 lymphocytes/ul) and severe TRL (<500 lymphocytes/ul) were in accordance with the Common Terminology Criteria for Adverse Events (CTCAE) criteria (22). Publication bias was estimated using a funnel plot, which involved visual assessments of symmetry, as well as Egger's regression asymmetry test (23). The statistical analyses were conducted using RevMan (Version 5.1; Cochrane Collaboration, Oxford, UK) and Stata software (version 12.0; Stata Corporation, College Station, TX).

Results

Database search and study retrieval

Figure 1 illustrates the procedure employed for conducting the literature search and study retrieval. Initially, a total of 781 records were acquired from the designated database, and subsequently, 172 duplicate entries were eliminated. Upon scrutinizing the titles and abstracts, an additional 583 studies were excluded due to their incompatibility with the objectives of the meta-analysis. Following comprehensive evaluations of the full texts of 26 studies, 16 were excluded based on the rationales outlined in Figure 1. Consequently, ten studies were deemed suitable for the subsequent meta-analysis (24–33).

Study characteristics

Overall, one prospective (27) and nine retrospective cohort studies (24–26, 28–33) were included in the meta-analysis. The characteristics of the studies incorporated in this analysis are concisely outlined in Table 1. These studies were conducted in the United States, Korea, and France, and were published within the timeframe of 2019 to 2023. All of the studies encompassed patients diagnosed with lung cancer who underwent treatment with ICIs. Among these studies, eight exclusively focused on patients with NSCLC (24, 25, 28–33), whereas the remaining two also encompassed patients with SCLC (26, 27). The drugs for ICIs varied among the included studies, which involved nivolumab, pembrolizumab, durvalumab, atezolizumab, ipilimumab, or a combination of nivolumab and ipilimumab. The cutoffs for the diagnosis of TRL also varied among the included studies, and accordingly, 427 patients (37.8%) were diagnosed as TRL. The follow-up durations varied from 4.7 months to 24.0 months, with the median follow-up duration of 13.0 months. Outcome of PFS was reported in nine studies (24, 26–33), while the outcome of OS was reported in eight studies (24–27, 29–31, 33). Univariate regression analysis was used in three studies when the association between TRL and survival of lung cancer patients on ICIs was reported (25, 26, 30), while in the other seven studies (24, 27–29, 31–33), multivariate regression analysis was used with the adjustment of confounding factors such as age, sex, performance status, histological type of cancer, and other concurrent anticancer treatments etc. The NOS of the included studies were six to nine, indicating that they were of moderate to good quality (Table 2).

Influence of TRL on PFS in lung cancer patients treated with ICIs

Nine studies (24, 26–33) evaluated the association between TRL and PFS in lung cancer patients treated with ICIs. Since one study reported the outcome in two cohorts of patients with different concurrent radiotherapy strategies (27), these two datasets were included independently into the meta-analysis. Pooled results showed that compared to those without TRL, lung cancer patients with TRL was associated with poor PFS (HR: 2.05, 95% CI: 1.62 to 2.60, $p < 0.001$; Figure 2A) with mild heterogeneity ($I^2 = 22\%$). Sensitivity analysis limited to patients with NSCLC showed similar results (HR: 2.26, 95% CI: 1.76 to 2.91, $p < 0.001$; $I^2 = 0\%$). Further subgroup analysis showed consistent association between TRL and poor PFS in studies with TRL diagnosed as ALC < 1000 and < 500/ul (p for subgroup difference = 0.64; Figure 2B), in studies with univariate and multivariate analysis (p for subgroup difference =

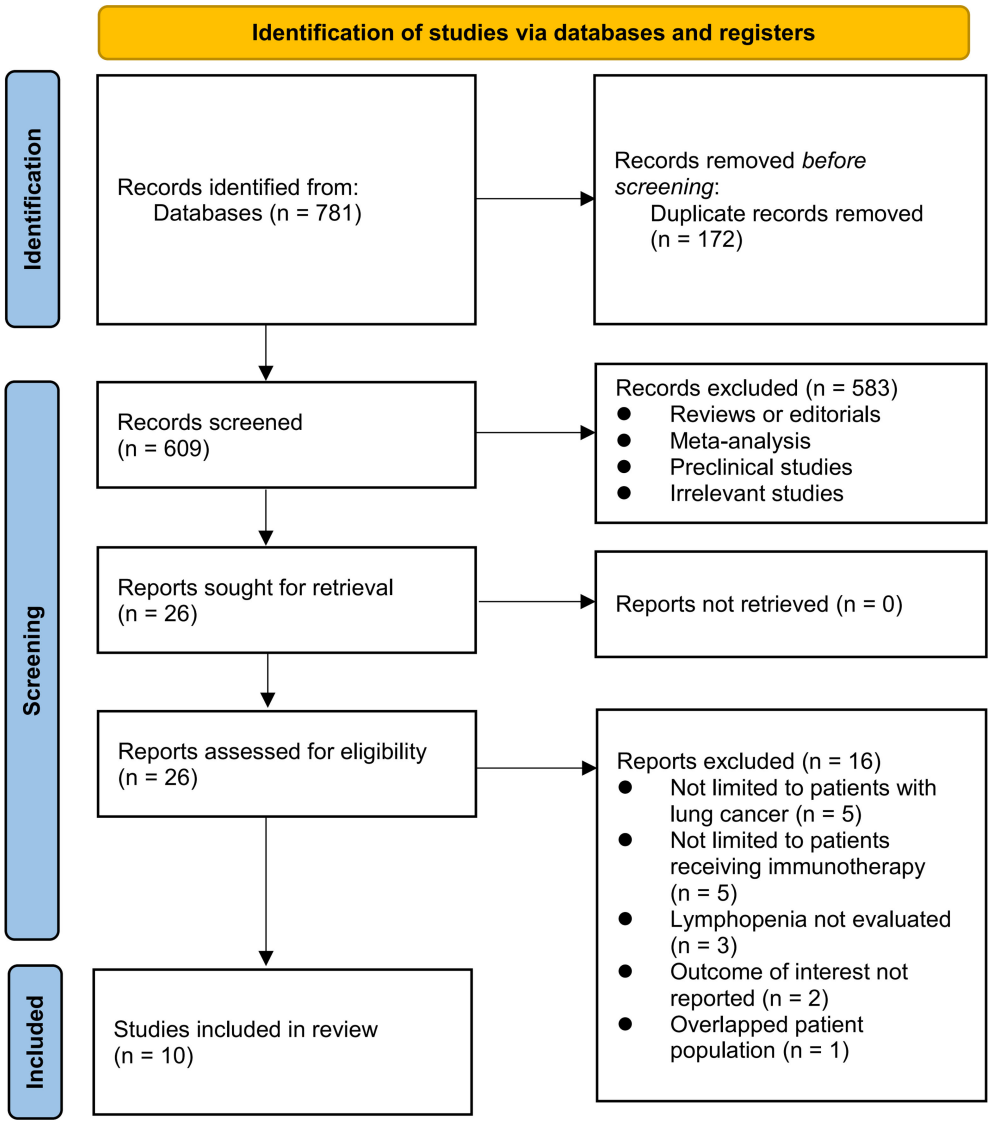

FIGURE 1
Flowchart of database search and study inclusion.

0.69; Figure 2C), and in studies with ICIs for locally advanced or advanced lung cancer (p for subgroup difference = 0.73; Figure 2D).

Influence of TRL on OS in lung cancer patients treated with ICIs

Eight studies (24–27, 29–31, 33) with nine datasets were included for the meta-analysis of the association between TRL and OS in lung cancer patients on ICIs. Results of the meta-analysis showed that TRL was associated with poor OS (HR: 2.69, 95% CI: 2.10 to 3.43, $p < 0.001$; Figure 3A) with no significant heterogeneity ($I^2 = 0\%$). Consistent results were observed in sensitivity analysis limited to NSCLC only (HR: 2.62, 95% CI: 1.99 to 3.44, $p < 0.001$; $I^2 = 0\%$). Moreover, subgroup analyses according to the diagnostic criteria of TRL (p for subgroup difference = 0.80, Figure 3B), the analytic models (p for subgroup difference = 0.26, Figure 3C), and indications of ICIs (p for subgroup difference = 0.63, Figure 3D) also showed similar results.

Publication bias

The funnel plots depicting the meta-analyses of the correlation between TRL and survival outcomes among lung cancer patients receiving ICIs are presented in Figure 4. Upon visual inspection, the plots exhibit symmetrical patterns, indicating a minimal presence of publication bias. Furthermore, the application of Egger's regression tests yielded p-values of 0.37 and 0.49, further supporting the notion of a low probability of publication bias.

TABLE 1 Characteristics of the included studies.

Study	Country	Design	Diagnosis	Number of patients	Mean age (years)	Male (%)	ICIs used	Definition of lymphopenia	Number of patients with lymphopenia	Median follow-up duration (months)	Outcomes reported	Variables adjusted
Karantanos 2019 (25)	USA	RC	Advanced NSCLC	22	62	54.5	Nivolumab	ALC < 900/ul at baseline or 6 months after the initiation of ICIs	6	10	OS	None
Cho 2019 (24)	Korea	RC	Advanced NSCLC	268	64	67.9	Nivolumab, pembrolizumab, or a combination of nivolumab and ipilimumab	ALC < 1000/ul at baseline or during ICIs	146	6.4	PFS and OS	Age, sex, ECOG PS, histological type, PD-L1 expression, EGFR mutation, disease extent, previous treatment, use or RT, and medications of ICIs
Li 2019 (26)	USA	RC	Lung cancer patients with brain metastases (NSCLC 93.6%)	20	65	46	Any ICIs	ALC < 1000/ul at baseline or during ICIs	15	13.2	PFS and OS	None
Chen 2020 (27)	USA	PC	Lung cancer patients receiving combined immunotherapy and radiotherapy (NSCLC 36.4%)	165	65	56.4	Ipilimumab or pembrolizumab	ALC < 1300/ul at baseline or during ICIs	69	21	PFS and OS	Age, sex, race, ECOG PS, histological type, smoking, prior treatment, and medications of ICIs
Friedes 2021 (28)	USA	RC	Unresectable locally advanced NSCLC	78	66	55	Durvalumab or Ipilimumab + nivolumab	ALC < 500/ul at the initiation of ICIs	18	10.6	PFS	Age, sex, race, KPS, tumor size, previous treatment, and medications of ICIs
Jing 2022 (30)	USA	RC	Locally advanced NSCLC	117	NR	59	Durvalumab	ALC < 230/ul at baseline or during ICIs	28	24	PFS and OS	None
Cho 2022 (29)	Korea	RC	Stage III NSCLC	66	65	82	Durvalumab or pembrolizumab	ALC < 500/ul at the initiation and during ICIs	7	18	PFS and OS	Age, sex, histological type, PD-L1 expression, and medications of ICIs
Thor 2022 (32)	USA	RC	Stage III NSCLC	113	67	59	Durvalumab	ALC < 700/ul at the initiation of ICIs	56	17.5	PFS	Age, ECOG PS, and PD-L1 expression
Lee 2022 (31)	Korea	RC	Advanced NSCLC	231	66	78.5	Durvalumab, pembrolizumab, or atezolizumab	ALC < 1000/ul at baseline or during ICIs	57	4.7	PFS and OS	Age, sex, ECOG PS, histological type, and smoking

(Continued)

10.3389/fonc.2023.1287555

TABLE 1 Continued

Study	Country	Design	Diagnosis	Number of patients	Mean age (years)	Male (%)	ICIs used	Definition of lymphopenia	Number of patients with lymphopenia	Median follow-up duration (months)	Outcomes reported	Variables adjusted
Pasquier 2023 (33)	France	RC	Unresectable locally advanced NSCLC	50	61.5	76	Durvalumab	ALC < 500/ul at the initiation of ICIs	25	23.2	PFS and OS	Age, sex, ECOG PS, histological type, and smoking

RC, retrospective cohort; PC, prospective cohort; NSCLC, non-small cell lung cancer; ICIs, immune checkpoint inhibitors; ALC, absolute lymphocyte count; PFS, progression-free survival; OS, overall survival; ECOG PS, the Eastern Cooperative Oncology Group Performance Status; PD-L, programmed death ligand 1; EGFR, epidermal growth factor receptor; RT, radiotherapy; KPS, Karnofsky performance status.

Discussion

This study conducted a systematic review and meta-analysis, incorporating data from ten cohort studies, to examine the correlation between TRL and survival outcomes in lung cancer patients undergoing ICIs treatment. The results of our analysis suggest that the presence of TRL at the start or during ICIs treatment is linked to unfavorable PFS and OS in lung cancer patients. Additionally, when focusing solely on studies involving patients with NSCLC, the findings remained consistent. Furthermore, subgroup analyses based on the cutoff value for diagnosing TRL, the chosen analytical model, and indications of ICIs also yielded consistent results. Taken together, these results suggest that TRL may be a risk factor of poor survival of lung cancer patients on the treatment of ICIs.

To the best of our knowledge, this study represents a potentially pioneering meta-analysis that examines the impact of TRL on the effectiveness of ICIs in individuals diagnosed with lung cancer. It is worth highlighting several notable advantages inherent in the employed meta-analysis methodologies. For instance, an extensive search of four widely utilized databases was conducted, thereby yielding up-to-date evidence pertaining to the association between TRL and the survival outcomes of lung cancer patients undergoing ICIs treatment. Moreover, it is worth mentioning that all the studies included in this analysis were cohort studies, indicating a possible longitudinal association between TRL and heightened risk of disease progression and mortality in these individuals. Furthermore, subgroup analysis based on the threshold values of ALC for diagnosing TRL yielded consistent findings, implying that even a mild TRL of ALC < 1000/ul may have a detrimental impact on the prognosis of lung cancer patients receiving ICIs. Finally, consistent results were obtained for subgroups of univariate and multivariate regression analyses, which suggested that the association between TRL and poor survival of lung cancer patients on ICIs may be independent of variables such as age, sex, functional status, and previous anticancer treatments. Collectively, these findings highly suggest the importance of monitoring lymphocyte count in peripheral circulating during the treatment with ICIs for patients with lung cancer.

The negative consequences observed in patients experiencing lymphopenia may be ascribed to modifications in the tumor microenvironment. These alterations can be linked to the accumulation of myeloid-derived suppressor cells, type-2 macrophages, or regulatory T cells, along with the generation of suppressive cytokines and metabolites, which can foster tumor advancement (15). Additionally, it has been postulated that neoantigen-specific T cells can be detected in the peripheral blood of patients with NSCLC undergoing anti-PD-L1 therapy. Notably, patients who exhibited an objective response demonstrated an increased presence of neoantigen-reactive T cells, which exhibited distinct phenotypic characteristics compared to non-responsive patients (34). The migration of these T cells to metastatic sites following immune checkpoint blockade stimulation is believed to play a crucial role in eliciting an effective antitumor response. However, the inhibition of T-cell function and subsequent lymphopenia in the peripheral blood may impede the transfer of

TABLE 2 Study quality assessment via the Newcastle-Ottawa Scale.

Study	Representativeness of the exposed cohort	Selection of the non-exposed cohort	Ascertainment of exposure	Outcome not present at baseline	Control for age	Control for other confounding factors	Assessment of outcome	Enough long follow-up duration	Adequacy of follow-up of cohorts	Total
Karantanos 2019 (25)	0	1	1	1	0	0	1	1	1	6
Cho 2019 (24)	0	1	1	1	1	1	1	1	1	8
Li 2019 (26)	0	1	1	1	0	0	1	1	1	6
Chen 2020 (27)	1	1	1	1	1	1	1	1	1	9
Friedes 2021 (28)	0	1	1	1	1	1	1	1	1	8
Jing 2022 (30)	0	1	1	1	0	0	1	1	1	6
Cho 2022 (29)	0	1	1	1	1	1	1	1	1	8
Thor 2022 (32)	0	1	1	1	1	1	1	1	1	8
Lee 2022 (31)	0	1	1	1	1	1	1	0	1	7
Pasquier 2023 (33)	0	1	1	1	1	1	1	1	1	8

T cells to the tumor site. In this particular scenario, lymphopenia serves as a surrogate marker indicating resistance to ICIs, necessitating the need for treatment modifications to overcome this resistance (35, 36). Notably, a recent investigation involving lung cancer patients with TRL who received ICIs revealed that inadequate lymphocyte recovery correlated with a shorter PFS, an increase in regulatory T cells, and a depletion of CD8+ T cells in the peripheral blood. These findings suggest that prompt recovery from TRL may hold significance in enhancing the prognosis of these patients (37).

For patients with cancer, radiation is a common cause of TRL, which is called radiation-induced lymphopenia (RIL). In lung cancer patients, the risk factors of RIL include advanced age, ALC before treatment, higher mean lung dose, larger volume of lung and heart receiving low dose (V5), longer treatment duration, and longer total beam-on time etc. (38–40). Among the studies included in the current meta-analysis, TRL caused by radiation therapy most frequently occurred at or within the six months after the initiation of the ICIs therapy. Results of the meta-analysis suggested that TRL may be associated with poor survival of lung cancer patients receiving ICIs, which is consistent with the results of studies in other types of tumors. A previous study of 105 patients with recurrent metastatic esophageal cancer receiving immunotherapy showed that lymphopenia is associated with a poorer immunotherapy prognosis in these patients (41). In another study of patients treated with nivolumab for recurrent/metastatic head and neck cancer, head and neck cancer, persistence of lymphopenia during immunotherapy was shown to be a predictor of worse OS (42). One attractive question at current stage is whether a prompt recovery from TRL may hold significance in enhancing the prognosis of patients with lung cancer on ICIs. A recently published pilot observational study in stage III NSCLC patients undergoing durvalumab consolidation therapy have suggested that recovery from TRL at the initiation of ICIs were associated with improved PFS and OS as compared to those without lymphocyte recovery (43). From a clinical standpoint, the restriction of radiotherapy dosage to the lungs, heart, and vertebrae presents modifiable risk factors that could potentially decrease the occurrence of RIL and PFS and OS, particularly in patients with non-modifiable risk factors such as advanced age, lower pre-radiotherapy ALC, and larger tumor size. However, modifying Lung V5 may pose technical challenges as it could lead to an increase in V20, thereby exacerbating fibrosis. Alternatively, shorter treatment duration may prove to be a more effective strategy when combined with immunotherapy to mitigate lymphopenia (44). Moreover, in the case of metastatic lung cancers, the utilization of stereotactic body radiotherapy to irradiate a specific portion of the tumor, as opposed to conventional radiotherapy targeting the entire tumor, has the potential to reduce RIL, while simultaneously preserving lung function and promoting antigen release. This, in turn, can contribute to the abscopal response (45). To comprehensively comprehend the relationship between TRL and unfavorable survival, as well as to devise efficacious approaches for improving the prognosis of patients experiencing lymphopenia during ICIs therapy, further translational investigations and clinical trials are imperative.

This study has several limitations that should be acknowledged. Firstly, the protocol of the meta-analysis was not prospectively

10.3389/fonc.2023.1287555

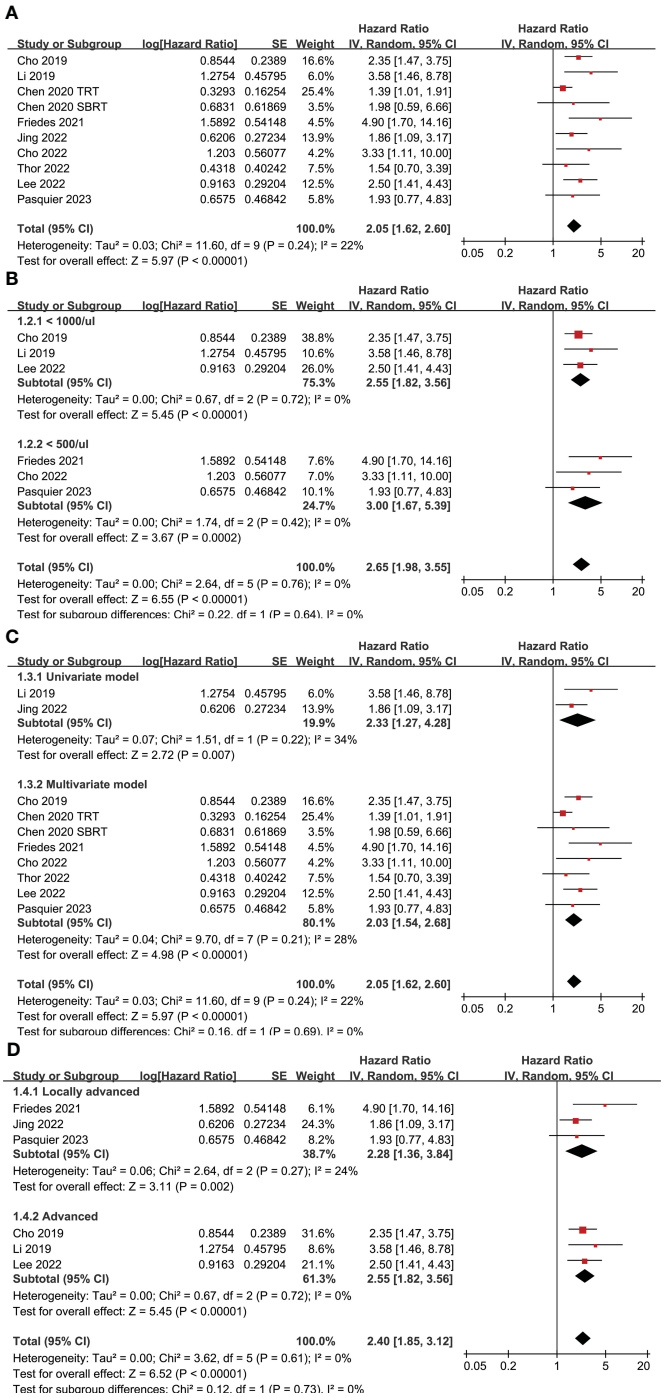

FIGURE 2
Forest plots for the meta-analyses regarding the association between TRL and PFS of lung cancer patients on ICIs; **(A)** overall meta-analysis; **(B)** subgroup analysis according to the cutoff for the diagnosis of TRL; **(C)** subgroup analysis according to the different analytic models used in the original studies; and **(D)** subgroup analysis according to the indications of ICIs.

registered, which is acknowledged as a limitation. Secondly, majority of the studies included in this analysis were retrospective, which introduces the possibility of selection and recall biases. To validate the findings, it is necessary to conduct large-scale prospective studies. Thirdly, among eight of the ten included studies, patients with NSCLC were included, while the other two studies included patients with NSCLC and SCLC. Accordingly, we could only observe the association between TRL and survival in NSCLC patients with ICIs via a sensitivity analysis limited to studies of patients with NSCLC only, instead of a subgroup analysis of NSCLC versus SCLC. It is important to considering subgroup analysis in NSCLC versus SCLC, because

10.3389/fonc.2023.1287555

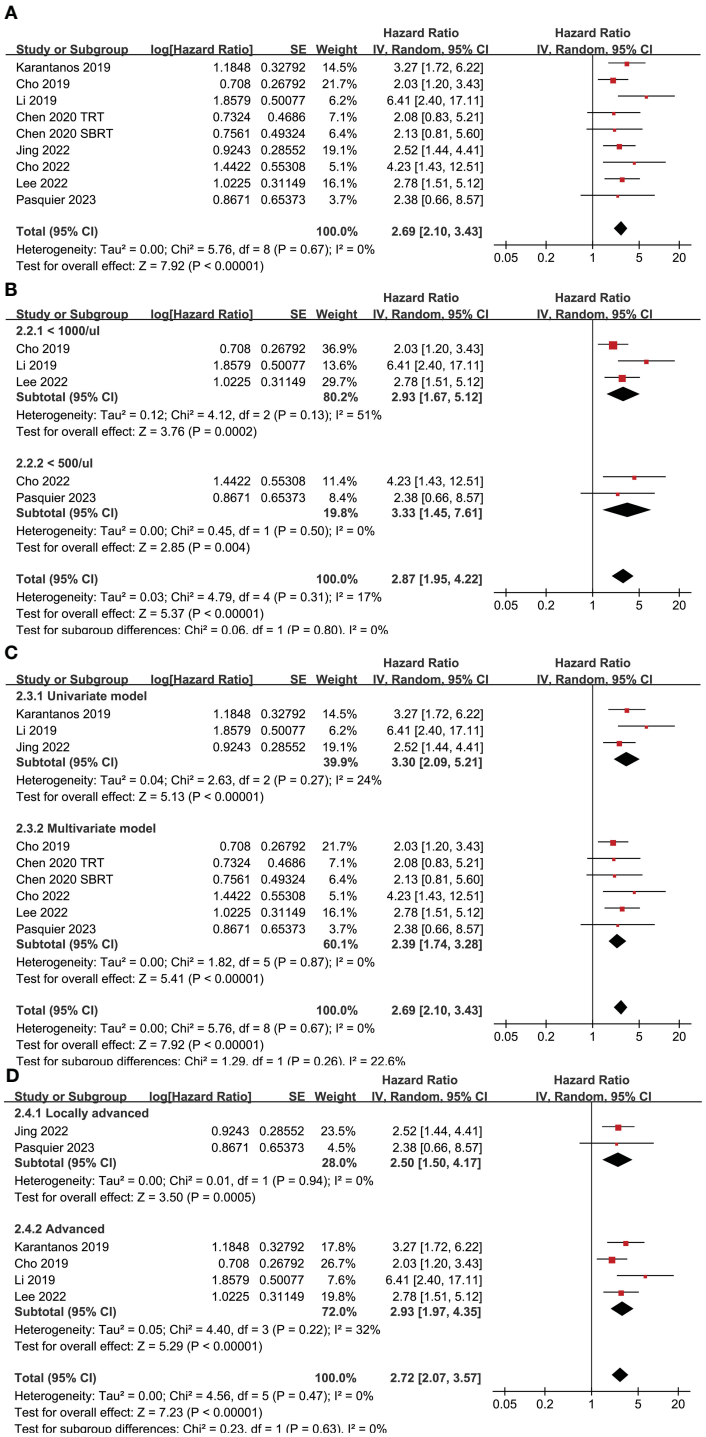

FIGURE 3
Forest plots for the meta-analyses regarding the association between TRL and OS of lung cancer patients on ICIs; **(A)** overall meta-analysis; **(B)** subgroup analysis according to the cutoff for the diagnosis of TRL; **(C)** subgroup analysis according to the different analytic models used in the original studies; and **(D)** subgroup analysis according to the indications of ICIs.

compared to NSCLC, SCLC is characterized by an exceptionally high proliferative rate, strong tendency for early widespread metastasis, and acquired chemoresistance (46). Currently, we could not determine if the association between TRL and survival of patients with SCLC on ICIS could be different from those of NSCLC, and studies are needed to address this association in patients with SCLC in the future. Furthermore, although the subset of studies employing multivariate regression analyses yielded comparable findings, it is important to acknowledge that the influence of residual factors on the correlation between TRL and

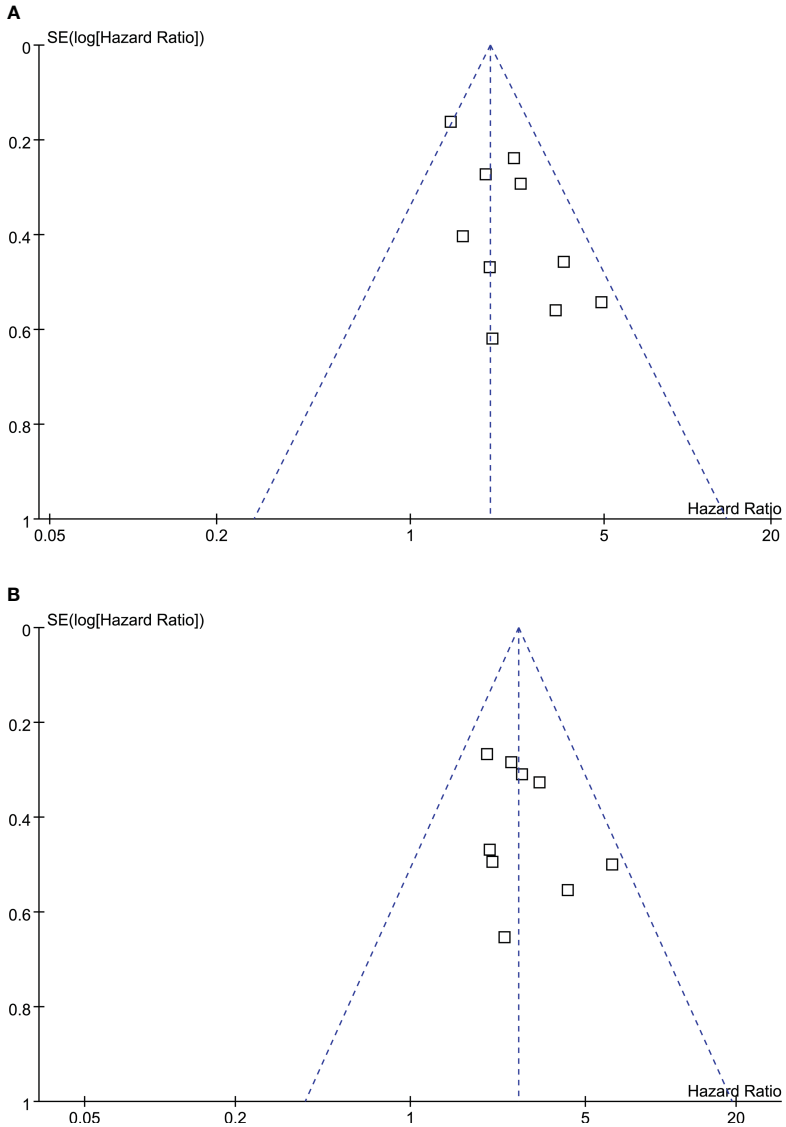

FIGURE 4
Funnel plots for the publication bias underlying the meta-analyses of the association between TRL and survival outcomes of lung cancer patients on ICIs; **(A)** funnel plots for the meta-analysis of the association between TRL and PFS; and **(B)** funnel plots for the meta-analysis of the association between TRL and OS.

unfavorable survival outcomes in these patients cannot be definitively dismissed. Ultimately, due to the nature of this meta-analysis being based on observational studies, it is not possible to establish a causal relationship between TRL and the heightened risk of cancer progression and mortality in lung cancer patients undergoing ICIs. Therefore, it is imperative to conduct clinical studies to ascertain if effective prevention or recovery of TRL could favorably influence the survival of lung cancer patients with ICIs treatment.

Conclusions

The results of the meta-analysis suggest a correlation between TRL and decreased survival rates among lung cancer patients receiving ICIs, particularly in those with NSCLC. However, further prospective studies are necessary to confirm these findings. On the other hand, the meta-analysis underscores the significance of monitoring peripheral lymphocyte counts in lung cancer patients undergoing ICI treatment. Additionally, it is crucial to investigate whether interventions aimed at preventing or expediting the recovery of TRL are linked to improved survival outcomes for lung cancer patients undergoing ICIs treatment.

Data availability statement

The original contributions presented in the study are included in the article/supplementary material. Further inquiries can be directed to the corresponding author.

Author contributions

YZ: Conceptualization, Data curation, Formal Analysis, Investigation, Methodology, Writing – original draft. CH: Data curation, Formal Analysis, Investigation, Validation, Writing – review & editing. SL: Conceptualization, Data curation, Formal Analysis, Investigation, Methodology, Supervision, Validation, Writing – review & editing.

Funding

The author(s) declare that no financial support was received for the research, authorship, and/or publication of this article.

Conflict of interest

The authors declare that the research was conducted in the absence of any commercial or financial relationships that could be construed as a potential conflict of interest.

Publisher's note

References

1. Siegel RL, Miller KD, Wagle NS, Jemal A. Cancer statistics, 2023. *CA Cancer J Clin* (2023) 73(1):17–48. doi: 10.3322/caac.21763

2. Sung H, Ferlay J, Siegel RL, Laversanne M, Soerjomataram I, Jemal A, et al. Global cancer statistics 2020: GLOBOCAN estimates of incidence and mortality worldwide for 36 cancers in 185 countries. *CA Cancer J Clin* (2021) 71(3):209–49. doi: 10.3322/caac.21660

3. Alduais Y, Zhang H, Fan F, Chen J, Chen B. Non-small cell lung cancer (NSCLC): A review of risk factors, diagnosis, and treatment. *Med (Baltimore)* (2023) 102(8): e32899. doi: 10.1097/MD.0000000000032899

4. Megyesfalvi Z, Gay CM, Popper H, Pirker R, Ostoros G, Heeke S, et al. Clinical insights into small cell lung cancer: Tumor heterogeneity, diagnosis, therapy, and future directions. *CA Cancer J Clin* (2023) 73(6):620–52. doi: 10.3322/caac.21785

5. Muenst S, Laubli H, Soysal SD, Zippelius A, Tzankov A, Hoeller S. The immune system and cancer evasion strategies: therapeutic concepts. *J Intern Med* (2016) 279 (6):541–62. doi: 10.1111/joim.12470

6. Abbott M, Ustoyev Y. Cancer and the immune system: the history and background of immunotherapy. *Semin Oncol Nurs* (2019) 35(5):150923. doi: 10.1016/j.soncn.2019.08.002

7. Lee J, Kim EH. Mechanisms underlying response and resistance to immune checkpoint blockade in cancer immunotherapy. *Front Oncol* (2023) 13:1233376. doi: 10.3389/fonc.2023.1233376

8. Reck M, Remon J, Hellmann MD. First-line immunotherapy for non-small-cell lung cancer. *J Clin Oncol* (2022) 40(6):586–97. doi: 10.1200/JCO.21.01497

9. Carlisle JW, Leal T. Advancing immunotherapy in small cell lung cancer. *Cancer* (2023) 129(22):3525–34. doi: 10.1002/cncr.34977

10. Xiao Q, Yu X, Shuai Z, Yao T, Yang X, Zhang Y. The influence of baseline characteristics on the efficacy of immune checkpoint inhibitors for advanced lung cancer: A systematic review and meta-analysis. *Front Pharmacol* (2022) 13:956788. doi: 10.3389/fphar.2022.956788

11. Koukourakis MI, Giatromanolaki A. Lymphopenia and intratumoral lymphocytic balance in the era of cancer immuno-radiotherapy. *Crit Rev Oncol Hematol* (2021) 159:103226. doi: 10.1016/j.critrevonc.2021.103226

12. de Kermenguy F, Meziani L, Mondini M, Clemenson C, Morel D, Deutsch E, et al. Radio-induced lymphopenia in the era of anti-cancer immunotherapy. *Int Rev Cell Mol Biol* (2023) 378:1–30. doi: 10.1016/bs.ircmb.2023.03.002

13. Upadhyay R, Venkatesulu BP, Giridhar P, Kim BK, Sharma A, Elghazawy H, et al. Risk and impact of radiation related lymphopenia in lung cancer: A systematic review and meta-analysis. *Radiother Oncol* (2021) 157:225–33. doi: 10.1016/j.radonc.2021.01.034

14. Damen PJJ, Kroese TE, van Hillegersberg R, Schuit E, Peters M, Verhoeff JJC, et al. The influence of severe radiation-induced lymphopenia on overall survival in solid tumors: A systematic review and meta-analysis. *Int J Radiat Oncol Biol Phys* (2021) 111 (4):936–48. doi: 10.1016/j.ijrobp.2021.07.1695

15. Menetrier-Caux C, Ray-Coquard I, Blay JY, Caux C. Lymphopenia in Cancer Patients and its Effects on Response to Immunotherapy: an opportunity for combination with Cytokines? *J Immunother Cancer* (2019) 7(1):85. doi: 10.1186/s40425-019-0549-5

16. Page MJ, Moher D, Bossuyt PM, Boutron I, Hoffmann TC, Mulrow CD, et al. PRISMA 2020 explanation and elaboration: updated guidance and exemplars for reporting systematic reviews. *BMJ* (2021) 372:n160. doi: 10.1136/bmj.n160

17. Page MJ, McKenzie JE, Bossuyt PM, Boutron I, Hoffmann TC, Mulrow CD, et al. The PRISMA 2020 statement: an updated guideline for reporting systematic reviews. *BMJ* (2021) 372:n71. doi: 10.1136/bmj.n71

18. Higgins J, Thomas J, Chandler J, Cumpston M, Li T, Page M, et al. *Cochrane Handbook for Systematic Reviews of Interventions version 6.2*. London, UK: The Cochrane Collaboration (2021). Available at: www.training.cochrane.org/handbook.

19. Wells GA, Shea B, O'Connell D, Peterson J, Welch V, Losos M, et al. *The Newcastle-Ottawa Scale (NOS) for assessing the quality of nonrandomised studies in meta-analyses* (2010). Available at: http://www.ohri.ca/programs/clinical_epidemiology/oxford.asp.

20. Higgins J, Green S. *Cochrane Handbook for Systematic Reviews of Interventions Version 5.1.0*. London, UK: The Cochrane Collaboration (2011). Available at: www.cochranehandbook.org.

21. Higgins JP, Thompson SG. Quantifying heterogeneity in a meta-analysis. *Stat Med* (2002) 21(11):1539–58. doi: 10.1002/sim.1186

22. Zhong X, Lim EA, Hershman DL, Moinpour CM, Unger J, Lee SM. Identifying severe adverse event clusters using the national cancer institute's common terminology criteria for adverse events. *J Oncol Pract* (2016) 12(3):e270–80, 45-6. doi: 10.1200/JOP.2015.006106

23. Egger M, Davey Smith G, Schneider M, Minder C. Bias in meta-analysis detected by a simple, graphical test. *BMJ* (1997) 315(7109):629–34. doi: 10.1136/bmj.315.7109.629

24. Cho Y, Park S, Byun HK, Lee CG, Cho J, Hong MH, et al. Impact of treatment-related lymphopenia on immunotherapy for advanced non-small cell lung cancer. *Int J Radiat Oncol Biol Phys* (2019) 105(5):1065–73. doi: 10.1016/j.ijrobp.2019.08.047

25. Karantanos T, Karanika S, Seth B, Gignac G. The absolute lymphocyte count can predict the overall survival of patients with non-small cell lung cancer on nivolumab: a clinical study. *Clin Transl Oncol* (2019) 21(2):206–12. doi: 10.1007/s12094-018-1908-2

26. Li YD, Lamano JB, Kaur G, Veliceasa D, Biyashev D, Kruser T, et al. Lymphopenia predicts response to stereotactic radiosurgery in lung cancer patients with brain metastases. *J Neurooncol* (2019) 143(2):337–47. doi: 10.1007/s11060-019-03169-0

27. Chen D, Patel RR, Verma V, Ramapriyan R, Barsoumian HB, Cortez MA, et al. Interaction between lymphopenia, radiotherapy technique, dosimetry, and survival outcomes in lung cancer patients receiving combined immunotherapy and radiotherapy. *Radiother Oncol* (2020) 150:114–20. doi: 10.1016/j.radonc.2020.05.051

28. Friedes C, Chakrabarti T, Olson S, Prichett L, Brahmer JR, Forde PM, et al. Association of severe lymphopenia and disease progression in unresectable locally advanced non-small cell lung cancer treated with definitive chemoradiation and immunotherapy. *Lung Cancer* (2021) 154:36–43. doi: 10.1016/j.lungcan.2021.01.022

29. Cho Y, Kim Y, Chamseddine I, Lee WH, Kim HR, Lee IJ, et al. Lymphocyte dynamics during and after chemo-radiation correlate to dose and outcome in stage III NSCLC patients undergoing maintenance immunotherapy. *Radiother Oncol* (2022) 168:1–7. doi: 10.1016/j.radonc.2022.01.007

30. Jing W, Xu T, Wu L, Lopez PB, Grassberger C, Ellsworth SG, et al. Severe radiation-induced lymphopenia attenuates the benefit of durvalumab after concurrent chemoradiotherapy for NSCLC. *JTO Clin Res Rep* (2022) 3(9):100391. doi: 10.1016/j.jtocrr.2022.100391

31. Lee YJ, Park YS, Lee HW, Park TY, Lee JK, Heo EY. Peripheral lymphocyte count as a surrogate marker of immune checkpoint inhibitor therapy outcomes in patients with non-small-cell lung cancer. *Sci Rep* (2022) 12(1):626. doi: 10.1038/s41598-021-04630-9

32. Thor M, Shepherd AF, Preeshagul I, Offin M, Gelblum DY, Wu AJ, et al. Pre-treatment immune status predicts disease control in NSCLCs treated with chemoradiation and durvalumab. *Radiother Oncol* (2022) 167:158–64. doi: 10.1016/j.radonc.2021.12.016

33. Pasquier C, Chaltiel L, Massabeau C, Rabeau A, Lebas L, Lusque A, et al. Impact of radiation on host immune system in patients treated with chemoradiotherapy and durvalumab consolidation for unresectable locally advanced non-small cell lung cancer. *Front Oncol* (2023) 13:1186479. doi: 10.3389/fonc.2023.1186479

34. Fehlings M, Jhunjhunwala S, Kowanetz M, O'Gorman WE, Hegde PS, Sumatoh H, et al. Late-differentiated effector neoantigen-specific CD8+ T cells are enriched in peripheral blood of non-small cell lung carcinoma patients responding to atezolizumab treatment. *J Immunother Cancer* (2019) 7(1):249. doi: 10.1186/s40425-019-0695-9

35. Li S, Simoni Y, Zhuang S, Gabel A, Ma S, Chee J, et al. Characterization of neoantigen-specific T cells in cancer resistant to immune checkpoint therapies. *Proc Natl Acad Sci U.S.A.* (2021) 118(30). doi: 10.1073/pnas.2025570118

36. Caushi JX, Zhang J, Ji Z, Vaghasia A, Zhang B, Hsiue EH, et al. Transcriptional programs of neoantigen-specific TIL in anti-PD-1-treated lung cancers. *Nature* (2021) 596(7870):126–32. doi: 10.1038/s41586-021-03752-4

37. Cheng B, Ding K, Chen P, Ji J, Luo T, Guo X, et al. Anti-PD-L1/TGF-betaR fusion protein (SHR-1701) overcomes disrupted lymphocyte recovery-induced resistance to PD-1/PD-L1 inhibitors in lung cancer. *Cancer Commun (Lond)* (2022) 42(1):17–36. doi: 10.1002/cac2.12244

38. Zhao Q, Li T, Chen G, Zeng Z, He J. Prognosis and risk factors of radiation-induced lymphopenia in early-stage lung cancer treated with stereotactic body radiation therapy. *Front Oncol* (2019) 9:1488. doi: 10.3389/fonc.2019.01488

39. Xie X, Lin SH, Welsh JW, Wei X, Jin H, Mohan R, et al. Radiation-induced lymphopenia during chemoradiation therapy for non-small cell lung cancer is linked with age, lung V5, and XRCC1 rs25487 genotypes in lymphocytes. *Radiother Oncol* (2021) 154:187–93. doi: 10.1016/j.radonc.2020.09.002

40. Kim Y, Chamseddine I, Cho Y, Kim JS, Mohan R, Shusharina N, et al. Neural network based ensemble model to predict radiation induced lymphopenia after concurrent chemo-radiotherapy for non-small cell lung cancer from two institutions. *Neoplasia* (2023) 39:100889. doi: 10.1016/j.neo.2023.100889

41. Zhao Q, Bi Y, Xue J, Liu Y, Zhu J, Qin S. Prognostic value of absolute lymphocyte count in patients with advanced esophageal cancer treated with immunotherapy: a retrospective analysis. *Ann Transl Med* (2022) 10(13):744. doi: 10.21037/atm-22-2669

42. Cesaire M, Rambeau A, Clatot F, Johnson A, Heutte N, Thariat J. Impact of lymphopenia on efficacy of nivolumab in head and neck cancer patients. *Eur Arch Otorhinolaryngol* (2023) 280(5):2453–61. doi: 10.1007/s00405-022-07800-1

43. Kuge T, Shiroyama T, Tamiya A, Tamiya M, Kanazu M, Kinehara Y, et al. Impact of lymphopenia recovery after chemoradiotherapy on durvalumab consolidation therapy in stage III NSCLC. *JTO Clin Res Rep* (2023) 4(5):100505. doi: 10.1016/j.jtocrr.2023.100505

44. Zhao Q, Li T, Du S, He J, Zeng Z. Shortened radiation time promotes recovery from radiation-induced lymphopenia in early-stage non-small cell lung cancer patients treated with stereotactic body radiation therapy. *Technol Cancer Res Treat* (2022) 21:15330338221112287. doi: 10.1177/15330338221112287

45. Tubin S, Khan MK, Salerno G, Mourad WF, Yan W, Jeremic B. Mono-institutional phase 2 study of innovative Stereotactic Body RadioTherapy targeting PArtial Tumor HYpoxic (SBRT-PATHY) clonogenic cells in unresectable bulky non-small cell lung cancer: profound non-targeted effects by sparing peri-tumoral immune microenvironment. *Radiat Oncol* (2019) 14(1):212. doi: 10.1186/s13014-019-1227-y

46. Meijer JJ, Leonetti A, Airo G, Tiseo M, Rolfo C, Giovannetti E, et al. Small cell lung cancer: Novel treatments beyond immunotherapy. *Semin Cancer Biol* (2022) 86:376–85. doi: 10.1016/j.semcancer.2022.05.004

Frontiers in Oncology

Advances knowledge of carcinogenesis and tumor progression for better treatment and management

The third most-cited oncology journal, which highlights research in carcinogenesis and tumor progression, bridging the gap between basic research and applications to imrpove diagnosis, therapeutics and management strategies.

Discover the latest Research Topics

See more →

Frontiers

Avenue du Tribunal-Fédéral 34
1005 Lausanne, Switzerland
frontiersin.org

Contact us

+41 (0)21 510 17 00
frontiersin.org/about/contact